

Neurodevelopment & Risk Factors in Schizophrenia

Vasileios Ioakeimidis

This thesis is submitted for the degree of
Doctor of Philosophy (PhD)

City, University of London
School of Arts and Social Sciences
Department of Psychology

April 2021

Table of contents

TABLE OF CONTENTS.....	3
TABLE OF FIGURES.....	6
TABLE OF TABLES.....	9
ACKNOWLEDGMENTS.....	10
THESIS ABSTRACT.....	11
GENERAL INTRODUCTION.....	12
THESIS OVERVIEW.....	18
REFERENCES.....	24
CHAPTER 1: DISSOCIATING TRAIT AND STATE ANXIETY EFFECTS ON MISMATCH NEGATIVITY AND SENSORY GATING EVENT-RELATED POTENTIALS.....	31
1. INTRODUCTION.....	32
2. METHODS.....	35
2.1. <i>Participants and self-report measures</i>	35
2.2. <i>Stimuli and design</i>	35
2.3. <i>EEG acquisition and pre-processing</i>	37
2.4. <i>Statistical analysis</i>	39
3. RESULTS.....	41
3.1. <i>Questionnaire data</i>	41
3.2. <i>MMN</i>	41
3.3. <i>P50 suppression</i>	43
4. DISCUSSION.....	45
REFERENCES.....	49
TABLES.....	55
CHAPTER 2: STATE ANXIETY INFLUENCES P300 AND P600 EVENT-RELATED POTENTIALS OVER PARIETAL REGIONS IN THE HOLLOW MASK ILLUSION EXPERIMENT*.....	58
1. INTRODUCTION.....	59
2. METHODS.....	63
2.1. <i>Participants</i>	63
2.2. <i>The NEO PI-R and STAI self-report questionnaires</i>	63
2.3. <i>Stimuli and Design</i>	64
2.4. <i>EEG acquisition and ERP analysis</i>	66
2.5. <i>Statistical analysis</i>	68
3. RESULTS.....	70
3.1. <i>Personality and anxiety scores</i>	70
3.2. <i>Behavioural data</i>	70
3.3. <i>ERP results</i>	71
4. DISCUSSION.....	76
REFERENCES.....	84
TABLES.....	90

CHAPTER 3: A META-ANALYSIS OF STRUCTURAL AND FUNCTIONAL BRAIN ABNORMALITIES IN EARLY-ONSET SCHIZOPHRENIA: NEUROIMAGING FINDINGS OF EARLY-ONSET SCHIZOPHRENIA*92

1. INTRODUCTION.....	93
2. METHODS.....	97
2.1. Literature search and study selection.....	97
2.2. Database construction.....	98
2.3. Activation likelihood estimation.....	99
2.4. Follow-up analyses for fMRI ALE.....	100
3. RESULTS.....	103
3.1. VBM.....	103
3.2. fMRI.....	103
3.3. Follow-up: Meta-analytic co-activation modelling (MACM).....	105
3.4. Follow-up: Cognitive associations.....	108
4. DISCUSSION.....	110
4.1. VBM.....	110
4.2. fMRI.....	111
4.3. Meta-analytic co-activation modelling (MACM): Saliency dysfunction.....	115
4.4. Conclusions.....	116
REFERENCES.....	118
TABLES.....	128

CHAPTER 4: DORSOLATERAL PREFRONTAL CORTEX AND DEFAULT MODE NETWORK DYSCONNECTIVITY UNDERLIES WORKING MEMORY PERFORMANCE IN YOUNG ADULTS WITH EARLY-ONSET SCHIZOPHRENIA: AN FMRI FOLLOW-UP STUDY 144

1. INTRODUCTION.....	145
2. METHODS.....	147
2.1. Participants.....	147
2.2. N-back task.....	148
2.3. Image acquisition.....	149
2.4. Image analysis.....	150
3. RESULTS.....	153
3.1. Participants.....	153
3.2. GLM analysis.....	153
3.3. Psychophysiological Interactions.....	155
4. DISCUSSION.....	157
REFERENCES.....	163
TABLES.....	167

CHAPTER 5: FUNCTIONAL NEURODEVELOPMENT OF WORKING MEMORY IN EARLY-ONSET SCHIZOPHRENIA: A LONGITUDINAL FMRI STUDY FROM ADOLESCENCE TO EARLY ADULTHOOD

171

1. INTRODUCTION.....	172
2. METHODS.....	177
2.1. Participants.....	177
2.2. N-back task.....	178
2.3. Image acquisition.....	179
2.4. Image analysis.....	179
3. RESULTS.....	182

3.1.	<i>Participants</i>	182
3.2.	<i>Longitudinal BOLD activity change in the entire sample</i>	183
3.3.	<i>Longitudinal BOLD activity change within and between groups</i>	184
3.4.	<i>Prediction of longitudinal BOLD activity change by clinical characteristics of EOS</i>	186
4.	DISCUSSION	188
	REFERENCES	193
	TABLES	201
	GENERAL DISCUSSION	206
	SUMMARY OF MAIN GOALS AND FINDINGS	206
	IS ANXIETY A RISK FACTOR FOR SCHIZOPHRENIA?	209
	IS SALIENCE NETWORK DYSFUNCTION THE CONNECTIVE LINK ACROSS PARADIGMS AND DIAGNOSES?	213
	WORKING MEMORY NEURODEVELOPMENT AS AN ENDOPHENOTYPIC MARKER FOR EOS	216
	STRENGTHS	219
	LIMITATIONS & FUTURE DIRECTIONS	220
	REFERENCES	226
	APPENDIX	235

Table of figures

Figure 1.1. Schematic representation of the auditory roving oddball paradigm reproduced from Garrido et al. (2009)	37
Figure 1.2. 64-channel ActiCAP and electrodes of interest for the MMN and P50 ERPs	38
Figure 1.3. A) Deviant (continuous black line) and standard (dotted grey line) stimuli ERP waveforms in the entire sample (N = 34). B) MMN waveform (deviant minus standard) at Fz electrode site for all participants (dashed line) C) Scatterplot showing the negative relationship of MMN amplitude at Fz with the trait anxiety measure. Partial correlation coefficient and associated p-value show the strength of the correlation and the probability this is being observed due to chance. Abbreviations: μV : microvolt; MMN: mismatch negativity; p: p-value; rp: partial correlation coefficient.....	41
Figure 1.4. A) MMN waveform (deviant minus standard) at Fz electrode site for HTA (continuous line) versus LTA (dotted line) groups. B) Bar graphs showing the MMN amplitude at Fz between HTA and LTA subjects following median split; * indicates significant differences; error bars represent standard error of the mean. Abbreviations: HTA: high-trait anxiety LTA: low-trait anxiety; μV : microvolt; MMN: mismatch negativity.....	42
Figure 1.5. A) Grand average waveforms for the S1 (black continuous line) and S2 (grey dotted line) stimuli at Cz superimposed onto each other for the entire sample. B) Scatterplots displaying the linear associations of the S2 amplitude, P50 difference, and P50 ratio with state anxiety on the left-hand side. Partial correlation coefficients and associated p-values show the strength of these correlations and the probability these were observed due to chance. Abbreviations: μV : microvolt; p: p-value; rp: partial correlation coefficient; S1: stimulus S1; S2: stimulus S2	43
Figure 1.6. Grand average waveforms for the S1 (black continuous line) and S2 (grey dotted line) stimuli at Cz superimposed onto each other A) for the subaverage of the high-state anxious, and B) low-state anxious participants. C) Bar plots for the four P50 suppression parameters (S1 and S2 amplitude, P50 difference and ratio) comparing the differences between HSA and LSA groups following median split; * indicates significant differences; error bars represent standard error of the mean. Abbreviations: HSA: high-state anxiety; LSA: low-state anxiety; μV : microvolt; S1: stimulus S1; S2: stimulus S2.....	44
Figure 2.1. Hollow mask stimulus generation. Using the stereoscope and by alternating Left and Right perspective images on the display we constructed concave, convex, and flat face stimuli.....	65
Figure 2.2. 64-electrode ActiCAP layout and electrode regions-of-interest.....	67
Figure 2.3. Grand average ERP waveforms for 3D normal faces, 3D inverted faces and flat faces in the whole sample (N=20) in the twenty ROI electrodes. Y-axis represents the amplitude of the ERP with tick marks every $1\mu\text{V}$ and X-axis represents the time before and after the stimulus presentation with tick marks every 100ms	72
Figure 2.4. Grand average ERP difference waves for 3D normal faces minus flat faces and 3D inverted faces minus flat faces in the whole sample (N=20) in the twenty ROI electrodes. Y-axis represents the amplitude of the ERP with tick marks every $1\mu\text{V}$ and X-axis represents the time before and after the stimulus presentation with tick marks every 100ms.....	74
Figure 2.5. Mean difference amplitude (μV) of concave and convex ERPs minus flat for high-state anxiety and low-state anxiety groups by median split, in A) the P300 central, B) P300 parietal and	

C) P600 parietal time windows; error bars represent standard error of the mean. * $p < .05$; ** $p < .01$ for between- and within-group comparisons.....75

Figure 3.1. Preferred Reporting Items for Systematic Reviews and Meta-Analyses (PRISMA) flowchart shows the detailed selection process of the studies used in the VBM and fMRI meta-analyses. Abbreviations: AOS (adolescent-onset schizophrenia); COS (childhood-onset schizophrenia); EOS (early-onset schizophrenia); SVC (small-volume correction); ROI (region-of-interest analysis).....98

Figure 3.2. Clusters of EOS hypoactivation in the Cognition ALE and WM ALE. A) Significant convergence across all cognitive experiments was found in the ACC and rTPJ for the HC > EOS contrasts. B) The WM ALE showed significant convergence at the lPreC, rIPL and rTPJ. Results are cluster-FWE corrected at 0.05 with cluster forming value at $p < 0.01$. The same clusters were later used as seed-ROIs for the MACM and functional associations analyses. Abbreviations: rACC (right anterior cingulate cortex); rIPL (right inferior parietal lobule); lPreC (left precuneus); rTPJ (right temporoparietal junction).....105

Figure 3.3. Schematic representation of the relative positions of the suprathreshold Cognition ALE clusters in blue and WM ALE clusters in orange, with their respective associate behavioural domains. The core network resulting from the conjunction analysis of the respective MACM maps, in purple. Axial brain slice from Colin27_T1_MN1 at $z = 15$106

Figure 3.4. Cognitive associations for the seed-ROIs resulting from (A) the Cognition ALE in blue and (B) WM ALE in orange. A 2-by-2 contingency table approach was used along with Fisher's test as a method of reverse inference to determine the odds of detecting a behavioural domain given activation of a certain ROI relative to the odds of detecting it given activation elsewhere in the brain. Only significant (FDR corrected) behavioural domains are presented in bar graphs, with odds of activating the ROI higher than 1. * $p < 0.05$; ** $p < 0.01$; *** $p < 0.001$108

Figure 4.1. Schematic representation of the letter n-back paradigm that was used during fMRI scanning.....149

Figure 4.2. Axial layout of brain areas with main effects of two-back activations (2-back > 0-back) in controls (red overlay) and EOS patients (blue overlay). Colour bars represent the T-values of the overlain clusters. Brain template is Colin27_T1_MN1overalyed with thresholded SPM corrected for multiple comparisons correction at FWE $p < 0.05$154

Figure 4.3. Sagittal layout of brain areas with main effects of two-back deactivations (0-back > 2-back) in controls (red overlay) and EOS patients (blue overlay). Colour bars represent the T-values of the overlain clusters. Brain template is Colin27_T1_MN1overalyed with thresholded SPM corrected for multiple comparisons correction at FWE $p < 0.05$154

Figure 4.4. Axial layout of brain areas that display negative psychophysiological interactions (PPI) with the right DLPFC seed in control subjects. EOS patients had no significant clusters for neither positive nor negative PPI, in neither the left nor right DLPFC. Brain template is Colin27_T1_MN1overalyed with thresholded SPM corrected for multiple comparisons correction at FWE $p < 0.05$155

Figure 4.5. Sagittal slice showing at $x = 0$ showing the medial prefrontal cortex and posterior cingulate cortex, areas where controls displayed increased negative PPI of the right DLPFC compared to EOS. Brain template is Colin27_T1_MN1overalyed with thresholded SPM $p < 0.001$ uncorrected, $k_e > 10$156

Figure 5.1. The graph shows the age distribution (in years) of the participants (Y axis) from baseline and follow-up scans. Age of illness-onset for EOS patients is also shown. It also shows the interscan

interval for each participant (follow-up age minus baseline age) as well as the duration of illness for EOS patients at each scan (age minus illness-onset)183

Figure 5.2. A) Brain areas with main effects of task on process-general $\Delta_{\text{BOLD}(t1>t2)}$ from baseline to follow-up in the entire sample of developing adolescents; B) Brain areas with process-general $\Delta_{\text{BOLD}(t1>t2)}$ in typically developing adolescents (red) and in adolescents with EOS (blue) and C) Sagittal layout of $\Delta_{\text{BOLD}(t1>t2)}$ in typical adolescents (red) and adolescents with EOS (blue), showing the non-overlapping reductions in ACC (red) and SMA (blue) areas at three-back trials. The EOS threshold SPM was extracted from the model with the additional covariates, i.e., onset-age, cumulative antipsychotic medication, and interscan interval, but it is not showing the left middle/superior temporal cluster because we wanted to show the absence of overlap in the two midline areas. Colour bars represent the T-values of the overlain clusters. Multiple comparisons correction at FWE $p < 0.05$ 184

Figure 5.3. A) PANSS total symptoms at baseline negatively predicted $\Delta_{\text{BOLD}(t1>t2)}$ in the middle cingulate gyrus during two-back blocks. Higher initial symptoms predicted lower longitudinal reduction. B), C) PANSS total and positive positively predicted $\Delta_{\text{BOLD}(t1>t2)}$ in the left inferior frontal and the right middle frontal gyri during one-back blocks. Higher initial symptoms predicted increased longitudinal reduction. Negative and positive $\Delta_{\text{BOLD}(t1>t2)}$ values represent increased and decreased BOLD at t2, respectively. Multiple comparisons correction at FWE $p < 0.05$ 186

Table of tables

Table 1.1. Demographics and questionnaire characteristics for all participants and anxiety subgroups.....	55
Table 1.2. Trait anxiety group characteristics for MMN.....	56
Table 2.1. Demographic and questionnaire data in the entire sample (N = 94).....	90
Table 2.2. Demographic, questionnaire, and behavioural data in the EEG sample (N = 20).....	91
Table 3.1. Summary of the demographic and clinical variables for the 7 VBM studies and the 8 fMRI studies.....	128
Table 3.2. Paradigm and coordinate data for the experiments (and contrasts) within the 7 VBM studies followed by the 8 fMRI studies.....	131
Table 3.3. Clusters showing significant convergence of hypoactivation in EOS.....	137
Table 3.4. Foci contribution from each fMRI study to the resultant ALE clusters of hypoactivation in EOS.....	138
Table 3.5. Functional connectivity for the Cognitive ALE-derived seeds and conjunctions between each using the minimum statistic.....	139
Table 3.6. Functional connectivity for the WM ALE-derived seeds and conjunctions between each seed using the minimum statistic.....	141
Table 4.1. Demographic, clinical, and behavioural characteristics for the EOS and HC groups.....	167
Table 4.2. BOLD activations at two-back in healthy controls and patients with EOS.....	168
Table 4.3. BOLD deactivations at two-back in healthy controls and patients with EOS.....	169
Table 4.4. Peak coordinates of within- and between-group PPI for left and right DLPFC seed.....	170
Table 5.1. Demographic, clinical, and behavioural characteristics for adolescents with EOS and TD adolescent groups at baseline and follow-up with respective p-values for longitudinal within-group change.....	201
Table 5.2. Main effects of task on Δ_{BOLD} while controlling for gender and age at follow-up.....	202
Table 5.3. Main effects of group (\times task) on Δ_{BOLD} while controlling for gender and age at follow-up.....	203
Table 5.4. Main effects of task on $\Delta_{\text{BOLD}(t_1>t_2)}$ for EOS patients while controlling for gender, age at follow-up, age-of-illness onset, cumulative antipsychotic medication, and interscan interval.....	204
Table 5.5. Brain areas with $\Delta_{\text{BOLD}(t_1>t_2)}$ predicted by baseline PANSS (total, positive, negative) scores in developing adolescents with EOS.....	205

Acknowledgments

Reflecting on my thoughts around the possibility of doing a PhD before its actual start, I remember being terrified at the idea of getting into one. This was due to the anecdotal horror stories from students whose misery made it seem that a PhD would not be the right path for me. My personal experience as a PhD student in the last 3.5 years, though often isolating, it was anything but horrific and I owe this to the wonderful network of support that I found at City and to my chosen family.

I'm most thankful to my marvellous supervisor, Danai. Thank you for being a role model who inspired me to be more assertive and helped me find confidence in my abilities. Thank you for the hours you spent replying to my emails, meeting in person or on Skype and for lifting me up when the little voice in my head insisted I'm not good enough. Your encouragement and your trust they mean the world to me and I am incredibly lucky to have had you as my supervisor.

Thanks to City, University of London for the funded studentship programme and the financial support. Thanks to the wonderful departmental staff Tanya Shennan and Jay Leighton who made mundane and frustrating admin issues seem remarkably simpler. Thank you to the Senior Tutor for Research Students Dr Dermot Bowler for being so helpful and always on our side.

So many thank yous to my lovely friends from City, Saoirse, Nareg, and Sonia. Thanks are given to the PhDs, Laura, Vasiliki, Ingrid, Prince, and all my peers who made it so fun going to work every day at Rhind building. Since the start of the pandemic, it became even more obvious how important it is to have a community of peers who support each other and who understand exactly what each of us is going through. I am really grateful to have had that mutual support in the first 2.5 years and for the continuing community that we maintain online.

A huge thank you to my parents Dimitri and Kiki for the sacrifices you made to make sure that me and my sisters can go to university (and for that many years!). And finally, a big thank you to my partner, Olly, whose vast resources of love, care, and creativity made these last few (nearly apocalyptic) months so much easier to go by.

Thank you all for making this journey feel a lot less lonely and a lot more exciting ❤️

Thesis abstract

Schizophrenia is a complex psychiatric disorder with positive, negative, and cognitive symptoms. The causes are not yet fully understood, but it is believed that together with a strong genetic foundation, a 'second environmental hit' may be responsible to triggering a psychotic episode. Early-onset schizophrenia (EOS) a rare and more severe form of the disorder compared to its adult-onset counterpart and it is regarded to be more genetically loaded. This being as children and adolescents are less likely to have accumulated environmental triggers that are often considered risks to develop schizophrenia. Neurotic personality and anxiety symptoms are considered candidate schizophrenia risk factors. Working memory (WM) performance, the ability to hold information "online" in the matter of a few seconds, as well as its neural correlates are severely impaired in EOS, and such impairment is considered endophenotypic to the disorder. In addition, the expression of neurophysiological indices of cognition such as the mismatch negativity (MMN) and P300 event-related potentials (ERPs) are consistently demonstrated to be reliable biomarkers for the disorder, as shown by electroencephalography. This thesis on one hand, explores the influence of neuroticism and anxiety levels in healthy participants in ERPs during the auditory roving oddball and the hollow mask illusion experiments that are continually shown to be affected in schizophrenia literature. On the other hand, it explores meta-analytically convergent structural and functional brain abnormalities in EOS literature and follows a longitudinal fMRI cohort of EOS and healthy adolescents who were scanned twice in a 4-year span, while they performed the n-back task (WM task). These experiments are aimed to reveal brain areas that may qualify as endophenotypic markers of impaired WM neurodevelopment in schizophrenia. Our results showed that anxiety and neuroticism do not fully explain their status as schizophrenia risk factors by their relationship with the schizophrenia biomarker ERPs (P50 sensory gating, MMN, P300 and P600). The meta-analysis strongly indicates that a dysfunction in the functional network that underlies salience and other executive functions related to incentive and goal-oriented processes may be central across cognitive paradigms in EOS. Longitudinally, functional connectivity and maturation impairments are prevalent in the WM functional substrate of adolescents with EOS as they undergo neurodevelopmental processes by transitioning into early adulthood.

General introduction

Schizophrenia is a psychiatric disorder with a lifetime prevalence of approximately 1%. It is expressed by positive and negative symptoms, whose continuous presence of over a six-month period is required for diagnosis according to the Diagnostic and Statistical Manual for Mental Disorders-5th edition (American Psychiatric Association, 2013). Positive symptoms include delusions, hallucinations and thought disorder, while negative symptoms consist of apathy, social withdrawal, avolition, alogia, anhedonia. Schizophrenia is also characterised by cognitive symptoms, which are not currently used as diagnostic criteria, but are prominent in clinical research. Cognitive abnormalities are primarily seen in executive processes such as attentional control, working memory, change detection, information filtering (Dima et al., 2012; Jansen et al., 2010; Lee & Park, 2006; Luck & Gold, 2008; Park & Gooding, 2014). Whereas antipsychotic medication is predominantly used to improve positive symptoms, cognitive and negative ones are less responsive to known antipsychotic treatments (Insel, 2010). Schizophrenia can cause a severe decline on day-to-day functioning; therefore, it is imperative to design efficient prognostic measures and biomarkers that assess the neural correlates relative to increased risk. This could be accomplished by assessing the relationship of cognitive function with neural signatures of (1) well-established risk factors for schizophrenia in the unaffected population as well as (2) illness-related brain function and trajectory in patients with schizophrenia.

Schizophrenia symptoms can manifest as early as early childhood (Gochman et al., 2011), but it typically gets diagnosed in young adulthood. Onset before 18 years of age is rare and accounts for approximately 5% of all patients diagnosed with the illness (Cannon et al., 1999). Childhood onset schizophrenia and adolescent onset

schizophrenia are subtypes that refer to different developmental stages of first onset, and sometimes are studied separately. More commonly, the term early onset schizophrenia (EOS) is used as an umbrella that encompasses any case in developing youths below 18 years old. EOS is neurobiologically continuous with its adult onset counterpart, however it is seen as a more severe form of the disorder often having worse prognosis, and more severe symptom expression (Rapoport & Gogtay, 2011). Nevertheless, recent reports have challenged this view (Amminger et al., 2011). Research in EOS has implied that it may be more genetically loaded as it has higher prevalence of rare genetic structural variants than adult-onset schizophrenia (Walsh et al., 2008) while it is considered to be influenced by environmental factors to a lesser degree (Rapoport & Gogtay, 2011). Children and adolescents are less likely to have accumulated exposure to later life behaviours such as cannabis use, and life stressors or traumatic events that are believed to increase the occurrence of schizophrenia in vulnerable individuals. Nonetheless, if schizophrenia had been purely genetic the expected concordance rate among monozygotic twins would be 100%, whereas the observed congruence in developing schizophrenia is around 50% (Rapoport et al., 2005). Environment-gene interactions can affect neurodevelopmental processes of brain maturation (Fatemi & Folsom, 2009). Indeed, many of the genetic variations that are observed in individuals with schizophrenia and other psychiatric syndromes, are implicated with signalling events of brain development and synaptic neurotransmission (Birnbaum & Weinberger, 2017; Walsh et al., 2008).

It has been hypothesized that schizophrenia symptoms and associated cognitive deficits are the outcome of atypical brain development that disrupts the acquisition of typical cognitive abilities before the onset of the disorder. Cognitive abilities that are mostly affected in schizophrenia include working memory, inhibitory and cognitive

control; functions whose development coincides with the typical development of their cortical substrates (e.g., prefrontal, temporal, parietal, and cingulate cortices) and with schizophrenia onset in adolescence (Catts et al., 2013). These deficits can manifest as premorbid deviances in high-risk individuals and are more pronounced in those who will later convert into full-blown schizophrenia. Hence, a growing consensus among scientists and clinicians (Bora, 2015; Fatemi & Folsom, 2009; Rapoport et al., 2012) increasingly regards schizophrenia to be neurodevelopmental in origin. In this model, cognitive deficits are the result of neurodevelopmental delay (Reichenberg et al., 2010), rather than loss of function, that are displayed early (prior to official diagnosis) and remain stable without further deteriorating as the illness progresses (Birnbaum & Weinberger, 2017; Zanelli et al., 2019). Brain morphological changes are seen in those at risk, before the onset of the illness, and they progress as they convert to psychosis (Sugranyes et al., 2020). Accordingly, aberrant brain activation associated with cognitive function is also evident in those with subclinical psychotic symptoms, such as delusional beliefs and hallucinatory experiences, including in children (Jacobson et al., 2010). Altered processes of brain development such as neuronal migration, synaptic pruning, axon myelination, dendritic arborisation are potential targets of genetic and environmental insults that can contribute to the neurodevelopment of the disorder, to the cognitive impairment that characterises it (Birnbaum & Weinberger, 2017; Bora, 2015) and to the progressive grey matter reduction in patients with EOS during adolescence (Sporn et al., 2003).

Anxiety is often considered a premorbid characteristic of schizophrenia (Pallanti et al., 2013), while it is known to impair cognition (Eysenck et al., 2007) and its neural correlates (Ansari & Derakshan, 2011; Modi et al., 2018). Anxiety disorders are prevalent in individuals with at-risk mental state (Fusar-Poli et al., 2014) and may be a

core feature of psychopathology in adolescents at high risk for schizophrenia (Mazzoni et al., 2009; McAusland et al., 2017). At age 15, individuals who were later on diagnosed with schizophrenia were reported to show increased levels of anxiety by their teachers in a UK 1946 birth cohort (P. Jones et al., 1994). Therefore, anxiety can be a risk factor or a premorbid characteristic for psychosis. Furthermore, it has been proposed that anxiety may be a core symptom dimension in schizophrenia (Muller et al., 2004) as more than 1/3 of schizophrenia patients have a comorbid anxiety disorder (Braga et al., 2013; Temmingh & Stein, 2015). Such high comorbidity rate suggests that there might exist a shared susceptibility between anxiety and psychosis (Muller et al., 2004). Importantly, positive psychotic symptoms are associated with anxiety in individuals with schizophrenia and with worse disease prognosis (Hartley et al., 2013). This includes anxiety disorders (Huppert & Smith, 2005) and subclinical anxiety measures (Cowles & Hogg, 2019; Guillem et al., 2005) that have been found to affect the severity of paranoia, hallucinations, and delusions. While it is unclear whether transition of high-risk individuals to frank psychosis is mediated by their heightened anxiety levels (Addington et al., 2017; Fusar-Poli et al., 2014), anxiety is seen more commonly in first-episode than chronic patients (Temmingh & Stein, 2015). Notably, high genetic risk for schizophrenia is associated with anxiety disorders and negative symptoms, in adolescence, but not with psychotic experiences (H. J. Jones et al., 2016). It was argued that positive symptoms might occur later in those individuals who later convert to psychosis, whereas anxiety is a prodromal symptom. This is supported by a study that found increased anxiety in individuals that were both at familial and clinical high risk compared to those at only familial risk (Stowkowy & Addington, 2013). Hence conversion to psychosis may be exacerbated by anxiety and its association with positive symptoms and thought disorder (Temmingh & Stein, 2015). This increased

susceptibility could be mediated by anxiety through neurobiological mechanisms that affect salience processing, attention, and inhibition of irrelevant information (Braunstein-Bercovitz, 2000; Heinz & Schlagenhauf, 2010).

Neuroticism, a stable personality trait that is characterised by vulnerability to stressors, is considered crucial for its role in the manifestation of psychopathology (Caspi et al., 2014). Similar to anxiety, it can shape cognitive processes, for example by focusing attention to irrelevant stimuli (Dhinakaran et al., 2014) and by altering the dynamics of the working memory network (Dima et al., 2015). Anxiety is a property of the neurotic personality trait. In the model of Costa and McCrae, neuroticism is consisted of six facets, namely anxiety, angry hostility, depression, self-consciousness, impulsiveness, and vulnerability (McCrae & Costa, 1992). Van Os & Jones (2001) found that higher neuroticism at age 15 predicted higher likelihood for the diagnosis of schizophrenia at a later age. This observed association was independent of anxiety and depressive symptoms (Van Os & Jones, 2001). More recently, a large meta-analysis on longitudinal studies found that neuroticism is a stable vulnerability factor that contributes to the development of psychopathology, including that of anxiety and schizophrenia (Jeronimus et al., 2016). Neuroticism was also consistently high for schizophrenia patients in a meta-analysis assessing 460 patients (Ohi et al., 2016). Thus, neuroticism – similar to anxiety – is both a risk factor and comorbid with schizophrenia. Moreover, neuroticism shares common genetic risk factors with schizophrenia and with anxiety, although these genetic correlations are medium ($r \approx 0.20$) for schizophrenia and stronger for anxiety (≈ 0.85) (Nagel et al., 2018; Smith et al., 2016). Interference of neuroticism with cognitive processes that can link negative attention bias, dysfunctional coping attitude, rumination, anxiety sensitivity, heightened reactivity (Jeronimus et al.,

2016) could be some of the mechanisms that explain neuroticism's involvement in the vulnerability to schizophrenia.

Owing to the widely distributed alterations in brain connectivity, schizophrenia is broadly considered a disconnection syndrome (Friston et al., 2016). Changes in networks supported by brain areas located in frontal, temporal, parietal, and occipital lobes as well as subcortical structures are extensively implicated in cognitive dysfunction as well as in positive and negative symptoms. Neurobiologically, schizophrenia has been associated with dysregulation in neurotransmitter systems such as dopamine, glutamate and GABA, which can explain schizophrenia symptoms and functional changes, and these neurotransmitter systems can also explain anxiety. Three major networks that rely on those neurotransmitter pathways, have been identified through their roles in perception, emotion, and cognition, the central executive, salience, and default mode (DMN) networks. During the last decade, psychopathology has been described under the framework of this triple-network dysregulation that can explain dysfunction in schizophrenia and other psychiatric symptoms, such as anxiety (Menon, 2011). Aberrant cross-network connectivity in schizophrenia patients is centred in the salience network and likely explains the challenges in shutting inner thought-related processes of the DMN and orient cognitive resources to goal-directed behaviour (Supekar et al., 2019). While salience network abnormality predicts psychotic symptoms in schizophrenia (Supekar et al., 2019), salience network disorganisation is featured in individuals with high trait anxiety (Massullo et al., 2020) and its nodes demonstrate aberrant function in neuroticism (Feinstein et al., 2006).

So far, we have described schizophrenia as a collection of positive, negative, and cognitive symptoms with accumulating evidence pointing to a neurodevelopmental origin. This becomes more evident through the study of EOS and at-risk patients, who

demonstrate widespread functional brain changes during childhood and adolescence when the brain still matures. Moreover, cognitive brain function is influenced by subclinical anxiety levels, with anxiety seen as a risk factor for schizophrenia, as it associates with the genetic risk and with positive symptoms. High anxiety levels and/or high neuroticism can lead to a higher risk of developing schizophrenia with the correct combination of genetic and environmental factors. What is fascinating, is that the neural correlates of cognitive and sensory processes can be influenced by anxiety and neuroticism in non-clinical samples (Berggren et al., 2015; Bishop et al., 2004; Fucci et al., 2019; Huang et al., 2009; Modi et al., 2018; Wang et al., 2004), often in similar ways as in schizophrenia.

Thesis overview

The aims of this PhD thesis are threefold: *First*, to examine subclinical measures of anxiety and neuroticism in healthy individuals against known neurophysiological and cognitive/perceptual endophenotypes of schizophrenia by using the auditory roving oddball and hollow mask experiments. Using electroencephalography (EEG) the first two experimental chapters (**Chapter 1** and **Chapter 2**) investigate how individual differences in neuroticism, state and trait anxiety, influence the generation of event-related potentials (ERP) that are aberrant in schizophrenia. *Second*, to determine the regional convergence of brain areas with aberrant structure and function in EOS, across published studies (**Chapter 3**). In order to achieve this structural and functional imaging studies with EOS samples were gathered and coordinate-based meta-analytic techniques were used. Additionally, the core functional network that supports the aberrant brain regions in EOS was also explored. Our *final aim* was to directly address the longitudinal changes in the neural correlates of working memory in EOS. The next two experimental chapters (**Chapter 4** and **Chapter 5**) follow up a patient cohort with EOS and healthy

individuals. In this cohort, a sample of typically developing (TD) adolescents and adolescents with EOS were scanned with functional magnetic resonance imaging (fMRI) during a working memory paradigm across two time points that spanned 4.5 years (first time point mean age in years = 16.5, second time point mean age = 21). The fourth chapter (**Chapter 4**) examines the cross-sectional differences between EOS and typical developing individuals in working memory function and connectivity, whereas the fifth and last chapter (**Chapter 5**) explores the longitudinal functional trajectory relevant to working memory neurodevelopment in these adolescents.

The auditory P50 and mismatch negativity (MMN) ERPs are indices of sensory gating and change detection, respectively (Turetsky et al., 2007). The P50 represents information filtering processes when two identical stimuli are presented one after the other. Typically, the amplitude of the second stimulus will be suppressed at around 50-100ms post-stimulus presentation – inhibiting the response to the repeated, redundant, stimulus. Individuals with schizophrenia and anxiety disorders do not inhibit the response to the repeated stimulus showing attenuated sensory gating. In a train of repeated auditory tones with the same properties (e.g., frequency) the auditory response at around 150-250ms post-stimulus will increase in amplitude until it habituates, and the tone eventually becomes “standard”. When a tone of different frequency interrupts the stimulus train, this creates a mismatch between the current stimulus and the predicted model resulting in sharp drop in amplitude (around 150-250ms) after the “deviant” stimulus. Proposed underlying mechanisms of this response are adaptation, change detection, and error prediction. Patients with schizophrenia and patients with anxiety disorders show opposing effects, with the former usually exhibiting an attenuated response and the latter having a more negative MMN. **Chapter 1** employs a well-studied paradigm, the auditory roving oddball to study the function of P50 and MMN

responses relative to levels of state and trait anxiety in individuals free from mental health diagnoses. This study aims to assess the effects of subclinical levels of anxiety, which are known risk factors to schizophrenia and influence symptom expression, on neurophysiological biomarkers that associate with functional impairments in sensory inhibition and salience.

The hollow mask experiment (**Chapter 2**) entails the presentation of concave faces that falsely appear as convex. This illusion originates from the prior expectation of human faces being convex, and it is driven by top-down signals that override the bottom-up stimulus characteristics (Gregory, 1997; Papathomas & Bono, 2004). Thus, there is a mismatch of the concave face percept and the stored memory representation for faces being convex, and this phenomenon could be explained under the predictive coding account (Adams et al., 2013; Friston, 2005; Keane et al., 2013). The hollow mask experiment is an important tool in the distinction of top-down versus bottom-up processing in psychiatry, as the illusory experience is more prevalent in individuals without any mental health diagnoses, whilst schizophrenia patients are less susceptible to experiencing the illusion (Schneider et al., 2002). This has led to the discovery that veridical perception of the concave faces in schizophrenia patients is accompanied by alterations in late perceptual electrophysiological signals and by impaired top-down network connectivity (Dima et al., 2010, 2011). Notably, increased veridical perception of the concave faces is associated with positive psychotic symptoms in individuals with schizophrenia (Keane et al., 2013), while it is considered a state-dependent effect (Adams et al., 2013; Schneider et al., 2002). Furthermore, similar effects as in schizophrenia are also observed in youth at psychosis high-risk (Gupta et al., 2016) and in anxiety patients (Passie et al., 2013). Alterations in top-down connectivity and simultaneous strengthening of the bottom-up signals could be relevant to the

dysregulation of the salience network leading up to increased salience processing of stimulus-driven characteristics. This could also point to a difficulty of schizophrenia patients' brains to use previous experiences to model expectations about the world surrounding them (Adams et al., 2013). The second experimental chapter investigates the assumption that ERPs during the hollow mask illusion will be affected by different levels of neuroticism, state and trait anxiety in healthy participants, based on the evidence that risk factors can impact brain function in similar ways as in schizophrenia. Similar to **Chapter 1**, EEG is employed to study late perceptual ERPs that index memory processes, but this time in the visual modality. These ERPs have already been proposed as endophenotypes, together with the P50 and MMN ERPs, of impaired deviance detection in schizophrenia (Turetsky et al., 2007). Exploring the influence of these psychometric measures on experiments known to have behavioural and biological effects on schizophrenia can help with the discovery of new biomarkers that can improve the identification of vulnerable individuals.

EOS is an extremely rare disorder. Neuroimaging research in EOS patients (with an onset < 18 years of age) is scarce and study samples are often small. This renders issues with low statistical power. One way to overcome this caveat lies in utilising a meta-analysis approach. Therefore, **Chapter 3** unifies structural and functional neuroimaging studies in patients with EOS in the context of coordinate-based meta-analysis. This method allows to locate clusters with convergent morphometric and functional brain changes. The functional meta-analysis looks for aberrant function separately in cognition and in working memory, which is the most studied executive function in EOS. For those brain clusters with convergent abnormalities, their functional associations and co-activations are meta-analytically assessed through a database of neuroimaging studies.

The final two chapters (**Chapter 4** and **Chapter 5**) explore the cross-sectional and longitudinal changes in working memory function in developing adolescents with EOS. The same two samples of EOS and TD adolescents were scanned twice with fMRI in the same scanner and using the same n-back paradigm, which is extensively used to elicit working memory function. The baseline study, found that the adolescents with EOS had hypoactivation in the left dorsolateral prefrontal cortex (DLPFC) and frontal operculum, and in the anterior cingulate (ACC) gyrus (Kyriakopoulos et al., 2012). Furthermore, EOS adolescents had hypoconnectivity of the DLPFC with ACC (Kyriakopoulos et al., 2012), which can suggest an executive-salience network disruption. **Chapter 4** examines the follow-up functional differences in EOS and TD individuals, as they transition into young adulthood, at age 21 years old. Similar to Kyriakopoulos and colleagues (2012), this chapter investigates the cross-sectional changes between groups in brain activation and connectivity with the DLPFC as they perform at the n-back task. **Chapter 5**, the last experimental chapter, explores the longitudinal trajectory of working memory function in these two groups. Brain activity relative to the n-back is assessed between the two time points for each group of developing adolescents, separately, and the trajectory of this change is also being compared. It is also of interest whether baseline clinical symptoms from the first time of scan can predict longitudinal functional changes in the brain of EOS patients.

In the following sections, each experimental chapter is written in a journal article format, with its own abstract, introduction, methods, results, discussion, and references. **Chapter 1** is being prepared for journal submission, **Chapter 2** is published in *Personality Neuroscience* (see [Appendix A](#)), **Chapter 3** is published in *Schizophrenia Bulletin Open* (see [Appendix B](#)), whereas **Chapter 5** is also being prepared to be submitted for publication. Finally, the thesis ends with a general

discussion summarising and integrating the findings in **Chapters 1** through **5**, while considering its strengths and limitations.

References

- Adams, R. A., Stephan, K. E., Brown, H. R., Frith, C. D., & Friston, K. J. (2013). The Computational Anatomy of Psychosis. *Frontiers in Psychiatry*, 4(May), 47. <https://doi.org/10.3389/fpsyt.2013.00047>
- Addington, J., Piskulic, D., Liu, L., Lockwood, J., Cadenhead, K. S., Cannon, T. D., Cornblatt, B. A., McGlashan, T. H., Perkins, D. O., Seidman, L. J., Tsuang, M. T., Walker, E. F., Bearden, C. E., Mathalon, D. H., & Woods, S. W. (2017). Comorbid diagnoses for youth at clinical high risk of psychosis. *Schizophrenia Research*, 190, 90–95. <https://doi.org/10.1016/j.schres.2017.03.043>
- American Psychiatric Association. (2013). *Diagnostic and statistical manual of mental disorders* (5th ed.). Arlington, VA: Author.
- Amminger, G. P., Henry, L. P., Harrigan, S. M., Harris, M. G., Alvarez-Jimenez, M., Herrman, H., Jackson, H. J., & McGorry, P. D. (2011). Outcome in early-onset schizophrenia revisited: Findings from the Early Psychosis Prevention and Intervention Centre long-term follow-up study. *Schizophrenia Research*, 131(1–3), 112–119. <https://doi.org/10.1016/j.schres.2011.06.009>
- Ansari, T. L., & Derakshan, N. (2011). The neural correlates of impaired inhibitory control in anxiety. *Neuropsychologia*, 49(5), 1146–1153. <https://doi.org/10.1016/j.neuropsychologia.2011.01.019>
- Berggren, N., Blonievsky, T., & Derakshan, N. (2015). Enhanced visual detection in trait anxiety. *Emotion*, 15(4), 477–483. <https://doi.org/10.1037/a0039449>
- Birnbaum, R., & Weinberger, D. R. (2017). Genetic insights into the neurodevelopmental origins of schizophrenia. *Nature Reviews Neuroscience*, 18(12), 727–740. <https://doi.org/10.1038/nrn.2017.125>
- Bishop, S., Duncan, J., Brett, M., & Lawrence, A. D. (2004). Prefrontal cortical function and anxiety: Controlling attention to threat-related stimuli. *Nature Neuroscience*, 7(2), 184–188. <https://doi.org/10.1038/nn1173>
- Bora, E. (2015). Neurodevelopmental origin of cognitive impairment in schizophrenia. *Psychological Medicine*, 45(1), 1–9. <https://doi.org/10.1017/S0033291714001263>
- Braga, R. J., Reynolds, G. P., & Siris, S. G. (2013). Anxiety comorbidity in schizophrenia. *Psychiatry Research*, 210(1), 1–7. <https://doi.org/10.1016/j.psychres.2013.07.030>
- Braunstein-Bercovitz, H. (2000). Is the attentional dysfunction in schizotypy related to anxiety? *Schizophrenia Research*, 46(2–3), 255–267. [https://doi.org/10.1016/S0920-9964\(00\)00021-9](https://doi.org/10.1016/S0920-9964(00)00021-9)
- Cannon, M., Jones, P., Huttunen, M. O., Tanskanen, A., Huttunen, T., Rabe-Hesketh, S., & Murray, R. M. (1999). School performance in Finnish children and later development of schizophrenia: A population-based longitudinal study. *Archives of General Psychiatry*, 56(5), 457–463.

<https://doi.org/10.1001/archpsyc.56.5.457>

- Caspi, A., Houts, R. M., Belsky, D. W., Goldman-Mellor, S. J., Harrington, H., Israel, S., Meier, M. H., Ramrakha, S., Shalev, I., Poulton, R., & Moffitt, T. E. (2014). The p Factor: One General Psychopathology Factor in the Structure of Psychiatric Disorders? *Clinical Psychological Science*, 2(2), 119–137. <https://doi.org/10.1177/2167702613497473>
- Catts, V. S., Fung, S. J., Long, L. E., Joshi, D., Vercammen, A., Allen, K. M., Fillman, S. G., Rothmond, D. A., Sinclair, D., Tiwari, Y., Tsai, S. Y., Weickert, T. W., & Weickert, C. S. (2013). Rethinking schizophrenia in the context of normal neurodevelopment. *Frontiers in Cellular Neuroscience*, 7(MAY), 1–27. <https://doi.org/10.3389/fncel.2013.00060>
- Cowles, M., & Hogg, L. (2019). An Experimental Investigation into the Effect of State-Anxiety on State-Paranoia in People Experiencing Psychosis. *Behavioural and Cognitive Psychotherapy*, 47(1), 52–66. <https://doi.org/10.1017/S1352465818000401>
- Dhinakaran, J., De Vos, M., Thorne, J. D., & Kranczioch, C. (2014). Neuroticism focuses attention: Evidence from SSVEPs. *Experimental Brain Research*, 232(6), 1895–1903. <https://doi.org/10.1007/s00221-014-3881-5>
- Dima, D., Dietrich, D. E., Dillo, W., & Emrich, H. M. (2010). Impaired top-down processes in schizophrenia: A DCM study of ERPs. *NeuroImage*, 52(3), 824–832. <https://doi.org/10.1016/j.neuroimage.2009.12.086>
- Dima, D., Dillo, W., Bonnemann, C., Emrich, H. M., & Dietrich, D. E. (2011). Reduced P300 and P600 amplitude in the hollow-mask illusion in patients with schizophrenia. *Psychiatry Research - Neuroimaging*, 191(2), 145–151. <https://doi.org/10.1016/j.psychresns.2010.09.015>
- Dima, D., Frangou, S., Burge, L., Braeutigam, S., & James, A. C. (2012). Abnormal intrinsic and extrinsic connectivity within the magnetic mismatch negativity brain network in schizophrenia: A preliminary study. *Schizophrenia Research*, 135, 23–27. <https://doi.org/10.1016/j.schres.2011.12.024>
- Dima, D., Friston, K. J., Stephan, K. E., & Frangou, S. (2015). Neuroticism and conscientiousness respectively constrain and facilitate short-term plasticity within the working memory neural network. *Human Brain Mapping*, 36(10), 4158–4163. <https://doi.org/10.1002/hbm.22906>
- Eysenck, M. W., Derakshan, N., Santos, R., & Calvo, M. G. (2007). Anxiety and cognitive performance: Attentional control theory. *Emotion*, 7(2), 336–353. <https://doi.org/10.1037/1528-3542.7.2.336>
- Fatemi, S. H., & Folsom, T. D. (2009). The neurodevelopmental hypothesis of Schizophrenia, revisited. *Schizophrenia Bulletin*, 35(3), 528–548. <https://doi.org/10.1093/schbul/sbn187>
- Feinstein, J. S., Stein, M. B., & Paulus, M. P. (2006). Anterior insula reactivity during certain decisions is associated with neuroticism. *Social Cognitive and Affective Neuroscience*, 1(2), 136–142. <https://doi.org/10.1093/scan/nsl016>

- Friston, K. (2005). A theory of cortical responses. *Philosophical Transactions of the Royal Society B: Biological Sciences*, 360(1456), 815–836. <https://doi.org/10.1098/rstb.2005.1622>
- Friston, K., Brown, H. R., Siemerkus, J., & Stephan, K. E. (2016). The dysconnection hypothesis (2016). *Schizophrenia Research*, 176(2–3), 83–94. <https://doi.org/10.1016/j.schres.2016.07.014>
- Fucci, E., Abdoun, O., & Lutz, A. (2019). Auditory perceptual learning is not affected by anticipatory anxiety in the healthy population except for highly anxious individuals: EEG evidence. *Clinical Neurophysiology*, 130(7), 1135–1143. <https://doi.org/10.1016/j.clinph.2019.04.010>
- Fusar-Poli, P., Nelson, B., Valmaggia, L., Yung, A. R., & McGuire, P. K. (2014). Comorbid Depressive and Anxiety Disorders in 509 Individuals With an At-Risk Mental State: Impact on Psychopathology and Transition to Psychosis. *Schizophrenia Bulletin*, 40(1), 120–131. <https://doi.org/10.1093/schbul/sbs136>
- Gochman, P., Miller, R., & Rapoport, J. L. (2011). Childhood-onset schizophrenia: The challenge of diagnosis. *Current Psychiatry Reports*, 13(5), 321–322. <https://doi.org/10.1007/s11920-011-0212-4>
- Gregory, R. L. (1997). Knowledge in perception and illusion. *Philosophical Transactions of the Royal Society of London. Series B, Biological Sciences*, 352(1358), 1121–1127. <https://doi.org/10.1098/rstb.1997.0095>
- Guillem, F., Pampoulova, T., Stip, E., Lalonde, P., & Todorov, C. (2005). The relationships between symptom dimensions and dysphoria in schizophrenia. *Schizophrenia Research*, 75(1), 83–96. <https://doi.org/10.1016/j.schres.2004.06.018>
- Gupta, T., Silverstein, S. M., Bernard, J. A., Keane, B. P., Papatomas, T. V., Pelletier-Baldelli, A., Dean, D. J., Newberry, R. E., Ristanovic, I., & Mittal, V. A. (2016). Disruptions in neural connectivity associated with reduced susceptibility to a depth inversion illusion in youth at ultra high risk for psychosis. *NeuroImage: Clinical*, 12, 681–690. <https://doi.org/10.1016/j.nicl.2016.09.022>
- Hartley, S., Barrowclough, C., & Haddock, G. (2013). Anxiety and depression in psychosis: A systematic review of associations with positive psychotic symptoms. In *Acta Psychiatrica Scandinavica* (Vol. 128, Issue 5, pp. 327–346). <https://doi.org/10.1111/acps.12080>
- Heinz, A., & Schlagenhauf, F. (2010). Dopaminergic dysfunction in schizophrenia: Salience attribution revisited. *Schizophrenia Bulletin*, 36(3), 472–485. <https://doi.org/10.1093/schbul/sbq031>
- Huang, Y. X., Bai, L., Ai, H., Li, W., Yu, C., Liu, J., & Luo, Y. J. (2009). Influence of trait-anxiety on inhibition function: Evidence from ERPs study. *Neuroscience Letters*, 456(1), 1–5. <https://doi.org/10.1016/j.neulet.2009.03.072>
- Huppert, J. D., & Smith, T. E. (2005). Anxiety and schizophrenia: The interaction of subtypes of anxiety and psychotic symptoms. *CNS Spectrums*, 10(9), 721–731. <https://doi.org/10.1017/S1092852900019714>
- Insel, T. R. (2010). Rethinking schizophrenia. *Nature*, 468(7321), 187–193.

<https://doi.org/10.1038/nature09552>

- Jacobson, S., Kelleher, I., Harley, M., Murtagh, A., Clarke, M., Blanchard, M., Connolly, C., O'Hanlon, E., Garavan, H., & Cannon, M. (2010). Structural and functional brain correlates of subclinical psychotic symptoms in 11-13 year old schoolchildren. *NeuroImage*, *49*(2), 1875–1885. <https://doi.org/10.1016/j.neuroimage.2009.09.015>
- Jansen, B. H., Hu, L., & Boutros, N. N. (2010). Auditory evoked potential variability in healthy and schizophrenia subjects. *Clinical Neurophysiology*, *121*(8), 1233–1239. <https://doi.org/10.1016/j.clinph.2010.03.006>
- Jeronimus, B. F., Kotov, R., Riese, H., & Ormel, J. (2016). Neuroticism's prospective association with mental disorders halves after adjustment for baseline symptoms and psychiatric history, but the adjusted association hardly decays with time: A meta-analysis on 59 longitudinal/prospective studies with 443 313 pa. *Psychological Medicine*, *46*(14), 2883–2906. <https://doi.org/10.1017/S0033291716001653>
- Jones, H. J., Stergiakouli, E., Tansey, K. E., Hubbard, L., Heron, J., Cannon, M., Holmans, P., Lewis, G., Linden, D. E. J., Jones, P. B., Smith, G. D., O'Donovan, M. C., Owen, M. J., Walters, J. T., & Zammit, S. (2016). Phenotypic manifestation of genetic risk for schizophrenia during adolescence in the general population. *JAMA Psychiatry*, *73*(3), 221–228. <https://doi.org/10.1001/jamapsychiatry.2015.3058>
- Jones, P., Rodgers, B., Murray, R., & Marmot, M. (1994). Child developmental risk factors for adult schizophrenia in the British 1946 birth cohort. *The Lancet*, *344*(8934), 1398–1402. [https://doi.org/10.1016/S0140-6736\(94\)90569-X](https://doi.org/10.1016/S0140-6736(94)90569-X)
- Keane, B. P., Silverstein, S. M., Wang, Y., & Papatomas, T. V. (2013). Reduced depth inversion illusions in schizophrenia are state-specific and occur for multiple object types and viewing conditions. *Journal of Abnormal Psychology*, *122*(2), 506–512. <https://doi.org/10.1037/a0032110>
- Kyriakopoulos, M., Dima, D., Roiser, J. P., Corrigall, R., Barker, G. J., & Frangou, S. (2012). Abnormal Functional Activation and Connectivity in the Working Memory Network in Early-Onset Schizophrenia. *Journal of the American Academy of Child & Adolescent Psychiatry*, *51*(9), 911–920.e2. <https://doi.org/10.1016/j.jaac.2012.06.020>
- Lee, J., & Park, S. (2006). The role of stimulus salience in CPT-AX performance of schizophrenia patients. *Schizophrenia Research*, *81*(2–3), 191–197. <https://doi.org/10.1016/j.schres.2005.08.015>
- Luck, S. J., & Gold, J. M. (2008). The Construct of Attention in Schizophrenia. *Biological Psychiatry*, *64*(1), 34–39. <https://doi.org/10.1016/j.biopsych.2008.02.014>
- Massullo, C., Carbone, G. A., Farina, B., Panno, A., Capriotti, C., Giacchini, M., Machado, S., Budde, H., Murillo-Rodríguez, E., & Imperatori, C. (2020). Dysregulated brain salience within a triple network model in high trait anxiety individuals: A pilot EEG functional connectivity study. *International Journal of Psychophysiology*, *157*(June), 61–69. <https://doi.org/10.1016/j.ijpsycho.2020.09.002>

- Mazzoni, P., Kimhy, D., Khan, S., Posner, K., Maayan, L., Eilenberg, M., Messinger, J., Kestenbaum, C., & Corcoran, C. (2009). Childhood onset diagnoses in a case series of teens at clinical high risk for psychosis. *Journal of Child and Adolescent Psychopharmacology*, *19*(6), 771–776.
<https://doi.org/10.1089/cap.2008.0105>
- McAusland, L., Buchy, L., Cadenhead, K. S., Cannon, T. D., Cornblatt, B. A., Heinssen, R., McGlashan, T. H., Perkins, D. O., Seidman, L. J., Tsuang, M. T., Walker, E. F., Woods, S. W., Bearden, C. E., Mathalon, D. H., & Addington, J. (2017). Anxiety in youth at clinical high risk for psychosis. *Early Intervention in Psychiatry*, *11*(6), 480–487. <https://doi.org/10.1111/eip.12274>
- McCrae, R., & Costa, P. (1992). An introduction to the five-factor model and its applications. *Journal of Personality*, *60*, 175–215. <https://doi.org/10.1111/j.1467-6494.1992.tb00970.x>
- Menon, V. (2011). Large-scale brain networks and psychopathology: A unifying triple network model. In *Trends in Cognitive Sciences* (Vol. 15, Issue 10, pp. 483–506). Elsevier Ltd.
<https://doi.org/10.1016/j.tics.2011.08.003>
- Modi, S., Kumar, M., Nara, S., Kumar, P., & Khushu, S. (2018). Trait anxiety and neural efficiency of abstract reasoning: An fMRI investigation. *Journal of Biosciences*, *43*(5), 877–886.
<https://doi.org/10.1007/s12038-018-9800-3>
- Muller, J. E., Koen, L., Seedat, S., Emsley, R. A., & Stein, D. J. (2004). Anxiety disorders and schizophrenia. *Current Psychiatry Reports*, *6*(4), 255–261. <https://doi.org/10.1007/s11920-004-0074-0>
- Nagel, M., Jansen, P. R., Stringer, S., Watanabe, K., De Leeuw, C. A., Bryois, J., Savage, J. E., Hammerschlag, A. R., Skene, N. G., Muñoz-Manchado, A. B., Agee, M., Alipanahi, B., Auton, A., Bell, R. K., Bryc, K., Elson, S. L., Fontanillas, P., Furlotte, N. A., Hinds, D. A., ... Posthuma, D. (2018). Meta-analysis of genome-wide association studies for neuroticism in 449,484 individuals identifies novel genetic loci and pathways. *Nature Genetics*, *50*(7), 920–927.
<https://doi.org/10.1038/s41588-018-0151-7>
- Ohi, K., Shimada, T., Nitta, Y., Kihara, H., Okubo, H., Uehara, T., & Kawasaki, Y. (2016). The Five-Factor Model personality traits in schizophrenia: A meta-analysis. *Psychiatry Research*, *240*, 34–41. <https://doi.org/10.1016/j.psychres.2016.04.004>
- Pallanti, S., Cantisani, A., & Grassi, G. (2013). Anxiety as a core aspect of schizophrenia. *Current Psychiatry Reports*, *15*(5), 1–5. <https://doi.org/10.1007/s11920-013-0354-7>
- Papathomas, T. V., & Bono, L. M. (2004). Experiments with a hollow mask and a reverspective: Top-down influences in the inversion effect for 3-D stimuli. *Perception*, *33*, 1129–1138.
<https://doi.org/10.1068/p5086>
- Park, S., & Gooding, D. C. (2014). Working memory impairment as an endophenotypic marker of a schizophrenia diathesis. *Schizophrenia Research: Cognition*, *1*(3), 127–136.
<https://doi.org/10.1016/j.scog.2014.09.005>

- Passie, T., Schneider, U., Borsutzky, M., Breyer, R., Emrich, H. M., Bandelow, B., & Schmid-Ott, G. (2013). Impaired perceptual processing and conceptual cognition in patients with anxiety disorders: A pilot study with the binocular depth inversion paradigm. *Psychology, Health & Medicine, 18*(3), 363–374. <https://doi.org/10.1080/13548506.2012.722649>
- Rapoport, J. L., Addington, A. M., Frangou, S., & Psych, M. R. C. (2005). The neurodevelopmental model of schizophrenia: update 2005. *Molecular Psychiatry, 10*(5), 434–449. <https://doi.org/10.1038/sj.mp.4001642>
- Rapoport, J. L., Giedd, J. N., & Gogtay, N. (2012). Neurodevelopmental model of schizophrenia: update 2012. *Molecular Psychiatry, 17*(12), 1228–1238. <https://doi.org/10.1038/mp.2012.23>
- Rapoport, J. L., & Gogtay, N. (2011). Childhood onset schizophrenia: Support for a progressive neurodevelopmental disorder. *International Journal of Developmental Neuroscience, 29*(3), 251–258. <https://doi.org/10.1016/j.ijdevneu.2010.10.003>
- Reichenberg, A., Caspi, A., Harrington, H., Houts, R., Keefe, R. S. E., Murray, R. M., Poulton, R., & Moffitt, T. E. (2010). Static and dynamic cognitive deficits in childhood preceding adult schizophrenia: A 30-year study. *American Journal of Psychiatry, 167*(2), 160–169. <https://doi.org/10.1176/appi.ajp.2009.09040574>
- Schneider, U., Borsutzky, M., Seifert, J., Leweke, F. M., Huber, T. J., Rollnik, J. D., & Emrich, H. M. (2002). Reduced binocular depth inversion in schizophrenic patients. *Schizophrenia Research, 53*(1–2), 101–108. [https://doi.org/10.1016/S0920-9964\(00\)00172-9](https://doi.org/10.1016/S0920-9964(00)00172-9)
- Smith, D. J., Escott-Price, V., Davies, G., Bailey, M. E. S., Colodro-Conde, L., Ward, J., Vedernikov, A., Marioni, R., Cullen, B., Lyall, D., Hagenaars, S. P., Liewald, D. C. M., Luciano, M., Gale, C. R., Ritchie, S. J., Hayward, C., Nicholl, B., Bulik-Sullivan, B., Adams, M., ... O'Donovan, M. C. (2016). Genome-wide analysis of over 106 000 individuals identifies 9 neuroticism-associated loci. *Molecular Psychiatry, 21*(6), 749–757. <https://doi.org/10.1038/mp.2016.49>
- Sporn, A. L., Greenstein, D. K., Gogtay, N., Jeffries, N. O., Lenane, M., Gochman, P., Clasen, L. S., Blumenthal, J., Giedd, J. N., & Rapoport, J. L. (2003). Progressive brain volume loss during adolescence in childhood-onset schizophrenia. *American Journal of Psychiatry, 160*(12), 2181–2189. <https://doi.org/10.1176/appi.ajp.160.12.2181>
- Stowkowy, J., & Addington, J. (2013). Predictors of a clinical high risk status among individuals with a family history of psychosis. *Schizophrenia Research, 147*(2–3), 281–286. <https://doi.org/10.1016/j.schres.2013.03.030>
- Sugranyes, G., Serna, E., Ilzarbe, D., Pariente, J. C., Borrás, R., Romero, S., Rosa, M., Baeza, I., Moreno, M. D., Bernardo, M., Vieta, E., & Castro-Fornieles, J. (2020). Brain structural trajectories in youth at familial risk for schizophrenia or bipolar disorder according to development of psychosis spectrum symptoms. *Journal of Child Psychology and Psychiatry*. <https://doi.org/10.1111/jcpp.13321>

- Supekar, K., Cai, W., Krishnadas, R., Palaniyappan, L., & Menon, V. (2019). Dysregulated Brain Dynamics in a Triple-Network Saliency Model of Schizophrenia and Its Relation to Psychosis. *Biological Psychiatry*, 85(1), 60–69. <https://doi.org/10.1016/j.biopsych.2018.07.020>
- Temmingh, H., & Stein, D. J. (2015). Anxiety in Patients with Schizophrenia: Epidemiology and Management. *CNS Drugs*, 29(10), 819–832. <https://doi.org/10.1007/s40263-015-0282-7>
- Turetsky, B. I., Calkins, M. E., Light, G. A., Olincy, A., Radant, A. D., & Swerdlow, N. R. (2007). Neurophysiological endophenotypes of schizophrenia: The viability of selected candidate measures. *Schizophrenia Bulletin*, 33(1), 69–94. <https://doi.org/10.1093/schbul/sbl060>
- Van Os, J., & Jones, P. B. (2001). Neuroticism as a risk factor for schizophrenia. *Psychological Medicine*, 31(6), 1129–1134. <https://doi.org/10.1017/S0033291701004044>
- Walsh, T., McClellan, J. M., McCarthy, S. E., Addington, A. M., Pierce, S. B., Cooper, G. M., Nord, A. S., Kusenda, M., Malhotra, D., Bhandari, A., Stray, S. M., Rippey, C. F., Roccanova, P., Makarov, V., Lakshmi, B., Findling, R. L., Sikich, L., Stromberg, T., Merriman, B., ... Sebat, J. (2008). Rare structural variants disrupt multiple genes in neurodevelopmental pathways in schizophrenia. *Science*, 320(5875), 539–543. <https://doi.org/10.1126/science.1155174>
- Wang, J., Miyazato, H., Hokama, H., Hiramatsu, K. I., & Kondo, T. (2004). Correlation between P50 suppression and psychometric schizotypy among non-clinical Japanese subjects. *International Journal of Psychophysiology*, 52(2), 147–157. <https://doi.org/10.1016/j.ijpsycho.2003.06.001>
- Zanelli, J., Mollon, J., Sandin, S., Morgan, C., Dazzan, P., Pilecka, I., Marques, T. R., David, A. S., Morgan, K., Fearon, P., Doody, G. A., Jones, P. B., Murray, R. M., & Reichenberg, A. (2019). Cognitive change in schizophrenia and other psychoses in the decade following the first episode. *American Journal of Psychiatry*, 176(10), 811–819. <https://doi.org/10.1176/appi.ajp.2019.18091088>

Chapter 1: Dissociating trait and state anxiety effects on mismatch negativity and sensory gating event-related potentials

Abstract: We investigated whether individual differences in self-reported anxiety, associate with mismatch negativity (MMN) – a neural response to change detection – and the earlier P50 component – a neural index of information filtering. The state-trait anxiety inventory questionnaire was used to assess the effects of anxiety on MMN amplitude and P50 ratio, by using EEG during the auditory roving oddball paradigm in healthy participants (N = 34). Trait anxiety exhibited a negative effect on the MMN amplitude at Fz electrode site ($F_{(1,31)} = 13.038$, $p = 0.001$, $\eta_p^2 = 0.296$) while state anxiety positively affected P50 ratio ($F_{(1,30)} = 13.117$, $p = 0.001$, $\eta_p^2 = 0.304$) at Cz electrode. This study provides evidence that (1) high trait-anxious participants demonstrate hypervigilant change detection to deviant tones that appear more salient and (2) increasing state anxiety associates with failure to filter out irrelevant stimuli.

1. Introduction

Mismatch negativity (MMN) is an event-related potential (ERP) that is generated by the presentation of an unusual (deviant) stimulus preceded by a series of regular (standard) ones. It occurs at approximately 200ms post-stimulus, with frontocentral topography on the midline of the scalp (Garrido, Kilner, Stephan, et al., 2009). In this paper we are utilising a special version of the oddball, the roving paradigm, in which the physical properties of the auditory stimuli are unimportant in the MMN response, as the deviants and standards have identical characteristics and stimulus frequency (Garrido et al., 2008; Haenschel et al., 2005). In the auditory modality, the MMN wave is said to reflect a pre-attentive mechanism of sensory memory trace formation (Näätänen et al., 2011). It is generated as a result of the brain's failure to predict the auditory input, based on its mismatch with the encoded memory trace (Näätänen et al., 2011). For over 25 years research on the MNN has focused on schizophrenia after it was shown that schizophrenic patients exhibit attenuated MMN amplitude compared to controls (Salisbury et al., 2002; Shelley et al., 1991), as well as ultra-high risk and first-episode patients (Nagai et al., 2013) and adolescents with early-onset psychosis (Rydkjær et al., 2017). In contrast, larger MMN responses have been found as a function of trait (Chen et al., 2017; Fucci et al., 2019), state (Schirmer & Escoffier, 2010) or anticipatory anxiety (Cornwell et al., 2007) or in individuals with anxiety disorders, such as PTSD (Bangel et al., 2017; Ge et al., 2011; Morgan & Grillon, 1999) and panic disorder (Y. Chang et al., 2015).

P50, an earlier ERP, is relevant to sensory gating processes. Sensory gating is a pre-attentive process that occurs as early as 50ms post-stimulus presentation and enables the brain to filter out redundant sensory information, such as repetitive auditory

stimuli. It can be tested with the presentation of identical tones as in the case of the paired click (Light et al., 2010) or the roving oddball paradigm, utilized in this study (Boutros et al., 1995; Haenschel et al., 2005). The brain response usually exhibits a strong potential to the first new tone (S1) at approximately 50ms, whereas the P50 amplitude is inhibited in subsequent repetition of the same tone (S2), acting as a protective mechanism against sensory flooding of higher association areas (Boutros et al., 1995). Individuals with schizophrenia exhibit impairments in P50 suppression that can either be expressed as failure to gate in or gate out the auditory stimuli, by exhibiting smaller S1 amplitudes (Hazlett et al., 2015; B. H. Jansen et al., 2010) or larger S2 (J.-C. Shan et al., 2010), respectively; specifically S2 amplitude-driven differences in P50 ratio, indicates an impairment driven by lack of inhibition to the repeating stimulus (W. P. Chang et al., 2011). P50 suppression abnormalities similar to those of schizophrenic patients are found in individuals with anxiety disorders such as panic disorder (Cheng et al., 2019; Ghisolfi et al., 2006), PTSD (Ghisolfi et al., 2004; Holstein et al., 2010; Neylan et al., 1999) and obsessive-compulsive disorder (Nakazawa et al., 2009). Additionally, P50 sensory gating is reduced in non-clinical populations under stressful or fearful conditions (Ermutlu et al., 2005; Kurayama et al., 2012), as well as a function of psychometric schizotypy (Wang et al., 2004). Interestingly, P50 suppression deficits in infants predicted parent-reported difficulties in attention, anxiety and externalizing symptoms at the age of 40-months old (Hutchison et al., 2017).

Trait anxiety is considered a stable personality characteristic, whereas state anxiety is more of a transitory response to a situation (Meijer, 2001). It has been argued that trait anxiety influences state anxiety levels, and state anxiety negatively associates with cognitive performance (Meijer, 2001). Under a neuroimaging perspective, state

and trait anxiety share commonalities and differences. Here we are interested about the effect of state and trait anxiety measures on change detection and sensory gating when performing the roving oddball during EEG under emotionally neutral conditions. In particular, we investigated whether individual differences in self-reported anxiety, using the state-trait anxiety inventory (STAI) questionnaire, associate with the MMN – a response to change detection – and the earlier P50 component – an index of information filtering – in a sample of healthy participants. Based on previous research in clinical and healthy populations, we expected to find associations of MMN and P50 suppression with either one measure of anxiety, while controlling for the other.

2. Methods

2.1. Participants and self-report measures

Data were collected from thirty-four healthy participants from 18 to 59 years of age ($M = 32.59$, $SD = 12.54$), of which sixteen were female and eighteen were male. Exclusion criteria consisted of: (1) lifetime history of mental disorder or substance use disorder, (2) reported head injury or medical disorder and (3) intake of prescribed psychiatric medication. Participants provided written informed consent prior to their inclusion in the study and the study was approved by the Psychology Department Ethics Committee of City, University of London (PSYETH (S_L) 16_17 06).

Self-reported measures of anxiety were collected using the STAI (Spielberger et al., 1983) questionnaire ([Table 1.1](#)). The State-Trait Anxiety Inventory (STAI) is a 40-item self-report devised by Spielberger et al. (1983). It is used to measure state and trait measures of anxiety in patients and in a healthy population, which result from its two forms, Y-1 and Y-2 respectively, each consisting of 20 items. The STAI has been previously shown to be a reliable psychometric scale with Cronbach's alpha > 0.7 (Marteau & Bekker, 1992; Vitasari, Wahab, Herawan, Othman, & Sinnadurai, 2011). Responses for each item have a four-point scale: "not at all", "somewhat", "moderately so" and "very much so". The STAI was administered by a trained psychologist prior the roving oddball paradigm and EEG recording.

2.2. Stimuli and design

We recorded EEG activity during the same auditory roving oddball paradigm used in previous studies (Dima et al., 2012; Garrido et al., 2008). This paradigm consists of stimulus trains of changing (roving) sinusoidal tones that range in frequency from 500Hz to 800Hz in random steps with integer multiples of 50Hz. Within each stimulus

train, all tones were of one frequency and were followed by a train of a different frequency. The first tone of a train was a deviant, which eventually became a standard after few repetitions. This means that deviants and standards have the same physical properties, differing only in the number of times they have been presented. The number of times a tone of the same frequency was presented varied pseudo-randomly between one and eleven. The probability that the same tone was presented once or twice was 2.5%; for three and four times the probability was 3.75% and for five to eleven times it was 12.5%. Each tone was presented through a speaker positioned on the left-hand side next to the computer monitor for 70ms, with 5ms rise and fall times and an interstimulus interval (ISI) of 500ms. Repeated tones of a specific frequency are included within each stimulus train and are followed by a sequence of tones with different frequency. The first tone in a stimulus train is considered the *deviant* (about 250 trials) and *standard* after six or more repetitions (approximately 200 trials). Each subject adjusted the loudness of the tones to a comfortable level, which was maintained throughout the experiment. Figure 1.1 offers a schematic representation of the roving oddball stimuli.

Concurrently with the oddball paradigm, participants performed a distracting visual task, a fixation cross changed colour from black to grey and vice versa. The instruction given to participants was to allocate their attention to the colour-changing cross presented in the middle of the screen and respond to it by pressing the ‘space’ button of the keyboard standing in front of them with their right index finger. The use of the visual task was to keep participants active during EEG recording and eliminate alpha waves as much as possible. We were interested to examine MMN and P50 suppression at the absence of active attentional allocation to the auditory roving oddball paradigm as per the literature (Fucci et al., 2019; Hsieh et al., 2019). Colour change

occurred in a pseudo-random ISI of 2 to 5s and did not overlap with the tone frequency changes. The duration of the entire paradigm was 15 minutes.

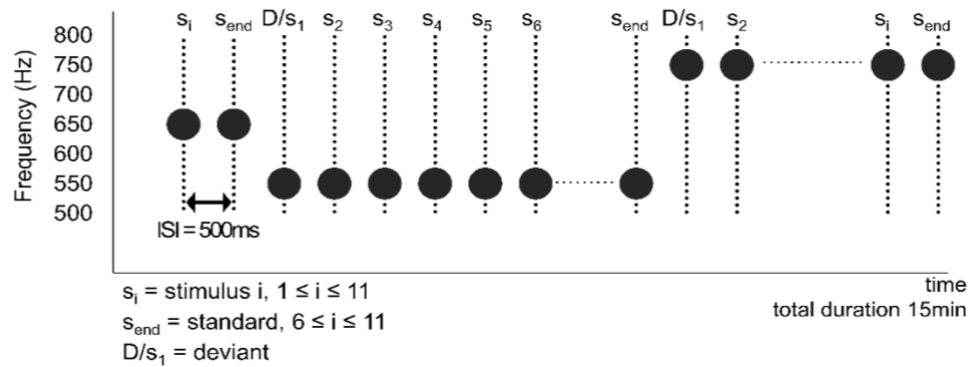


Figure 1.1. Schematic representation of the auditory roving oddball paradigm reproduced from Garrido et al. (2009)

2.3. EEG acquisition and pre-processing

EEG was recorded with a 64-channel BrainVision BrainAmp series amplifier (Brain Products, Herrsching, Germany; 63 active electrodes in a ActiCAP 64Ch EEG cap) with a 1000 Hz sampling rate. Data were recorded with reference to FC_z electrode and the ground electrode at AF_z. Electrooculography (EOG) signal was recorded with an electrode placed below the left eye. All pre-processing steps were carried through in BrainVision Analyzer (Brain Products, Herrsching, Germany) and during pre-processing EEG data were down sampled to 250Hz. We corrected for ocular movements with an automated independent component analysis procedure using the mean sloped algorithm Gratton et al. (1983), then re-referenced to TP₉ and TP₁₀ mastoid electrodes. Similar to Hsieh et al. (2019), and as suggested by Light et al. (2010), we applied different filter settings and artifact rejection to the stimuli providing the MMN (deviant and standard segments) and P50 suppression (S1-S2 segments).

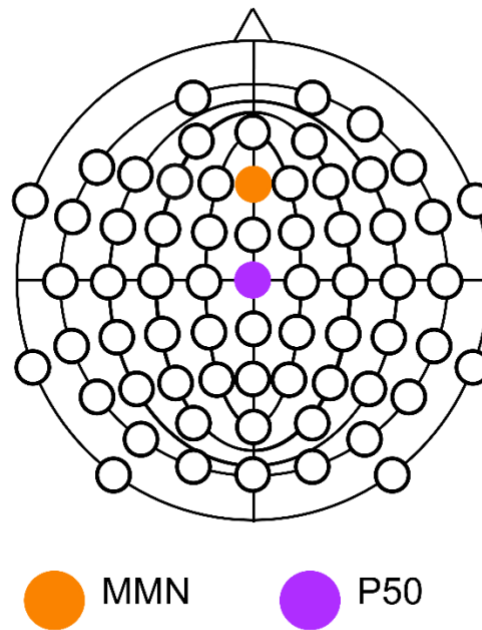


Figure 1.2. 64-channel ActiCAP and electrodes of interest for the MMN and P50 ERPs

For the MMN, data were segmented for (1) the first new tone in a stimulus train (deviant) that followed a stimulus train with six or more repetitions of the previous tone and (2) for the sixth repetition (standard) in a prestimulus window of 500ms spanning from -100ms pre- to 400ms. Deviant and standard segments were band-pass filtered (with infinite impulse response filters; IIR) at 0.5 - 30Hz, with a 12 dB/oct slope. Using automatic artifact rejection, we excluded segments with a slope of $50\mu\text{V}/\text{ms}$, min-max difference of $200\mu\text{V}$ in a 200ms interval and low activity of $0.5\mu\text{V}$ in a 100ms interval. Before averaging data were baseline corrected at the 100ms interval preceding the stimulus. The MMN is considered the difference wave of the standard stimulus from the deviant one and was selected at Fz electrode in the time window from 110 – 220ms (Figure 1.2), to be in line with research using the same roving oddball paradigm (Garrido et al., 2008). There were approximately 190 standard and 190 deviant segments per participant after averaging.

For the P50 suppression, to mimic the paired-click paradigm (Light et al., 2010), following the re-referencing step mentioned above, we segmented the EEG data into a peristimulus window of 1050ms, from -100ms to 950ms post stimulus, containing the first (S1) and second (S2) tones of same frequency in a new stimulus train. Segments containing artifacts of $-50\mu\text{V}$ to $50\mu\text{V}$ were automatically detected and rejected before being baseline corrected and averaged. An average of 200 artifact-free segments (min-max range = 110-240) containing S1 and S2 were used for averaging, per participant. Finally, averaged segments were band-pass filtered from 10Hz to 50Hz (IIR) (12 dB/oct slope), to prevent aliasing (Hsieh et al., 2019; Light et al., 2010). The P50 peak was detected at the C_z electrode (Figure 1.2), according to the protocol of Light and colleagues (2010). Hence, it was defined as the most positive deflection occurring between 40 – 80ms and 540 – 580ms for S1 and S2, respectively. P50 amplitude was calculated by subtracting the highest preceding negativity between 30 – 60ms and 530 – 560ms from the P50 peak at S1 and S2, respectively. The parameters for P50 suppression were the S1 and S2 amplitude, P50 difference (S1-S2) and P50 ratio (S2/S1). To exclude outliers, we used a maximum ratio of 2 (Hsieh et al. 2019). We calculated the square root for the amplitudes of S1 and S2 and the P50 ratio to achieve a normal distribution in these variables for our analysis (Wang et al., 2004), but not for the P50 difference since it was already normally distributed and it contained negative values. There was one subject in our sample without a positive S1 amplitude (no preceding negativity at 30 – 60ms), which was excluded from the analysis. Participants without an obvious S2 P50 peak were assigned the value of $0.01\mu\text{V}$ (Light et al., 2010).

2.4. Statistical analysis

Statistical analysis of the mean amplitudes of the MMN and the P50 were conducted in SPSS (SPSS 25, Armonk, NY: IBM Corp). For the MMN, we first performed a paired-

sample t-test for stimulus type (deviant/standard) to evaluate whether the roving oddball paradigm was successful in eliciting change detection in our experimental setup. We then performed partial correlations between state and trait anxiety with MMN, standard, and deviant stimulus amplitudes at the Fz electrode site, while controlling for trait and state anxiety, respectively. We further performed ANCOVA for the MMN amplitude at Fz with group (high-trait/low-trait anxiety OR high-state/low-state anxiety) as a fixed factor, while controlling for the other anxiety subtype (state anxiety OR trait anxiety as a covariate, respectively). The high and low state/ trait anxiety groups were created by median split of state ($mdn = 32.5$) and trait ($mdn = 41$) scores. As is shown in [Table 1.1](#), subjects with scores above the median were included in the ‘high-’ group and those with scores below the median were in the ‘low-’ group, similar to previous studies (e.g., Bishop, Jenkins, & Lawrence, 2007).

For P50 suppression, we performed partial correlations between state/trait anxiety measures and S1 and S2 amplitude, P50 difference and P50 ratio, controlling for trait/state anxiety measures respectively. For variables showing significant correlations, group level differences were assessed with ANCOVA, again while covarying for the other anxiety subtype.

3. Results

3.1. Questionnaire data

A total of thirty-four subjects were recruited and completed the STAI questionnaire and EEG during the oddball paradigm. Mean scores on the STAI measures, as well as demographics, are reported in [Table 1.1](#). State and trait anxiety were positively correlated with each other ($r = .537, p < .001$). Age and sex did not associate significantly with either of the STAI measures ($p > .243$).

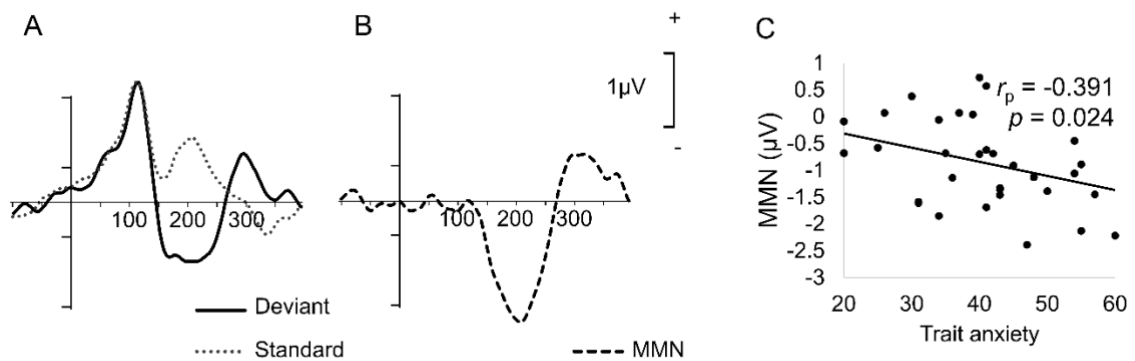


Figure 1.3. A) Deviant (continuous black line) and standard (dotted grey line) stimuli ERP waveforms in the entire sample ($N = 34$). B) MMN waveform (deviant minus standard) at Fz electrode site for all participants (dashed line) C) Scatterplot showing the negative relationship of MMN amplitude at Fz with the trait anxiety measure. Partial correlation coefficient and associated p-value show the strength of the correlation and the probability this is being observed due to chance. Abbreviations: μV : microvolt; MMN: mismatch negativity; p : p-value; r_p : partial correlation coefficient

3.2. MMN

A paired-sample t-test indicated a strong effect of stimulus ($t_{(33)} = -6.945, p = 6.160 \times 10^{-8}$; *Cohen's d* = -1.191), indicating change detection in our experimental setup. Figure 1.3A shows the waveforms for deviant and standard stimuli and Figure 1.3B shows the MMN waveforms in the entire sample.

Partial correlations for state anxiety while controlling for trait were not significant for neither standard ($p = 0.345$), deviant ($p = 0.639$) or MMN ($p = 0.466$) amplitudes.

Trait anxiety did not correlate with standard ($p = 0.359$) or deviant ($p = 0.593$) amplitudes, covarying for state anxiety. MMN amplitude was negatively correlated with trait anxiety, when controlling for state anxiety at the Fz site ($r_p = -0.391$, $p = 0.024$), demonstrating that higher trait anxiety levels associate with more negative MMN amplitude (Figure 1.3C).

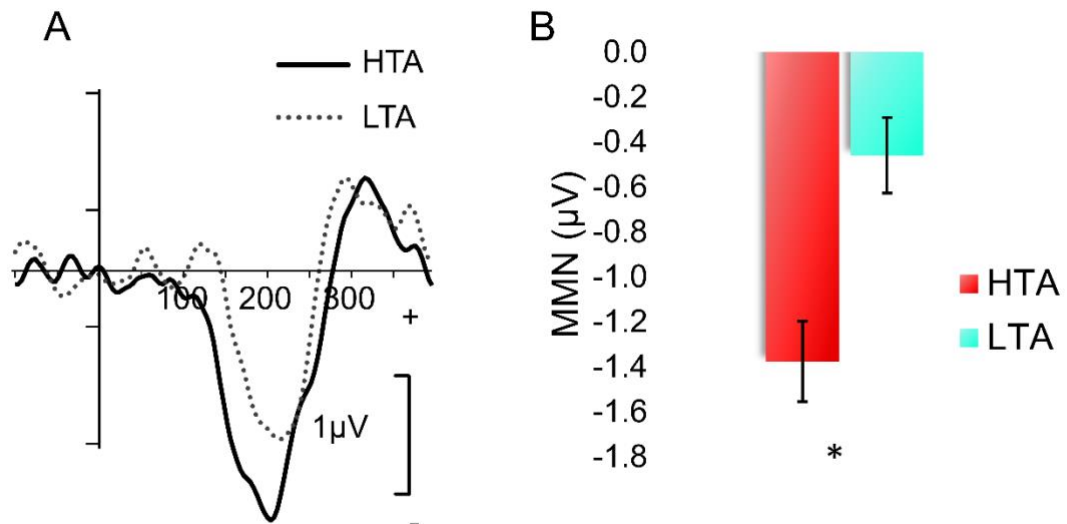


Figure 1.4. A) MMN waveform (deviant minus standard) at Fz electrode site for HTA (continuous line) versus LTA (dotted line) groups. B) Bar graphs showing the MMN amplitude at Fz between HTA and LTA subjects following median split; * indicates significant differences; error bars represent standard error of the mean. Abbreviations: HTA: high-trait anxiety LTA: low-trait anxiety; μV : microvolt; MMN: mismatch negativity

We followed up the significant partial correlations of MMN with trait anxiety using ANCOVA, with trait anxiety as group factor and state anxiety as a covariate. This revealed a significant main effect of the median-split trait anxiety group factor in the MMN at Fz ($F_{(1,31)} = 13.038$, $p = 0.001$, $\eta_p^2 = 0.296$) (Figure 1.4). Thus, as is shown in [Table 1.2](#), high trait-anxious individuals had significantly enhanced (negative) MMN amplitudes.

To find out if the MMN difference in high- vs low-trait anxiety was driven by either the standard or deviant tones we followed up with a post-hoc 2×2 ANCOVA for stimulus \times group. This analysis revealed a significant stimulus \times trait-anxiety group

interaction ($F_{(2,62)} = 12.801, p = 0.001, \eta_p^2 = 0.292$). MMN differences between high- and low-trait anxiety groups were driven by increased amplitudes for standard and reduced amplitudes for deviant tones in high-trait anxiety, however they were not significantly different to those of low-trait anxious individuals ($p > 0.204$) (Table 1.2).

3.3. P50 suppression

P50 sensory gating was analysed at the Cz electrode. The identical repeated stimulus (S2) was successfully gated in our sample as a whole, as revealed by paired-sample t-test that showed a significant reduction in P50 S2 amplitude compared to S1 ($t_{(32)} = 2.520, p = 0.017, \text{Cohen's } d = 0.439$) in the entire sample, suggesting successful sensory gating in our experimental setup (Figure 1.5A).

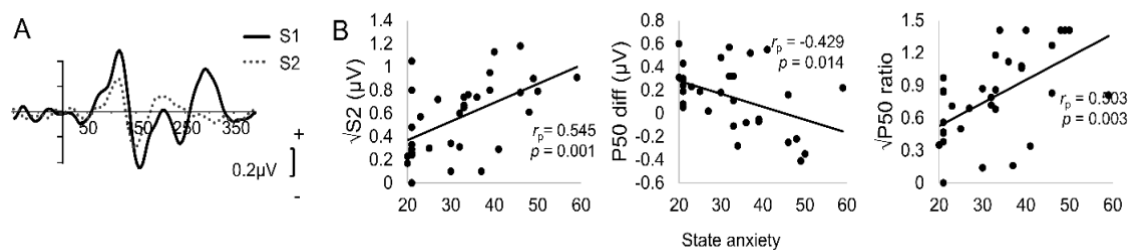


Figure 1.5. A) Grand average waveforms for the S1 (black continuous line) and S2 (grey dotted line) stimuli at Cz superimposed onto each other for the entire sample. B) Scatterplots displaying the linear associations of the S2 amplitude, P50 difference, and P50 ratio with state anxiety on the left-hand side. Partial correlation coefficients and associated p-values show the strength of these correlations and the probability these were observed due to chance. Abbreviations: μV : microvolt; p: p-value; r_p : partial correlation coefficient; S1: stimulus S1; S2: stimulus S2

Significant partial correlations were detected with state anxiety and S2 amplitude ($r_p = 0.545, p = 0.001$), P50 difference ($r_p = -0.429, p = 0.014$) and P50 ratio ($r_p = 0.503, p = 0.003$), controlling for trait anxiety (Figure 1.5B). None of the P50 suppression parameters correlated significantly with trait anxiety ($p > 0.060$), while controlling for state anxiety.

Following up the significant correlations of the P50 parameters with state anxiety we median-split participants into groups of high- and low-state anxiety and

explored the groups' differences using ANCOVA while controlling for trait anxiety. Sub-average ERP waveforms for S1 and S2 are shown in Figure 1.6A for high-state anxious participants and in Figure 1.6B for low-state anxious individuals. Low-state anxious participants had significantly lower S2 amplitude ($F_{(1,30)} = 9.102, p = 0.005, \eta_p^2 = 0.233$) compared to high-state anxious participants (Figure 1.6C). Additionally, P50 suppression was significantly different between the groups in both P50 difference ($F_{(1,30)} = 10.642, p = 0.003, \eta_p^2 = 0.262$) and P50 ratio ($F_{(1,30)} = 13.117, p = 0.001, \eta_p^2 = 0.304$) indicating inefficient suppression of the second stimulus at the Cz electrode in the high-state anxiety group (Table 1.3; Figure 1.6C). Accordingly, early auditory response to the S2 stimulus was not filtered in the high-state anxious individuals in our sample, whereas low-state anxious participants successfully gated the repeated S2 tone.

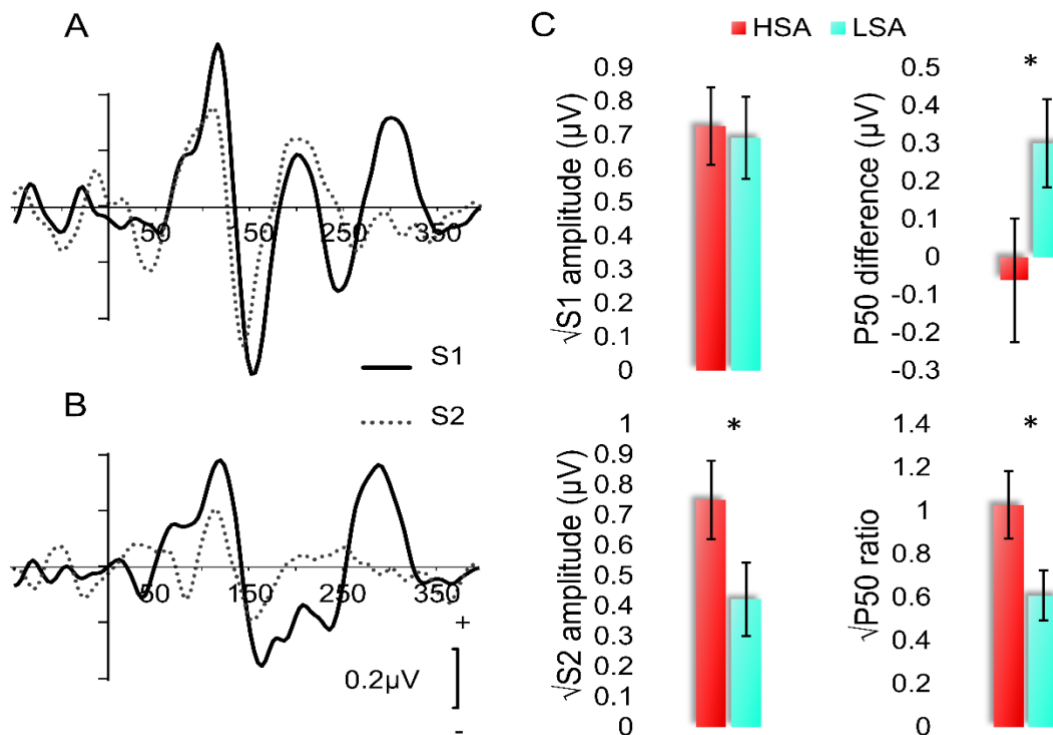


Figure 1.6. Grand average waveforms for the S1 (black continuous line) and S2 (grey dotted line) stimuli at Cz superimposed onto each other A) for the subaverage of the high-state anxious, and B) low-state anxious participants. C) Bar plots for the four P50 suppression parameters (S1 and S2 amplitude, P50 difference and ratio) comparing the differences between HSA and LSA groups following median split; * indicates significant differences; error bars represent standard error of the mean. Abbreviations: HSA: high-state anxiety; LSA: low-state anxiety; μV: microvolt; S1: stimulus S1; S2: stimulus S2

4. Discussion

We found that high-trait anxious participants had significantly increased MMN waves. High-trait anxious participants showed more negative responses to deviant tones compared to low-trait anxious participants. Under the predictive coding hypothesis, the failure of top-down connections to suppress prediction error causes strengthening of the bottom-up ones, resulting in strong error detection and MMN (Garrido et al., 2008). Hence, MMN is mediated by a complex interplay of top-down and bottom-up connection dynamics (Garrido et al., 2008), with frontal feedback signals mediating attentional reorienting and temporal feedforward connections regulating sensory memory encoding (Baldeweg et al., 2004; Garrido, Kilner, Kiebel, et al., 2009). This bidirectional modulation is affected in high-trait anxiety resulting in a hypervigilant response against the oddball stimulus.

Diminished top-down modulation and bottom-up connectivity enhancement in anxiety (Cornwell et al., 2017), together with impaired prefrontal activity in high-trait anxious individuals (Bishop, 2009), potentially drive increased sensitivity and hyperarousal to deviant stimuli that are perceived as more salient. These mechanisms could then compromise attentional capture that affect attentional shifting and control, as bottom-up processes are prioritized over top-down ones to drive attention to the deviant stimulus (Eysenck et al., 2007); in our experiment, such impairment could be expressed as a heightened pre-attentive MMN response, as is also evidenced by clinical anxiety disorders (Y. Chang et al., 2015; Morgan & Grillon, 1999) and in pre-clinical anxiety states (Fucci et al., 2019; Schirmer & Escoffier, 2010).

P50 suppression (sensory gating) has been shown to correlate with attentional control (Wan et al., 2008) manifested as increasing S1 and decreasing S2 amplitudes

when healthy participants are asked to allocate their attention to the stimuli (Dalecki et al., 2016). In addition, inhibitory processes govern the suppression of the repeated stimulus (Dalecki et al., 2015). Indeed, supporting evidence reveals associations of sensory gating and goal-directed attention, as P50 suppression correlates significantly with latent inhibition and sustained attention (Jones et al., 2016). Early sensory gating could reflect a combination of top-down and bottom-up processes allowing to identify stimulus irrelevance and orient selective attention towards the relevant ones (Jones et al., 2016). Such P50 inhibition was argued to be related with cognitive mechanisms (rather than sensory / motor ones) as its neural substrates are located in forebrain regions, (i.e., prefrontal, cingulate and parietal areas), revealed by electrophysiological recordings in epileptic patients (Boutros et al., 2013). Therefore, diminished P50 suppression can be a cause of sensory overload due to insufficient filtering of irrelevant stimuli, as it increases attention to distraction (Yadon et al., 2009). Furthermore, by demonstrating an effect of state anxiety on sensory gating, we extend previous studies reporting that state anxiety only affected bottom-up attention processes (Pacheco-Unguetti et al., 2010), since P50 gating is a process involving an interplay of top-down and bottom-up dynamics (Golubic et al., 2019).

State anxiety is regarded as a transient state influenced by trait anxiety and environmental effects on mood (Bishop, 2009). Our results point out that individual differences in state anxiety are marked by increases in S2 amplitudes (similar to clinical populations such as in Ghisolfi et al., 2004; Holstein et al., 2010; J. C. Shan et al., 2013) and sensory gating failure is indexed by both measures of P50 ratio and P50 difference. S2 amplitude-driven sensory gating differences support the notion that the P50 suppression impairment explains deficits in information filtering rather than registration. This effect has been shown to anti-correlate with benzodiazepine use in

panic disorder (Ghisolfi et al., 2006). Accordingly, anxiety-related sensory gating impairment could potentially be reversed with administration of anxiolytic drugs, supporting the idea that gating deficits could be generated by states of mental distress.

Similar to our results, sensory gating reduction has been observed under physical stress-inducing conditions, an effect driven by enhanced S2 amplitude (Ermutlu et al., 2005). However, our study provides evidence that impaired inhibitory control, can arise under neutral conditions and without explicitly inducing stressful conditions. Thus, we showed that inhibitory processes of attentional control can be compromised under acute worrying states (heightened state anxiety) and we expand current knowledge regarding the same effects under threatening conditions (Roxburgh et al., 2019) or in relation to increased trait anxiety (Osinsky et al., 2012) only.

Limitations on the comparability of the P50 suppression results across the literature are posed by the relative heterogeneity in preprocessing pipelines with regards to offline filter specifications and the detection of the P50 peak. Band-pass filter ranges can vary; from 10-45Hz (Dalecki et al., 2015), to 10-50Hz (Cadenhead et al., 2005; Hsieh et al., 2019; Light et al., 2010), or 10-75Hz (Yadon et al., 2009). Moreover, there is relative variability in the P50 peak detection strategies. There are papers that assess the P50 peak as the highest positive deflection in a preselected time-window either relative (1) to the baseline (Dalecki et al., 2015, 2016), (2) to its preceding negativity (Cadenhead et al., 2005; Ghisolfi et al., 2006; Hsieh et al., 2019; Jones et al., 2016; Light et al., 2010; Nagamoto et al., 1989; Olincy et al., 2010; J. C. Shan et al., 2013), or (3) the averaged amplitude over the selected time-window (Ermutlu et al., 2005). Despite the absence of absolute homogeneity in the methods sections of individual studies, the effect of P50 suppression has been repeatedly demonstrated, indicating that early sensory gating filters out redundant auditory stimuli. Such is the case in our study,

in which we additionally show that P50 suppression is reduced in high-state anxious participants under stressor-free conditions.

We used an auditory roving oddball paradigm in healthy participants to explore change detection and sensory gating processes in relation to psychometric measures of anxiety. The former was assessed with the MMN response and the latter was determined by P50 suppression. There are two main findings in this study. First, the MMN response was enhanced (more negative) in high-trait anxious versus low-trait anxious participants at the Fz electrode site. Second, P50 suppression is compromised in high-state anxious participants which is shown by significant differences in both the P50 difference and ratio between high- and low-state anxiety groups at the Cz electrode site. The P50 suppression deficit in high-state anxious participants is driven by the S2 amplitude (gating out) that is significantly increased in this group. Trait anxiety relates to hypervigilant attention shifting to deviant stimuli (MMN) as they become more salient, whereas state anxiety is responsible for diminished inhibitory control (P50) failing to suppress irrelevant information. We have also showed that heightened levels of state and trait anxiety in healthy individuals bear similarities with anxiety disorders at the level of MMN and sensory gating ERP measures. Both state and trait anxiety tap into attentional processing, however the former has an effect on inhibiting or gating redundant information, which could be a more transient effect, and the latter associates with hypervigilant detection of salient features, a change of potentially more stable nature. Hence, our study provides evidence of a dissociation between the two anxiety subtypes, whilst showing that both interfere with cognitive mechanisms involved in the same paradigm.

References

- Baldeweg, T., Klugman, A., Gruzelier, J., & Hirsch, S. R. (2004). Mismatch negativity potentials and cognitive impairment in schizophrenia. *Schizophrenia Research*, *69*(2–3), 203–217.
<https://doi.org/10.1016/j.schres.2003.09.009>
- Bangel, K. A., Van Buschbach, S., Smit, D. J. A., Mazaheri, A., & Olf, M. (2017). Aberrant brain response after auditory deviance in PTSD compared to trauma controls: An EEG study. *Scientific Reports*, *7*(1), 1–9. <https://doi.org/10.1038/s41598-017-16669-8>
- Bishop, S. J. (2009). Trait anxiety and impoverished prefrontal control of attention. *Nature Neuroscience*, *12*(1), 92–98. <https://doi.org/10.1038/nn.2242>
- Bishop, S. J., Jenkins, R., & Lawrence, A. D. (2007). Neural processing of fearful faces: Effects of anxiety are gated by perceptual capacity limitations. *Cerebral Cortex*, *17*(7), 1595–1603.
<https://doi.org/10.1093/cercor/bhl070>
- Boutros, N. N., Gjini, K., Eickhoff, S. B., Urbach, H., & Pflieger, M. E. (2013). Mapping repetition suppression of the P50 evoked response to the human cerebral cortex. *Clinical Neurophysiology*, *124*(4), 675–685. <https://doi.org/10.1016/j.clinph.2012.10.007>
- Boutros, N. N., Torello, M. W., Barker, B. A., Tueting, P. A., Wu, S.-C., & Nasrallah, H. A. (1995). The P50 evoked potential component and mismatch detection in normal volunteers: implications for the study of sensory gating. *Psychiatry Research*, *57*(1), 83–88. [https://doi.org/10.1016/0165-1781\(95\)02637-C](https://doi.org/10.1016/0165-1781(95)02637-C)
- Cadenhead, K. S., Light, G. A., Shafer, K. M., & Braff, D. L. (2005). P50 suppression in individuals at risk for schizophrenia: The convergence of clinical, familial, and vulnerability marker risk assessment. *Biological Psychiatry*, *57*(12), 1504–1509.
<https://doi.org/10.1016/j.biopsych.2005.03.003>
- Chang, W. P., Arfken, C. L., Sangal, M. P., & Boutros, N. N. (2011). Probing the relative contribution of the first and second responses to sensory gating indices: A meta-analysis. *Psychophysiology*, *48*(7), 980–992. <https://doi.org/10.1111/j.1469-8986.2010.01168.x>
- Chang, Y., Xu, J., Pang, X., Sun, Y., Zheng, Y., & Liu, Y. (2015). Mismatch negativity indices of enhanced preattentive automatic processing in panic disorder as measured by a multi-feature paradigm. *Biological Psychology*, *105*, 77–82. <https://doi.org/10.1016/j.biopsycho.2015.01.006>
- Chen, C., Hu, C. H., & Cheng, Y. (2017). Mismatch negativity (MMN) stands at the crossroads between explicit and implicit emotional processing. *Human Brain Mapping*, *38*(1), 140–150.
<https://doi.org/10.1002/hbm.23349>
- Cheng, C. H., Chan, P. Y. S., Hsu, S. C., & Liu, C. Y. (2019). Abnormal frontal generator during auditory

- sensory gating in panic disorder: An MEG study. *Psychiatry Research - Neuroimaging*, 288(5), 60–66. <https://doi.org/10.1016/j.psychresns.2019.04.006>
- Cornwell, B. R., Baas, J. M. P., Johnson, L., Holroyd, T., Carver, F. W., Lissek, S., & Grillon, C. (2007). Neural responses to auditory stimulus deviance under threat of electric shock revealed by spatially-filtered magnetoencephalography. *NeuroImage*, 37(1), 282–289. <https://doi.org/10.1016/j.neuroimage.2007.04.055>
- Cornwell, B. R., Garrido, M. I., Overstreet, C., Pine, D. S., & Grillon, C. (2017). The Unpredictive Brain Under Threat: A Neurocomputational Account of Anxious Hypervigilance. *Biological Psychiatry*, 82(6), 447–454. <https://doi.org/10.1016/j.biopsych.2017.06.031>
- Dalecki, A., Green, A. E., Johnstone, S. J., & Croft, R. J. (2016). The relevance of attention in schizophrenia P50 paired stimulus studies. *Clinical Neurophysiology*, 127(6), 2448–2454. <https://doi.org/10.1016/j.clinph.2016.03.013>
- Dalecki, A., Johnstone, S. J., & Croft, R. J. (2015). Clarifying the functional process represented by P50 suppression. *International Journal of Psychophysiology*, 96(3), 149–154. <https://doi.org/10.1016/j.ijpsycho.2015.04.011>
- Dima, D., Frangou, S., Burge, L., Braeutigam, S., & James, A. C. (2012). Abnormal intrinsic and extrinsic connectivity within the magnetic mismatch negativity brain network in schizophrenia: A preliminary study. *Schizophrenia Research*, 135, 23–27. <https://doi.org/10.1016/j.schres.2011.12.024>
- Ermütlu, M. N., Karamürsel, S., Ugur, E. H., Senturk, L., & Gokhan, N. (2005). Effects of cold stress on early and late stimulus gating. *Psychiatry Research*, 136(2–3), 201–209. <https://doi.org/10.1016/j.psychres.2003.03.002>
- Eysenck, M. W., Derakshan, N., Santos, R., & Calvo, M. G. (2007). Anxiety and cognitive performance: Attentional control theory. *Emotion*, 7(2), 336–353. <https://doi.org/10.1037/1528-3542.7.2.336>
- Fucci, E., Abdoun, O., & Lutz, A. (2019). Auditory perceptual learning is not affected by anticipatory anxiety in the healthy population except for highly anxious individuals: EEG evidence. *Clinical Neurophysiology*, 130(7), 1135–1143. <https://doi.org/10.1016/j.clinph.2019.04.010>
- Garrido, M. I., Friston, K. J., Kiebel, S. J., Stephan, K. E., Baldeweg, T., & Kilner, J. M. (2008). The functional anatomy of the MMN: A DCM study of the roving paradigm. *NeuroImage*, 42(2), 936–944. <https://doi.org/10.1016/j.neuroimage.2008.05.018>
- Garrido, M. I., Kilner, J. M., Kiebel, S. J., Stephan, K. E., Baldeweg, T., & Friston, K. J. (2009). Repetition suppression and plasticity in the human brain. *NeuroImage*, 48, 269–279. <https://doi.org/10.1016/j.neuroimage.2009.06.034>
- Garrido, M. I., Kilner, J. M., Stephan, K. E., & Friston, K. J. (2009). The mismatch negativity: A review of underlying mechanisms. In *Clinical Neurophysiology* (Vol. 120, Issue 3, pp. 453–463).

- International Federation of Clinical Neurophysiology. <https://doi.org/10.1016/j.clinph.2008.11.029>
- Ge, Y., Wu, J., Sun, X., & Zhang, K. (2011). Enhanced mismatch negativity in adolescents with posttraumatic stress disorder (PTSD). *International Journal of Psychophysiology*, *79*(2), 231–235. <https://doi.org/10.1016/j.ijpsycho.2010.10.012>
- Ghisolfi, E. S., Heldt, E., Zanardo, A. P., Strimitzer, I. M., Prokopiuk, A. S., Becker, J., Cordioli, A. V., Manfro, G. G., & Lara, D. R. (2006). P50 sensory gating in panic disorder. *Journal of Psychiatric Research*, *40*(6), 535–540. <https://doi.org/10.1016/j.jpsychires.2006.02.006>
- Ghisolfi, E. S., Margis, R., Becker, J., Zanardo, A. P., Strimitzer, I. M., & Lara, D. R. (2004). Impaired P50 sensory gating in post-traumatic stress disorder secondary to urban violence. *International Journal of Psychophysiology*, *51*(3), 209–214. <https://doi.org/10.1016/j.ijpsycho.2003.09.002>
- Golubic, S. J., Jurasic, M. J., Susac, A., Huonker, R., Gotz, T., & Haueisen, J. (2019). Attention modulates topology and dynamics of auditory sensory gating. *Human Brain Mapping*, *40*(10), 2981–2994. <https://doi.org/10.1002/hbm.24573>
- Haenschel, C., Vernon, D. J., Dwivedi, P., Gruzelier, J. H., & Baldeweg, T. (2005). Event-Related Brain Potential Correlates of Human Auditory Sensory Memory-Trace Formation. *Journal of Neuroscience*, *25*(45), 10494–10501. <https://doi.org/10.1523/JNEUROSCI.1227-05.2005>
- Hazlett, E. A., Rothstein, E. G., Ferreira, R., Silverman, J. M., Siever, L. J., & Olincy, A. (2015). Sensory gating disturbances in the spectrum: Similarities and differences in schizotypal personality disorder and schizophrenia. *Schizophrenia Research*, *161*(2–3), 283–290. <https://doi.org/10.1016/j.schres.2014.11.020>
- Holstein, D. H., Vollenweider, F. X., Jäncke, L., Schopper, C., & Csomor, P. A. (2010). P50 suppression, prepulse inhibition, and startle reactivity in the same patient cohort suffering from posttraumatic stress disorder. *Journal of Affective Disorders*, *126*(1–2), 188–197. <https://doi.org/10.1016/j.jad.2010.02.122>
- Hsieh, M. H., Lin, Y.-T., Chien, Y.-L., Hwang, T.-J., Hwu, H.-G., Liu, C.-M., & Liu, C.-C. (2019). Auditory Event-Related Potentials in Antipsychotic-Free Subjects With Ultra-High-Risk State and First-Episode Psychosis. *Frontiers in Psychiatry*, *10*(April), 1–11. <https://doi.org/10.3389/fpsy.2019.00223>
- Hutchison, A. K., Hunter, S. K., Wagner, B. D., Calvin, E. A., Zerbe, G. O., & Ross, R. G. (2017). Diminished Infant P50 Sensory Gating Predicts Increased 40-Month-Old Attention, Anxiety/Depression, and Externalizing Symptoms. *Journal of Attention Disorders*, *21*(3), 209–218. <https://doi.org/10.1177/1087054713488824>
- Jansen, B. H., Hu, L., & Boutros, N. N. (2010). Auditory evoked potential variability in healthy and schizophrenia subjects. *Clinical Neurophysiology*, *121*(8), 1233–1239. <https://doi.org/10.1016/j.clinph.2010.03.006>

- Jones, L. A., Hills, P. J., Dick, K. M., Jones, S. P., & Bright, P. (2016). Cognitive mechanisms associated with auditory sensory gating. *Brain and Cognition*, *102*, 33–45.
<https://doi.org/10.1016/j.bandc.2015.12.005>
- Kurayama, T., Matsuzawa, D., Komiya, Z., Nakazawa, K., Yoshida, S., & Shimizu, E. (2012). P50 suppression in human discrimination fear conditioning paradigm using danger and safety signals. *International Journal of Psychophysiology*, *84*(1), 26–32.
<https://doi.org/10.1016/j.ijpsycho.2012.01.004>
- Light, G. A., Williams, L. E., Minow, F., Sprock, J., Rissling, A., Sharp, R., Swerdlow, N. R., & Braff, D. L. (2010). Electroencephalography (EEG) and Event-Related Potentials (ERPs) with Human Participants. *Current Protocols in Neuroscience*, *52*(1), 6.25.1-6.25.24.
<https://doi.org/10.1002/0471142301.ns0625s52>
- Meijer, J. (2001). Stress in the Relation between Trait and State Anxiety. *Psychological Reports*, *88*(3_suppl), 947–964. <https://doi.org/10.2466/pr0.2001.88.3c.947>
- Morgan, C. A., & Grillon, C. (1999). Abnormal mismatch negativity in women with sexual assault-related posttraumatic stress disorder. *Biological Psychiatry*, *45*(7), 827–832.
[https://doi.org/10.1016/S0006-3223\(98\)00194-2](https://doi.org/10.1016/S0006-3223(98)00194-2)
- Näätänen, R., Kujala, T., & Winkler, I. (2011). Auditory processing that leads to conscious perception: A unique window to central auditory processing opened by the mismatch negativity and related responses. *Psychophysiology*, *48*(1), 4–22. <https://doi.org/10.1111/j.1469-8986.2010.01114.x>
- Nagai, T., Tada, M., Kirihara, K., Yahata, N., Hashimoto, R., Araki, T., & Kasai, K. (2013). Auditory mismatch negativity and P3a in response to duration and frequency changes in the early stages of psychosis. *Schizophrenia Research*, *150*(2–3), 547–554.
<https://doi.org/10.1016/j.schres.2013.08.005>
- Nagamoto, H. T., Adler, L. E., Waldo, M. C., & Freedman, R. (1989). Sensory gating in schizophrenics and normal controls: Effects of changing stimulation interval. *Biological Psychiatry*, *25*(5), 549–561. [https://doi.org/10.1016/0006-3223\(89\)90215-1](https://doi.org/10.1016/0006-3223(89)90215-1)
- Nakazawa, K., Nanbu, M., Iyo, M., Shimizu, E., Yoshida, S., Kurayama, T., Ogura, H., Hashimoto, T., Matsuzawa, D., Haraguchi, T., & Komiya, Z. (2009). Impaired P50 suppression in fear extinction in obsessive–compulsive disorder. *Progress in Neuro-Psychopharmacology and Biological Psychiatry*, *34*(2), 317–322. <https://doi.org/10.1016/j.pnpbp.2009.12.005>
- Neylan, T. C., Fletcher, D. J., Lenoci, M., McCallin, K., Weiss, D. S., Schoenfeld, F. B., Marmar, C. R., & Fein, G. (1999). Sensory gating in chronic posttraumatic stress disorder: Reduced auditory p50 suppression in combat veterans. *Biological Psychiatry*, *46*(12), 1656–1664.
[https://doi.org/10.1016/S0006-3223\(99\)00047-5](https://doi.org/10.1016/S0006-3223(99)00047-5)
- Olincy, A., Braff, D. L., Adler, L. E., Cadenhead, K. S., Calkins, M. E., Dobie, D. J., Green, M. F., Greenwood, T. A., Gur, R. E., Gur, R. C., Light, G. A., Mintz, J., Nuechterlein, K. H., Radant, A.

- D., Schork, N. J., Seidman, L. J., Siever, L. J., Silverman, J. M., Stone, W. S., ... Freedman, R. (2010). Inhibition of the P50 cerebral evoked response to repeated auditory stimuli: Results from the Consortium on Genetics of Schizophrenia. *Schizophrenia Research*, *119*(1–3), 175–182. <https://doi.org/10.1016/j.schres.2010.03.004>
- Osinsky, R., Gebhardt, H., Alexander, N., & Hennig, J. (2012). Trait anxiety and the dynamics of attentional control. *Biological Psychology*, *89*(1), 252–259. <https://doi.org/10.1016/j.biopsycho.2011.10.016>
- Pacheco-Unguetti, A. P., Acosta, A., Callejas, A., & Lupiáñez, J. (2010). Attention and anxiety: Different attentional functioning under state and trait anxiety. *Psychological Science*, *21*(2), 298–304. <https://doi.org/10.1177/0956797609359624>
- Roxburgh, A. D., Hughes, M. E., & Cornwell, B. R. (2019). Threat-induced anxiety weakens inhibitory control. *Biological Psychology*, *144*(December 2018), 99–102. <https://doi.org/10.1016/j.biopsycho.2019.03.009>
- Rydkjær, J., Møllegaard Jepsen, J. R., Pagsberg, A. K., Fagerlund, B., Glenthøj, B. Y., & Oranje, B. (2017). Mismatch negativity and P3a amplitude in young adolescents with first-episode psychosis: A comparison with ADHD. *Psychological Medicine*, *47*(2), 377–388. <https://doi.org/10.1017/S0033291716002518>
- Salisbury, D. F., Shenton, M. E., Griggs, C. B., Bonner-Jackson, A., & McCarley, R. W. (2002). Mismatch negativity in chronic schizophrenia and first-episode schizophrenia. *Archives of General Psychiatry*, *59*(8), 686–694. <https://doi.org/10.1001/archpsyc.59.8.686>
- Schirmer, A., & Escoffier, N. (2010). Emotional MMN: Anxiety and heart rate correlate with the ERP signature for auditory change detection. *Clinical Neurophysiology*, *121*(1), 53–59. <https://doi.org/10.1016/j.clinph.2009.09.029>
- Shan, J.-C., Hsieh, M. H., Liu, C.-M., Chiu, M.-J., Jaw, F.-S., & Hwu, H.-G. (2010). More evidence to support the role of S2 in P50 studies. *Schizophrenia Research*, *122*(1–3), 270–272. <https://doi.org/10.1016/j.schres.2010.05.026>
- Shan, J. C., Liu, C. M., Chiu, M. J., Liu, C. C., Chien, Y. L., Hwang, T. J., Lin, Y. T., Hsieh, M. H., Jaw, F. S., & Hwu, H. G. (2013). A Diagnostic Model Incorporating P50 Sensory Gating and Neuropsychological Tests for Schizophrenia. *PLoS ONE*, *8*(2), 1–7. <https://doi.org/10.1371/journal.pone.0057197>
- Shelley, A. M., Ward, P. B., Catts, S. V., Michie, P. T., Andrews, S., & McConaghy, N. (1991). Mismatch negativity: An index of a preattentive processing deficit in schizophrenia. *Biological Psychiatry*, *30*(10), 1059–1062. [https://doi.org/10.1016/0006-3223\(91\)90126-7](https://doi.org/10.1016/0006-3223(91)90126-7)
- Spielberger, C. D., Gorsuch, R. L., Lushene, R., Vagg, P. R., Jacobs, G. A. (1983). *Manual for the State-Trait Anxiety Inventory*. Palo Alto, CA: Consulting Psychologists Press

- Vitasari, P., Wahab, M. N. A., Herawan, T., Othman, A., & Sinnadurai, S. K. (2011). Re-test of State Trait Anxiety Inventory (STAI) among Engineering Students in Malaysia: Reliability and Validity tests. *Procedia - Social and Behavioral Sciences*, *15*, 3843–3848.
<https://doi.org/https://doi.org/10.1016/j.sbspro.2011.04.383>
- Wan, L., Friedman, B. H., Boutros, N. N., & Crawford, H. J. (2008). P50 sensory gating and attentional performance. *International Journal of Psychophysiology*, *67*(2), 91–100.
<https://doi.org/10.1016/j.ijpsycho.2007.10.008>
- Wang, J., Miyazato, H., Hokama, H., Hiramatsu, K. I., & Kondo, T. (2004). Correlation between P50 suppression and psychometric schizotypy among non-clinical Japanese subjects. *International Journal of Psychophysiology*, *52*(2), 147–157. <https://doi.org/10.1016/j.ijpsycho.2003.06.001>
- Yadon, C. A., Bugg, J. M., Kisley, M. A., & Davalos, D. B. (2009). P50 sensory gating is related to performance on select tasks of cognitive inhibition. *Cognitive, Affective and Behavioral Neuroscience*, *9*(4), 448–458. <https://doi.org/10.3758/CABN.9.4.448>

Tables

Table 1.1. Demographics and questionnaire characteristics for all participants and anxiety subgroups						
	All participants	High-Trait Anxious	Low-Trait Anxious	High-State Anxious	Low-State Anxious	Statistics
N	34	16	18	17	17	
Age (SD)	32.59 (12.54)	30.19 (11.77)	34.72 (13.14)	34.12 (14.47)	31.06 (10.48)	HTA vs LTA: ns HSA vs LSA: ns
Sex (F:M)	16:18	9:7	11:7	10:7	6:11	HTA vs LTA: ns HSA vs LSA: ns
STAI						
State anxiety	32.62 (10.64)	38.00 (10.55)	27.83 (8.37)	41.29 (7.34)	23.94 (4.44)	
Trait anxiety	41.94 (11.65)	51.56 (7.58)	33.39 (6.95)	47.52 (8.24)	36.35 (12.08)	

Abbreviations: **F**: female; **HSA**: high-State Anxious; **HTA**: high-Trait Anxious; **LSA**: low-State Anxious; **LTA**: low-Trait Anxious; **M**: male; **N**: sample size; **ns**: not significant; **SD**: standard deviation; **STAI**: State-Trait Anxiety Inventory

Table 1.2. Trait anxiety group characteristics for MMN			
	Trait anxiety mean (SD)		Statistics
	High (N = 16)	Low (N = 18)	η_p^2
Age	30.19 (11.77)	34.72 (13.14)	
Sex (F:M)	(9:7)	(11:7)	
Fz (μV)			
MMN	-1.30 (0.58)	-0.52 (0.80)	0.296
Deviant	-0.38 (1.15)	0.04 (1.12)	0.025
Standard	0.96 (0.95)	0.62 (1.23)	0.051

Abbreviations: **F**: female; **Fz**: Fz electrode; **M**: male; **μV** : microvolt; **MMN**: mismatch negativity; **N**: sample size; η_p^2 : partial eta-squared; **SD**: standard deviation

Table 1.3. State anxiety group characteristics for P50 suppression			
	State anxiety mean (SD)		Statistics
	High (N = 16)	Low (N = 17)	η_p^2
Age	34.25 (14.93)	31.06 (10.48)	
Sex (F:M)	9:7	6:11	
P50 (Cz)			
S1 amplitude	0.73 (0.21)	0.69 (0.26)	$7.133 \cdot 10^{-4}$
S2 amplitude	0.75 (0.27)	0.42 (0.25)	0.233
P50 difference	-0.024 (0.31)	0.27 (0.17)	0.262
P50 ratio	1.03 (0.39)	0.61 (0.23)	0.304

Abbreviations: **Cz**: Cz electrode; **F**: female; **M**: male; **μV** : microvolt; **N**: sample size; **η_p^2** : partial eta-squared; **SD**: standard deviation

Chapter 2: State anxiety influences P300 and P600 event-related potentials over parietal regions in the hollow mask illusion experiment*

Abstract: The hollow mask illusion is an optical illusion where a concave face is perceived as convex. It has been demonstrated that individuals with schizophrenia and anxiety are less susceptible to the illusion than controls. Previous research has shown that the P300 and P600 event-related potentials (ERPs) are affected in individuals with schizophrenia. Here, we examined whether individual differences in neuroticism and anxiety scores, traits that have been suggested to be risk factors for schizophrenia and anxiety disorders, affect ERPs of healthy participants while they view concave faces. Our results confirm that the participants were susceptible to the illusion, misperceiving concave faces as convex. We additionally demonstrate significant interactions of the concave condition with state anxiety in central and parietal electrodes for P300 and parietal areas for P600, but not with neuroticism and trait anxiety. The state anxiety interactions were driven by low-state anxiety participants, showing lower amplitudes for concave faces compared to convex. The P300 and P600 amplitudes were smaller when a concave face activated a convex face memory representation, since the stimulus did not match the active representation. The opposite pattern was evident in high-state anxiety participants in regard to state anxiety interaction and the hollow mask illusion, demonstrating larger P300 and P600 amplitudes to concave faces suggesting impaired late information processing in this group. This could be explained by impaired allocation of attentional resources in high state anxiety leading to hyperarousal to concave faces that are unexpected mismatches to standard memory representations, as opposed to expected convex faces.

* Ioakeimidis Vasileios, Khachatoorian Nareg, Haenschel Corinna, Papatomas Thomas, Farkas Attila, Kyriakopoulos Marinos, and Dima Danai. (2020) State anxiety influences P300 and P600 event related potentials over parietal regions in the hollow-mask illusion experiment. *Personality Neuroscience*. 4(e02), 1-10. doi.org/10.1017/pen.2020.16; [See appendix](#)

1. Introduction

Visual illusions are primarily, for research, a great tool to understand human perception (Carbon, 2014) and they occur when the subjective percept does not match the real physical properties of the observed object. This mismatch can be a result of stimulus-driven assumptions made by the visual system and other times they constitute an active recalibration of higher-level cognitive areas (Eagleman, 2001). They can be distinguished in two categories based on the brain networks which contribute to the illusory percept; illusions resulting from bottom-up signals are called physiological or low-level, whereas those occurring from top-down regulatory activity are cognitive illusions (Dima, Dillo, Bonnemann, Emrich, & Dietrich, 2011; King, Hodgekins, Chouinard, Chouinard, & Sperandio, 2017).

An interesting class of cognitive illusions are the binocular depth-inversion illusions that result in objects perceived in reverse depth, with distant points perceived to be closer than near points; thus, concavities are perceived as convexities. The best-known binocular depth-inversion illusion is the hollow mask illusion. One way to experience it is to swap the images of the left and right eyes of a stereoscopic pair; despite the strong stereoscopic cues that signal a concave mask, viewers report perceiving a normal convex face (Farkas et al., 2016; Georgeson, 1979; Van den Eenden & Spekrijse, 1989). A similar experience can be perceived by using a physical hollow mask, prompting a misperception of the concave 3D surface as convex, despite visual depth cues suggesting the opposite (concave when a face is perceived as 3D going inwards and convex when it was going outwards, like a normal face) (Gregory, 1973; H. Hill & Bruce, 1993; Harold Hill & Johnston, 2007; Papathomas & Bono, 2004). Healthy controls from six-month of age (Corrow et al., 2011) throughout adulthood

incorrectly perceive concave faces as convex. Individuals with schizophrenia perceive the illusion to a much lesser degree than controls; instead, they have a veridical perception of the truthful concavity of the mask (Schneider et al., 2002). Schneider et al. (2002) argued that this incongruence is the result of disturbed top-down processes in individuals with schizophrenia, which can be reversed after the course of antipsychotic medication. This discrepancy in schizophrenia has been shown to be due to strengthened bottom-up and weakened top-down processing that allows schizophrenia patients to interpret the sensory cues of a hollow face that deviate from stored knowledge of faces being convex as concave (Danai Dima et al., 2009, 2010, 2011). Apart from schizophrenic patients, individuals with other psychosis-prone states are also less likely to perceive the hollow mask illusion, such as cannabis users (Leweke et al., 2000; Semple et al., 2003), alcohol withdrawal (Schneider et al., 1996), sleep deprivation (Sternemann et al., 1997), youth at ultra-high risk for psychosis (Gupta et al., 2016), and anxiety patients (Passie et al., 2013). Therefore, disposition of veridical perception of concaveness in faces in the psychotic and pro-psychotic states mentioned above, could be of use in research aiming to identify susceptibility to mental illness.

In this study, we explore the electrophysiological signature of perception of the hollow mask illusion. We use the P300 and P600 event-related potentials (ERPs), occurring between 300 to 600 milliseconds and 600 to 800 milliseconds after stimulus onset, respectively, to explore the timeline of the hollow mask illusion. These ERPs have been previously shown to be significantly reduced in amplitude in schizophrenia patients who respond to the hollow mask illusion experiment compared to controls (Dima et al., 2011). The P300 occurrence involves attentional engagement responsible for memory functioning and stimulus evaluation, with familiar stimuli activating context- and familiarity-related temporo-parietal top-down control. The P600 has been

traditionally thought to reflect any linguistic processes, however studies have also implicated it to similar processes as the P300, in that it is triggered when a subject encounters an “improbable” stimulus (Coulson et al., 1998). Since ungrammatical sentences are relatively rare in natural speech, a P600 may not be simply a linguistic response but rather an effect of the subject's "surprise" upon encountering an unexpected stimulus (Coulson et al., 1998). Higher amplitudes in P300 and P600 are believed to be associated with stimulus novelty and significance, which are modulated by late perceptual processes, such as remembering and attention (Stelmack et al., 1993), and lower amplitude in P300 and P600 during perceiving concave faces was assumed to be a result in late perceptual processing dysregulation in patients with schizophrenia (Dima et al., 2011). Electroencephalography (EEG) studies have associated these late positive event-related components with frontal, temporal and parietal scalp distribution (Polich, 2007).

In this study, we investigate the P300 and P600 ERPs during the presentation of hollow mask stimuli in healthy participants in relation to their individual differences in neuroticism and anxiety self-report measures. Neuroticism, from the five-factor model (McCrae & Costa, 1992), is of particular interest in psychiatry, as it reflects dysregulation of the emotional equilibrium, anxiety proneness and susceptibility to stress (Hettema et al., 2006). As such, high scores in neuroticism are also associated with comorbidity of schizophrenia and anxiety disorders (Caspi et al., 2015; Khan et al., 2005). A meta-analysis on the five-factor model has found that higher levels of neuroticism in individuals with schizophrenia come in conjunction with lower levels of extroversion, with large effect sizes, and lower openness, agreeableness and conscientiousness, but with more moderate effect sizes (Ohi et al., 2016). Additionally, there is evidence that schizophrenia appears to be co-occurring along with anxiety

disorders (Muller et al., 2004; Temmingh & Stein, 2015). There is a complex relationship between anxiety and positive symptom expression in psychotic states. Trait and state anxiety (STAI; Spielberger et al., 1983) can be seen as predictors of paranoia in psychosis spectrum disorders (Freeman and Fowler, 2009; Cowles and Hogg 2019), whereas state anxiety mediates intrusive thoughts in hallucinating schizophrenia patients (Bortolon and Raffard, 2015). Previous reports have shown that trait anxiety is significantly associated with positive psychotic symptoms and auditory hallucinations in schizophrenia patients, making it a potential causal factor for the disorder (Guillem et al., 2005). However, when the authors controlled for state anxiety, the correlation with hallucinations became non-significant whilst a significant relationship with bizarre delusions was revealed (Guillem et al., 2005). Hence, state anxiety concealed the delusion-trait anxiety relationship and revealed that delusions mediate the relationship between hallucinations and trait anxiety (Guillem et al., 2005). Accordingly, there is a complex relationship of self-reported neuroticism and anxiety self-reports with psychopathology, and particularly with psychosis which is known to be implicated with abnormal ERPs during the presentation of hollow mask stimuli.

Given the predisposition of elevated neuroticism and anxiety levels with general psychopathology and psychosis, we hypothesised that self-reported neuroticism and anxiety levels will have an effect on the late positive ERPs that reflect high-order cognitive processes and are generated by hollow mask stimuli. Furthermore, based on the presented evidence, it is expected that our sample consisting of healthy participants will be susceptible to the illusion behaviourally and show no difference in P300 and P600 amplitude for the concave and convex face stimuli. However, we expect to find an effect of neuroticism and anxiety scores on the amplitude of the ERPs generated by the concave and convex faces.

2. Methods

2.1. Participants

Neuroticism data using the Neuroticism Extroversion Openness Personality Inventory-Revised (NEO PI-R) (Costa & McCrae, 1992) were collected from ninety-four participants from 18 to 59 years of age ($M = 26.21$, $SD = 11.67$), of which 72 were female and 22 were male ([Table 2.1](#)). Exclusion criteria consisted of: (1) lifetime history of mental disorder or substance use, (2) reported head injury or medical disorder and (3) intake of prescribed psychiatric medication. Participants provided written informed consent prior to their inclusion and the study was approved by the Psychology Department Ethics Committee of City, University of London. Participants were self-referred from study advertisements throughout the university and word-of-mouth recommendation. All participants completed the mini-international neuropsychiatric interview (MINI) (Sheehan et al., 1998).

Upon analysis of the neuroticism trait, 20 out of the 94 subjects were invited to participate in the hollow mask illusion EEG paradigm. The selection was designed to include a normal distribution of neuroticism scores ([Table 2.2](#)). Those who took part in the EEG session first completed the State-Trait Anxiety Inventory (STAI) to assess state and trait measures of anxiety (Spielberger, Gorsuch, Lushene, Vagg, & Jacobs, 1983). Following this, they participated in the hollow mask illusion experiment while their brain activity was being recorded with EEG.

2.2. The NEO PI-R and STAI self-report questionnaires

The NEO PI-R is a 240 item self-report questionnaire, grouped in 5 meta-factors, each having six distinct facets. It is used to measure five broad dimensions of personality traits in adults, namely neuroticism, extroversion, openness, agreeableness and

conscientiousness resulting from the scores of their corresponding facets (McCrae & Costa, 1992). Responses for each item have a five-point scale ranging from strongly disagree to strongly agree. In our analysis, we only focus on neuroticism.

The State-Trait Anxiety Inventory (STAI) is a 40-item self-report questionnaire and was devised by Spielberger et al. (1983). It is used to measure state and trait measures of anxiety, which result from its two forms, Y-1 and Y-2 respectively, each consisting of 20 items. Responses for each item have a four-point scale: “not at all”, “somewhat”, “moderately so” and “very much so”.

2.3. Stimuli and Design

Participants were included in the study only if their vision was normal or corrected to normal, had normal colour vision and had functional stereoscopic vision. Stereoscopic vision was tested using the TNO test, designed by the by the Institute for Perception, Netherlands Organisation for Applied Scientific Research (Lameris Ootech BV, Utrecht, Netherlands; (<http://www.ootech.nl/>)). Furthermore, prior to the hollow mask illusion experiment, participants took a further test to evaluate if they have functional stereopsis. They viewed images of 15 geometric shapes of three possible surface curvatures (concave, convex and flat) and were asked to respond according to their perception. They were included in the study only if they got all 15 correct.

Subsequently, the hollow mask illusion experiment was conducted to test the perception of binocular depth inversion (Dima et al., 2011). During this experiment, participants observed images of upright or upside-down faces (real faces) on a computer monitor with the aid of a Wheatstone mirror stereoscope (Wheatstone, 1838, 1852). They were told that the curvature (depth perception) of the faces will vary and were instructed to press one of three keys according to their perception of the depth of the image: ‘Concave’ when a face was perceived as 3D going inwards to the screen,

‘Convex’ when it was going outwards (like normal faces) and ‘Flat’ when they perceived the face as two-dimensional.

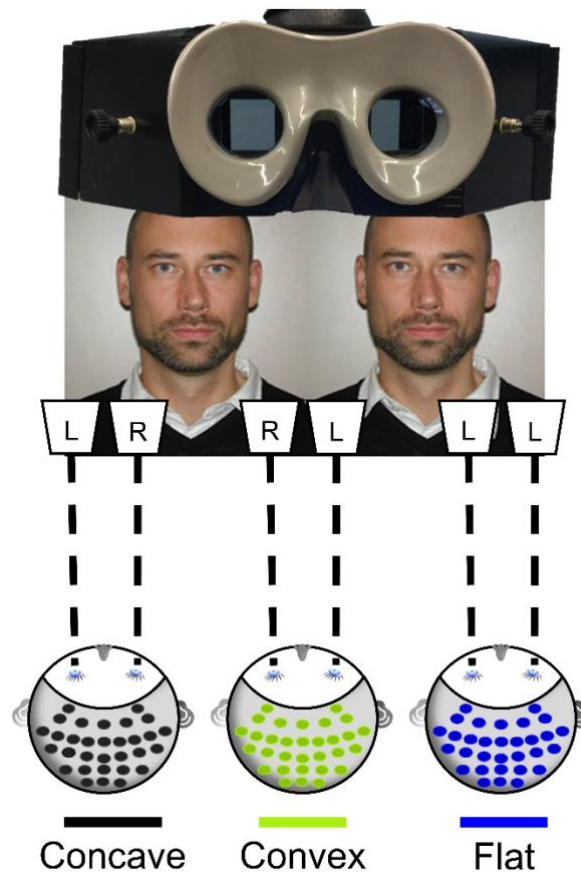


Figure 2.1. Hollow mask stimulus generation. Using the stereoscope and by alternating Left and Right perspective images on the display we constructed concave, convex, and flat face stimuli.

In order to create the impression of three-dimensionality, each eye was presented with a photo of the same face taken from two angles that corresponded to the views of the left and right eyes (Figure 2.1). The participant was able to perceive a 3D face that was fused in the middle of the screen while looking through the stereoscope. The effect of binocular depth inversion was generated by swapping the images for the right and left eyes; this swapping has the effect of creating a stereo pair with opposite binocular disparities to those of the convex face and produce, a concave face. Flat (2D)

faces were produced by presenting images from the same angle (i.e. the same photo) to both eyes, as seen in Figure 2.1.

Participants performed twelve blocks, each containing 24 stimuli (12 upright and 12 upside-down), one third concave, one third convex and the other third flat, presented in a random order. This led to six different conditions (upright convex, upright concave, upright flat; upside-down convex, upside-down concave, upside-down flat), resulting in 288 images per participant during the course of a complete experimental session. Each stimulus was presented until participants responded. A tone was heard 1.2 seconds after stimulus onset that signalled to participants that they were free to make a response according to their depth perception of the stimulus. The inter-stimulus interval, following response, was 0.5 seconds and the whole session lasted for an average of 45 minutes, including breaks. In all subsequent analyses, only upright faces are included.

2.4. EEG acquisition and ERP analysis

The EEG signal was recorded using a 64-channels (Figure 2.2), BrainVision BrainAmp series amplifier (Brain Products, Herrsching, Germany) with a 1000 Hz sampling rate. The data were recorded with respect to FCz electrode reference. Ocular activity was recorded with an electrode placed underneath the left eye. Pre-processing was conducted in BrainVision Analyzer (Brain Products, Herrsching, Germany) and the statistical analysis of the ERP was conducted in the Statistical Package for the Social Sciences software (SPSS 23, Armonk, NY: IBM Corp).

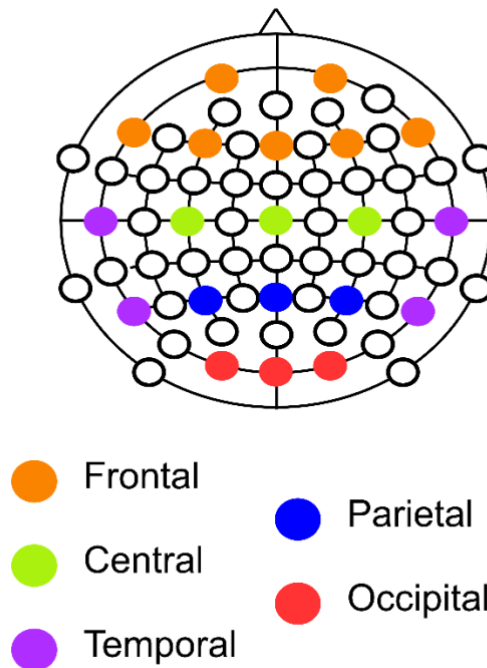


Figure 2.2. 64-electrode ActiCAP layout and electrode regions-of-interest

Pre-processing steps are described in their order of application. First, all EEG channels were individually inspected for high-frequency noise artefacts and slow drift. Those which were noisy throughout the whole EEG session, were topographically interpolated by spherical splines. Subsequently, EEG data were down-sampled to 250 Hz and a high-pass filtered with a cut-off frequency of 0.5 Hz was applied. An automatic ocular correction was performed with the independent component analysis in BrainVision Analyzer. Following re-referencing to TP9 and TP10 electrodes, data were segmented from 200 ms prior to 1000 ms after stimulus presentation for each condition. A low-pass filter of 30 Hz was applied followed by automatic artefact rejection which excluded segments with a slope of $100 \mu\text{V}/\text{ms}$, min-max difference of $200 \mu\text{V}$ in a 200 ms interval and low activity of $0.5 \mu\text{V}$ in a 100 ms interval. Baseline correction was applied using the 200 ms interval preceding the stimulus and averaging was performed across each condition (convex, flat, concave). Averaging included all trials per

condition (≈ 48), as opposed to only focusing on accurate-only responses, since concave faces were almost impossible to identify correctly ([Table 2.2](#)). For illustration purposes, a high cut-off filter of 20 Hz was applied to the grand average ERPs in Figure 2.3 and Figure 2.4.

2.5. Statistical analysis

After pre-processing, the grand average data were extracted from BrainVision Analyzer and were taken into SPSS for statistical analysis. The mean amplitudes of the ERPs were separately analysed for the 300–600 ms (P300) and the 600–800 ms (P600) time windows after stimulus onset. The waveforms of the flat faces were used as a baseline to calculate the difference waves for the concave and convex faces. As discussed by Luck (2014), this process can be used to eliminate identical components between separate conditions and isolate those that differ. Difference waves of ‘concave minus flat’ and ‘convex minus flat’ were used to moderate for face processing-related activity and allow comparison of the different 3D features between depth-inverted and depth non-inverted conditions. This led to the creation of two new variables that were used in the analysis as the ‘condition’ factor with two levels: (1) the mean amplitude of the concave minus the flat (Concave) and (2) the mean amplitude of the convex minus flat (Convex).

Electrodes from five separate regions-of-interest (ROIs) were included in the analyses: frontal (Fp1-Fp2-F7-F8-F3-F4-Fz), central (C3-C4-Cz), temporal (T7-T8-P7-P8), parietal (P3-P4-Pz) and occipital (O1-O2-Oz) (Figure 2.2). The electrode ROIs were chosen to correspond with those used in Dima et al. (2011). Repeated measures analyses of variance (RM ANOVA) with factors electrode ROI \times condition as well as repeated measures analyses of covariance (RM ANCOVA), with a 0.01 alpha-level (α) after Bonferroni correction (0.05/5: for the five electrode ROIs) were run in SPSS to

examine the main effects the condition factor (Concave vs Convex) and its interactions with neuroticism, state and trait anxiety scores as covariates. Additionally, Pearson's correlations were used to test the associations of the anxiety and neuroticism measures.

3. Results

3.1. Personality and anxiety scores

Mean scores of neuroticism, state and trait anxiety and their standard deviations are shown in [Table 2.2](#) for the twenty participants in the EEG session. Neuroticism, state, and trait anxiety scores were distributed normally based on Shapiro-Wilk tests ($p > .05$). Correlation analysis showed that neuroticism had a positive correlation with trait anxiety ($r = 0.673, p = .001$) and state anxiety ($r = 0.480, p = .032$). Also, state and trait anxiety were positively correlated with each other ($r = 0.447, p = .048$). Age or sex had no effect on neuroticism nor on state and trait anxiety ($p \geq .265$).

3.2. Behavioural data

[Table 2.2](#) shows the percentages of correct classification of the stimuli in the three conditions (concave, convex and flat), as well as their corresponding response times (RT). Correct responses for the concave faces, as expected, accounted only for 16% ($SD = \pm 23\%$) of the trials, far below the convex ($M = 87\%; SD = \pm 17\%$) and flat ($M = 66\%; SD = \pm 28\%$) faces. Correct responses for convex faces were significantly higher than for concave faces ($t_{19} = 11.330, p < .001$) but not for flat ones ($t_{19} = 2.390, p = .270$). Whereas correct responses for flat faces were significantly higher than the concave responses ($t_{19} = 9.120, p < .001$). Concave faces were misclassified equally as flat ($M = 47\%, SD = 21\%$) or convex ($M = 39\%, SD = 21\%$), $t_{19} = 1.000, p = .329$. RT for concave faces were significantly longer than convex RT ($t_{19} = 3.094, p = .006$), but not for the flat ones ($t_{19} = 1.939, p = .067$). Also, flat RT was not significantly different from convex RT ($t_{19} = 1.911, p = .071$).

RT and correct responses for the three types of stimuli (concave, convex and flat faces) did not significantly correlate with neuroticism or either measure of anxiety.

3.3. ERP results

3.3.1. Main effects

Figure 2.3 illustrates the grand average ERP waveforms for the concave, convex and flat stimuli trials in all electrode ROIs. The difference waves for the two conditions (concave minus flat; convex minus flat) are illustrated in Figure 2.4.

Repeated measures ANOVA revealed a significant main effect of condition (convex vs concave) in the mean amplitudes of the P300 difference wave in the temporal area ($F_{1,19} = 6.267, p = .022$), that did not survive Bonferroni correction. For the remaining four electrode groups, namely the frontal, central, parietal and occipital no significant main effects were detected in the P300 or P600 time windows ($p > .05$).

3.3.2. Neuroticism

Neuroticism did not interact significantly with condition (concave/convex) in either P300 or P600 time window in any of the five electrode-ROIs that were tested ($p \geq .099$).

3.3.3. State Anxiety

RM ANCOVA for the P300 ERP showed significant interactions for the condition \times covariate in the central ($F_{1,18} = 10.044, p = .005, \eta_p^2 = 0.358$) and parietal ($F_{1,18} = 9.243, p = .007, \eta_p^2 = 0.339$) ROIs. A significant interaction was found in the frontal ROI ($F_{1,18} = 4.820, p = .041, \eta_p^2 = 0.211$) that did not survive multiple correction.

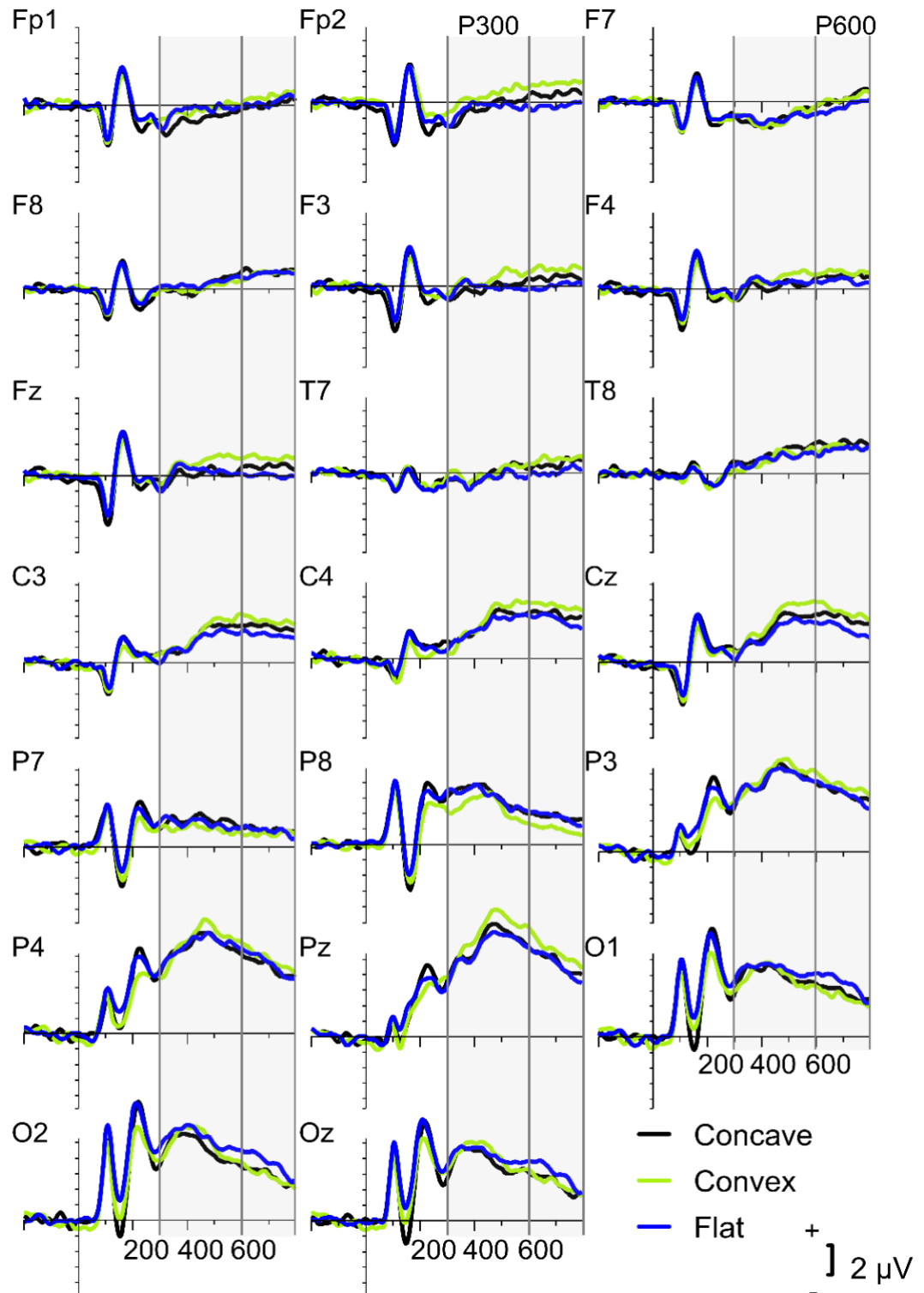


Figure 2.3. Grand average ERP waveforms for 3D normal faces, 3D inverted faces and flat faces in the whole sample ($N=20$) in the twenty ROI electrodes. Y-axis represents the amplitude of the ERP with tick marks every $1\mu\text{V}$ and X-axis represents the time before and after the stimulus presentation with tick marks every 100ms

In the P600, a condition \times state anxiety interaction that was significant for multiple comparisons was observed in the parietal ROI ($F_{1,18} = 13.270$, $p = .002$, $\eta_p^2 = 0.424$). For the temporal ($F_{1,18} = 4.772$, $p = .042$, $\eta_p^2 = 0.210$), central ($F_{1,18} = 4.712$, $p = .044$, $\eta_p^2 = 0.207$) and occipital ($F_{1,18} = 5.023$, $p = .037$, $\eta_p^2 = 0.218$) ROIs, significant interactions were found, however they did not survive Bonferroni correction.

Subsequently, significant interactions of the continuous state anxiety covariate were explored by creating a categorical variable for state anxiety. Participants were separated according to their state anxiety scores by median split ($Mdn = 33$) into two groups of high-state and low-state anxiety (Bishop et al., 2007). Hence, nine participants were included in the high-state anxiety group and eleven in the low-state anxiety group. There was no significant difference for behavioural scores between the two groups, except for correct responses to convex faces with low-state anxiety participants identifying them more correctly ($p = .031$). Subsequently, the mean difference amplitudes and standard errors were calculated for each electrode ROI that showed a significant interaction with the 3D condition, namely the central and parietal for the P300 time window and the parietal for the P600 (Figure 2.5). Post-hoc independent t-tests showed high- vs low-state anxious participants had significantly higher amplitudes for concave faces in the parietal ROI for the P300 ($t_{18} = 2.498$, $p = .022$, *Cohen's d* = 1.123) and P600 ($t_{18} = 2.359$, $p = .030$, *Cohen's d* = 1.060), but not in the central P300 ($t_{18} = 1.507$, $p = .149$, *Cohen's d* = 0.678). Concurrently, paired-sample t-tests revealed significant differences between the 3D conditions only in the low-state anxiety group participants. The difference amplitude in the concave condition was significantly lower in the central and parietal P300

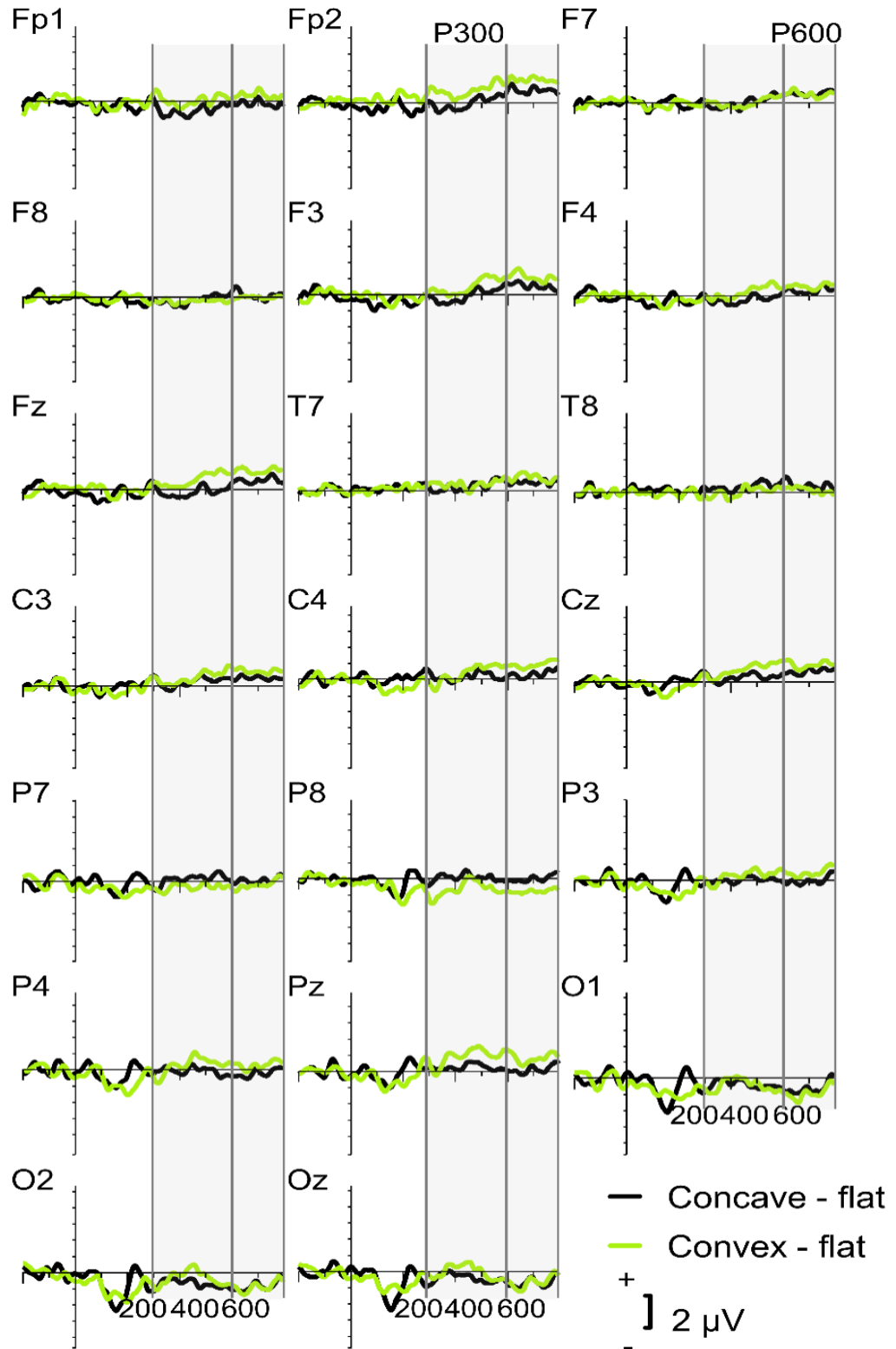


Figure 2.4. Grand average ERP difference waves for 3D normal faces minus flat faces and 3D inverted faces minus flat faces in the whole sample ($N=20$) in the twenty ROI electrodes. Y-axis represents the amplitude of the ERP with tick marks every $1\mu\text{V}$ and X-axis represents the time before and after the stimulus presentation with tick marks every 100ms

($t_{10} = 3.810, p = .003, \text{Cohen's } d = 1.149; t_{10} = 3.527, p = .005, \text{Cohen's } d = 1.064$) and the parietal P600 ($t_{10} = 2.818, p = .018, \text{Cohen's } d = 0.850$) (Figure 2.5).

3.3.4. Trait Anxiety

For the P300 time window, trait anxiety showed significant interactions with the condition factor at frontal ($F_{1,18} = 5.310, p = .033, \eta_p^2 = 0.228$) and central ($F_{1,18} = 5.879, p = .026, \eta_p^2 = 0.246$) ROIs, not surviving Bonferroni correction.

In the P600 time window, significant condition \times trait anxiety interactions in frontal ($F_{1,18} = 4.819, p = .042, \eta_p^2 = 0.211$) and central ($F_{1,18} = 6.732$ and $p = .018, \eta_p^2 = 0.272$) ROIs did not survive Bonferroni correction.

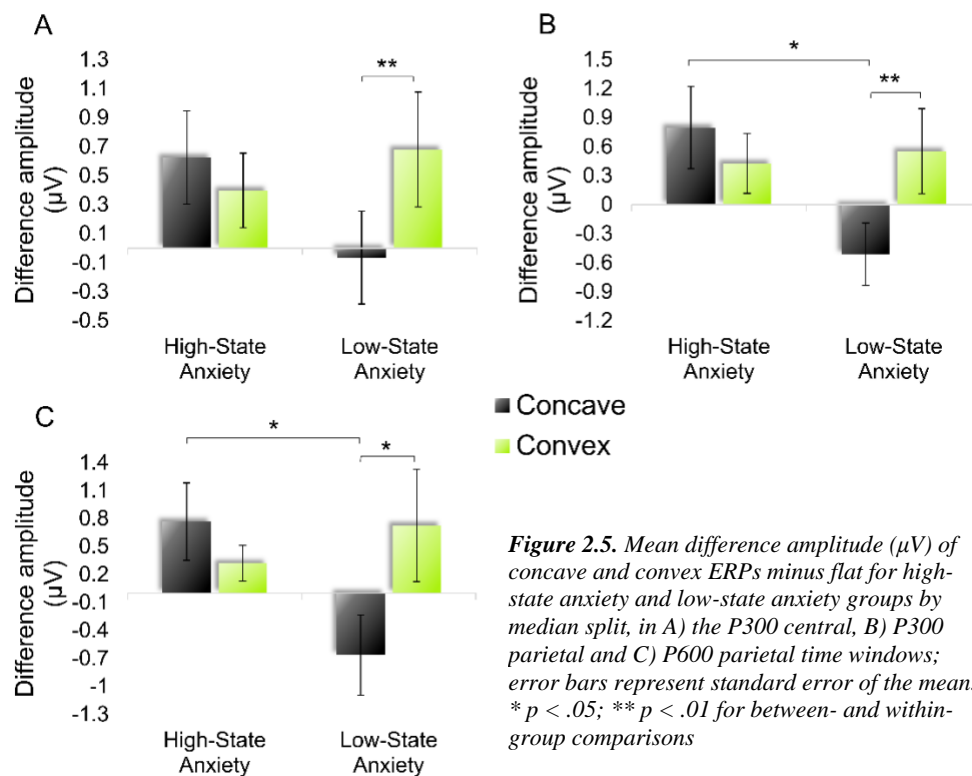


Figure 2.5. Mean difference amplitude (μV) of concave and convex ERPs minus flat for high-state anxiety and low-state anxiety groups by median split, in A) the P300 central, B) P300 parietal and C) P600 parietal time windows; error bars represent standard error of the mean. * $p < .05$; ** $p < .01$ for between- and within-group comparisons

4. Discussion

To our knowledge, this is the first study to assess neuroticism, state, and trait anxiety in ERPs during the hollow-mask illusion. There are three key findings from our study. First, as expected, (1) controls rarely perceive concave 3D faces as they fail to correctly categorise them as such and (2) there were no main significant effects of condition (convex/concave) in the P300 and P600 time windows (Dima et al., 2011). Second, there was no interaction of neuroticism or trait anxiety and concave/convex condition in the P300 and P600 time windows while viewing the hollow mask illusion, not supporting our initial hypothesis. Third, there was a significant interaction of state anxiety with the condition (concave/convex) in the P300 time window at central and parietal electrodes, and in the P600 time window at parietal ones.

The interaction effect between concave/convex faces and state anxiety revealed that the difference of amplitudes of the concave condition for the P300 ERP were significantly lower compared to the convex, only in the low-state anxiety group (Figure 2.5). This was the case despite the absence of conscious perception of concave stimuli in both groups. The P300 component is traditionally associated with the detection of an expected but unpredictable target in a series of stimuli, like the oddball task. The P300 is thought to be composed of two subcomponents, the ‘novelty’ component (P300a), a large fronto-central positive wave elicited by novel stimuli that mainly reflects involuntary attention shifts to changes in the environment and the ‘target’ component (P300b), more relevant to our study (Polich, 2007). The ‘target’ component is generated in posterior-parietal brain areas and reflects memory access processes that are activated by stimuli that require an evaluation or input (Giraudet et al., 2015).

In the low-state anxiety group the concave condition elicited significantly smaller P300 amplitude than the convex condition. Although participants rarely reported concave faces as concave and misclassified them as convex or flat, they were highly accurate in correctly reporting both convex and flat faces. A recent study that tested different types of expectations (target stimuli could either confirm or disconfirm passive or active expectations) has shown that expected stimuli like the convex faces used in our study, could be related to larger P300 amplitudes (Król & El-Deredy, 2015). The authors argued that conscious expectations can indirectly affect expectancy and thus have an opposite direction effect of automatically formed expectations. Additionally, Kok (1988) showed that the P300 tends to be smaller when the stimulus does not match the active representation (template mismatch). In line with this, the P300 in our study was smaller when the concave face activated a convex face representation, compared to when a stimulus is less probable (probability mismatch) in the low-state anxiety group. There has also been evidence that the P300 is smaller for difficult tasks, especially when uncertainty is greater and a resolution much harder to reach (Polich, 1987); this uncertainty becomes evident by the longer RTs for concave faces. Our results also question the prevailing theory that the P300 amplitude increases with greater mental resource allocation (Polich & Kok, 1995) and increased informational content of the stimulus, reflecting extraction and utilisation of information (Gratton et al., 1990).

The high-state anxiety group compared to the low-state anxiety group showed a stronger P300 in response to the concave condition. Only a few studies have investigated the P300 in patients with anxiety disorders. In a study using the auditory oddball stimuli, the results showed not only clear differences between subjects who suffered from anxiety and controls but also showed opposite results between anxious

patients and anxious controls: while anxious patients compared to controls showed a decreased P300, the group of anxious controls compared to anxious patients showed an increase of the P300 (Boudarene & Timsit-Berthier, 1997). Anxious participants have also been shown to display higher emotional sensitivity and enhanced P300 peak amplitude to negative emotional words compared to non-anxious participants (De Pascalis et al., 2004; Naumann et al., 1992). An early P300 subcomponent (P315) was also larger in patients having an anxiety disorder alone when compared to depressed patients with or without an anxiety disorder and controls when performing an auditory oddball task; whereas a late P300 subcomponent (P400) was larger in patients having comorbidity of anxiety and depressive disorders than in the controls and depressed patients (Bruder et al., 2002). Another study looking at source characteristics of the P300b showed an anxiety-related pattern of hyperactive ventral attention networks for the anxiety group, indicating increased stimulus-driven attention to task-relevant stimuli (Li et al., 2015). In a recent meta-analysis of ERPs in post-traumatic stress disorder, results demonstrated that seven studies (out of eight) showed increased P300 responses to trauma related or aversive stimuli in the post-traumatic stress disorder group compared to the control group (Javanbakht et al., 2011). In terms of P300, the present study disclosed a greater sensitivity to concave faces in anxious subjects, with a higher P300 amplitude indicating a greater effort investment for these subjects (Brocke et al., 1997). There might be increased attentional resource allocation in anxious subjects to the concave faces showing sensitisation (sensitisation is a learning process in which repeated exposure of a stimulus results in the progressive amplification of a response) to stimuli that are not consciously correctly reported as concave. Our results therefore add support to the notion of impaired attentional resources in anxious participants leading to

shifting more resources - hyperarousal - to stimuli that are mismatches (concave faces) compared to stimuli that are expected (convex faces).

The same pattern of interaction between state anxiety and condition can be seen in the P600 time window at parietal electrodes. The P600 is a centro-parietal late positive EPR that has been associated with syntactic operations such as successful retrieval and recollection (Kaan & Swaab, 2003). The P600 amplitude is known to increase with words being consciously remembered (Smith, 1993), as well as remembering not only the words but also the context of encoding (Wilding et al., 1995; Wilding & Rugg, 1996). Furthermore, it is larger for deeply encoded items implying sensitivity to the levels of processing manipulation (Rugg et al., 1998). The language specificity of the P600 has been challenged with studies showing salience and probability of stimulus occurrence affecting P600 amplitude (Coulson et al., 1998; Gunter et al., 1997). In the Coulson et al. study (1998), both ungrammatical and improbable stimuli elicited larger P600 amplitude, while in the Gunter et al. (1997) study stimulus probability and sentence complexity had similar influence on the P600. Thus, it is not surprising that in the low-state anxiety group, convex faces elicit a strong P600 while the concave faces that are rarely correctly classified and are misrepresented as convex or flat faces elicit a much smaller P600. However, the opposite effect is seen in the high-state anxiety group implying the same mechanism we see in the P300 time window. Studies have demonstrated significantly higher amplitudes of the P600 in an obsessive-compulsive disorder patient group compared to controls in a working memory paradigm (Papageorgiou & Rabavilas, 2003) as well as in a selective attention task (Towey et al., 1994). Thus, the pattern of the results obtained in the current study suggests that the high-state anxiety group demonstrated impairments in the later stages

of information processing as they are reflected by the stronger P600 elicited while viewing the concave face that involve or affect parietal brain areas.

Accordingly, it appears that the late perceptual ERPs of low-state anxiety participants are more like the group as a whole, i.e., the response to the convex stimuli is higher than the concave (when flat is subtracted). Increased sensitisation to novel stimuli (concave faces) at the higher end of the state anxiety levels interferes with the allocation of attention to the expected ones (convex faces). Fucci, Abdoun & Lutz (2019) have demonstrated increased amplitude in an earlier auditory component (P2) corresponding to standard stimuli compared to deviant ones under safe but not under threatening conditions (Fucci et al., 2019). Likewise, under anxiety-inducing conditions the authors observed increased frontal P2 response to the deviant stimuli (Fucci et al., 2019). Similarly, increased P300 response was also observed in a sample of behaviourally inhibited adolescents with a history of an anxiety disorder compared to adolescents with no such history (Reeb-Sutherland et al., 2009). Our results suggest a dimensional effect of state anxiety on the attentional processes that underlie the hollow mask illusion, the low state-anxiety individuals do not need to allocate as much attention to mismatch stimuli (concave faces) while individuals experiencing high anxiety orient excessive attention to them.

Even though the interaction between trait anxiety and neural correlates of the hollow mask stimulus did not survive Bonferroni correction, it showed the same pattern as state anxiety. Anxiety in general has been related to hypervigilance and attentional biases (in terms of intrinsic negativity by selecting threatening stimuli instead of neutral or positive stimuli) (Eysenck, 1997), however the effects of state versus trait on these processes are not well established. Trait anxiety influences state anxiety levels and is considered a stable personality characteristic, whereas state anxiety is more of a

transitory response to a situation (Meijer, 2001). There have been theories that posit that the two subtypes influence cognition differently; state anxiety decreases a person's threshold for threat stimuli and this occurs more frequently in participants with a high score on trait anxiety (Mathews & Mackintosh, 1998; Williams et al., 1997). It seems that state anxiety is more sensitive to electrophysiological changes related to the hollow mask illusion paradigm compared to trait anxiety, although both subtypes influence it in similar ways. It is, however, important to acknowledge that, in our sample, state anxiety levels are moderate. Future studies should recruit participants representing a wider range of state anxiety scores to include anxiety measures at the higher end of the spectrum. This could be better addressed by incorporating a bigger sample size, despite our large effect sizes, which would ensure the inclusion of a more substantial number of individuals to capture the whole gamut of state and trait anxiety measures. Finally, it would be important that future studies should control for effects of physiological arousal by measuring heart rate and cortisol levels, although one previous study did not find these to correlate with state anxiety (Jansen et al., 2000).

With this study we intended to explore the relationship between the electrophysiological response to hollow mask stimuli and traits of personality and anxiety states in controls, to indirectly inform us as to whether certain individuals are more vulnerable to psychopathology. We expected to find a relationship between neuroticism and the ERPs generated by the concave and convex faces due to neuroticism's high occurrence in disorders that interact with the hollow mask illusion, though this was not the case. Neuroticism has been indicated as an important risk factor for psychiatric traits including anxiety disorders (Hettema et al., 2006) and schizophrenia (Hayes et al., 2017; Van Os & Jones, 2001). A recent meta-analysis has found that a neurotic personality remained a significant risk factor for common mental

disorders including anxiety, it was only identified as a vulnerability factor for psychotic disorders (Jeronimus et al., 2016). Research has yet to clarify whether the associations between neurotic traits and psychiatric disorders indicate whether neurotic personality characteristics are a causal factor or a consequence of psychiatric illnesses or both. In our study, we did however find significant correlations between neuroticism and state/trait anxiety. Neuroticism, also known as emotional instability (McCrae & Costa, 1997) and anxiety are closely related measures. This becomes apparent as anxiety itself makes up one of the six facets of neuroticism in the five-factor model of McCrae & Costa (1992). Trait anxiety positively correlated with neuroticism in a sample of patients with panic disorder (Foot & Koszycki, 2004). In a different study, high state anxiety was associated with higher neuroticism scores in a healthy sample (Bonsaksen et al., 2019). In turn, state and trait anxiety were found to intercorrelate in a sample of patients with schizophrenia (Guillem et al., 2005) and schizophrenia patients tend to score higher in STAI measures than controls (Jansen et al., 2000). While state anxiety is thought more of as an effect of psychosis (Guillem et al., 2005) and has been demonstrated to be a predictor of state-paranoia (Cowles & Hogg, 2019), trait and state anxiety were shown to be related with positive symptoms of schizophrenia, such as bizarre delusions and auditory hallucinations (Guillem et al., 2005). Importantly, both anxiety measures affect cognitive control and attentional processes in controls (Pacheco-Unguetti et al., 2010). Hence, the interaction of state anxiety with the hollow mask ERPs could explain an indirect relationship of self-report measures and proneness to mental illness. Our paper serves as a stepping-stone to understanding psychiatric disorders and future research should parse out whether high and low state anxiety in different disorders, and especially in schizophrenia, alters the results found here.

In summary, our study points to a potential relationship between ERPs in the hollow-mask illusion and state anxiety. The most robust findings include a significant interaction of state anxiety with 3D condition in the P300 time window at central and parietal electrodes, and in the P600 time window at parietal ones. The high-state anxiety group shows disproportionately big P300 and P600 amplitudes to concave faces implying impaired late information processing in this group. Finally, anxious participants have impaired attentional resources by transferring more resources to the concave faces that are stimuli mismatches to our memory representations compared to convex faces that are expected.

References

- Bishop, S. J., Jenkins, R., & Lawrence, A. D. (2007). Neural processing of fearful faces: Effects of anxiety are gated by perceptual capacity limitations. *Cerebral Cortex*, *17*, 1595–1603. <https://doi.org/10.1093/cercor/bhl070>
- Bonsaksen, T., Heir, T., Ekeberg, Ø., Grimholt, T. K., Lerdal, A., Skogstad, L., & Schou-Bredal, I. (2019). Self-evaluated anxiety in the Norwegian population: Prevalence and associated factors. *Archives of Public Health*, *77*, 1–8. <https://doi.org/10.1186/s13690-019-0338-0>
- Boudarene, M., & Timsit-Berthier, M. (1997). [Stress, anxiety and and event related potentials]. *Encephale*, *23*, 237–250.
- Brocke, B., Tasche, K. G., & Beauducel, A. (1997). Biopsychological foundations of extraversion: Differential effort reactivity and state control. *Personality and Individual Differences*, *21*, 727–738. [https://doi.org/10.1016/S0191-8869\(96\)00226-7](https://doi.org/10.1016/S0191-8869(96)00226-7)
- Bruder, G. E., Kayser, J., Tenke, C. E., Leite, P., Schneier, F. R., Stewart, J. W., & Quitkin, F. M. (2002). Cognitive ERPs in Depressive and Anxiety Disorders during Tonal and Phonetic Oddball Tasks. *Clinical EEG and Neuroscience*, *22*, 119–124. <https://doi.org/10.1177/155005940203300308>
- Carbon, C. C. (2014). Understanding human perception by human-made illusions. *Frontiers in Human Neuroscience*. <https://doi.org/10.3389/fnhum.2014.00566>
- Caspi, A., Houts, R. M., Belsky, D. W., & Goldman-mellor, S. J. (2015). The p Factor: One General Psychopathology Factor in the Structure of Psychiatric Disorders? *Clin Psychol Sci*, *2*, 119–137. <https://doi.org/10.1177/2167702613497473>.The
- Corrow, S., Granrud, C. E., Mathison, J., & Yonas, A. (2011). Six-month-old infants perceive the hollow-face illusion. *Perception*, *40*, 1376–1383. <https://doi.org/10.1068/p7110>
- Coulson, S., King, J. W., & Kutas, M. (1998). Expect the Unexpected: Event-related Brain Response to Morphosyntactic Violations. *Language and Cognitive Processes*, *13*, 21–58. <https://doi.org/10.1080/016909698386582>
- Cowles, M., & Hogg, L. (2019). An Experimental Investigation into the Effect of State-Anxiety on State-Paranoia in People Experiencing Psychosis. *Behavioural and Cognitive Psychotherapy*, *47*, 52–66. <https://doi.org/10.1017/S1352465818000401>
- De Pascalis, V., Strippoli, E., Riccardi, P., & Vergari, F. (2004). Personality, event-related potential (ERP) and heart rate (HR) in emotional word processing. *Personality and Individual Differences*, *36*, 873–891. [https://doi.org/10.1016/S0191-8869\(03\)00159-4](https://doi.org/10.1016/S0191-8869(03)00159-4)
- Dima, D., Dietrich, D. E., Dillo, W., & Emrich, H. M. (2010). Impaired top-down processes in schizophrenia: A DCM study of ERPs. *NeuroImage*, *52*, 824–832.

<https://doi.org/10.1016/j.neuroimage.2009.12.086>

- Dima, D., Dillo, W., Bonnemann, C., Emrich, H. M., & Dietrich, D. E. (2011). Reduced P300 and P600 amplitude in the hollow-mask illusion in patients with schizophrenia. *Psychiatry Research - Neuroimaging*, *191*, 145–151. <https://doi.org/10.1016/j.psychres.2010.09.015>
- Dima, D., Roiser, J. P., Dietrich, D. E., Bonnemann, C., Lanfermann, H., Emrich, H. M., & Dillo, W. (2009). Understanding why patients with schizophrenia do not perceive the hollow-mask illusion using dynamic causal modelling. *NeuroImage*, *46*, 1180–1186. <https://doi.org/10.1016/j.neuroimage.2009.03.033>
- Eagleman, D. M. (2001). Visual illusions and neurobiology. *Nature Reviews Neuroscience*, *2*, 920–926. <https://doi.org/10.1038/35104092>
- Eysenck, M. W. (1997). *Anxiety and cognition: A unified theory*. <https://doi.org/10.1017/CBO9781107415324.004>
- Farkas, A., Papatomas, T. V., Silverstein, S. M., Kourtev, H., & Papayanopoulos, J. F. (2016). Dynamic 3-D computer graphics for designing a diagnostic tool for patients with schizophrenia. *Visual Computer*, *32*, 1499–1506. <https://doi.org/10.1007/s00371-015-1152-5>
- Foot, M., & Koszycki, D. (2004). Gender differences in anxiety-related traits in patients with panic disorder. *Depression and Anxiety*, *20*, 123–130. <https://doi.org/10.1002/da.20031>
- Fucci, E., Abdoun, O., & Lutz, A. (2019). Auditory perceptual learning is not affected by anticipatory anxiety in the healthy population except for highly anxious individuals: EEG evidence. *Clinical Neurophysiology*, *130*, 1135–1143. <https://doi.org/10.1016/j.clinph.2019.04.010>
- Georgeson, M. A. (1979). Random-dot stereograms of real objects: Observations on stereo faces and moulds. *Perception*, *8*, 585–588. <https://doi.org/10.1068/p080585>
- Giraudet, L., St-Louis, M. E., Scannella, S., & Causse, M. (2015). P300 event-related potential as an indicator of inattentive deafness? *PLoS ONE*, *10*. <https://doi.org/10.1371/journal.pone.0118556>
- Gratton, G., Bosco, C. M., Kramer, A. F., Coles, M. G. H., Wickens, C. D., & Donchin, E. (1990). Event-related brain potentials as indices of information extraction and response priming. *Electroencephalography and Clinical Neurophysiology*, *75*, 419–432. [https://doi.org/10.1016/0013-4694\(90\)90087-Z](https://doi.org/10.1016/0013-4694(90)90087-Z)
- Guillem, F., Pampoulova, T., Stip, E., Lalonde, P., & Todorov, C. (2005). The relationships between symptom dimensions and dysphoria in schizophrenia. *Schizophrenia Research*, *75*, 83–96. <https://doi.org/10.1016/j.schres.2004.06.018>
- Gunter, T. C., Stowe, L. A., & Mulder, G. (1997). When syntax meets semantics. *Psychophysiology*, *34*, 660–676.
- Gupta, T., Silverstein, S. M., Bernard, J. A., Keane, B. P., Papatomas, T. V., Pelletier-Baldelli, A., ...

- Mittal, V. A. (2016). Disruptions in neural connectivity associated with reduced susceptibility to a depth inversion illusion in youth at ultra high risk for psychosis. *NeuroImage: Clinical, 12*, 681–690. <https://doi.org/10.1016/j.nicl.2016.09.022>
- Hayes, J. F., Osborn, D. P. J., Lewis, G., Dalman, C., & Lundin, A. (2017). Association of late adolescent personality with risk for subsequent serious mental illness among men in a swedish nationwide cohort study. *JAMA Psychiatry, 74*, 703–711. <https://doi.org/10.1001/jamapsychiatry.2017.0583>
- Hettema, J. M., Neale, M. C., Myers, J. M., Prescott, C. A., & Kendler, K. S. (2006). A Population-Based Twin Study of the Relationship Between Neuroticism and Internalizing Disorders. *American Journal of Psychiatry, 163*, 857–864. <https://doi.org/10.1176/ajp.2006.163.5.857>
- Hill, H., & Bruce, V. (1993). Independent Effects of Lighting, Orientation, and Stereopsis on the Hollow-Face Illusion. *Perception, 22*, 887–897. <https://doi.org/10.1068/p220887>
- Hill, H., & Johnston, A. (2007). The Hollow-Face Illusion: Object-Specific Knowledge, General Assumptions or Properties of the Stimulus? *Perception, 36*, 199–223. <https://doi.org/10.1068/p5523>
- Jansen, L. M. C., Gispén-de Wied, C. C., & Kahn, R. S. (2000). Selective impairments in the stress response in schizophrenic patients. *Psychopharmacology, 149*, 319–325. <https://doi.org/10.1007/s002130000381>
- Javanbakht, A., Liberzon, I., Amirsadri, A., Gjini, K., & Boutros, N. N. (2011). Event-related potential studies of post-traumatic stress disorder: A critical review and synthesis. *Biology of Mood & Anxiety Disorders, 1*(1). <https://doi.org/10.1186/2045-5380-1-5>
- Jeronimus, B. F., Kotov, R., Riese, H., & Ormel, J. (2016). Neuroticism's prospective association with mental disorders halves after adjustment for baseline symptoms and psychiatric history, but the adjusted association hardly decays with time: A meta-analysis on 59 longitudinal/prospective studies with 443 313 participants. *Psychological Medicine, 46*, 2883–2906. <https://doi.org/10.1017/S0033291716001653>
- Kaan, E., & Swaab, T. Y. (2003). Repair, revision, and complexity in syntactic analysis: An electrophysiological differentiation. *Journal of Cognitive Neuroscience, 15*, 98–110. <https://doi.org/10.1162/089892903321107855>
- Khan, A. a, Jacobson, K. C., Gardner, C. O., Prescott, C. a, & Kendler, K. S. (2005). Personality and comorbidity of common psychiatric disorders. *British Journal of Psychiatry, 186*, 190–196. <https://doi.org/10.1192/bjp.186.3.190>
- King, D. J., Hodgekins, J., Chouinard, P. A., Chouinard, V.-A., & Sperandio, I. (2017). A review of abnormalities in the perception of visual illusions in schizophrenia. *Psychonomic Bulletin & Review, 24*, 734–751. <https://doi.org/10.3758/s13423-016-1168-5>
- Kok, A. (1988). Probability mismatch and template mismatch: A paradox in P300 amplitude? *Behavioral and Brain Sciences, 11*, 388–389. <https://doi.org/10.1017/S0140525X00058143>

- Król, M., & El-Deredy, W. (2015). The clash of expectancies: Does the P300 amplitude reflect both passive and active expectations? *Quarterly Journal of Experimental Psychology*, *68*, 1723–1724. <https://doi.org/10.1080/17470218.2014.996166>
- Leweke, F. M., Schneider, U., Radwan, M., Schmidt, E., & Emrich, H. M. (2000). Different effects of nabilone and cannabidiol on binocular depth inversion in man. *Pharmacology Biochemistry and Behavior*, *66*, 175–181. [https://doi.org/10.1016/S0091-3057\(00\)00201-X](https://doi.org/10.1016/S0091-3057(00)00201-X)
- Li, Y., Wang, W., Liu, T., Ren, L., Zhou, Y., Yu, C., ... Hu, Y. (2015). Source analysis of P3a and P3b components to investigate interaction of depression and anxiety in attentional systems. *Scientific Reports*, *5*, 17138. <https://doi.org/10.1038/srep17138>
- Mathews, A., & Mackintosh, B. (1998). A cognitive model of selective processing in anxiety. *Cognitive Therapy and Research*, *22*, 539–560. <https://doi.org/10.1023/A:1018738019346>
- McCrae, R., & Costa, P. (1992). An introduction to the five-factor model and its applications. *Journal of Personality*, *60*, 175–215. <https://doi.org/10.1111/j.1467-6494.1992.tb00970.x>
- Muller, J. E., Koen, L., Seedat, S., Emsley, R. A., & Stein, D. J. (2004). Anxiety disorders and schizophrenia. *Current Psychiatry Reports*, *6*, 255–261. <https://doi.org/10.1007/s11920-004-0074-0>
- Naumann, E., Bartussek, D., Diedrich, O., & Laufer, M. E. (1992). Assessing cognitive and affective information processing functions of the brain by means of the late positive complex of the event-related potential. *Journal of Psychophysiology*, *6*, 285–298.
- Ohi, K., Shimada, T., Nitta, Y., Kihara, H., Okubo, H., Uehara, T., & Kawasaki, Y. (2016). The Five-Factor Model personality traits in schizophrenia: A meta-analysis. *Psychiatry Research*, *240*, 34–41. <https://doi.org/10.1016/j.psychres.2016.04.004>
- Pacheco-Unguetti, A. P., Acosta, A., Callejas, A., & Lupiáñez, J. (2010). Attention and anxiety: Different attentional functioning under state and trait anxiety. *Psychological Science*, *21*, 298–304. <https://doi.org/10.1177/0956797609359624>
- Papageorgiou, C. C., & Rabavilas, A. D. (2003). Abnormal P600 in obsessive-compulsive disorder. A comparison with healthy controls. *Psychiatry Research*, *119*, 133–143. [https://doi.org/10.1016/S0165-1781\(03\)00109-4](https://doi.org/10.1016/S0165-1781(03)00109-4)
- Papathomas, T. V., & Bono, L. M. (2004). Experiments with a hollow mask and a reverspective: Top-down influences in the inversion effect for 3-D stimuli. *Perception*, *33*, 1129–1138. <https://doi.org/10.1068/p5086>
- Passie, T., Schneider, U., Borsutzky, M., Breyer, R., Emrich, H. M., Bandelow, B., & Schmid-Ott, G. (2013). Impaired perceptual processing and conceptual cognition in patients with anxiety disorders: A pilot study with the binocular depth inversion paradigm. *Psychology, Health & Medicine*, *18*, 363–374. <https://doi.org/10.1080/13548506.2012.722649>
- Polich, J. (1987). Task difficulty, probability, and inter-stimulus interval as determinants of P300 from

- auditory stimuli. *Electroencephalography and Clinical Neurophysiology/ Evoked Potentials*, 68, 311–320. [https://doi.org/10.1016/0168-5597\(87\)90052-9](https://doi.org/10.1016/0168-5597(87)90052-9)
- Polich, J. (2007). Updating P300: An integrative theory of P3a and P3b. *Clinical Neurophysiology*, 118, 2128–2148. <https://doi.org/10.1016/j.clinph.2007.04.019>
- Polich, J., & Kok, A. (1995). Cognitive and biological determinants of P300: An integrative review. *Biological Psychology*, 41, 103–146. [https://doi.org/10.1016/0301-0511\(95\)05130-9](https://doi.org/10.1016/0301-0511(95)05130-9)
- Reeb-Sutherland, B. C., Vanderwert, R. E., Degnan, K. A., Marshall, P. J., Pérez-Edgar, K., Chronis-Tuscano, A., ... Fox, N. A. (2009). Attention to novelty in behaviorally inhibited adolescents moderates risk for anxiety. *Journal of Child Psychology and Psychiatry*, 50, 1365–1372. <https://doi.org/10.1111/j.1469-7610.2009.02170.x>
- Rugg, M. D., Mark, R. E., Walla, P., Schloerscheidt, A. M., Birch, C. S., & Allan, K. (1998). Dissociation of the neural correlates of implicit and explicit memory. *Nature*, 392, 595–598. <https://doi.org/10.1038/33396>
- Schneider, U., Borsutzky, M., Seifert, J., Leweke, F. M., Huber, T. J., Rollnik, J. D., & Emrich, H. M. (2002). Reduced binocular depth inversion in schizophrenic patients. *Schizophrenia Research*, 53, 101–108. [https://doi.org/10.1016/S0920-9964\(00\)00172-9](https://doi.org/10.1016/S0920-9964(00)00172-9)
- Schneider, U., Leweke, F. M., Niemczyk, W., Sternemann, U., Bevilacqua, M., & Emrich, H. M. (1996). Impaired binocular depth inversion in patients with alcohol withdrawal. *Journal of Psychiatric Research*, 30, 469–474. [https://doi.org/10.1016/S0022-3956\(96\)00031-3](https://doi.org/10.1016/S0022-3956(96)00031-3)
- Semple, D. M., Ramsden, F., & McIntosh, A. M. (2003). Reduced binocular depth inversion in regular cannabis users. *Pharmacology Biochemistry and Behavior*, 75, 789–793. [https://doi.org/10.1016/S0091-3057\(03\)00140-0](https://doi.org/10.1016/S0091-3057(03)00140-0)
- Sheehan, D. V., Lecrubier, Y., Sheehan, K. H., Amorim, P., Janavs, J., Weiller, E., ... Dunbar, G. C. (1998). The Mini-International Neuropsychiatric Interview (M.I.N.I.): The development and validation of a structured diagnostic psychiatric interview for DSM-IV and ICD-10. *Journal of Clinical Psychiatry*, 59, 22–23.
- Smith, M. E. (1993). Neurophysiological manifestations of recollective experience during recognition memory judgments. *Journal of Cognitive Neuroscience*, 5, 1–13. <https://doi.org/10.1162/jocn.1993.5.1.1>
- Spielberger, C. D., Gorsuch, R. L., Lushene, R., Vagg, P. R., Jacobs, G. A. (1983). *Manual for the State-Trait Anxiety Inventory*. Palo Alto, CA: Consulting Psychologists Press
- Stelmack, R. M., Houlihan, M., & McGarry-Roberts, P. A. (1993). Personality, reaction time, and event-related potentials. *Journal of Personality and Social Psychology*, 65, 399–409. <https://doi.org/10.1037//0022-3514.65.2.399>
- Sternemann, U., Schneider, U., Leweke, F. M., Bevilacqua, C. M., Dietrich, D. E., & Emrich, H. M.

- (1997). Pro-psychotic change of binocular depth inversion by sleep deprivation. *Der Nervenarzt*, 68, 593–596. <https://doi.org/10.1007/s001150050167>
- Temmingh, H., & Stein, D. J. (2015). Anxiety in Patients with Schizophrenia: Epidemiology and Management. *CNS Drugs*, 29, 819–832. <https://doi.org/10.1007/s40263-015-0282-7>
- Towey, J. P., Tenke, C. E., Bruder, G. E., Leite, P., Friedman, D., Liebowitz, M., & Hollander, E. (1994). Brain event-related potential correlates of overfocused attention in obsessive-compulsive disorder. *Psychophysiology*, 31, 535–543. <https://doi.org/10.1111/j.1469-8986.1994.tb02346.x>
- Van den Enden, A., & Spekreijse, H. (1989). Binocular depth reversals despite familiarity cues. *Science*, 244, 959–961. <https://doi.org/10.1126/science.2382135>
- Van Os, J., & Jones, P. B. (2001). Neuroticism as a risk factor for schizophrenia. *Psychological Medicine*, 31, 1129–1134. <https://doi.org/10.1017/S0033291701004044>
- Wheatstone, C. (1838). Contributions to the physiology of vision: I. On some remarkable, and hitherto unobserved, phenomena of binocular vision. *Philosophical Transactions of the Royal Society London*, 128, 371–394.
- Wheatstone, C. (1852). Contributions to the physiology of vision: II. On some remarkable, and hitherto unobserved, phenomena of binocular vision (continued). *Philosophical Transactions of the Royal Society London*, 142, 1–17.
- Wilding, E. L., Doyle, M. C., & Rugg, M. D. (1995). Recognition memory with and without retrieval of context: An event-related potential study. *Neuropsychologia*, 33, 1–25. [https://doi.org/10.1016/0028-3932\(95\)00017-W](https://doi.org/10.1016/0028-3932(95)00017-W)
- Wilding, E. L., & Rugg, M. D. (1996). An event-related potential study of recognition memory with and without retrieval of source. *Brain*, 119, 889–905. <https://doi.org/10.1093/brain/119.3.889>
- Williams, J. M. G., Watts, F. N., MacLeod, C. M., & Mathews, A. (1997). Cognitive psychology and emotional disorders. In *The Wiley series in clinical psychology*.

Tables

Table 2.1. Demographic and questionnaire data in the entire sample (N = 94)	
<i>Demographic data</i>	
Gender (male: female)	22:72
Age in years, <i>M</i> (<i>SD</i>)	26.21 (11.67)
Age range	18 – 59
<i>NEO PI-R scores</i>	
Neuroticism, <i>M</i> (<i>SD</i>)	97.74 (22.76)
Neuroticism range	46 – 162

NEO PI-R: Neuroticism Extroversion Openness Personality Inventory-Revised; **STAI:** State-Trait Anxiety Inventory

Table 2.2. Demographic, questionnaire, and behavioural data in the EEG sample (N = 20)	
<i>Demographic data</i>	
Gender (male: female)	3:17
Age in years, <i>M (SD)</i>	25.70 (8.96)
Age range	18 – 59
<i>NEO PI-R scores</i>	
Neuroticism, <i>M (SD)</i>	103.60 (25.77)
Neuroticism range	46 – 142
<i>STAI scores</i>	
State anxiety, <i>M (SD)</i>	33.75 (9.42)
Trait anxiety, <i>M (SD)</i>	43.75 (9.95)
<i>Correct responses to face stimuli (% correct), M (SD)</i>	
Concave	16% (23%)
Convex	86% (18%)
Flat	69% (26%)
<i>Response time for face stimuli in milliseconds, M (SD)</i>	
Concave	4117.68 (2070.36)
Convex	3181.45 (1202.75)
Flat	3400.43 (1072.18)

EEG: Electroencephalography; **NEO PI-R:** Neuroticism Extroversion Openness Personality Inventory-Revised; **STAI:** State-Trait Anxiety Inventory

Chapter 3: A meta-analysis of structural and functional brain abnormalities in early-onset schizophrenia: Neuroimaging findings of early-onset schizophrenia*

Abstract: Early-onset schizophrenia (EOS) patients demonstrate brain changes that are similar to severe cases of adult-onset schizophrenia. Neuroimaging research in EOS is limited due to the rarity of the disorder. The present meta-analysis aims to consolidate MRI and functional MRI findings in EOS. Seven voxel-based morphometry (VBM) and eight functional MRI studies met the inclusion criteria, reporting whole-brain analyses of EOS versus healthy controls. Activation likelihood estimation (ALE) was conducted to identify aberrant anatomical or functional clusters across the included studies. Separate ALE analyses were performed, first for all task-dependent studies (Cognition ALE) and then only for working memory ones (WM ALE). The VBM ALE revealed no significant clusters for grey matter volume reductions in EOS. Significant hypoactivations peaking in the right anterior cingulate cortex (rACC) and the right temporoparietal junction (rTPJ) were detected in the Cognition ALE. In the WM ALE, consistent hypoactivations were found in the left precuneus (IPreC), the right inferior parietal lobule (rIPL) and the rTPJ. These hypoactivated areas show strong associations with language, memory, attention, spatial and social cognition. The functional co-activated networks of each suprathreshold ALE cluster, identified using the BrainMap database, revealed a core co-activation network with similar topography to the salience network. Our results add support to posterior parietal, ACC and rTPJ dysfunction in EOS, areas implicated in the cognitive impairments characterizing EOS. The salience network lies at the core of these cognitive processes, co-activating with the hypoactivating regions, and thus highlighting the importance of salience dysfunction in EOS.

* Ioakeimidis Vasileios, Haenschel Corinna, Yarrow Kielan, Kyriakopoulos Marinos, Dima Danai (2020). A Meta-analysis of Structural and Functional Brain Abnormalities in Early-Onset Schizophrenia. *Schizophrenia Bulletin Open*, 1(1), 1–12. doi.org/10.1093/schizbullopen/sgaa016; [See appendix](#)

1. Introduction

Early-onset schizophrenia (EOS) is a rare and severe form of schizophrenia which has its onset before early adulthood. Research usually distinguishes between childhood- and adolescent-onset cases; the former considering diagnoses up to 13 and the latter from 13 to 18 years old (Kyriakopoulos & Frangou, 2007). In this paper, the term EOS encompasses both childhood- and adolescent-onset schizophrenia and is used as an umbrella term for all diagnosed cases of schizophrenia up to the 18th year of age. Schizophrenia is diagnosed in 1% of the worldwide population (Zwicker et al., 2018), but epidemiological findings for EOS suggest a rate of prevalence in less than 5% of all schizophrenia cases (Cannon et al., 1999), making the literature for the disorder scarce. EOS patients have higher premorbid developmental and social deficits, more hospitalizations and poorer psychosocial outcome compared to adult schizophrenia patients (Vyas et al., 2011). Like adult schizophrenia, EOS is characterized by diverse symptomatology which includes the presence of positive and negative symptoms, along with cognitive impairments. Cognitive processes that are affected include working memory (WM) (Park & Gooding, 2014), attention (Luck & Gold, 2008) and processing of salience (Kapur, 2003).

Regional grey matter volume loss and cortical thinning in EOS, although inconsistent, has been reported in numerous brain areas; these are seen bilaterally in the ventral prefrontal cortex, dorsolateral prefrontal cortex, superior parietal cortex (SPL), middle temporal gyrus, inferior temporal gyrus, thalamus and the cerebellum; whereas left-sided reductions have been observed in the anterior cingulate cortex (ACC), paracingulate gyrus, cuneus, precuneus (PreC) and superior temporal gyrus (STG) (Kyriakopoulos & Frangou, 2007; Rapoport et al., 2005). EOS patients also

demonstrate decreased insular volumes (Moran et al., 2014). Other findings in EOS include sensorimotor areas, namely the right pre- and post-central gyri, the SMA and pre-SMA areas (Douaud et al., 2009). Juuhl-Langseth et al. (2012), found subcortical volume increases in the ventricles and bilaterally in the caudate, but no other differences were detected (2012). However, a recent meta-analysis on longitudinal volumetric changes in early-onset psychosis has identified only frontal grey matter loss (Fraguas et al., 2016), whereas only frontal lobe grey matter decreases were found in a different study (Janssen et al., 2014). Reduced grey matter thickness was found bilaterally in the anterior midcingulate gyrus and sulcus, the insula and the middle frontal sulci, as well as in the left hemisphere in superior temporal, the parietooccipital, the postcentral and superior frontal sulci (Palaniyappan et al., 2019). Right hemisphere cortical thickness reductions were observed in the posterior midcingulate gyrus and sulcus, subparietal sulcus, the STG and inferior frontal gyrus. Longitudinal studies have revealed that the cortical reductions observed in EOS are dynamically spreading during adolescence and follow a back to front and top-to-bottom pattern (Gogtay et al., 2006); the medial frontal wall is affected early, whereas the ACC volume decreases later on (Vidal et al., 2006). Thompson et al. (2001), reported that the accelerated pattern of grey matter loss in an EOS sample is not a medication-related side effect and begins in parietal and motor areas, with reductions in superior and dorsolateral frontal cortices and temporal regions following later in adolescence.

Correspondingly, grey matter volume decreases in adult-onset schizophrenia that converge meta-analytically across studies include bilaterally the insula, the thalamus, the ACC (ventral, dorsal and subgenual), and the left parahippocampal gyrus, postcentral gyrus and middle frontal gyrus (Glahn et al., 2008). A more recent meta-analysis of schizophrenia by the ENIGMA consortium also found bilateral decreases of

cortical thickness in the fusiform gyrus, the inferior temporal gyrus, the cingulate cortex, the STG and the superior temporal sulcus, and lateralized reductions included the right inferior frontal gyrus and right posterior cingulate cortex, whereas left-hemisphere thickness decreases were found on the middle temporal gyrus and lateral orbitofrontal cortex (van Erp et al., 2018). van Erp et al. (2018), also found cortical thickness increases in the SPL, PreC and paracentral lobule bilaterally, and right-side increases in the inferior parietal lobule (IPL), the rostral ACC and precentral gyrus.

Schizophrenia is characterized by cognitive deficits, especially in WM (Park & Gooding, 2014) and attentional processing (Luck & Gold, 2008), linked with aberrant activation of their neural substrates. EOS patients demonstrate impairments in change detection (Rydkjær et al., 2017) that are dependent on ACC and STG activity (Oknina et al., 2005) and are associated with positive symptoms (Rydkjær et al., 2017).

Furthermore, WM-related dysfunction in schizophrenia is tied to reduced activity in the prefrontal cortex which is more specific to an encoding malfunction (Bittner et al., 2015). However, there are inconsistent reports revealing cases of prefrontal (Thormodsen et al., 2011) and anterior cingulate (Glahn et al., 2005; White, Hongwanishkul, et al., 2011) hyperactivation in EOS and adult schizophrenia.

Correspondingly, increasing WM load predicts suppression deficiency in the medial frontal and bilateral posterior parietal cortices in EOS (Fryer et al., 2013) and such suppression reduction is associated with WM capacity deficits (Van Snellenberg et al., 2016). Reduced activity during WM performance is also shown in the temporoparietal junction (TPJ) (Bittner et al., 2015; Pauly et al., 2008) as well as the ACC (Kyriakopoulos et al., 2012; Pauly et al., 2008). WM encoding deficits are further associated with functional connectivity disruptions between the ACC and the temporal lobes (White, Schmidt, et al., 2011). ACC- and TPJ-related dysfunction in EOS has also

been observed during emotional (Seiferth et al., 2009), language processing (Borofsky et al., 2010), as well as change detection (Oknina et al., 2005) tasks.

In the present study, we used the activation likelihood estimation (ALE) meta-analysis method, a coordinate-based meta-analytic technique, using the available voxel-based morphometry (VBM) and task-dependent fMRI literature in EOS. To our knowledge, this is the first coordinate-based meta-analysis for the VBM and fMRI literature in EOS and we sought to identify brain areas with grey matter volume abnormalities and aberrant activation that converge across studies. In addition, we conducted post-hoc analyses using meta-data from a large-scale neuroimaging database (BrainMap) to decode any cognitive correlates that associate with these brain areas and to identify functional networks which embed these areas in the healthy population. The overarching goal of the study was to draw inferences about the structural, functional cognitive and connectivity profiles of brain dysfunction that lies in EOS.

2. Methods

2.1. Literature search and study selection

We conducted a systematic PubMed search to identify all neuroimaging studies on EOS up to January 2020, using the PRISMA guidelines (Moher et al., 2009). The search was performed by two independent investigators using the following set of keywords:

“(schizophrenia [Title/Abstract]) AND (early onset schizophrenia OR childhood onset schizophrenia OR adolescent onset schizophrenia) AND (VBM [Title/Abstract] OR fMRI [Title/Abstract] OR magnetic resonance imaging [Title/Abstract] OR MRI [Title/Abstract] OR voxel-based morphometry [Title/Abstract] OR cortical thickness [Title/Abstract])”

This process returned a total of 530 abstracts that were initially screened for inclusion. Studies were included if they: 1) were conducted in an EOS sample with age of illness onset below 18 years old, 2) employed whole-brain analysis using VBM or fMRI, and 3) presented group comparisons of EOS and healthy controls (HC). Full-text review of the pre-selected studies was followed to determine eligibility. Studies were excluded if they: 1) did not report coordinate data on standard stereotactic space, 2) performed region-of-interest (ROI) or small-volume correction analyses, 3) did not report second-level analysis of case-control contrasts, 4) analysed samples reported by a previous study, 5) were longitudinal studies but did not report cross-sectional contrasts, 6) were case-studies or 7) were resting-state fMRI studies. Whole-brain analyses were preferred over seed-based

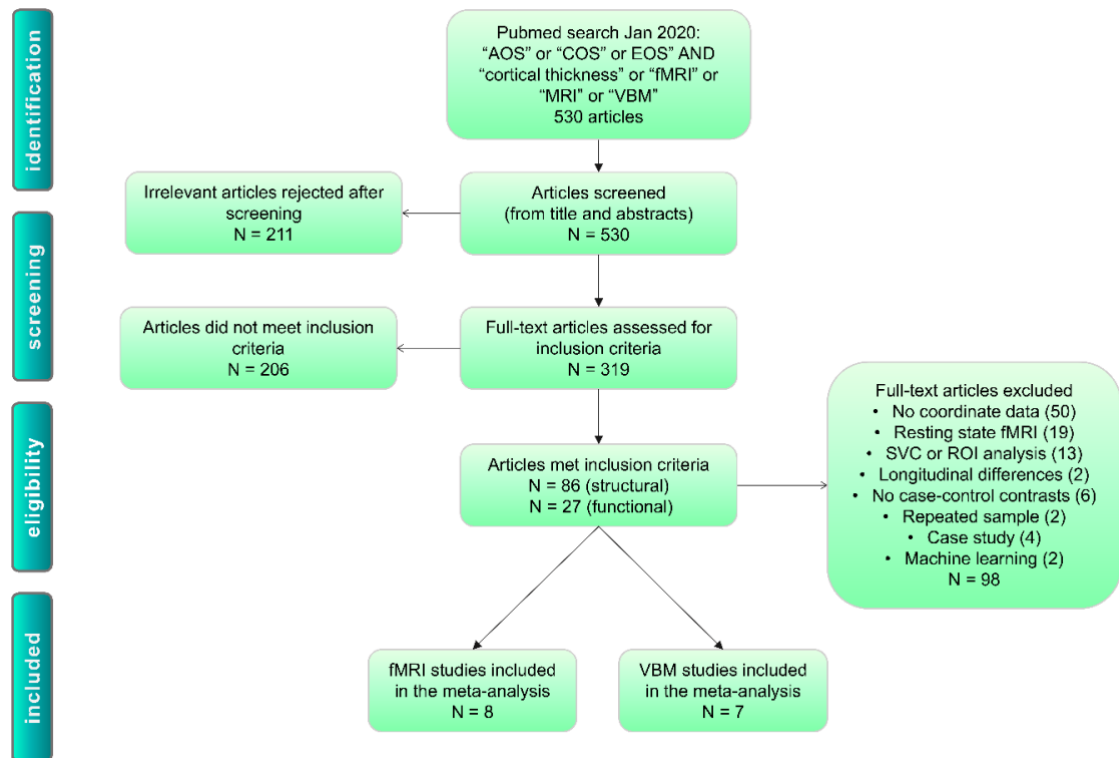


Figure 3.1. Preferred Reporting Items for Systematic Reviews and Meta-Analyses (PRISMA) flowchart shows the detailed selection process of the studies used in the VBM and fMRI meta-analyses. Abbreviations: AOS (adolescent-onset schizophrenia); COS (childhood-onset schizophrenia); EOS (early-onset schizophrenia); SVC (small-volume correction); ROI (region-of-interest analysis)

ones, that were excluded to eliminate risk-of-bias (Müller et al., 2018; Tahmasian et al., 2017). Figure 1 displays the flow-diagram of the search and selection process.

2.2. Database construction

The complete selection process yielded a total of 15 whole-brain analysis studies that met criteria and reached consensus by two researchers (Table 3.1). These were then divided into VBM and fMRI, with seven and eight studies, respectively (Figure 3.1).

For each of the studies we extracted data on sample size, participants' mean age and sex. For the patients, we also extracted age of illness onset and duration of illness, mean and standard deviation of symptom severity as well as chlorpromazine equivalents, where available (Table 3.1).

We use the term 'study' to refer to each published article, and 'experiment' to reflect a single contrast or analysis. For all experiments, we recorded all foci with

significant case-control differences and their respective p-values and peak coordinates, as well as the direction of the signal change compared to the control group. For each fMRI study, we also recorded the experimental design and type of task. Coordinates reported in the Talairach & Tournoux (Laitinen, 1989) space were transformed into MNI (Evans et al., 1993) space.

Together the VBM studies included seven experiments (or contrasts), from which only the HC > EOS contrast yielded significant differences, which located around 37 anatomical foci. The fMRI studies revealed 147 foci obtained from 36 cognitive experiments. These were then separated into HC > EOS contrasts (EOS hypoactivations; 22 experiments and 98 foci) and EOS > HC contrasts (EOS hyperactivations; 14 experiments and 49 foci). The fMRI studies were further organized into WM-only experiments which yielded 15 experiments and 55 foci for EOS hypoactivation and 10 experiments and 35 foci for EOS hyperactivations ([Table 3.2](#)). In the analysis, we only included coordinate data shown in case-control comparisons. To control for within-group effects, datasets were conservatively organized ‘per subject group’ instead of ‘per experiment’, to avoid inflating the contribution of studies with more than one experiments and retain more balanced distribution of contributing foci from each study (Turkeltaub et al., 2012).

2.3. Activation likelihood estimation

All statistical analyses were carried out separately for the VBM and fMRI experiments following the same procedure. We used the revised version of the activation likelihood estimation (ALE) algorithm (Eickhoff et al., 2012) implemented in GingerALE version 2.3.6 (Eickhoff et al., 2009, 2012; Turkeltaub et al., 2012) (www.brainmap.org/ale) to identify clusters of convergent activation across experiments. The ALE algorithm tests whether peak coordinates from the primary studies with activation differences were

significantly higher than a random spatial null distribution (Eickhoff et al., 2009). For each experiment every coordinate was modelled as the centre of a random 3D Gaussian probability distribution, instead of being modelled as a single point, for which full width at half maximum is determined by the study's sample size (Eickhoff et al., 2009). A modelled activation (MA) map was then created for a given experiment by combining the maximum across the Gaussian probability distributions of each focus (Turkeltaub et al., 2012). Foci were organised by subject group instead of being organised by experiment, in order to prevent multiple foci from a single study influencing the MA values (Turkeltaub et al., 2012). Also, within the fMRI studies we performed separate ALE studies, one for all cognitive experiments (Cognition ALE) and the other including only the working memory (WM ALE) ones. The combination of each individual MA map across experiments resulted in a respective ALE map that represented the convergence of foci for each brain region. The ALE map was then compared against a null-distribution map using a random effects model of random association between experiments to find convergence of above-chance level (Eickhoff et al., 2009) (Eickhoff et al., 2009). To correct for multiple comparisons we applied a cluster-level FWE correction at $p < 0.05$ with a cluster-forming threshold of $p < 0.01$ (Beissner et al., 2013; Rasgon et al., 2017). Anatomical labels and Brodmann areas (BA) were assigned to ALE suprathreshold peaks through the Talairach Daemon that is incorporated in GingerALE.

2.4. Follow-up analyses for fMRI ALE

2.4.1. Meta-analytic co-activation modelling

Meta-analytic co-activation modelling (MACM) is a meta-analytic technique that investigates significant whole-brain task-dependent co-activation patterns of user-specified ROI (Robinson et al., 2010, 2012). MACM allows one to make inferences about functional connectivity between the ROIs (seeds) and the rest of the brain (Laird

et al., 2013). The suprathreshold clusters of convergent activation from our ALE studies were used as seeds in the search criteria of the BrainMap database. In our study, this technique allowed the exploration of the networks which our ALE suprathreshold clusters (two resulting from the Cognitive ALE and three from the WM ALE) co-activate, and subsequently could point to a network dysfunction.

First, ROI images of the clusters were created in Mango (<http://ric.uthscsa.edu/mango/>) and then used as seeds separately in Sleuth 2.4 (<http://brainmap.org/sleuth>) (Fox et al., 2005; Laird et al., 2005), to identify fMRI experiments in the BrainMap database reporting at least one focus of activation within the respective seed in healthy controls. The resulting co-activation foci from each seed-search were exported into separate datasets and a single ALE analysis was performed for each dataset. A threshold of voxel-level FWE at 0.05 was applied, with a minimum cluster volume of 50 mm³ for all co-activation maps of each of our ROIs (Eickhoff et al., 2016).

Secondly, the resultant voxel-level FWE thresholded functional connectivity (i.e. MACM) maps for each seed were used in conjunction analyses to find where these maps overlap using the minimum statistic method (Nichols et al., 2005). We explored the conjunction across significantly co-activating brain regions resulting from the cognition ALE and WM ALE separately. This method was chosen to locate the core network that was formed by the impaired ALE clusters in EOS.

2.4.2. Cognitive associations

Finally, we explored the cognitive associations of our significantly impaired clusters in EOS that resulted from our Cognition and WM ALE studies. This procedure helped elucidate the roles of these clusters in cognition in the healthy population. We explored these cognitive associations by using the BrainMap meta-data that provide information

on the *behavioural domains* of each neuroimaging experiment included in the database (Fox et al., 2005). Behavioural domains describe the mental processes presumed to be isolated by the statistical contrasts and comprise five main categories: action, cognition, emotion, interoception, and perception, as well as their subcategories (Fox et al., 2005).

Each seed search in the Sleuth software additionally provides the counts of activations of each behavioural domain category and subcategory that appears in the BrainMap database and that are identified by the search criteria each time. We took advantage of this feature and used our significant ALE clusters as ROIs to filter our Sleuth searches to identify the counts of activations of each behavioural domain within each seed-ROI. We also performed one additional control search to explore the counts of activations within each behavioural domain in the whole brain of healthy controls.

We used the contingency table approach to calculate the odds ratio of finding a behavioural domain given activation within a particular ROI relative to finding that same domain given activation elsewhere in the brain, similar to the reverse inference approach (Poldrack, 2006). Significance was assessed with the Fisher's exact test in MATLAB (`fishertest` function) and was corrected for multiple comparison using FDR of 0.05 (`mafdr` function) with the linear step-up procedure (Benjamini & Hochberg, 1995). We were only interested in odds ratios when the odds of behavioural domains given ROI activation were higher than the odds of finding the behavioural domain given activation anywhere else in the brain. Hence as a final step, the FDR corrected p value was halved to reflect our directional hypothesis. The benefit of the reverse inference method is that it allows us to assign multiple mental processes to a certain ROI (Yarkoni et al., 2011) instead of associating only a single function to a brain region as in the classical forward inference method (Henson, 2006).

3. Results

The initial search returned 530 articles of which 319 full-text articles were assessed for eligibility and 15 were retained for the quantitative meta-analysis, seven of them for the VBM meta-analysis and eight for the task-dependent fMRI (Figure 3.1).

3.1. VBM

3.1.1. *Study sample and characteristics*

The VBM meta-analysis returned a sample of 194 EOS individuals (58% male) with range of sub-sample mean ages from 15.4 to 16.9 and range of mean age of illness onset (AIO) 14.9 – 16.5 (three studies had AIO < 18 but did not report the mean). The HC sample size was 254 (HC; 61% male) with range of mean ages 15.4 – 16.8 ([Table 3.1](#)). The HC > EOS study included contrasts from all seven experiments, however no studies reported EOS > HC contrasts (Castro-Fornieles et al., 2018; Douaud et al., 2007; Janssen et al., 2008; Tang et al., 2012; Yoshihara et al., 2008; C. Zhang et al., 2017; Y. Zhang et al., 2015).

3.1.2. *Anatomical likelihood estimation from VBM studies*

No significant clusters were found at $p < 0.05$ following cluster-level FWE correction for the contrasts HC > EOS in the VBM studies.

3.2. fMRI

3.2.1. *Study sample and characteristics*

The analysis across all functional studies (Cognition ALE) yielded a sample consisting of 148 EOS (69% male) with range of mean age from 13.3 to 21.3 and AIO range 10 – 16.5 (three studies did not mention the AIO but had ages of inclusion below 18 years).

The HC sample included 152 individuals (70% male) with range of mean age from 12.8 to 20 years ([Table 3.1](#)).

The studies with the WM experiments (WM ALE) returned a sample of 122 individuals with EOS (66% male), with range of mean age from 15 to 21.3 years old and AIO range from 10 to 16.5. The HC sample included 126 individuals (67% male) with range of mean age from 15-20 years old.

3.2.2. *Activation likelihood estimation from fMRI studies*

3.2.2.1. Cognition ALE

The analysis for all cognitive tasks yielded two significant clusters of reduced activation in EOS compared to HC ([Table 3.3](#); Figure 3.2A). One cluster was located at the right anterior cingulate cortex (rACC; $x = 6, y = 38, z = 14$) and the second cluster was located at the right superior temporal gyrus/ temporoparietal junction (rTPJ) ($x = 60, y = -46, z = 20$). No clusters of hyperactivation in EOS survived cluster-level FWE correction.

3.2.2.2. WM ALE

ALE revealed three significant clusters, where EOS individuals showed hypoactivation when engaging in WM tasks. These clusters were found at parietal and temporoparietal areas, with the first peaking at the left SPL/precuneus (IPreC; $x = -22, y = -66, z = 44$). The second cluster was centred at the right inferior parietal lobule (rIPL; $x = 38, y = -50, z = 46$) and the third at the right supramarginal gyrus/rTPJ ($x = 60, y = -46, z = 22$) ([Table 3.3](#); Figure 3.2B). No FWE corrected clusters were significant for the EOS > HC contrasts, reflecting hyperactivations in the EOS group. Diagnostics for both the Cognitive and WM ALEs are show in [Table 3.4](#).

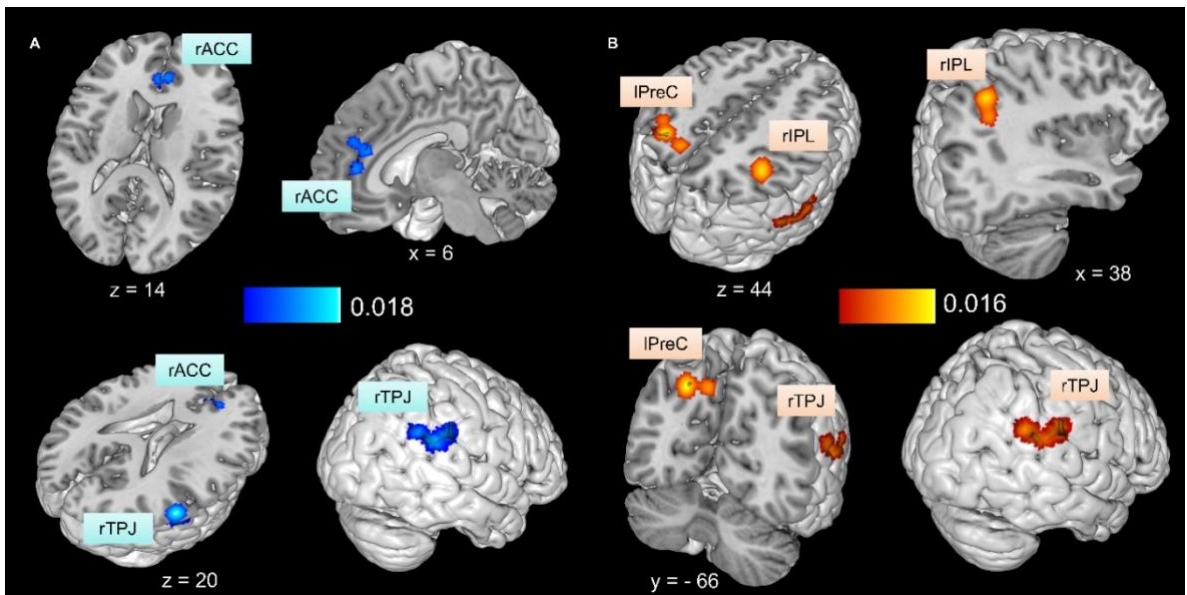


Figure 3.2. Clusters of EOS hypoactivation in the Cognition ALE and WM ALE. A) Significant convergence across all cognitive experiments was found in the ACC and rTPJ for the HC > EOS contrasts. B) The WM ALE showed significant convergence at the lPreC, rIPL and rTPJ. Results are cluster-FWE corrected at 0.05 with cluster forming value at $p < 0.01$. The same clusters were later used as seed-ROIs for the MACM and functional associations analyses. Abbreviations: rACC (right anterior cingulate cortex); rIPL (right inferior parietal lobule); lPreC (left precuneus); rTPJ (right temporoparietal junction)

3.3. Follow-up: Meta-analytic co-activation modelling (MACM)

As a first follow-up step to our ALE studies, we were interested to investigate whole-brain task-dependent co-activations with the five seed-ROIs (Figure 3.2) identified with the Cognition and WM ALE.

3.3.1. Seeds resulting from the Cognitive ALE study

3.3.1.1. rACC

At the time of the search (September 2019) the rACC seed resulted in 132 experiments consisting of 1909 foci in 1851 subjects for the rACC seed. This seed showed strong functional connectivity with the left claustrum, the right insula, the right inferior frontal gyrus, the right middle frontal gyrus, the right caudate body, the right and left medial dorsal nucleus and the cingulate gyrus (Table 3.5).

3.3.1.2. rTPJ

The rTPJ seed located 92 experiments consisting of 1762 foci in 1629 subjects. The left claustrum and right insula were found to be co-activated with the seed, along with the cingulate gyrus and medial frontal gyrus, the left STG, the right middle frontal gyrus, the thalamus (bilaterally), the right caudate body, the right superior frontal gyrus and a small area in the right STG ([Table 3.5](#)).

3.3.2. Seeds resulting from the WM ALE study

3.3.2.1. IPreC

Our BrainMap search for the IPreC seed yielded 250 experiments consisting of 4321 foci in 3087 subjects. Analysis for this seed revealed functional connectivity with a large area around the left inferior frontal, middle frontal and precentral gyri, a cluster around the left SPL and PreC, the medial frontal and cingulate gyri, and the right inferior frontal gyrus. In addition, the IPreC seed was found to be co-activated bilaterally with the insula. Further areas co-activating with the IPreC seed were the right precentral gyrus, right middle

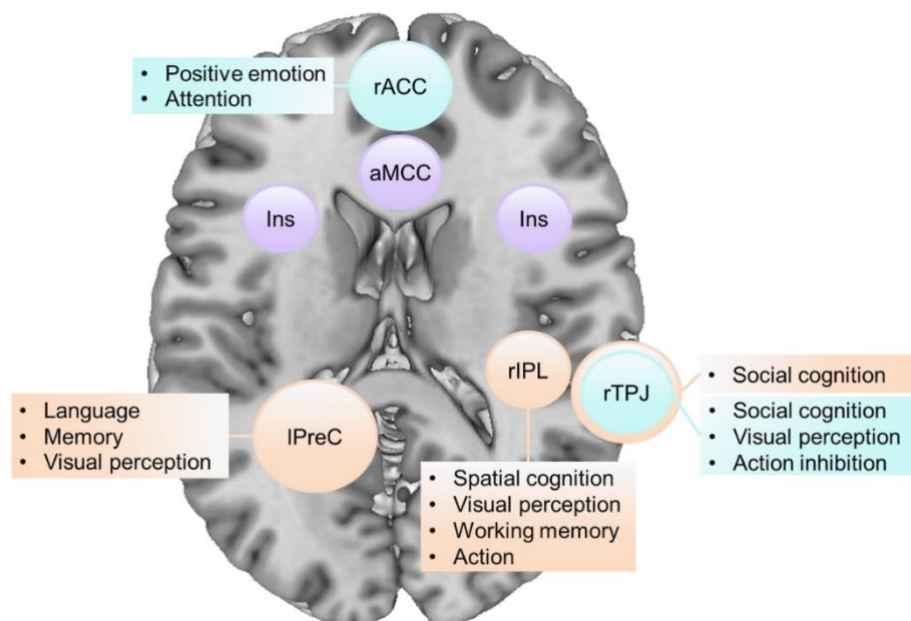


Figure 3.3. Schematic representation of the relative positions of the suprathreshold Cognition ALE clusters in blue and WM ALE clusters in orange, with their respective associate behavioural domains. The core network resulting from the conjunction analysis of the respective MACM maps, in purple. Axial brain slice from Colin27_T1_MNI at $z = 15$

frontal gyrus, left fusiform gyrus, left putamen of the lentiform nucleus and left superior frontal gyrus ([Table 3.6](#)).

3.3.2.2. rIPL

The rIPL seed resulted in 186 experiments consisting of 3231 foci coming from 2390 subjects. Analysis revealed a large cluster co-activating with this seed was located in the left parietal lobe and included peaks in the IPL, SPL and PreC. The next three clusters showing strong functional connectivity with the rIPL seed were located around the medial frontal gyrus and cingulate gyrus, the right inferior frontal gyrus and middle frontal gyrus, and the left precentral gyrus, and a smaller cluster was found in the left middle frontal gyrus. The bilateral insular cortices were also functionally connected to the rIPL seed. The putamen (bilaterally) and the left caudate body, the left (ventral posterior medial nucleus) and right thalamus, the left middle temporal gyrus and a small region in the right precuneus were also functionally connected to the seed ([Table 3.6](#)).

3.3.2.3. rTPJ

The database search for experiments with at least one focus of activation in the rTPJ seed returned 76 experiments consisting of 1322 foci coming from 1205 subjects. Analysis revealed significant connectivity with the left claustrum, the right insula, the medial frontal gyrus, the left SMG, left and right STG as well as the left IPL and a cluster around the left PreC ([Table 3.6](#)).

3.3.3. *Core co-activation network*

Secondly, clusters forming a conjunction between the MACM maps for the two seed-ROIs (rACC and rTPJ) of the Cognition ALE and the three seeds (lPreC, rIPL and rTPJ) from the WM ALE study are shown in [Tables 3.5](#) and [3.6](#), respectively. The core co-activation networks for Cognition ALE and WM ALE resulting from the conjunction

analyses were almost identical, with conjunctions bilaterally in the insula and the area of the anterior midcingulate gyrus (aMCC)/medial frontal gyrus (Figure 3.3).

3.4. Follow-up: Cognitive associations

We were interested to explore the mental processes that show cognitive associations with the significant clusters from our ALE studies.

The rACC ROI that resulted from the Cognition ALE was found to be significantly associated with positive emotion/reward, attention and broad cognition. The rTPJ ROI revealed a strong and significant association with social cognition and high associations with visual motion perception and action inhibition (Figure 3.4A).

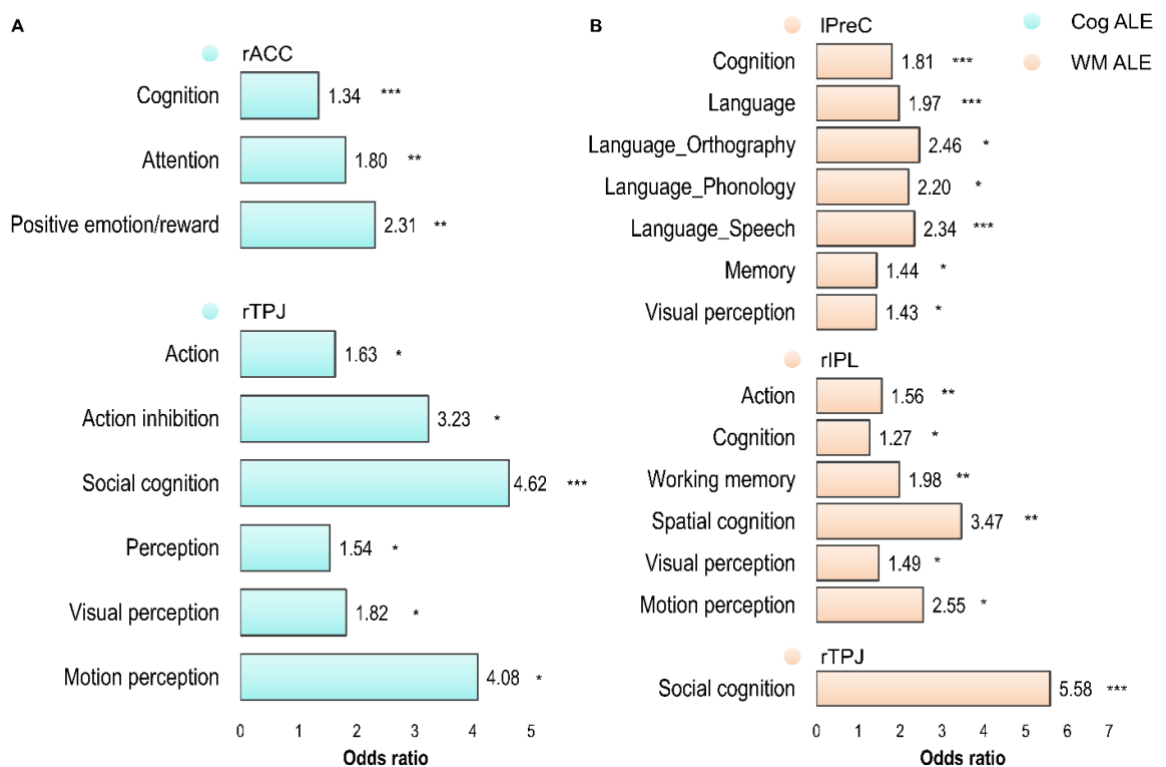


Figure 3.4. Cognitive associations for the seed-ROIs resulting from (A) the Cognition ALE in blue and (B) WM ALE in orange. A 2-by-2 contingency table approach was used along with Fisher's test as a method of reverse inference to determine the odds of detecting a behavioural domain given activation of a certain ROI relative to the odds of detecting it given activation elsewhere in the brain. Only significant (FDR corrected) behavioural domains are presented in bar graphs, with odds of activating the ROI higher than 1. * $p < 0.05$; ** $p < 0.01$; *** $p < 0.001$

Our ROIs deriving from the WM ALE study showed prevalent cognitive associations with behavioural domains of cognition, perception and action (Figure

3.4B). More specifically, the lPreC ROI was found to be predominantly associated with language processing (orthography, speech and phonology), memory and visual perception. The rIPL ROI was more strongly associated with spatial cognition. Additional cognitive associations were found for motion perception and WM, as well as the broad domain of action. The rTPJ ROI had a single, very strong and highly significant association with social cognition.

4. Discussion

In the present study, we investigated structural and functional changes in EOS versus HC using ALE, a coordinate-based meta-analysis method. By doing so, we sought to outline all structural and functional findings in EOS and to establish whether a structural or functional biomarker exists for the disorder. Additionally, we were interested to define brain regions with abnormal function across cognition and during WM performance, in the developing brains of EOS patients compared to typically developing controls. We followed-up with post-hoc analyses that sought to explore task-wide co-activation brain patterns of our ALE-derived clusters within the healthy population and their cognitive associations with behavioural domains. These analyses allowed us to explore the behavioural profile of the affected brain regions and to pinpoint where the EOS dysfunction lies in terms of functional network connectivity.

4.1. VBM

The VBM meta-analysis for grey matter volume reductions returned no significantly convergent clusters between controls and EOS patients. This result is consistent with previous studies that failed to demonstrate EOS – HC grey matter differences (Pagsberg et al., 2007; Thormodsen et al., 2013). However, our result could be due to limited statistical power owing to the very small number of studies ($n = 7$) (Eickhoff et al., 2016) that met our inclusion criteria, even though some individual studies have found brain-volume reductions in EOS (Douaud et al., 2007). Different brain areas follow different developmental trajectories in controls (Casey et al., 2011) and grey-matter volume loss in EOS is dynamic and follows a back-to-front pattern starting in parietal and progressing in temporal and prefrontal regions (Thompson et al., 2001). Thus, differences in age, duration of illness, AIO or medication in individual studies could be

some of the factors creating variability and contributing to the absence of structural convergence. Alternatively, lack of convergence in the VBM analysis could suggest the EOS brain volume reduction to be not specific to a particular brain region.

4.2. fMRI

4.2.1. ACC

In the Cognition ALE, the ACC and rTPJ were the two clusters showing reduced activation in the EOS patients when compared with typically developing controls. Following the post-hoc cognitive association analysis we found the ACC cluster activity to be related with attentional and reward-related processes.

The ACC shows sustained activity during WM delays (Petit et al., 1998), plays a role in conflict monitoring and avoidance learning (Botvinick, 2007), responds to errors (Polli et al., 2008) and drives the reallocation of attentional resources according to task-demands and salience (Crottaz-Herbette & Menon, 2006). These processes have been shown to be affected in schizophrenia patients and coupled with reduced activation in areas of the ACC compared to HC (Kerns et al., 2005; Laurens et al., 2005; Polli et al., 2008). Thus hypoactivation of the ACC in EOS is shared with the adult / chronic populations of the disorder (Kerns et al., 2005). One study has shown that the conflict- and error-monitoring related ACC activity reduction in schizophrenia relates to absence of behavioural adjustments to improve performance (Kerns et al., 2005). The ACC hypoactivation is believed to reflect impaired attribution of salience to errors which then leads to impaired performance (Polli et al., 2008). Hence, the ACC could serve as a neural substrate across a range of cognitive disturbances in EOS which are shared with adult schizophrenia patients.

4.2.2. *rTPJ*

Our meta-analysis provides evidence that the *rTPJ* has significantly reduced activation in EOS patients across different cognitive tasks and this dysfunction persists also within WM only tasks. Even though the *rTPJ* clusters from both functional ALE analyses overlap to a high degree, our cognitive associations analyses revealed a slightly different pattern of behavioural domains coded by each cluster. The *rTPJ* cluster corresponding to the Cognition ALE was primarily involved in social cognition, visual perception, and action inhibition, whereas the one corresponding to WM was primarily involved in social cognition-related behaviours.

Apart from attention reorienting to salient stimuli (Touroutoglou et al., 2012), the *rTPJ* also facilitates an individual's sense of agency (Hughes, 2018) which is impaired in schizophrenia (Koreki et al., 2019). The *rTPJ* plays a domain-general role in social cognition (such as mental state attribution) through gating low-level attentional processes that generate internal predictions about external sensory events (Decety & Lamm, 2007). Attentional shifting mediated by the *rTPJ* is done by detecting unexpected events in the environment and the formation of spatial or social predictions that are held in WM (Krall et al., 2015). Thus, the cognitive associations' findings of the Cognition ALE could be interpreted in light of the *rTPJ* sub-serving social cognitive processes through motor control (action inhibition) and the integration of sensory stimuli (visual perception). These processes could play a part in a wider cognitive framework that involves the detection of saliency, under any circumstances that require cognitive control (e.g. detection of performance errors) (Ham et al., 2013) and executive functioning, such as WM. Therefore, the hypoactivation we observed here could indicate inefficient salience processing of stimuli that are relevant for cognitive and

WM performance. The same dysfunctional processes could also explain impaired social cognition processes that are observed in the disorder.

Additionally, in schizophrenia, TPJ hypoactivation has previously been shown during auditory distraction from a visual attention task (Smucny et al., 2013). This suggests that deficient processing for exogenous/bottom-up cues is mediated by impaired TPJ activation, as observed in an adult and chronically ill sample (Smucny et al., 2013). In a recent meta-analysis, Kim (2018) supported the existence of a frontoparietal network involving the rTPJ activated for subsequent forgetting after repetition enhancement. The author inferred that rTPJ activation results in the suppression of task-irrelevant mind wandering (Kim, 2018). Hence, rTPJ hypoactivity as observed in our meta-analysis could signal the inefficiency of EOS subjects to ‘shut down’ distracting thoughts and focus their attention on WM performance. Additionally, morphological examination of rTPJ in adult patients has shown that an abnormal sulcal pattern was associated with deficits in sense of agency and auditory hallucinations (Plaze et al., 2015). We suggest that the rTPJ is tied to the neurodevelopment of the disorder, an idea which is reinforced by the early insult in its sulcal development, as sulcal patterns are determined in utero (Plaze et al., 2015), and by reduced activity related to cognitive and WM processes in the EOS population, as our results suggest.

4.2.3. *Posterior parietal cortices: Attentional and executive dysfunction*

Focusing only on the WM experiments, our results not only showed hypoactivation in the rTPJ cluster but also bilaterally in the posterior parietal cortex (IPreC and rIPL). The paradigms in this meta-analysis included verbal and visuospatial WM. In our ALE results, the cluster with the highest ALE value was located in the IPreC. Our cognitive

association analysis of this cluster showed it was associated with cognitive functions of language and memory, as well as visual perception. On the right hemisphere, the hypoactivation peaked on the more inferior part of the parietal lobe (rIPL) with activity related to WM, spatial cognition, action and motion perception.

Evidence from anatomical studies reveals parietal grey matter loss starting early in patients with childhood-onset schizophrenia, whereas bilateral SPL grey matter demonstrates the highest loss rate (Thompson et al., 2001). Early parietal abnormalities are a consistent finding in schizophrenia research (Burke et al., 2008; Zhao et al., 2018). There is supporting evidence that the lPreC volume is a successful classifier for EOS in a multivariate machine learning study (Greenstein et al., 2012), while rIPL and bilateral PreC resting state BOLD abnormalities accurately predicted adolescents with schizophrenia against typically developing controls (Liu et al., 2018). Yildiz et al. (2011) proposed the ‘parietal type’ of schizophrenia in which parietal, both anatomical and functional, impairments mark the second insult (the first insult being early in life before the overt manifestation of clinical symptoms in line with the neurodevelopmental model of the disorder including genetic, pregnancy and infancy factors) that triggers illness onset in some patients and is later progressing to frontal regions. This parietal impairment is first evidenced by WM impairment and sense of agency deficits (Yildiz et al., 2011) and hence could explain delusions of control seen in the disorder (Blakemore & Frith, 2003).

Functional imaging suggests that the posterior parietal areas that cover the PreC/IPS (BA: 7/40) are responsible for the manipulation of information in WM (Champod & Petrides, 2010), such as binding verbal and spatial stimuli (Grot et al., 2017) and for creating saliency maps for subsequent attentional selection (Bisley & Goldberg, 2010). Active binding in WM, which has been shown to be affected in

schizophrenia patients, is partially explained by insufficient allocation of attentional resources and has a neural substrate located in the IPreC and bilateral IPL (Grot et al., 2017). Our IPreC and rIPL clusters of hypoactivation in EOS could indicate patients' reduced ability to manipulate verbal and spatial information in WM, as the included tasks comprised of both modalities which our left and right parietal clusters were respectively functionally associated with. Additionally, reduced connectivity of the frontoparietal network has been observed in schizophrenia: Dysconnectivity of the IPreC and rIPL to dorsal cingulate cortex has been linked to lack of cognitive control (Fornito et al., 2011), while frontoparietal dysconnectivity during WM performance has been suggested as a potential biomarker of the disorder (Loeb et al., 2018). Andre et al. (2016) found evidence for decreased rIPL activation and IPreC activation increase with aging in healthy subjects. Developmentally, this could mean that EOS patients reach a posterior parietal activation plateau similar to adult levels before actually entering adulthood. The results in this meta-analysis together with previous studies in patients with schizophrenia highlight a parietal insult in multiple loci that extends from structure to activity.

4.3. Meta-analytic co-activation modelling (MACM):

Saliency dysfunction

We followed up our ALE meta-analyses of cognition and WM in EOS by exploring the task-dependent co-activation patterns of our suprathreshold clusters with aberrant activation. EOS is marked with convergent hypoactivation in areas of the ACC and rTPJ across different cognitive processes. Using our clusters as seeds to explore their task-dependent functional connectivity we discovered they are all co-activated with a more posterior part of the ACC or aMCC/medial frontal gyrus and bilateral insular cortices. Similarly, the posterior parietal and rTPJ seeds that demonstrate reduced

activation during WM activate the same core network. This core network maps heavily on the salience network (Seeley et al., 2007). As the salience network co-activates with the ACC, rTPJ and posterior parietal cortices – areas responsible for attention (endogenous and exogenous), reward, WM and visual perception – it becomes clear that this system integrates all these processes for successful cognitive and WM performance.

Decreased grey matter volume of the salience network (ACC/medial frontal gyrus and bilateral insula) has been a consistent finding across psychiatric conditions, and especially schizophrenia (Goodkind et al., 2015). In our meta-analysis, we did not detect consistent aberrant activity of the insular cortices in EOS, however, both our ALE results detected hypoactivation of the rTPJ. rTPJ is intimately linked to the ventral attentional network, responsible for reorienting attention to behaviourally relevant and salient stimuli (Corbetta et al., 2008). Kucyi and colleagues (2012) have previously argued that the ventral attention and salience networks are likely undifferentiated, owing to the high degree of functional and spatial overlap (Kucyi et al., 2012). Therefore, the rTPJ could be considered a node of the salience network, and together with the ACC they show hypoactivation in EOS which in turn could point to a central salience processing dysfunction relevant to general cognition.

4.4. Conclusions

This is the first coordinate-based meta-analysis of VBM and fMRI literature in EOS. The VBM meta-analysis did not reveal any reduction of grey matter volume in EOS patients. Our fMRI results highlight brain areas of consistently reduced activation across studies that are common for EOS. These areas include the ACC during general cognition, the bilateral posterior parietal cortices during WM and the rTPJ during cognition and WM. Furthermore, our post-hoc analysis showed that the salience network is functionally connected with these hypoactivating nodes identified here.

Evidence from previous studies supports the idea that a salience processing impairment is central to schizophrenia and patients demonstrate disruptions of within- and between-salience network connectivity with other functional networks. Thus, saliency dysfunction could play a central role in EOS and lead to cognitive symptoms in the disorder, such as poor WM and goal-directed attention.

References

- Andre, J., Picchioni, M., Zhang, R., & Touloupoulou, T. (2016). Working memory circuit as a function of increasing age in healthy adolescence: A systematic review and meta-analyses. *NeuroImage: Clinical*, *12*, 940–948. <https://doi.org/10.1016/j.nicl.2015.12.002>
- Beissner, F., Meissner, K., Bar, K.-J., & Napadow, V. (2013). The Autonomic Brain: An Activation Likelihood Estimation Meta-Analysis for Central Processing of Autonomic Function. *Journal of Neuroscience*, *33*(25), 10503–10511. <https://doi.org/10.1523/JNEUROSCI.1103-13.2013>
- Benjamini, Y., & Hochberg, Y. (1995). Controlling the False Discovery Rate: A Practical and Powerful Approach to Multiple Testing. *Journal of the Royal Statistical Society: Series B (Methodological)*, *57*(1), 289–300. <https://doi.org/10.1111/j.2517-6161.1995.tb02031.x>
- Bisley, J. W., & Goldberg, M. E. (2010). Attention, Intention, and Priority in the Parietal Lobe. *Annual Review of Neuroscience*, *33*(1), 1–21. <https://doi.org/10.1146/annurev-neuro-060909-152823>
- Bittner, R. A., Linden, D. E. J., Roebroek, A., Härtling, F., Rotarska-Jagiela, A., Maurer, K., Goebel, R., Singer, W., & Haenschel, C. (2015). The When and Where of Working Memory Dysfunction in Early-Onset Schizophrenia—A Functional Magnetic Resonance Imaging Study. *Cerebral Cortex*, *25*(9), 2494–2506. <https://doi.org/10.1093/cercor/bhu050>
- Blakemore, S. J., & Frith, C. (2003). Self-awareness and action. *Current Opinion in Neurobiology*, *13*(2), 219–224. [https://doi.org/10.1016/S0959-4388\(03\)00043-6](https://doi.org/10.1016/S0959-4388(03)00043-6)
- Borofsky, L. A., McNealy, K., Siddarth, P., Wu, K. N., Dapretto, M., & Caplan, R. (2010). Semantic processing and thought disorder in childhood-onset schizophrenia: Insights from fMRI. *Journal of Neurolinguistics*, *23*(3), 204–222. <https://doi.org/10.1016/j.jneuroling.2009.07.004>
- Botvinick, M. M. (2007). Conflict monitoring and decision making: Reconciling two perspectives on anterior cingulate function. *Cognitive, Affective and Behavioral Neuroscience*, *7*(4), 356–366. <https://doi.org/10.3758/CABN.7.4.356>
- Burke, L., Androustos, C., Jogia, J., Byrne, P., & Frangou, S. (2008). The Maudsley Early Onset Schizophrenia Study: The effect of age of onset and illness duration on fronto-parietal gray matter. *European Psychiatry*, *23*(4), 233–236. <https://doi.org/10.1016/j.eurpsy.2008.03.007>
- Cannon, M., Jones, P., Huttunen, M. O., Tanskanen, A., Huttunen, T., Rabe-Hesketh, S., & Murray, R. M. (1999). School performance in Finnish children and later development of schizophrenia: A population-based longitudinal study. *Archives of General Psychiatry*, *56*(5), 457–463. <https://doi.org/10.1001/archpsyc.56.5.457>

- Casey, B. J., Jones, R. M., & Somerville, L. H. (2011). Braking and accelerating of the adolescent brain. *Journal of Research on Adolescence*, *21*(1), 21–33. <https://doi.org/10.1111/j.1532-7795.2010.00712.x>
- Castro-Fornieles, J., Bargalló, N., Calvo, A., Arango, C., Baeza, I., Gonzalez-Pinto, A., Parellada, M., Graell, M., Moreno, C., Otero, S., Janssen, J., Rapado-Castro, M., & de la Serna, E. (2018). Gray matter changes and cognitive predictors of 2-year follow-up abnormalities in early-onset first-episode psychosis. *European Child & Adolescent Psychiatry*, *27*(1), 113–126. <https://doi.org/10.1007/s00787-017-1013-z>
- Champod, A. S., & Petrides, M. (2010). Dissociation within the Frontoparietal Network in Verbal Working Memory: A Parametric Functional Magnetic Resonance Imaging Study. *Journal of Neuroscience*, *30*(10), 3849–3856. <https://doi.org/10.1523/JNEUROSCI.0097-10.2010>
- Corbetta, M., Patel, G., & Shulman, G. L. (2008). The Reorienting System of the Human Brain: From Environment to Theory of Mind. *Neuron*, *58*(3), 306–324. <https://doi.org/10.1016/j.neuron.2008.04.017>
- Crottaz-Herbette, S., & Menon, V. (2006). Where and When the Anterior Cingulate Cortex Modulates Attentional Response: Combined fMRI and ERP Evidence. *Journal of Cognitive Neuroscience*, *18*(5), 766–780. <https://doi.org/10.1162/jocn.2006.18.5.766>
- Decety, J., & Lamm, C. (2007). The role of the right temporoparietal junction in social interaction: How low-level computational processes contribute to meta-cognition. *Neuroscientist*, *13*(6), 580–593. <https://doi.org/10.1177/1073858407304654>
- Douaud, G., MacKay, C., Andersson, J., James, S., Quested, D., Ray, M. K., Connell, J., Roberts, N., Crow, T. J., Matthews, P. M., Smith, S., & James, A. (2009). Schizophrenia delays and alters maturation of the brain in adolescence. *Brain*, *132*(9), 2437–2448. <https://doi.org/10.1093/brain/awp126>
- Douaud, G., Smith, S., Jenkinson, M., Behrens, T., Johansen-Berg, H., Vickers, J., James, S., Voets, N., Watkins, K., Matthews, P. M., & James, A. (2007). Anatomically related grey and white matter abnormalities in adolescent-onset schizophrenia. *Brain*, *130*(9), 2375–2386. <https://doi.org/10.1093/brain/awm184>
- Eickhoff, S. B., Bzdok, D., Laird, A. R., Kurth, F., & Fox, P. T. (2012). Activation likelihood estimation meta-analysis revisited. *NeuroImage*, *59*(3), 2349–2361. <https://doi.org/10.1016/j.neuroimage.2011.09.017>
- Eickhoff, S. B., Laird, A. R., Grefkes, C., Wang, L. E., Zilles, K., & Fox, P. T. (2009). Coordinate-based activation likelihood estimation meta-analysis of neuroimaging data: A random-effects approach based on empirical estimates of spatial uncertainty. *Human Brain Mapping*, *30*(9), 2907–2926.

<https://doi.org/10.1002/hbm.20718>

- Eickhoff, S. B., Nichols, T. E., Laird, A. R., Hoffstaedter, F., Amunts, K., Fox, P. T., Bzdok, D., & Eickhoff, C. R. (2016). Behavior, sensitivity, and power of activation likelihood estimation characterized by massive empirical simulation. *NeuroImage*, *137*, 70–85.
<https://doi.org/10.1016/j.neuroimage.2016.04.072>
- Evans, A. C., Collins, D. L., Mills, S. R., Brown, E. D., Kelly, R. L., & Peters, T. M. (1993). 3D statistical neuroanatomical models from 305 MRI volumes. *1993 IEEE Conference Record Nuclear Science Symposium and Medical Imaging Conference*, 1813–1817.
<https://doi.org/10.1109/NSSMIC.1993.373602>
- Fornito, A., Yoon, J., Zalesky, A., Bullmore, E. T., & Carter, C. S. (2011). General and specific functional connectivity disturbances in first-episode schizophrenia during cognitive control performance. *Biological Psychiatry*, *70*(1), 64–72. <https://doi.org/10.1016/j.biopsych.2011.02.019>
- Fox, P. T., Laird, A. R., Fox, S. P., Fox, P. M., Uecker, A. M., Crank, M., Koenig, S. F., & Lancaster, J. L. (2005). BrainMap taxonomy of experimental design: Description and evaluation. *Human Brain Mapping*, *25*(1), 185–198. <https://doi.org/10.1002/hbm.20141>
- Fraguas, D., Díaz-Caneja, C. M., Pina-Camacho, L., Janssen, J., & Arango, C. (2016). Progressive brain changes in children and adolescents with early-onset psychosis: A meta-analysis of longitudinal MRI studies. *Schizophrenia Research*, *173*(3), 132–139.
<https://doi.org/10.1016/j.schres.2014.12.022>
- Fryer, S. L., Woods, S. W., Kiehl, K. A., Calhoun, V. D., Pearlson, G. D., Roach, B. J., Ford, J. M., Srihari, V. H., McGlashan, T. H., & Mathalon, D. H. (2013). Deficient suppression of default mode regions during working memory in individuals with early psychosis and at clinical high-risk for psychosis. *Frontiers in Psychiatry*, *4*(SEP), 1–17. <https://doi.org/10.3389/fpsy.2013.00092>
- Glahn, D. C., Laird, A. R., Ellison-Wright, I., Thelen, S. M., Robinson, J. L., Lancaster, J. L., Bullmore, E., & Fox, P. T. (2008). Meta-Analysis of Gray Matter Anomalies in Schizophrenia: Application of Anatomic Likelihood Estimation and Network Analysis. *Biological Psychiatry*, *64*(9), 774–781.
<https://doi.org/10.1016/j.biopsych.2008.03.031>
- Glahn, D. C., Ragland, J. D., Abramoff, A., Barrett, J., Laird, A. R., Bearden, C. E., & Velligan, D. I. (2005). Beyond hypofrontality: A quantitative meta-analysis of functional neuroimaging studies of working memory in schizophrenia. *Human Brain Mapping*, *25*(1), 60–69.
<https://doi.org/10.1002/hbm.20138>
- Gogtay, N., Nugent, T. F., Herman, D. H., Ordonez, A., Greenstein, D., Hayashi, K. M., Clasen, L., Toga, A. W., Giedd, J. N., Rapoport, J. L., & Thompson, P. M. (2006). Dynamic mapping of normal human hippocampal development. *Hippocampus*, *16*(8), 664–672.

<https://doi.org/10.1002/hipo.20193>

- Goodkind, M., Eickhoff, S. B., Oathes, D. J., Jiang, Y., Chang, A., Jones-Hagata, L. B., Ortega, B. N., Zaiko, Y. V., Roach, E. L., Korgaonkar, M. S., Grieve, S. M., Galatzer-Levy, I., Fox, P. T., & Etkin, A. (2015). Identification of a common neurobiological substrate for mental illness. *JAMA Psychiatry*, *72*(4), 305–315. <https://doi.org/10.1001/jamapsychiatry.2014.2206>
- Greenstein, D., Malley, J. D., Weisinger, B., Clasen, L., & Gogtay, N. (2012). Using Multivariate Machine Learning Methods and Structural MRI to Classify Childhood Onset Schizophrenia and Healthy Controls. *Frontiers in Psychiatry*, *3*(June), 1–12. <https://doi.org/10.3389/fpsy.2012.00053>
- Grot, S., Légaré, V. P., Lipp, O., Soulières, I., Dolcos, F., & Luck, D. (2017). Abnormal prefrontal and parietal activity linked to deficient active binding in working memory in schizophrenia. *Schizophrenia Research*, *188*, 68–74. <https://doi.org/10.1016/j.schres.2017.01.021>
- Ham, T., Leff, A., de Boissezon, X., Joffe, A., & Sharp, D. J. (2013). Cognitive Control and the Salience Network: An Investigation of Error Processing and Effective Connectivity. *Journal of Neuroscience*, *33*(16), 7091–7098. <https://doi.org/10.1523/JNEUROSCI.4692-12.2013>
- Henson, R. (2006). Forward inference using functional neuroimaging: Dissociations versus associations. *Trends in Cognitive Sciences*, *10*(2), 64–69. <https://doi.org/10.1016/j.tics.2005.12.005>
- Hughes, G. (2018). The role of the temporoparietal junction in implicit and explicit sense of agency. *Neuropsychologia*, *113*(March), 1–5. <https://doi.org/10.1016/j.neuropsychologia.2018.03.020>
- Janssen, J., Alemán-Gómez, Y., Schnack, H., Balaban, E., Pina-Camacho, L., Alfaro-Almagro, F., Castro-Fornieles, J., Otero, S., Baeza, I., Moreno, D., Bargalló, N., Parellada, M., Arango, C., & Desco, M. (2014). Cortical morphology of adolescents with bipolar disorder and with schizophrenia. *Schizophrenia Research*, *158*(1–3), 91–99. <https://doi.org/10.1016/j.schres.2014.06.040>
- Janssen, J., Reig, S., Parellada, M., Moreno, D., Graell, M., Fraguas, D., Zabala, A., Garcia Vazquez, V., Desco, M., & Arango, C. (2008). Regional Gray Matter Volume Deficits in Adolescents With First-Episode Psychosis. *Journal of the American Academy of Child & Adolescent Psychiatry*, *47*(11), 1311–1320. <https://doi.org/10.1097/CHI.0b013e318184ff48>
- Juuhl-Langseth, M., Rimol, L. M., Rasmussen, I. A., Thormodsén, R., Holmén, A., Emblem, K. E., Due-Tønnessen, P., Rund, B. R., & Agartz, I. (2012). Comprehensive segmentation of subcortical brain volumes in early onset schizophrenia reveals limited structural abnormalities. *Psychiatry Research: Neuroimaging*, *203*(1), 14–23. <https://doi.org/10.1016/j.psychres.2011.10.005>
- Kapur, S. (2003). Psychosis as a state of aberrant salience: A framework linking biology, phenomenology, and pharmacology in schizophrenia. In *American Journal of Psychiatry* (Vol. 160,

Issue 1, pp. 13–23). <https://doi.org/10.1176/appi.ajp.160.1.13>

- Kerns, J. G., Cohen, J. D., Iii, A. W. M., Johnson, M. K., Stenger, A., Aizenstein, H., & Carter, C. S. (2005). Decreased Conflict- and Error-Related Activity in the Anterior Cingulate Cortex in Subjects With Schizophrenia. *American Journal of Psychiatry*, *162*(October), 1833–1839.
- Kim, H. (2018). Parietal control network activation during memory tasks may be associated with the co-occurrence of externally and internally directed cognition: A cross-function meta-analysis. *Brain Research*, *1683*, 55–66. <https://doi.org/10.1016/j.brainres.2018.01.022>
- Koreki, A., Maeda, T., Okimura, T., Terasawa, Y., Kikuchi, T., Umeda, S., Nishikata, S., Yagihashi, T., Kasahara, M., Nagai, C., Moriyama, Y., Den, R., Watanabe, T., Kikumoto, H., Kato, M., & Mimura, M. (2019). Dysconnectivity of the Agency Network in Schizophrenia: A Functional Magnetic Resonance Imaging Study. *Frontiers in Psychiatry*, *10*(April), 1–11. <https://doi.org/10.3389/fpsy.2019.00171>
- Krall, S. C., Rottschy, C., Oberwelling, E., Bzdok, D., Fox, P. T., Eickhoff, S. B., Fink, G. R., & Konrad, K. (2015). The role of the right temporoparietal junction in attention and social interaction as revealed by ALE meta-analysis. In *Brain Structure and Function* (Vol. 220, Issue 2, pp. 587–604). <https://doi.org/10.1007/s00429-014-0803-z>
- Kucyi, A., Hodaie, M., & Davis, K. D. (2012). Lateralization in intrinsic functional connectivity of the temporoparietal junction with salience- and attention-related brain networks. *Journal of Neurophysiology*, *108*(12), 3382–3392. <https://doi.org/10.1152/jn.00674.2012>
- Kyriakopoulos, M., Dima, D., Roiser, J. P., Corrigall, R., Barker, G. J., & Frangou, S. (2012). Abnormal Functional Activation and Connectivity in the Working Memory Network in Early-Onset Schizophrenia. *Journal of the American Academy of Child & Adolescent Psychiatry*, *51*(9), 911–920.e2. <https://doi.org/10.1016/j.jaac.2012.06.020>
- Kyriakopoulos, M., & Frangou, S. (2007). Pathophysiology of early onset schizophrenia. *International Review of Psychiatry*, *19*(4), 315–324. <https://doi.org/10.1080/09540260701486258>
- Laird, A. R., Eickhoff, S. B., Rottschy, C., Bzdok, D., Ray, K. L., & Fox, P. T. (2013). Networks of task co-activations. *NeuroImage*, *80*, 505–514. <https://doi.org/10.1016/j.neuroimage.2013.04.073>
- Laird, A. R., Lancaster, J. L., & Fox, P. T. (2005). The Social Evolution of a Human Brain Mapping Database. *Neuroinformatics*, *3*(5), 65–77.
- Laitinen, L. (1989). Co-planar stereotaxic atlas of the human brain. *Clinical Neurology and Neurosurgery*, *91*(3), 277–278. [https://doi.org/10.1016/0303-8467\(89\)90128-5](https://doi.org/10.1016/0303-8467(89)90128-5)
- Laurens, K. R., Kiehl, K. A., Ngan, E. T. C., & Liddle, P. F. (2005). Attention orienting dysfunction during salient novel stimulus processing in schizophrenia. *Schizophrenia Research*, *75*(2–3), 159–

171. <https://doi.org/10.1016/j.schres.2004.12.010>
- Liu, Y., Zhang, Y., Lv, L., Wu, R., Zhao, J., & Guo, W. (2018). Abnormal neural activity as a potential biomarker for drug-naïve first-episode adolescent-onset schizophrenia with coherence regional homogeneity and support vector machine analyses. *Schizophrenia Research*, *192*, 408–415. <https://doi.org/10.1016/j.schres.2017.04.028>
- Loeb, F. F., Zhou, X., Craddock, K. E. S., Shora, L., Broadnax, D. D., Gochman, P., Clasen, L. S., Lalonde, F. M., Berman, R. A., Berman, K. F., Rapoport, J. L., & Liu, S. (2018). Reduced Functional Brain Activation and Connectivity During a Working Memory Task in Childhood-Onset Schizophrenia. *Journal of the American Academy of Child and Adolescent Psychiatry*, *57*(3), 166–174. <https://doi.org/10.1016/j.jaac.2017.12.009>
- Luck, S. J., & Gold, J. M. (2008). The Construct of Attention in Schizophrenia. *Biological Psychiatry*, *64*(1), 34–39. <https://doi.org/10.1016/j.biopsych.2008.02.014>
- Moher, D., Liberati, A., Tetzlaff, J., Altman, D. G., Altman, D., Antes, G., Atkins, D., Barbour, V., Barrowman, N., Berlin, J. A., Clark, J., Clarke, M., Cook, D., D'Amico, R., Deeks, J. J., Devereaux, P. J., Dickersin, K., Egger, M., Ernst, E., ... Tugwell, P. (2009). Preferred reporting items for systematic reviews and meta-analyses: The PRISMA statement. *PLoS Medicine*, *6*(7). <https://doi.org/10.1371/journal.pmed.1000097>
- Moran, M. E., Weisinger, B., Ludovici, K., McAdams, H., Greenstein, D., Gochman, P., Miller, R., Clasen, L., Rapoport, J. L., & Gogtay, N. (2014). At the boundary of the self: The insular cortex in patients with childhood-onset schizophrenia, their healthy siblings, and normal volunteers. *International Journal of Developmental Neuroscience*, *32*, 58–63. <https://doi.org/10.1016/j.ijdevneu.2013.05.010>
- Müller, V. I., Cieslik, E. C., Laird, A. R., Fox, P. T., Radua, J., Mataix-Cols, D., Tench, C. R., Yarkoni, T., Nichols, T. E., Turkeltaub, P. E., Wager, T. D., & Eickhoff, S. B. (2018). Ten simple rules for neuroimaging meta-analysis. *Neuroscience and Biobehavioral Reviews*, *84*(November 2017), 151–161. <https://doi.org/10.1016/j.neubiorev.2017.11.012>
- Nichols, T., Brett, M., Andersson, J., Wager, T., & Poline, J. B. (2005). Valid conjunction inference with the minimum statistic. *NeuroImage*, *25*(3), 653–660. <https://doi.org/10.1016/j.neuroimage.2004.12.005>
- Oknina, L. B., Wild-Wall, N., Oades, R. D., Juran, S. A., Röpcke, B., Pfueller, U., Weisbrod, M., Chan, E., & Chen, E. Y. H. (2005). Frontal and temporal sources of mismatch negativity in healthy controls, patients at onset of schizophrenia in adolescence and others at 15 years after onset. *Schizophrenia Research*, *76*(1), 25–41. <https://doi.org/10.1016/j.schres.2004.10.003>
- Pagsberg, A. K., Baaré, W. F. C., Raabjerg Christensen, A. M., Fagerlund, B., Hansen, M.-B., LaBianca,

- J., Krabbe, K., Aarkrog, T., Paulson, O. B., & Hemmingsen, R. P. (2007). Structural brain abnormalities in early onset first-episode psychosis. *Journal of Neural Transmission*, *114*(4), 489–498. <https://doi.org/10.1007/s00702-006-0573-8>
- Palaniyappan, L., Das, T. K., Winmill, L., Hough, M., & James, A. (2019). Progressive post-onset reorganisation of MRI-derived cortical thickness in adolescents with schizophrenia. *Schizophrenia Research*, *208*, 477–478. <https://doi.org/10.1016/j.schres.2019.01.041>
- Park, S., & Gooding, D. C. (2014). Working memory impairment as an endophenotypic marker of a schizophrenia diathesis. *Schizophrenia Research: Cognition*, *1*(3), 127–136. <https://doi.org/10.1016/j.scog.2014.09.005>
- Pauly, K., Seiferth, N. Y., Kellermann, T., Backes, V., Vloet, T. D., Shah, N. J., Schneider, F., Habel, U., & Kircher, T. T. (2008). Cerebral Dysfunctions of Emotion—Cognition Interactions in Adolescent-Onset Schizophrenia. *Journal of the American Academy of Child & Adolescent Psychiatry*, *47*(11), 1299–1310. <https://doi.org/10.1097/CHI.0b013e318184ff16>
- Petit, L., Courtney, S. M., Ungerleider, L. G., & Haxby, J. V. (1998). Sustained Activity in the Medial Wall during Working Memory Delays. *The Journal of Neuroscience*, *18*(22), 9429–9437.
- Plaze, M., Mangin, J. F., Paillère-Martinot, M. L., Artiges, E., Olié, J. P., Krebs, M. O., Gaillard, R., Martinot, J. L., & Cachia, A. (2015). “Who is talking to me?” - Self-other attribution of auditory hallucinations and sulcation of the right temporoparietal junction. *Schizophrenia Research*, *169*(1–3), 95–100. <https://doi.org/10.1016/j.schres.2015.10.011>
- Poldrack, R. A. (2006). Can cognitive processes be inferred from neuroimaging data? *Trends in Cognitive Sciences*, *10*(2), 59–63. <https://doi.org/10.1016/j.tics.2005.12.004>
- Polli, F. E., Barton, J. J. S., Thakkar, K. N., Greve, D. N., Goff, D. C., Rauch, S. L., & Manoach, D. S. (2008). Reduced error-related activation in two anterior cingulate circuits is related to impaired performance in schizophrenia. *Brain*, *131*(4), 971–986. <https://doi.org/10.1093/brain/awm307>
- Rapoport, J. L., Addington, A. M., Frangou, S., & Psych, M. R. C. (2005). The neurodevelopmental model of schizophrenia: update 2005. *Molecular Psychiatry*, *10*(5), 434–449. <https://doi.org/10.1038/sj.mp.4001642>
- Rasgon, A., Lee, W. H., Leibu, E., Laird, A., Glahn, D., Goodman, W., & Frangou, S. (2017). Neural correlates of affective and non-affective cognition in obsessive compulsive disorder: A meta-analysis of functional imaging studies. *European Psychiatry*. <https://doi.org/10.1016/j.eurpsy.2017.08.001>
- Robinson, J. L., Laird, A. R., Glahn, D. C., Blangero, J., Sanghera, M. K., Pessoa, L., Fox, P. M., Uecker, A., Friebs, G., Young, K. A., Griffin, J. L., Lovallo, W. R., & Fox, P. T. (2012). The functional

- connectivity of the human caudate: An application of meta-analytic connectivity modeling with behavioral filtering. *NeuroImage*, 60(1), 117–129.
<https://doi.org/10.1016/j.neuroimage.2011.12.010>
- Robinson, J. L., Laird, A. R., Glahn, D. C., Lovallo, W. R., Fox, P. T., & Fox, T. (2010). Metaanalytic connectivity modeling: Delineating the functional connectivity of the human amygdala. *Human Brain Mapping*, 31(2), 173–184. <https://doi.org/10.1002/hbm.20854>
- Rydkjær, J., Møllegaard Jepsen, J. R., Pagsberg, A. K., Fagerlund, B., Glenthøj, B. Y., & Oranje, B. (2017). Mismatch negativity and P3a amplitude in young adolescents with first-episode psychosis: A comparison with ADHD. *Psychological Medicine*, 47(2), 377–388.
<https://doi.org/10.1017/S0033291716002518>
- Seeley, W. W., Menon, V., Schatzberg, A. F., Keller, J., Glover, G. H., Kenna, H., Reiss, A. L., & Greicius, M. D. (2007). Dissociable Intrinsic Connectivity Networks for Salience Processing and Executive Control. *Journal of Neuroscience*, 27(9), 2349–2356.
<https://doi.org/10.1523/jneurosci.5587-06.2007>
- Seiferth, N. Y., Pauly, K., Kellermann, T., Shah, N. J., Ott, G., Herpertz-Dahlmann, B., Kircher, T., Schneider, F., & Habel, U. (2009). Neuronal Correlates of Facial Emotion Discrimination in Early Onset Schizophrenia. *Neuropsychopharmacology*, 34(2), 477–487.
<https://doi.org/10.1038/npp.2008.93>
- Smucny, J., Rojas, D. C., Eichman, L. C., & Tregellas, J. R. (2013). Neural Effects of Auditory Distraction on Visual Attention in Schizophrenia. *PLoS ONE*, 8(4), 1–9.
<https://doi.org/10.1371/journal.pone.0060606>
- Tahmasian, M., Eickhoff, S. B., Giehl, K., Schwartz, F., Herz, D. M., Drzezga, A., van Eimeren, T., Laird, A. R., Fox, P. T., Khazaie, H., Zarei, M., Eggers, C., & Eickhoff, C. R. (2017). Resting-state functional reorganization in Parkinson's disease: An activation likelihood estimation meta-analysis. *Cortex*, 92, 119–138. <https://doi.org/10.1016/j.cortex.2017.03.016>
- Tang, J., Liao, Y., Zhou, B., Tan, C., Liu, W., Wang, D., Liu, T., Hao, W., Tan, L., & Chen, X. (2012). Decrease in Temporal Gyrus Gray Matter Volume in First-Episode, Early Onset Schizophrenia: An MRI Study. *PLoS ONE*, 7(7), e40247. <https://doi.org/10.1371/journal.pone.0040247>
- Thompson, P. M., Vidal, C., Giedd, J. N., Gochman, P., Blumenthal, J., Nicolson, R., Toga, A. W., & Rapoport, J. L. (2001). Mapping adolescent brain change reveals dynamic wave of accelerated gray matter loss in very early-onset schizophrenia. *Proceedings of the National Academy of Sciences*, 98(20), 11650–11655. <https://doi.org/10.1073/pnas.201243998>
- Thormodsen, R., Jensen, J., Holmèn, A., Juuhl-Langseth, M., Emblem, K. E., Andreassen, O. A., & Rund, B. R. (2011). Prefrontal hyperactivation during a working memory task in early-onset

- schizophrenia spectrum disorders: An fMRI study. *Psychiatry Research - Neuroimaging*, *194*(3), 257–262. <https://doi.org/10.1016/j.psychresns.2011.05.011>
- Thormodsen, R., Rimol, L. M., Tamnes, C. K., Juuhl-Langseth, M., Holmén, A., Emblem, K. E., Rund, B. R., & Agartz, I. (2013). Age-related cortical thickness differences in adolescents with early-onset schizophrenia compared with healthy adolescents. *Psychiatry Research - Neuroimaging*, *214*(3), 190–196. <https://doi.org/10.1016/j.psychresns.2013.07.003>
- Touroutoglou, A., Hollenbeck, M., Dickerson, B. C., & Feldman Barrett, L. (2012). Dissociable large-scale networks anchored in the right anterior insula subserve affective experience and attention. *NeuroImage*, *60*(4), 1947–1958. <https://doi.org/10.1016/j.neuroimage.2012.02.012>
- Turkeltaub, P. E., Eickhoff, S. B., Laird, A. R., Fox, M., Wiener, M., & Fox, P. (2012). Minimizing within-experiment and within-group effects in activation likelihood estimation meta-analyses. *Human Brain Mapping*, *33*(1), 1–13. <https://doi.org/10.1002/hbm.21186>
- van Erp, T. G., Walton, E., Hibar, D. P., Schmaal, L., Jiang, W., Glahn, D. C., Pearlson, G. D., Yao, N., Fukunaga, M., Hashimoto, R., Okada, N., Yamamori, H., Bustillo, J. R., Clark, V. P., Agartz, I., Mueller, B. A., Cahn, W., de Zwarte, S. M., Hulshoff Pol, H. E., ... Orhan, F. (2018). Cortical Brain Abnormalities in 4474 Individuals With Schizophrenia and 5098 Control Subjects via the Enhancing Neuro Imaging Genetics Through Meta Analysis (ENIGMA) Consortium. *Biological Psychiatry*, *84*(9), 644–654. <https://doi.org/10.1016/j.biopsych.2018.04.023>
- Van Snellenberg, J. X., Girgis, R. R., Horga, G., van de Giessen, E., Slifstein, M., Ojeil, N., Weinstein, J. J., Moore, H., Lieberman, J. A., Shohamy, D., Smith, E. E., & Abi-Dargham, A. (2016). Mechanisms of Working Memory Impairment in Schizophrenia. *Biological Psychiatry*, *80*(8), 617–626. <https://doi.org/10.1016/j.biopsych.2016.02.017>
- Vidal, C. N., Rapoport, J. L., Hayashi, K. M., Geaga, J. A., Sui, Y., McLemore, L. E., Alagband, Y., Giedd, J. N., Gochman, P., Blumenthal, J., Gogtay, N., Nicolson, R., Toga, A. W., & Thompson, P. M. (2006). Dynamically Spreading Frontal and Cingulate Deficits Mapped in Adolescents With Schizophrenia. *Archives of General Psychiatry*, *63*(January), 25–34.
- Vyas, N. S., Patel, N. H., & Puri, B. K. (2011). Neurobiology and phenotypic expression in early onset schizophrenia. *Early Intervention in Psychiatry*, *5*(1), 3–14. <https://doi.org/10.1111/j.1751-7893.2010.00253.x>
- White, T., Hongwanishkul, D., & Schmidt, M. (2011). Increased anterior cingulate and temporal lobe activity during visuospatial working memory in children and adolescents with schizophrenia. *Schizophrenia Research*, *125*(2–3), 118–128. <https://doi.org/10.1016/j.schres.2010.11.014>
- White, T., Schmidt, M., Kim, D. II, & Calhoun, V. D. (2011). Disrupted functional brain connectivity during verbal working memory in children and adolescents with schizophrenia. *Cerebral Cortex*,

21(3), 510–518. <https://doi.org/10.1093/cercor/bhq114>

Yarkoni, T., Poldrack, R. A., Nichols, T. E., Van Essen, D. C., & Wager, T. D. (2011). Large-scale automated synthesis of human functional neuroimaging data. *Nature Methods*, 8(8), 665–670. <https://doi.org/10.1038/nmeth.1635>

Yildiz, M., Borgwardt, S. J., & Berger, G. E. (2011). Parietal Lobes in Schizophrenia: Do They Matter? *Schizophrenia Research and Treatment*, 2011(February), 1–15. <https://doi.org/10.1155/2011/581686>

Yoshihara, Y., Sugihara, G., Matsumoto, H., Suckling, J., Nishimura, K., Toyoda, T., Isoda, H., Tsuchiya, K. J., Takebayashi, K., Suzuki, K., Sakahara, H., Nakamura, K., Mori, N., & Takei, N. (2008). Voxel-based structural magnetic resonance imaging (MRI) study of patients with early onset schizophrenia. *Annals of General Psychiatry*, 7, 1–11. <https://doi.org/10.1186/1744-859X-7-25>

Zhang, C., Wang, Q., Ni, P., Deng, W., Li, Y., Zhao, L., Ma, X., Wang, Y., Yu, H., Li, X., Zhang, P., Meng, Y., Liang, S., Li, M., & Li, T. (2017). Differential Cortical Gray Matter Deficits in Adolescent- and Adult-Onset First-Episode Treatment-Naïve Patients with Schizophrenia. *Scientific Reports*, 7(1), 1–9. <https://doi.org/10.1038/s41598-017-10688-1>

Zhang, Y., Zheng, J., Fan, X., Guo, X., Guo, W., Yang, G., Chen, H., Zhao, J., & Lv, L. (2015). Dysfunctional resting-state connectivities of brain regions with structural deficits in drug-naïve first-episode schizophrenia adolescents. *Schizophrenia Research*, 168(1–2), 353–359. <https://doi.org/10.1016/j.schres.2015.07.031>

Zhao, C., Zhu, J., Liu, X., Pu, C., Lai, Y., Chen, L., Yu, X., & Hong, N. (2018). Structural and functional brain abnormalities in schizophrenia: A cross-sectional study at different stages of the disease. *Progress in Neuro-Psychopharmacology and Biological Psychiatry*, 83(11), 27–32. <https://doi.org/10.1016/j.pnpbp.2017.12.017>

Zwicker, A., Denovan-Wright, E. M., & Uher, R. (2018). Gene–environment interplay in the etiology of psychosis. *Psychological Medicine*, 48(12), 1925–1936. <https://doi.org/10.1017/S003329171700383X>

Tables

Table 3.1. Summary of the demographic and clinical variables for the 7 VBM studies and the 8 fMRI studies

	No	Author	Sample (M/F)	Age Mean (SD/range)	Age of illness onset (AIO) Duration of illness (DI)	Medication Mean mg/day (SD/Range)	Symptom Scores Mean (SD)
VBM studies	1	Douaud et al 2007	EOS = 25 (18/7)	M: 16.5 (1.3)	AIO: 14.9 (1.6/11-16.8)	CPZE: 340 (180)	PANSS positive: 22 (5)
			HC = 25 (17/8)	F: 15.9 (1.5)	DI: 1.4 (0.7)		PANSS negative: 16 (5)
				M: 16.2 (1.7)			
				F: 15.6 (1.3)			
	2	Janssen et al 2008	Patients = 70 (51/19)			CPZE: 329.7 (211.5/80 -920)	PANSS positive: 25.7 (4.2)
			EOS = 25 (19/6)	15.4 (1.8/12-18)	AIO: 15 (1.8/11-17)		PANSS negative: 25.6 (6.8)
					DI: 15.0 (9.3/0-65) weeks (0.29 years)		PANSS general: 48.2 (8.0)
			HC = 51 (35/16)	15.4 (1.6/11-18)			
	3	Yoshihara et al 2008	EOS = 18 (9/9)	15.8 (1.8)	DI: 1.2 (0.9) years	Unspecified	PANSS positive: 13.8 (4.4)
			HC = 18 (9/9)	15.8 (1.3)	AIO <18 yrs		PANSS negative: 19.1 (10.0)
							PANSS global: 31.1 (10.7)
	4	Tang et al 2012	EOS = 29 (13/16)	16.5 (0.9)	AIO: 15.7 (1.0)	CPZE: 252.2 (189.2)	PANSS Positive: 22.3 (2.8)
			HC = 34 (16/18)	16.6 (0.8)	DI: 9.3 (4.6) months (0.76 years)		PANSS negative: 20.8 (3.0)
							PANSS general: 34.5 (3.7)
							PANSS total: 77.7 (5.7)
	5	Zhang Y et al 2015	EOS = 37 (17/20)	15.5 (1.8)	DI: 16.0 (14.4) months	Unspecified	PANSS Positive: 20.42 (5.72)
			HC = 30 (17/13)	15.3 (1.6)			PANSS negative: 20.91 (8.41)
							PANSS general: 33.28 (6.69)
							PANSS total: 74.62 (10.61)
	6	Zhang C et al 2017	EOS = 26 (13/13)	16.87 (1.05)	AIO: 16.51 (1.01)	N/A (treatment naïve)	PANSS positive: 25.12 (4.92)
			HC = 26 (13/13)	16.81 (0.75)	DI: 3.61 (3.50) months (0.30 years)		PANSS negative: 20.46 (8.19)
							PANSS general: 47.85 (9.88)
							PANSS total: 93.42 (16.43)
							PANSS thought disturbance: 13.65 (3.74)
							PANSS activation: 9.12 (2.86)
							PANSS paranoid: 10.62 (2.00)
							PANSS impulsive aggression: 16.85 (5.14)
							PANSS anergia: 9.77 (4.88)
						PANSS depression: 9.15 (3.94)	
7	Castro-Fornieles et al 2018	EOS = 34 (24/10)	15.2 (1.7) *	Not specified**	Cumulative CPZE: 215375.97 (267730.54)	PANSS positive: 14.7 (7.2) ***	
		HC = 70 (48/22)	15.3(1.5)			PANSS negative: 18.1 (8.1)	
						PANSS general: 31.1 (9.9)	
						PANSS total: 63.5 (22.3)	

fMRI studies	1	Pauly et al 2008	EOS = 12 (12/0)	17.5 (0.70)	AIO: 16.10 (0.88/15-17)	Unspecified	PANSS positive: 17.50 (9.19)
			HC = 12 (12/0)	17.5 (1.76)			PANSS negative: 12.70 (5.17)
							PANSS general: 25.30 (5.68)
							GAF: 60.91 (11.36)
	2	Seiferth et al 2009	EOS = 12 (12/0)	17.8 (1.4)	DI: 38 weeks (4-109)	CPZE: 231 (111)	PANSS positive: 16.2 (8.1)
			HC = 12 (12/0)	17.9 (1.5)	(0.73 years)		PANSS negative: 13.3 (6.9)
							PANSS global: 56.3 (22.2)
							GAS: 57.0 (15.8)
	3	Borofsky et al 2010	EOS = 14 (7/7)	13.34 (2.14)	Unspecified	Unspecified	Thought cohesion: 0.48 (0.206)
			HC = 14 (6/8)	12.37 (2.39)	(<13 years old)		Repair of the organization of thoughts: 0.49 (0.181)
							Revision of linguistic errors: 0.50 (0.081)
							Formal thought disorder: 0.41 (0.191)
	4	White et al 2011a	EOS = 22 (15/7)	15.0 (2.8)	AIO: 12.5 (2.4)	CPZE (Woods): 313.89 (153.78)	SANS: 2.8 (0.8)
			Schizophrenia paranoid = 10				SAPS (psychotic symptoms): 2.6 (1.1)
			Schizophrenia disorganised = 1		DI: 1.6 (1.3)		Disorganised symptoms: 1.9 (1.0)
			Schizophrenia undifferentiated = 8				
			Schizoaffective disorder = 2				
			Schizophreniform disorder = 1				
			HC = 24 (16/8)	15.0 (3.0)			
	5	White et al 2011b	EOS = 14 (12/2)	15.1 (2.6)	Unspecified	CPZE (Woods): 184.33 (unspecified)	SANS: 2.6 (0.8)
			Schizophrenia = 11				SAPS (psychotic symptoms): 2.5 (1.2)
			Schizoaffective disorder = 2				Disorganised symptoms: 2.0 (1.2)
			Schizophreniform disorder = 1				
			HC = 14 (12/2)	15.0 (2.8)			
	6	Kyriakopoulos et al 2012	EOS = 25 (14/11)	16.1 (1.5)	AIO: 14.8 (1.6)	CPZE: 285.9 (50 - 1200)	PANSS positive: 8.9 (2.1)
			HC = 20 (12/8)	16.3 (2.1)			PANSS negative: 12.4 (3.4)
							PANSS total: 44 (5.6)
	7	Bittner et al 2015	EOS = 17 (11/6)	17.9 (15.2 - 20.4)	AIO: 16.5 (1.2)	CPZE: 188.7 (166)	PANSS total: 44.92 (18.38)
		HC = 17 (11/6)	17.5 (15.1 - 19.9)				

8	Loeb et al 2018	EOS = 32 (16/16)	21.3 (1.1)	AIO: 10.0 (1.7)	CPZE: 943 (113)	SAPS: 9.8 (6.2)
				DI: 11.3 (1.1) years		SANS: 13.3 (7.6)
		HC = 39 (21/18)	20.0 (0.7)			

CPZE: Chlorpromazine equivalent, EOS: early-onset schizophrenia, GAF: Global Assessment of Functioning, GAS: Global Assessment Scale, HC: healthy controls,

PANSS: positive and negative schizophrenia symptoms, SANS: Scale for the Assessment of Negative Symptoms, SAPS: Scale for the Assessment of Positive Symptoms

* Ages in this sample are given in the baseline study, but cross-sectional EOS-HC differences only reported in the follow up, which was on average 26 months (EOS: M = 26, SD = 3.1; HC: M = 25.8, SD = 2.6)

** Study does not specify AIO, but age range of sample (11-17) presumes onset of illness < 18 years of age

*** PANSS scores are reported at the follow-up scanning time

Table 3.2. Paradigm and coordinate data for the experiments (and contrasts) within the 7 VBM studies followed by the 8 fMRI studies

First author	Year	Subjects		Imaging modality	Brain template	Behavioural task(s)	Design / Software	Subject-Level Analysis	Group-Level Analysis	p threshold	Anatomic labels	Coordinates		
		EOS	HC									x	y	z
Douaud	2007	25	25	VBM	MNI (FSL)	N/A	FSL & SPM2	N/A	HC > EOS	0.01 FWE corrected cluster-forming threshold 0.05	L-Heschl Gyrus	-48	-18	10
											L-Parietal Operculum	-38	-16	24
											R-Parietal Operculum	50	-24	20
											R-Heschl Gyrus	50	-22	8
											L-Pars Opercularis	-46	18	12
											L-Pars Opercularis	-50	8	20
											L/R-SMA	1	0	52
											L-Poste-Central Gyrus	-40	-36	46
											R-Pre-Central Gyrus	51	-10	41
											R-Post Central Gyrus	60	-16	44
											R-Pre-Central Gyrus	38	10	38
											L-FEF	-22	18	48
											R-Anterior Cingulate Gyrus	14	8	34
											R-Anterior Cingulate Gyrus	14	40	30
											R-Anterior Cingulate Gyrus	10	22	25
											R-Dorsolateral Prefrontal Cortex	20	44	20
											R-Dorsolateral Prefrontal Cortex	20	44	32
											R-Precuneus	24	-70	32
											R-Parieto-Occipital Fissure	20	-60	14
											L-Precuneus	-12	-61	49
											L-Calcarine Fissure	-12	-90	6
											L-Inferior Temporal Gyrus	-50	-16	-22
											R-Middle Temporal Gyrus	58	-11	-16
Janssen	2008	25	51	VBM	MNI152	N/A	SPM2	N/A	HC > EOS	cluster-level correction 0.05	L-Middle Frontal Gyrus	-39	10	51
											L-Medial Frontal Gyrus	-3	54	16
Yoshihara	2008	18	18	VBM	T & T	N/A	BAMM (Brain Analysis Morphological Mapping)	N/A	HC > EOS	0.05 FWE corrected	L-Parahippocampal Gyrus	-57	2	-4
Tang	2012	29	34	VBM	MNI	N/A	SPM5	N/A	HC > EOS	FDR 0.05	L-Middle & Superior Temporal Gyrus	-54	-22	-11
Zhang Y	2015	37	30	VBM	MNI	N/A	SPM8	N/A	HC > EOS	0.05 corrected, cluster-forming p < 0.005, k > 1115	R-Middle & Superior Temporal Gyrus	48	-9	-17
Zhang C	2017	26	26	VBM	MNI	N/A	SPM8	N/A	HC > EOS	cluster-level FWE 0.05	L-Parietal Postcentral Gyrus	-10	-38	70
										voxel-wise t > 3.12	L-Parahippocampal Gyrus	-31	-44	-7

											R-Cerebellum Posterior Pyramis	4	-70	-29
Castro-Fornieles	2018	34	70	VBM	MNI	N/A	SPM8	N/A	HC > EOS	p < 0.0001 uncorrected	R-Thalamus	8	-11	9
											L/R-Medial Frontal Gyrus	-2	42	37
											L/R-Medial Frontal Gyrus	-1	51	13
											R-Rectus	1	38	-20
Pauly	2008	12	12	fMRI	MNI	verbal n-back	Block / SPM2	2-back > 0-back	HC > EOS	0.001 uncorrected k > 15 voxels	R-Middle Frontal Gyrus	50	16	40
											R-Middle Frontal Gyrus	48	28	28
											L-Cuneus/Precuneus	-16	-74	32
											L-Middle Frontal Gyrus	-22	28	40
											R-Angular Gyrus	60	-56	26
											L-Anterior Cingulate Cortex	-2	36	26
						verbal n-back		2-back > 0-back	HC < EOS		L-Inferior Parietal Lobe	-62	-56	24
											R-Middle Occipital Lobe	44	-86	2
											R-Postcentral Gyrus	56	-14	50
											R-Superior Temporal Pole	42	12	-22
						negative emotion induction		negative odour > neutral odour	HC > EOS		L-Anterior Orbitofrontal Cortex	-36	56	-14
						negative emotion induction		negative odour > neutral odour	HC < EOS		L-Middle Cingulate Gyrus	-4	-16	44
											L-Lateral Orbitofrontal Cortex	-50	40	-6
											R-Precuneus	2	-52	32
											R-Precentral/Postcentral Gyrus	52	0	24
											R-Posterior Cingulum	6	-44	14
											R-Angular Gyrus	42	-70	36
											L-Middle Frontal Gyrus	-30	18	44
											L-Medial Prefrontal Gyrus	-20	40	18
Seiferth	2009	12	12	fMRI	MNI	facial emotion discrimination	Event-related / SMP2	Happy faces > neutral faces & blank screen	HC > EOS	0.05 FWE corrected	L-Inferior Occipital Gyrus	-36	-70	-10
										k > 5 voxels	R-Fusiform Gyrus	32	-78	-6
											Thalamus	0	-16	2
								Sad faces > neutral faces & blank screen			L-Inferior Occipital Gyrus	-34	-72	-8
											L-Parahippocampal Gyrus	-2	-22	-18
											L-Caudate	-14	-14	22
											R-Superior Temporal Gyrus	60	-44	20
											Posterior Cingulum	0	-36	24
											R-Thalamus	16	-34	16
											R-Middle Occipital Gyrus	48	-78	18

											R-Superior Occipital Gyrus	22	-80	30
											R-Middle Temporal Gyrus	44	-62	14
											R-Rolandic Operculum	60	-20	16
											R-Hippocampus	40	-8	-14
											R-Insula	30	-18	20
											L-Cerebellum	-16	-40	-20
											L-Superior Temporal Gyrus	-38	-38	12
											R-Middle Temporal Gyrus	66	-22	-4
											R-Cerebellum	20	-36	-20
											R-Supramarginal Gyrus	62	-48	40
											R-Inferior Parietal Cortex	50	-24	-6
								Angry > neutral faces & blank screen			L-Inferior Occipital Gyrus	-36	-70	-10
											R-Fusiform Gyrus	32	-78	-6
											L-Thalamus	-2	-18	2
								Fearful faces > neutral faces & blank screen			L-Fusiform Gyrus	-26	-78	-8
											R-Fusiform Gyrus	32	-78	-8
											R-Superior Temporal Gyrus	46	-38	6
								Happy faces > neutral faces & blank screen	HC < EOS		R-Cuneus	8	-82	18
								Angry > neutral faces & blank screen			R-Cuneus	8	-82	18
											L-Precuneus	-4	-54	8
											L-Precentral/Inferior Frontal Gyrus	-56	10	32
											L-Cuneus	-8	-66	22
								Fearful faces > neutral faces & blank screen			R-Calcarine Sulcus/Cuneus	8	-82	14
Borofsky	2010	14	14	fMRI	T & T	semantic and syntactic processing	Block / AIR within LONI; SPM2	Semantic condition > baseline	HC > EOS	0.05 cluster-level FWE	R-Inferior Frontal Gyrus	46	22	12
										cluster-forming threshold 0.001		32	30	-6
											R-Dorsal Medial Prefrontal Cortex	6	28	36
											R-Anterior Cingulate Cortex	10	30	28
											L-Superior Temporal Gyrus	-56	-54	14
											L-Middle Temporal Gyrus	-56	-50	6
											L-Putamen	-30	2	10
											R-Cerebellum	30	-68	-28

								Syntactic condition > baseline				L-Inferior Frontal Gyrus	-48	10	30
												L-Premotor Cortex	-38	2	44
												L-Dorsal Medial Prefrontal Cortex	-2	42	36
												2	26	46	
												R-Presupplementary Motor Area	2	16	54
												R-Caudate Nucleus	12	14	10
												L-Putamen	-24	2	8
White	2011a	22	24	fMRI	MNI	visuospatial SIRP	Block / AFNI & FSL, FMRIB	Encode load 3	HC > EOS	0.05 corrected	R-Parietal Lobe/Precuneus	6	-58	50	
												R-Superior Parietal Lobe	38	-52	46
												L-Lateral Occipital Cortex	-22	-68	44
								Encode load 2	HC < EOS			L-Anterior Cingulate Gyrus	-12	36	-4
												L-Planum Polare/Heschl's Gyrus/Superior Temporal Gyrus	-50	-14	-2
												L-Temporal Pole	-32	12	-42
												L-Cerebellum/Brainstem	-10	-16	-40
												L-Posterior Cingulate Gyrus	-6	-54	22
												L-Anterior Cerebellum	-2	-52	-6
												L-Hippocampus	-26	-10	-20
												R-Middle Temporal Gyrus	58	4	-22
												R-Orbital Frontal Cortex	26	14	-20
												R-Hippocampus/Amygdala	24	-6	-22
								Retrieval probe load 2				L-Temporal Pole	-28	10	-38
												L-Middle Temporal Gyrus	-56	-8	-24
												L-Hippocampus/Parahippocampal Gyrus	-20	-8	-28
												L-Paracingulate Gyrus	-14	42	-6
								Retrieval probe load 3				L-Middle Temporal Gyrus	-60	-2	-18
												L-Temporal Pole	-46	10	-24
												L-Parahippocampal Gyrus	-16	-14	-22
												L-Hippocampus/Amygdala	-16	-10	-16
White	2011b	14	14	fMRI	T & T	verbal SIRP	Block / AFNI & FSL, FMRIB	retrieval	HC > EOS	0.05 corrected	L-Occipital Lobe	-22	-98	-14	
Kyriakopoulos	2012	25	20	fMRI	T & T	verbal n-back	Block / SPM8	2-back > 0-back	HC > EOS	0.05 FWE corrected	L-Middle Frontal Gyrus	-28	32	33	
												L-Left Anterior Cingulate Gyrus	-2	30	19
												R-Right Anterior Cingulate Gyrus	4	32	20
												L-Inferior Frontal Gyrus	-52	9	16

Bittner	2015	17	17	fMRI	T & T	delayed visual discrimination	Event-related / BrainVoyager	encoding load 1, 2, 3	HC > EOS	0.05 corrected	L-Ventrolateral Prefrontal Cortex	-48	25	12
											L-Inferior Parietal Lobule	-54	-43	26
								encoding load 2, 3			L-Ventrolateral Prefrontal Cortex	-48	11	12
											L-Middle Temporal Gyrus	-50	-55	7
								encoding load 3			L-Precuneus	-6	-68	27
											L-Insula	-34	4	6
											R-Inferior Parietal Lobule	57	-41	26
								encoding load 2			R-Lingual Gyrus	18	-56	4
								early maintenance load 1, 2, 3			R-Posterior Cingulate	12	-30	41
											L-Posterior Cingulate	-10	-33	38
											R-Precuneus	7	-65	25
											L-Precuneus	-5	-68	23
											R-Middle Occipital Gyrus	24	-80	16
											L-Middle Occipital Gyrus	-24	-81	14
											L-Insula	-40	-26	17
											R-Central Sulcus	19	-32	58
											R-Supramarginal Gyrus	51	-25	24
											R-Superior Temporal Gyrus	51	-29	16
											R-Lingual Gyrus	8	-76	-11
								early maintenance load 2, 3			L-Intraparietal Sulcus	-30	-62	37
											L-Middle Temporal Gyrus	-45	-63	13
								early maintenance load 3			R-Superior Parietal Lobe	31	-49	42
											L-Dorsolateral Prefrontal Cortex	-37	10	38
											L-Intraparietal Sulcus	-23	-67	35
								late maintenance load 2, 3			L-Superior Temporal Gyrus	-45	-54	20
								late maintenance load 2			L-Posterior Cingulate Cortex	-5	-41	29
								retrieval load 1			L-Fusiform Gyrus	-30	-38	-11
											R-Anterior Cingulate Cortex	5	22	28
								encoding load 1	HC < EOS		L-Insula	-34	4	6
											R-Inferior Parietal Lobule	57	-41	26
											R-Lingual Gyrus	18	-56	4
								early maintenance load 2			L-Intraparietal Sulcus	-30	-62	37
								late maintenance load 1, 2, 3			L-Superior Frontal Gyrus	-16	-14	62
								retrieval load 2, 3			L-Anterior Cingulate Cortex	-8	27	26
											R-Ventrolateral Prefrontal Cortex	28	19	2
											L-Ventrolateral Prefrontal Cortex	-27	20	-3

											L-Prefrontal Cortex	-33	48	18
											R-Lingual Gyrus	11	-86	-7
								retrieval load 1, 2, 3			R-Inferior Parietal Lobule	38	-30	41
											L-Inferior Parietal Lobule	-49	-25	35
											L-Inferior Parietal Lobule	-37	-48	37
								retrieval load 2			R-Anterior Cingulate Cortex	5	22	28
Loeb	2018	32	39	fMRI	MNI	n-back	Block / SPM12	2- and 1-back > 0-back	HC > EOS	0.05 FWE corrected	L-Precuneus	-9	-67	45
											R-Lateral Posterior Parietal	36	-52	36
											R-Caudate	18	5	18
											L-Lateral Posterior Parietal	-27	-55	33
											R-Dorsolateral Prefrontal Cortex	36	29	30
											R-Lateral Posterior Temporal	60	-46	21
											L-Dorsolateral Prefrontal Cortex	-27	-7	48
											R-Premotor	30	2	48
											L-Premotor	-48	-1	39
											L-Caudate	-15	5	12
											L-Middle Occipital	-30	-76	27
											R-Cerebellum Crus	6	-85	-27

SIRP: Stenberg Item Recognition Paradigm

Table 3.3. Clusters showing significant convergence of hypoactivation in EOS								
					Local extrema			
Cluster	Volume	Location	BA	L/R	x	y	z	ALE value
	(mm³)							(10⁻³)
<i>Cognition ALE</i>								
Healthy controls > Early-onset schizophrenia								
1	1752	Anterior cingulate	32	R	6	38	14	9.78
		Cingulate gyrus	32	R	6	28	24	9.53
		Cingulate gyrus	32	R	12	36	22	9.23
		Anterior cingulate	24	L	0	36	14	9.16
		Medial frontal gyrus	6	R	8	34	32	9.06
		Cingulate gyrus	32	L	-2	36	26	8.94
2	1520	Superior temporal gyrus	13	R	60	-46	20	17.76
		Superior temporal gyrus	39	R	60	-56	26	8.90
<i>Working memory ALE</i>								
Healthy controls > Early-onset schizophrenia								
1	2488	Precuneus	7	L	-22	-66	44	16.06
		Middle temporal gyrus	39	L	-28	-56	34	9.31
		Precuneus	7	L	-10	-68	44	9.24
		Angular gyrus	39	L	-30	-60	44	9.19
2	1640	Inferior parietal lobule	40	R	38	-50	46	13.52
		Superior temporal gyrus	39	R	36	-52	36	10.43
3	1448	Supramarginal gyrus	40	R	60	-46	22	10.53
		Inferior parietal lobule	40	R	62	-40	26	9.14
		Superior temporal gyrus	39	R	60	-56	26	8.88

MNI coordinates, $p < 0.05$ cluster-level FWE, **BA**: Brodmann area, **HC**: healthy controls, **EOS**: early-onset schizophrenia

Table 3.4. Foci contribution from each fMRI study to the resultant ALE clusters of hypoactivation in EOS								
Study cluster	Pauly 2008	Seiferth 2009	Borofsky 2010	White 2011a	White 2011b	Kyriakop oulos 2012	Bittner 2015	Loeb 2018
Cognitive ALE								
rACC	1 focus	-	2 foci	-	-	2 foci	1 focus	-
rTPJ	1 focus	1 focus	-	-	-	-	1 focus	1 focus
WM ALE								
IPreC	-	n/a*	n/a	1 focus	-	-	2 foci	2 foci
rIPL	-	n/a	n/a	1 focus	-	-	1 focus	1 focus
rTPJ	1 focus	n/a	n/a	-	-	-	1 focus	1 focus

*Studies did not qualify to be included in the WM ALE

Table 3.5. Functional connectivity for the Cognitive ALE-derived seeds and conjunctions between each using the minimum statistic

Seed region	Cluster	Volume (mm ³)	Location	BA	L/R	MNI coordinates			ALE value (10 ^{^3})
						x	y	z	
rACC	1	11608	Anterior cingulate Gyrus	32	R	8	32	26	238.783
			Medial Frontal Gyrus	8	L	2	32	44	55.954
	2	2488	Insula		L	-32	22	-4	70.867
			Insula		R	38	20	-2	77.388
	4	592	Inferior Frontal Gyrus	9	R	52	16	26	51.014
	5	352	Middle Frontal Gyrus	9	R	44	36	28	55.677
	6	288	Caudate	Caudate Body	R	12	8	2	51.719
	7	168	Thalamus	Medial Dorsal Nucleus	R	8	-14	6	49.318
	8	168	Cingulate Gyrus	24	L	0	6	48	46.190
	9	160	Cingulate Gyrus	32	R	6	18	38	47.236
10	128	Cingulate Gyrus	31	L	2	-28	34	47.718	
	11	88	Thalamus	Medial Dorsal Nucleus	L	-10	-16	10	45.817
rTPJ	1	5816	Superior Temporal Gyrus	13	R	60	-44	22	208.639
	2	1536	Claustrium		L	-34	18	2	69.585

	3	1224	Insula		R	40	18	-2	60.965
			Insula	13	R	48	14	-2	49.711
	4	1144	Cingulate Gyrus	24	R	4	10	46	52.941
			Medial Frontal Gyrus	6	L	2	4	52	50.162
	5	272	Superior Temporal Gyrus	22	L	-60	-38	26	47.076
	6	248	Middle Frontal Gyrus	6	R	48	4	46	44.917
			Middle Frontal Gyrus	6	R	40	0	52	43.762
	7	216	Thalamus	Medial Dorsal Nucleus	R	10	-14	6	49.205
	8	136	Caudate	Caudate Body	R	16	2	8	46.025
	9	136	Superior Frontal Gyrus	6	R	12	2	66	48.640
	10	88	Thalamus		L	-10	-16	4	42.972
	11	80	Superior Temporal Gyrus	22	R	50	-32	-4	44.614
rACC \cap rTPJ	1	920	Insula	13	L	-36	18	0	63.560
	2	752	Insula	13	R	40	18	0	60.965
	3	128	Cingulate Gyrus	32	R	2	8	46	45.006
	4	64	Thalamus	Medial Dorsal Nucleus	R	10	-14	6	46.424

ALE: activation likelihood estimation, **rACC:** Right anterior cingulate cortex, **rTPJ:** right temporoparietal junction

Table 3.6. Functional connectivity for the WM ALE-derived seeds and conjunctions between each seed using the minimum statistic

Seed region	Cluster	Volume (mm ³)	Location	BA	L/R	MNI coordinates			ALE value (10 ³)
						x	y	z	
IPreC	1	15792	Precuneus	7	L	-24	-66	44	393.765
			Inferior Parietal Lobule	40	L	-44	-40	44	103.293
	2	11136	Inferior Frontal Gyrus	6	L	-46	6	32	143.849
			Middle Frontal Gyrus	6	L	-26	-4	54	96.743
			Precentral Gyrus	6	L	-44	-2	48	90.827
	3	9504	Superior Parietal Lobule	7	R	32	-60	46	149.588
			Precuneus	31	R	30	-74	34	86.114
	4	8120	Medial Frontal Gyrus	32	L	-2	16	48	165.478
			Cingulate Gyrus	32	R	4	24	38	100.191
	5	3440	Insula	13	R	36	22	0	164.074
	6	2808	Insula	13	L	-34	22	0	144.915
	7	1800	Inferior Frontal Gyrus	9	R	48	8	30	125.814
8	920	Precentral Gyrus	6	R	34	0	50	78.141	
9	424	Middle Frontal Gyrus	9	R	44	34	30	72.719	
10	408	Fusiform Gyrus	37	L	-42	-66	-10	74.036	
11	112	Lentiform Nucleus	Putamen	L	-18	6	4	66.586	
12	80	Superior Frontal Gyrus	9	L	38	44	26	66.627	
rIPL	1	9504	Inferior Parietal Lobule	40	R	36	-48	46	377.322
			Inferior Parietal Lobule	40	L	-34	-50	46	142.905
	2	9488	Superior Parietal Lobule	7	L	-26	-60	48	103.884
			Precuneus	7	L	-14	-64	56	65.156
			Medial Frontal Gyrus	6	R	2	20	46	128.635
	3	9272	Cingulate Gyrus	32	R	8	26	36	95.367
			Inferior Frontal Gyrus	9	R	46	10	30	115.976
	4	6808	Middle Frontal Gyrus	9	R	48	28	28	71.347
			Middle Frontal Gyrus	9	R	40	40	28	67.955
Middle Frontal Gyrus			6	R	28	-4	54	66.220	
Middle Frontal Gyrus			46	R	44	36	14	58.934	

	5	6496	Precentral Gyrus	6	L	-42	6	32	132.128
	6	3784	Insula	13	R	34	24	0	157.487
	7	2872	Insula	13	L	-34	22	2	123.725
	8	1024	Middle Frontal Gyrus	6	L	-26	-4	54	72.954
	9	344	Lentiform Nucleus	Putamen	L	-20	0	6	61.601
			Caudate	Caudate Body	L	-12	2	14	57.092
	10	328	Thalamus		R	10	-14	-2	65.608
	11	184	Middle Temporal Gyrus	22	L	-52	-46	6	64.287
	12	184	Thalamus	Ventral Posterior Medial Nucleus	L	-14	-20	6	62.552
	13	152	Lentiform Nucleus	Putamen	R	24	4	2	64.917
	14	56	Precuneus	7	R	14	-66	54	58.418
rTPJ	1	4952	Superior Temporal Gyrus	13	R	60	-44	22	157.309
	2	1240	Insula		L	-34	18	-2	61.482
	3	872	Insula	13	R	38	18	-4	51.795
			Insula	13	R	34	24	4	44.963
	4	424	Medial Frontal Gyrus	32	R	4	12	44	43.783
			Cingulate Gyrus	24	R	2	4	48	38.113
	5	304	Supramarginal Gyrus	40	L	-56	-50	32	41.484
			Superior Temporal Gyrus	39	L	-52	-56	30	40.259
	6	200	Inferior Parietal Lobule	40	L	-58	-38	26	43.058
	7	120	Superior Temporal Gyrus	22	R	50	-32	-4	41.815
	8	80	Precuneus	7	L	-2	-56	36	41.585
IPreC \cap rIPL	1	6968	Superior Frontal Gyrus	6	R	2	18	48	126.574
			Cingulate Gyrus	32	R	6	26	36	90.369
	2	6968	Inferior Parietal Lobule	40	L	-34	-52	46	134.438
			Superior Parietal Lobule	7	L	-26	-60	48	103.884
			Precuneus	7	L	-14	-64	54	62.009
	3	5776	Precentral Gyrus	6	L	-42	6	32	131.649
	4	5184	Superior Parietal Lobule	7	R	32	-56	46	138.810

	5	2720	Insula	13	R	36	22	0	153.704
	6	2304	Insula	13	L	-34	22	2	123.725
	7	1704	Inferior Frontal Gyrus	9	R	48	10	30	115.206
	8	896	Middle Frontal Gyrus	6	L	-26	-4	54	72.954
	9	392	Middle Frontal Gyrus	9	R	46	32	28	69.102
			Middle Frontal Gyrus	46	R	44	38	18	56.884
	10	296	Middle Frontal Gyrus	6	R	30	-2	52	63.133
			Middle Frontal Gyrus	6	R	40	0	46	55.712
	11	32	Precuneus	7	R	14	-66	52	57.436
	12	24	Lentiform Nucleus	Putamen	L	-20	2	4	61.076
	13	24	Superior Frontal Gyrus	9	R	38	42	26	62.276
rIPL \cap rTPJ	1	1104	Insula		L	-34	18	-2	61.482
	2	832	Insula	13	R	38	18	-4	51.795
			Insula	13	R	34	24	4	44.963
	3	344	Medial Frontal Gyrus	32	R	4	12	44	43.783
			Cingulate Gyrus	24	R	2	4	48	38.113
IPreC \cap rTPJ	1	1160	Insula		L	-34	18	-2	61.482
	2	696	Insula	13	R	38	18	-4	51.795
			Insula	13	R	34	24	4	44.963
	3	280	Medial Frontal Gyrus	32	R	4	12	44	43.783
	4	8	Cingulate Gyrus	32	R	8	16	40	36.119
	5	8	Cingulate Gyrus	24	R	2	6	48	36.546
IPreC \cap rIPL \cap rTPJ	1	1160	Insula		L	-34	18	-2	61.482
	2	696	Insula	13	R	38	18	-4	51.795
	3	280	Medial Frontal Gyrus	32	R	4	12	44	43.783

ALE: activation likelihood estimation, **WM**: working memory, **IPreC**: left precuneus, **rIPL**: right inferior parietal lobule, **rTPJ**: right temporoparietal junction

Chapter 4: Dorsolateral prefrontal cortex and default mode network dysconnectivity underlies working memory performance in young adults with early-onset schizophrenia: an fMRI follow-up study

Abstract: Cognitive dysfunction in schizophrenia is increasingly regarded to be neurodevelopmental in origin. This is due to the cognitive impairment in executive function that starts in adolescence; a critical period for working memory processes and its neural substrates, i.e., the dorsolateral prefrontal cortex (DLPFC). Following the first episode, working memory brain activity is frequently shown to normalise in patients. Meanwhile, schizophrenia is believed to be a disorder of dysconnectivity with prevalent dysregulation in connectivity between major cognitive networks. Follow-ups of functional magnetic resonance imaging (fMRI) studies in patients with an early onset (EOS) can help determine the neural correlates of working memory activity and connectivity concurrently with associated brain maturation. This study follows up the EOS patients and age- and gender-matched controls from Kyriakopoulos et al. (2012) 4 years after the initial scan. The participants were scanned with fMRI during the n-back to examine cross-sectional differences in brain activity and connectivity of the DLPFC. Performance in the n-back was similar across groups, while general linear model analysis showed comparable brain activation between the groups. Nevertheless, functional connectivity between the DLPFC and the default mode network was affected in EOS. Patients had reduced negative connectivity of the executive DLPFC node with the posterior cingulate, medial prefrontal and right angular gyrus. These results confirm that functional brain activity normalises in the years following the first episode while also points to disconnection that is relevant with EOS and was not detected in the four years before the second scan, therefore suggesting potential destabilisation in internetwork connectivity.

1. Introduction

Schizophrenia is a clinical syndrome with pronounced cognitive and functional brain disturbances, and it usually manifests in early adulthood. There is a small fraction of patients with an earlier onset that occurs in childhood or adolescence, referred here as early-onset schizophrenia (EOS). The existence of schizophrenia patients with this earlier onset-age agrees with the increasingly discussed neurodevelopmental model of schizophrenia, which sees the disorder as the end state of abnormal neurodevelopmental processes (Rapoport et al., 2012). It has been shown that neurocognitive abnormalities precede clinical symptom expression of schizophrenia (Bora, 2015) and in accordance, regional grey matter and functional abnormalities are more prominent following the first episode than in any other stage of the disease, like in individuals with genetic risk, ultra-high risk or chronic patients (Zhao et al., 2018). There are however variations in the trajectories of functional brain impairments in schizophrenia (Bora, 2015) and while patients are marked by a global cognitive deficit relative to controls in broad range of domains that includes working memory (Schaefer et al., 2013), it is not unusual that schizophrenia patients maintain their cognitive functioning or even improve following illness-onset (Bora & Murray, 2014).

Working memory (WM) is supported by a central executive network, frequently dependent on the activation of the dorsolateral prefrontal (DLPFC) (BAs 9, 46), anterior cingulate (BA 32), superior and inferior parietal (BAs 7, 40), occipital (BA 19), and temporal (BAs 13, 22, 37) cortices (Niendam et al., 2012) and function in these areas is often found to be compromised in schizophrenia (Minzenberg et al., 2009). In developmental as well as in schizophrenia research, the prefrontal cortex attracts a lot of attention as it is a central node of the cognitive control that is exerted upon other

performance guiding systems, while still being subjected to maturational processes throughout adolescence (Constantinidis & Luna, 2019). While the DLPFC is critical for the maintenance of information (Bittner et al., 2015) and inhibitory control (Hwang et al., 2010), schizophrenia patients are shown to have aberrant WM-related function (Bittner et al., 2015; Glahn et al., 2005; Karlsgodt et al., 2009) and connectivity profiles of this node with other areas (Loeb et al., 2018; Nielsen et al., 2017; Wu et al., 2017). Aberrant activation of the DLPFC, however, is not a consistent finding in the neuroimaging literature in EOS (Ioakeimidis et al., 2020), as the extent of DLPFC activation is often modulated by task performance in patients with schizophrenia (Karlsgodt et al., 2009; Wu et al., 2017) and is dependent on task demands and resource allocation (Burzynska et al., 2011). Consequently, studying the DLPFC connectivity profiles during WM tasks in schizophrenia might be a more reliable marker of the disease (Wu et al., 2017).

The present study is a follow-up to a baseline first reported in Kyriakopoulos et al. (2012) which consisted of adolescents with EOS with an age of illness onset at 14.4 years. In the baseline study, 25 adolescents with EOS and 20 healthy controls matched for age, gender, and hand dominance performed a verbal version of the n-back task while their BOLD activity was being recorded with fMRI at the Maudsley Hospital in South London. Four years later, the majority of the same adolescents returned to be assessed in the same n-back paradigm and in the same scanner. This study explores cross-sectional WM activation and de-activation during the n-back and functional connectivity of the DLPFC using psychophysiological interactions (PPI).

2. Methods

2.1. Participants

In this follow-up, seventeen youths with EOS aged 20.82 (± 1.71) and seventeen healthy controls (HC), who were matched for age and gender, aged 21.00 (± 2.11) years, returned to participate in the study ([Table 4.1](#)). At baseline (Kyriakopoulos et al., 2012), patients were recruited from the South London and Maudsley NHS Foundation Trust Child and Adolescent mental health services based on the following criteria: (a) fulfilling Diagnostic and Statistical Manual of Mental Disorders - Fourth Edition (DSM-IV) criteria for schizophrenia; (b) aged 12-19 years; (c) onset of schizophrenia before the 18th birthday; (d) no co-morbid Axis I diagnosis; and (e) $IQ > 70$. Psychopathology was assessed in patients with the Positive and Negative Syndrome Scale (PANSS) (Kay et al 1987). Total antipsychotic exposure was calculated in cumulative chlorpromazine equivalents (CPZE). The demographic, clinical and medication status of patients in the 4-year follow-up ($M = 4.35$, $SD = .79$) is summarized in [Table 4.1](#). Seventeen healthy individuals who had no personal history of psychiatric disorder and no family history of psychosis in their first-degree relatives, were recruited from the same geographic area via advertisements and participated in the follow-up study. Exclusion criteria for all participants were: (a) history of head injury; (b) lifetime history of substance dependence as defined by the DSM-IV; (c) substance abuse as defined by the DSM-IV within the 6 months preceding study entry; (d) any concomitant medical condition; and (e) history of hereditary neurological disorders. All participants were assessed by qualified child psychiatrists using the Structured Clinical Interview for DSM-IV Axis I Disorders (First et al 2002a, b). In all participants, the National Adult Reading Test (NART) (Nelson & Willison, 1991) was used to obtain an

estimate of general intellectual ability (IQ) and the Annette handedness scale to assess hand dominance. Patients were monitored to ensure that they were tested when clinically stable defined as scoring ≤ 3 on each item of the PANSS positive syndrome subscale for two consecutive weeks prior to scanning.

2.2. N-back task

The n-back task was administered as a block design, incorporating alternating active and control conditions (Figure 4.1). Prior to each block, participants were explicitly prompted to respond by button press to the target letter. In the control condition (X-back) the designated target letter was “X”. In the active conditions (one-, two-, and three-back), the target letter was defined as any letter that was identical to the one presented one, two or three trials back, respectively. In each condition, a series of 14 letters were presented visually, with each letter displayed for 2 seconds. The ratio of target to non-target letters presented per block ranged from 2:12 to 3:11. Responses were monitored via an MRI-compatible button box held in the subject’s dominant hand. There were 18 epochs in all, each lasting 30 seconds, with total experiment duration of 9 minutes. The number of correct responses (accuracy) and reaction time (RT; s) were recorded. All participants received training before scanning to ensure they understood the task instructions.

Group differences in task performance (% correct accuracy) were examined using Mann-Whitney U and differences in RT (s) were tested with independent sample t-tests, following inspection if data were parametric with the Shapiro-Wilk test of normality. Participants scoring lower than 50% correct in the X-back or one-back blocks were excluded from the analysis to ensure that participants were cognitively

engaged at the task. Consequently, two EOS participants with accuracy of 37% and 42% on the X-back were excluded from the initial sample of 17 patients.

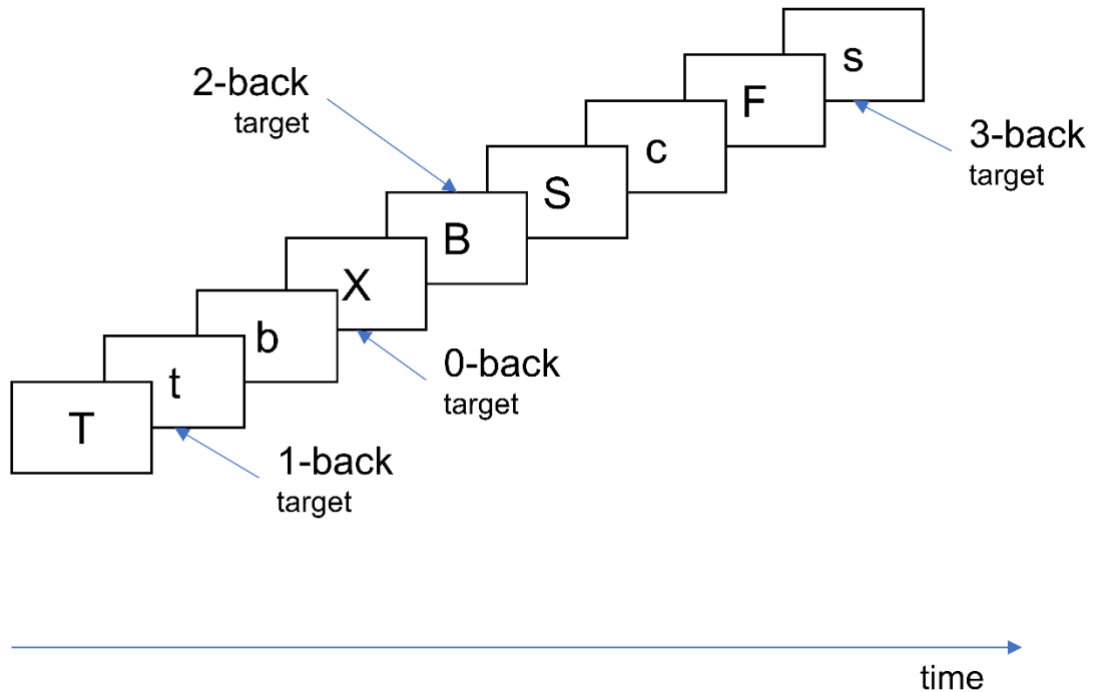


Figure 4.1. Schematic representation of the letter n-back paradigm that was used during fMRI scanning.

2.3. Image acquisition

fMRI and anatomical data were acquired during the same session on a 1.5-T imaging system (Signa; GE Medical Systems, Milwaukee, Wisconsin) using a gradient-echo echoplanar imaging sequence and a 3D T1-weighted Inversion Recovery prepared Spoiled GRASS sequence respectively. A total of 270 T2*-weighted EPI brain volumes depicting blood-oxygenation level-dependent (BOLD) contrast were acquired at each of 16 axial planes (echo time = 40ms, repetition time = 2s, voxel dimensions = 3.75 x 3.75 x 7mm³, interslice gap = 0.7mm, matrix size = 64 x 64, flip angle = 70°). Structural images were acquired using a 3D axial T1-weighted Inversion Recovery prepared Spoiled GRASS sequence from 128 slices (echo time = 5.1ms, repetition time = 2s,

inversion time = 450ms, voxel dimensions = $0.9375 \times 0.9375 \times 1.5$ mm³, matrix size = 256 x 192, field of view = 240 x 180 mm², flip angle = 20°, number of excitations = 1).

2.4. Image analysis

2.4.1. *Pre-processing*

Image processing and analysis were implemented using Statistical Parametric Mapping (SPM12) software (www.fil.ion.ucl.ac.uk/spm/). Pre-processing involved realignment (slice timing and motion correction) of the functional images, co-registration of the mean functional image to each participant's structural one, normalisation into standard stereotactic space to the Montreal Neurological Institute (MNI) template and smoothing with an isotropic Gaussian kernel of 8 mm full-width-at-half-maximum. No subjects were excluded due to excessive inter-scan motion (defined as >4 mm translation, >4° rotation).

2.4.2. *First- and second-level analysis*

fMRI responses were modelled using a canonical haemodynamic response function (hrf) convolved with the vectors of interest. We were only interested in the two-back blocks versus the implicit baseline (X-back), as this load is suggested to reflect higher WM demands (Luo et al., 2020; Meule, 2017) and it was also used in the baseline study (Kyriakopoulos et al., 2012). Movement parameters were entered as nuisance covariates.

At the second level, a general-linear model random effects analysis was conducted using a flexible factorial model with diagnosis status as between-subjects factor and two-back contrasts as dependent variable. We identified the neural signature of WM-related brain activations and deactivations for the two-back blocks within each

group separately, and we were also interested in group-level differences at two-back activation. Peak maxima are reported at FWE $p < .05$.

Post-hoc multiple regression analyses were employed to explore whether variance in two-back brain activation in EOS can be explained by accuracy, IQ, or clinical characteristics (age of illness onset, duration of illness, PANSS scores), with gender as covariate of no interest. Significance is reported at FWE $p < 0.05$.

2.4.3. *Psychophysiological Interaction analysis*

The aim of the PPI analysis was to examine functional connectivity of the dorsolateral prefrontal cortex (DLPFC) during the n-back task. The PPI analysis consists of a design matrix with three regressors: the “psychological variable”, representing the experimental task (here, the two-back blocks); the “physiological variable”, representing the neural response in the seed region (here the DLPFC); and a third variable representing the interaction between the first and the second variables. First, to select the volumes-of-interest (VOIs) we performed a ROI analysis using the left and right DLPFC (BAs 9 & 46) (Karlsgodt et al., 2009) with the WFU pickatlas to create the masks. We located the peak coordinates in the within-group analysis of the two-back contrast, thresholded to an uncorrected $p < .01$, $k > 30$ to ensure BOLD activity in all subjects. For each individual, the first eigenvariate time was extracted from a sphere of 5mm radius centred on the peak height coordinates for the left and right DLPFC VOIs for each group. A variable representing the interaction between each time series and the psychological variable was constructed for each subject. To directly compare group differences in functional connectivity at a second level a flexible factorial model with the between-factor for group was constructed for VOIs from each hemisphere, separately for each hemisphere. To identify positive and negative PPIs within groups we

represented contrasts with a weight of [1] and [-1], respectively. All PPI analyses were thresholded at cluster-FWE 0.05 with an uncorrected $p < 0.001$.

For both fMRI and PPI analyses, labels for the peak maxima were determined using the automated anatomical labelling (AAL3) atlas (Rolls et al., 2020). Brodmann areas were identified with the Talairach Daemon Client (www.talairach.org), after converting stereotactic coordinates from MNI to Talairach and Tournoux (www.mrc-cbu.cam.ac.uk/Imaging/mnispace.html).

3. Results

3.1. Participants

There were no between-group differences in age, gender, hand dominance ($p > .621$). Unlike the baseline study (Kyriakopoulos et al., 2012), NART scores were different between the groups ($p < .001$). Neither accuracy scores nor RT differ significantly between the groups in neither of the three n-back loads ($p > .085$) suggesting comparable task performance between patients and controls ([Table 4.1](#)).

3.2. GLM analysis

Within-group analysis revealed task-positive activation in the frontoparietal executive network (Rottschy et al., 2012) at two-back in both the HC and EOS groups (Figure 4.2). Specifically, controls had BOLD activations in the left inferior parietal lobule, the right angular gyrus, the right superior frontal gyrus, the left precentral gyrus, the left superior frontal gyrus/supplementary motor area, the bilateral inferior frontal gyrus, the left insula and bilateral middle frontal gyrus ([Table 4.2](#); Figure 4.2). Patients with EOS had BOLD activations relative to WM in the right angular gyrus, the right insula, the left inferior frontal gyrus extending to the superior gyrus, the left inferior parietal lobule, the right middle frontal gyrus, and the right inferior frontal extending to the superior frontal gyrus ([Table 4.2](#); Figure 4.2). There were no significant interactions for group \times task at cluster-FWE corrected threshold.

Deactivations in healthy controls were observed at posterior midline areas in the posterior cingulate, middle cingulate gyrus, the precuneus and anteriorly in the medial

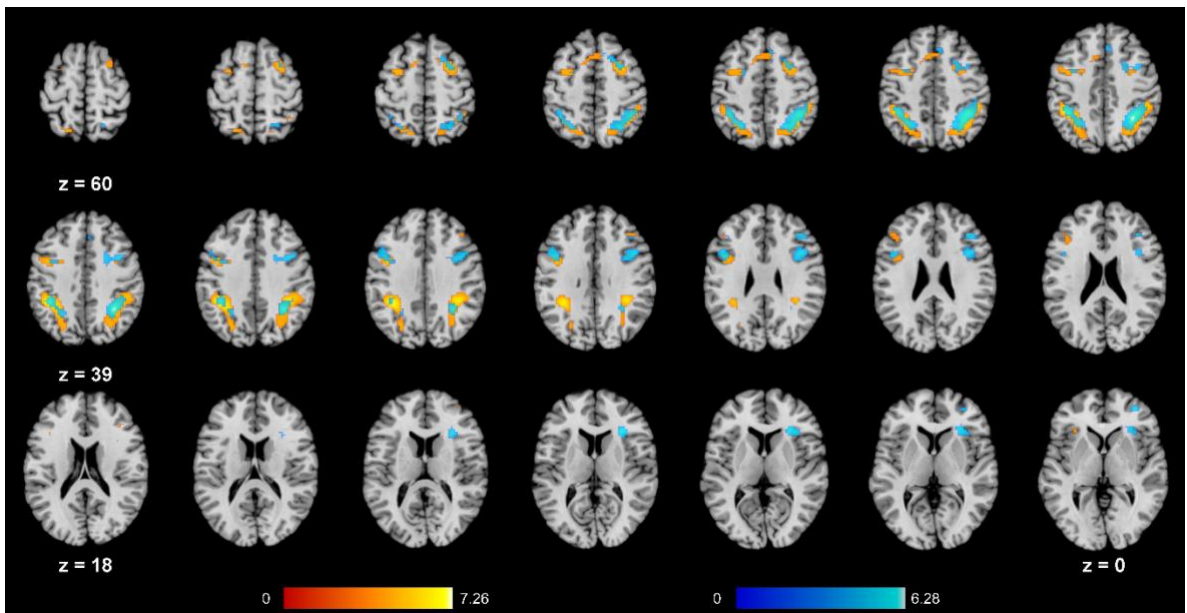


Figure 4.2. Axial layout of brain areas with main effects of two-back activations (2-back > 0-back) in controls (red overlay) and EOS patients (blue overlay). Colour bars represent the T-values of the overlain clusters. Brain template is Colin27_T1_MNI overlaid with thresholded SPM corrected for multiple comparisons correction at FWE $p < 0.05$

superior frontal gyrus. Patients with EOS showed deactivations in the right precuneus, the left medial superior frontal gyrus, the left cuneus, the left parahippocampal gyrus, the left precuneus, the right medial superior frontal gyrus and the right middle occipital gyrus (Table 4.3; Figure 4.3).

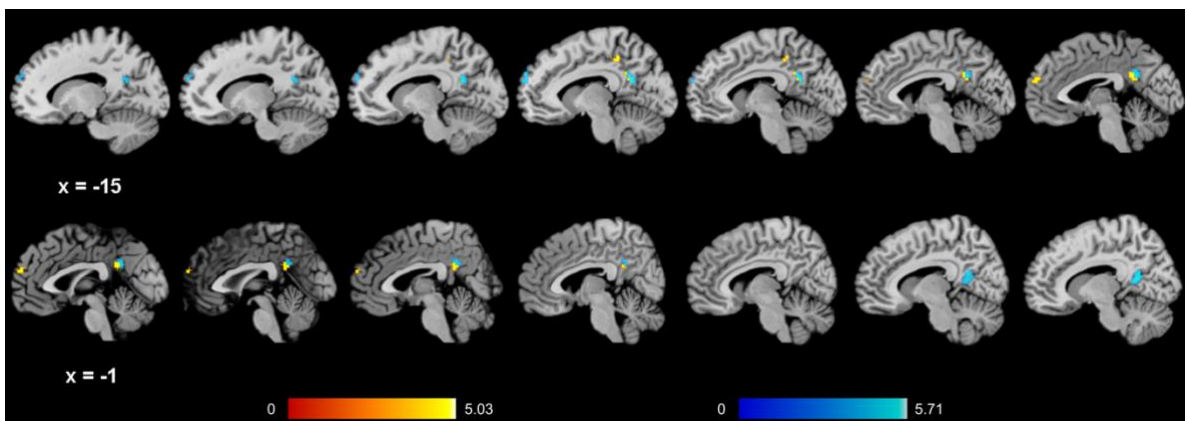


Figure 4.3. Sagittal layout of brain areas with main effects of two-back deactivations (0-back > 2-back) in controls (red overlay) and EOS patients (blue overlay). Colour bars represent the T-values of the overlain clusters. Brain template is Colin27_T1_MNI overlaid with thresholded SPM corrected for multiple comparisons correction at FWE $p < 0.05$

No effects were observed at FWE in EOS brain activation with multiple regressions for WM accuracy, IQ, age of illness onset, illness duration or PANSS (total, positive, negative) as regressors.

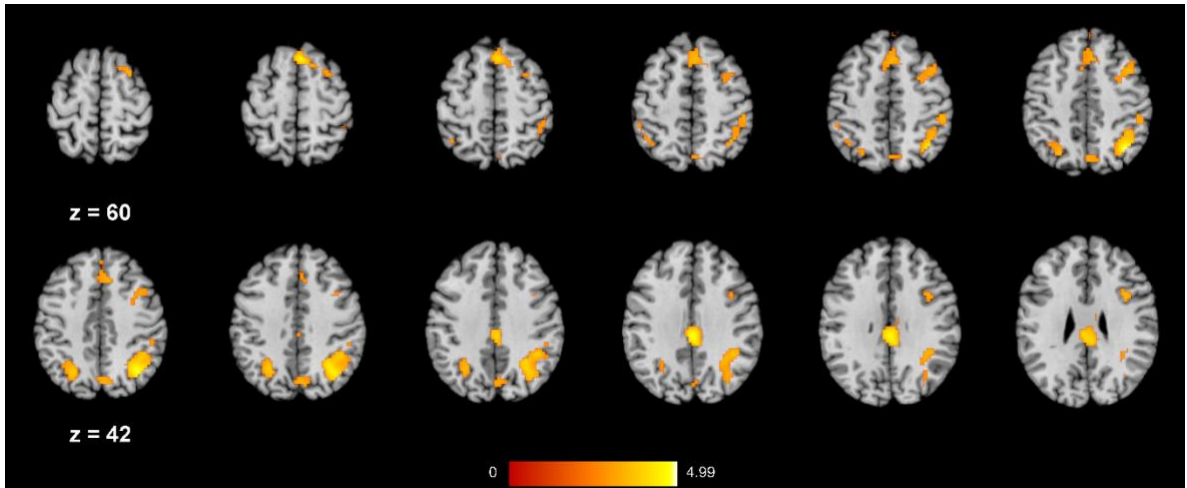


Figure 4.4. Axial layout of brain areas that display negative psychophysiological interactions (PPI) with the right DLPFC seed in control subjects. EOS patients had no significant clusters for neither positive nor negative PPI, in neither the left nor right DLPFC. Brain template is Colin27_T1_MN1 overlaid with thresholded SPM corrected for multiple comparisons correction at FWE $p < 0.05$

3.3. Psychophysiological Interactions

The MNI coordinates for the left DLPFC seed were $x = -42, y = 2, z = 32$ (z -value = 5.74) in HC and $x = -45, y = 11, z = 29$ (z -value = 5.57) in patients with EOS. The MNI coordinates for the right DLPFC seed were $x = 42, y = 29, z = 35$ (z -value = 4.35) in HC and $x = 39, y = 5, z = 38$ (z -value = 5.41) in EOS patients.

In healthy controls, PPI analysis showed that the left and right DLPFC seeds were negatively coupled with the right angular gyrus. The right DLPFC was further functionally connected to the middle cingulate, the right supplementary motor area, the precuneus and left superior parietal lobule (Table 4.4; Figure 4.4). Patients with EOS showed no brain areas significantly connected with neither the right nor the left DLPFC seed, nor any group differences were detected at FWE correction. Using a more lenient threshold ($p < 0.001$ uncorrected, $k_e > 10$), controls had increased right DLPFC negative

connectivity compared to patients with EOS in the posterior cingulate gyrus, the right angular gyrus and the medial superior frontal gyrus ([Table 4.4](#); Figure 4.5).

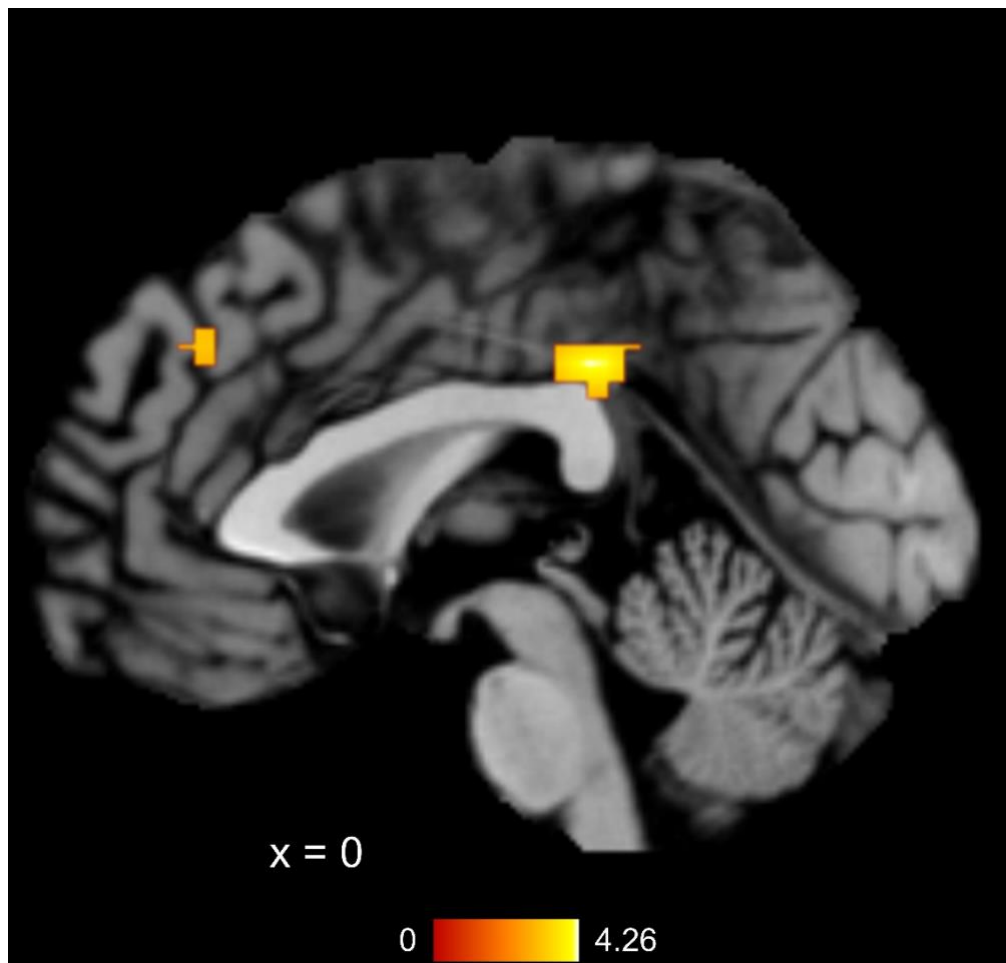


Figure 4.5. Sagittal slice showing at $x = 0$ showing the medial prefrontal cortex and posterior cingulate cortex, areas where controls displayed increased negative PPI of the right DLPFC compared to EOS. Brain template is Colin27_T1_MNI overlaid with thresholded SPM $p < 0.001$ uncorrected, $k_e > 10$

4. Discussion

Here we examine the 4-year follow-up of a longitudinal cohort consisting of patients with EOS and age- and gender-matched healthy controls. Participants were scanned during a version of the n-back paradigm that taps into verbal WM activity. Controls and patients performed with similar accuracy and processing speed (reaction times) at the n-back paradigm in all levels of the task. WM performance at two-back engaged executive frontoparietal activity in both healthy controls and in patients with EOS, whereas posterior and anterior midline areas were deactivated. WM activity was comparable in patients and controls, suggesting normalisation of WM function and no detectable signs of further functional decline, in support of the neurodevelopmental model of schizophrenia. Finally, functional connectivity of the DLPFC was prominent in posterior and medial areas of the default mode network in healthy controls but not in individuals with schizophrenia.

At baseline, patients with EOS and controls, being matched for IQ (measured by NART score) and WM accuracy, activated areas of the frontoparietal WM network (Kyriakopoulos et al., 2012), whilst EOS patients manifested hypoactivation in the left DLPFC, left inferior frontal gyrus and bilateral ACC (Kyriakopoulos et al., 2012). Here, in a 4-year follow-up period, patients with EOS still successfully activate the executive WM network (Rottschy et al., 2012), while concurrently performing the two-back task with analogous accuracy, however, they did not differ from controls in their WM activation profiles. Difference in IQ scores between the groups was caused by an IQ increase in controls rather than worsening in EOS, from the time of the first to the second scan, as it will be shown in the longitudinal analysis in the next chapter. Hence, we examined potentially confounding effects of current IQ levels on WM function

using post-hoc multiple regression and found that IQ did not explain any variance in brain activation at two-back. Thus, absence of group differences in WM performance and function lends further support to the neurodevelopmental origin of schizophrenia (Bora, 2015). Neurodevelopmental accounts of schizophrenia posit that the cognitive dysfunction is expressed as a slower acquisition of cognitive skills instead of a loss of already acquired skills; something that is further reinforced by a meta-analysis of longitudinal studies with first-episode and ultra-high risk subjects (Bora & Murray, 2014). Bora & Murray found cognitive performance in various skills to remain stable or to even improve, at varied follow-up periods of 6 months to 7 years (Bora & Murray, 2014). Similarly, our EOS sample showed no evidence of IQ decline or WM performance differences relative to controls. It is likely that patients also benefitted by normalisation of the WM brain dysfunction that was initially observed 4 years earlier, as they show no evidence of progressive functional neurodegeneration, concurrently with stabilised WM accuracy and reaction times.

This is not the first study that fails to detect WM activation changes in schizophrenia patients relative to healthy controls during a two-back task (Nielsen et al., 2017). However, other studies have found whole-brain functional abnormalities in schizophrenia during the two-back task, including the baseline study in this sample (Kyriakopoulos et al., 2012). A study similar to ours, that included an EOS sample and employed the n-back to explore WM brain function in 21 year old patients with EOS, did report significant BOLD reductions (Loeb et al., 2018) unlike our study. The authors found hypoactivation in areas of the posterior parietal lobules, temporoparietal junction and bilateral prefrontal cortex; discrepancy in this study and ours could be due to behavioural, clinical, or methodological differences. In Loeb et al. (2018), the authors used both two-back & one-back blocks to compare group level differences. Adding

more scans for analysis could increase the likelihood of observing significant group-level activation abnormalities. Furthermore, the EOS sample in Loeb et al. (2018) was more severely impaired having significantly lower accuracy at one- and two-back compared to the control sample. Additionally, mean onset-age and duration of illness were 10 and 11 years, respectively, whereas our patients had on average a higher age of onset and lower illness duration, while being only mildly impaired, which was controlled by scanning patients while they had low and stable PANSS scores. Another study that used the two-back but recruited patients with more severe psychotic symptoms (PANSS total > 60) also reported extensive group effects in brain activation in WM that also interacted with performance (Wu et al., 2017). Hence, it cannot be ruled out that discrepant findings of WM function in schizophrenia could stem from differences in behaviour or secondary clinical characteristics. Again, exploratory multiple regression analyses for either accuracy at two-back, age of onset, illness duration, or PANSS scores as regressors did not significantly explain any variance in brain activity during two-back performance. Accordingly, it has been reported that illness duration does not affect cognitive impairment (Schaefer et al., 2013), and brain activity is not reduced with younger age of illness onset (Niendam et al., 2018) or symptom severity (Grot et al., 2017). Consequently, the source of discrepancy (absence or presence of group effects) in this and various other WM studies of brain activation in schizophrenia remains inconclusive, as the initial differences in WM function that were observed in this sample at baseline are now normalised and WM activation is not explained by WM performance, current PANSS symptoms scores, onset-age, or illness duration.

We have also shown that haemodynamic activity in the DLPFC in controls was functionally negatively coupled with the posterior cingulate, medial frontal, and

bilateral posterior parietal cortices; areas associated with the task-negative or the default mode network (Buckner et al., 2008). Furthermore, negative interactions were more prominent than positive, signifying anticorrelated activities in the central executive and in the DMN which could be relevant to an inhibitory role of the seed exerted upon the task-negative system. The right DLPFC seed interacted negatively with nodes that are traditionally discussed as part of the task-negative network (some of those are reported here as two-back deactivations) and EOS patients failed to show such negative connectivity of the DLPFC. In accordance with our results, Fryer and colleagues (2013) have previously shown that the default mode network is insufficiently suppressed during a WM task in young patients and at-risk individuals with psychosis (Fryer et al., 2013) dysconnectivity of the DLPFC and the default mode network is already apparent in early-course unmedicated patients (Anticevic et al., 2015). Even though we failed to replicate activation differences, we hypothesise that diminished DMN suppression could result from poor functional connectivity between the central executive network and brain regions with task-negative related activity. The negative interactions of the DLPFC node with the default mode system may be relevant to DLPFC's role in exerting inhibitory control signals (Soltaninejad et al., 2019) that suppress task-negative activity (including self-referential processes of the DMN). EOS patients fail to make use of such inhibitory control through their DLPFC. Similarly, during a cognitive control paradigm functional brain activation did not differ between patients with schizophrenia and healthy controls, but negative PPI connectivity from the left and right DLPFC was prominent with nodes of the default mode network only in the controls while it was decreased in patients (Barbalat & Franck, 2020). Therefore, DLPFC activity that is modulated by WM or more general cognitive control processes, may in turn modulate inhibitory functional interactions with the default mode network. While DMN

connectivity with the cognitive control network increases to reach maturity and such greater connectivity associates with better cognitive performance (Gu et al., 2015), adolescents with increased psychiatric symptoms experience destabilisation and delayed maturation of these two networks (Kaufmann et al., 2017). Therefore, our results suggest that despite normalised WM activation and accuracy, our chronic patient sample with EOS is characterised by aberrant functional connectivity. Our results contribute to the accumulating literature in support of schizophrenia being a disorder of dysconnectivity (Friston, 1999) as well as the view that aberrant interactions between discrete networks (such as the executive control and the default mode) are central to psychopathology (Menon, 2011).

Overall, we report comparable WM performance and brain activity in patients with EOS and controls in a 4-year follow-up of the n-back task, a finding that provides further evidence for the neurodevelopmental model of schizophrenia. This states that cognitive abnormalities do not progress further with disease chronicity and that functional efficiency can be optimised by using alternative cognitive strategies (Bora, 2015), which in the case of our sample may be expressed as differential functional connectivity dynamics. Similar with injury in other parts of the body and recovery from it in developing individuals, it is likely that brain deficits in EOS patients, who manifest schizophrenia symptoms during a sensitive period in brain development, benefit from neuroprotective factors that promote neuroplasticity and facilitate normalisation of WM or other cognitive functions (Lee et al., 2012). We also reported dysconnectivity of the DLPFC and areas associated with the default mode network of mentalising processing to be prominent in the EOS sample. It is likely that destabilisation of functional network dynamics is a more sensitive marker of the psychopathology of schizophrenia, as abnormal default mode network connectivity is common finding in EOS (Tang et al.,

2013; S. Zhang et al., 2019) and dysconnectivity between the default mode and central executive networks may be related to the emergence of psychotic syndromes (Mennigen et al., 2019). Therefore, our study supports a neurodevelopmental account of schizophrenia and the influential theory that schizophrenia is increasingly considered as a dysconnectivity syndrome (Friston et al., 2016; Keshavan & Paus, 2015).

References

- Anticevic, A., Hu, X., Xiao, Y., Hu, J., Li, F., Bi, F., ... Gong, Q. (2015). Early-course unmedicated schizophrenia patients exhibit elevated prefrontal connectivity associated with longitudinal change. *Journal of Neuroscience*, *35*(1), 267–286. <https://doi.org/10.1523/JNEUROSCI.2310-14.2015>
- Barbalat, G., & Franck, N. (2020). Dysfunctional connectivity in posterior brain regions involved in cognitive control in schizophrenia: A preliminary fMRI study. *Journal of Clinical Neuroscience*, *78*(xxxx), 317–322. <https://doi.org/10.1016/j.jocn.2020.04.089>
- Bittner, R. A., Linden, D. E. J., Roebroek, A., Härtling, F., Rotarska-Jagiela, A., Maurer, K., ... Haenschel, C. (2015). The When and Where of Working Memory Dysfunction in Early-Onset Schizophrenia—A Functional Magnetic Resonance Imaging Study. *Cerebral Cortex*, *25*(9), 2494–2506. <https://doi.org/10.1093/cercor/bhu050>
- Bora, E. (2015). Neurodevelopmental origin of cognitive impairment in schizophrenia. *Psychological Medicine*, *45*(1), 1–9. <https://doi.org/10.1017/S0033291714001263>
- Bora, E., & Murray, R. M. (2014). Meta-analysis of cognitive deficits in ultra-high risk to psychosis and first-episode psychosis: Do the cognitive deficits progress over, or after, the onset of psychosis? *Schizophrenia Bulletin*, *40*(4), 744–755. <https://doi.org/10.1093/schbul/sbt085>
- Buckner, R. L., Andrews-Hanna, J. R., & Schacter, D. L. (2008). The brain's default network: Anatomy, function, and relevance to disease. *Annals of the New York Academy of Sciences*, *1124*, 1–38. <https://doi.org/10.1196/annals.1440.011>
- Burzynska, A. Z., Nagel, I. E., Preuschhof, C., Li, S. C., Lindenberger, U., Bäckman, L., & Heekeren, H. R. (2011). Microstructure of frontoparietal connections predicts cortical responsivity and working memory performance. *Cerebral Cortex*, *21*(10), 2261–2271. <https://doi.org/10.1093/cercor/bhq293>
- Constantinidis, C., & Luna, B. (2019). Neural Substrates of Inhibitory Control Maturation in Adolescence. *Trends in Neurosciences*, Vol. 42, pp. 604–616. <https://doi.org/10.1016/j.tins.2019.07.004>
- First M. B., Spitzer R. L., Gibbon M., Williams J. B. W. (2002a). *Structured Clinical Interview for DSM-IV-TR Axis I Disorders, Research Version, Non-patient Edition*. (SCID-I/NP). New York: Biometrics Research, New York State Psychiatric Institute
- First M. B., Spitzer R. L., Gibbon M., Williams J. B. W. (2002b). *Structured Clinical Interview for DSM-IV-TR Axis I Disorders, Research Version, Patient Edition*. (SCID-I/P). New York: Biometrics Research, New York State Psychiatric Institute
- Friston, K. (1999). Schizophrenia and the disconnection hypothesis. *Acta Psychiatrica Scandinavica*, *99*(s395), 68–79. <https://doi.org/10.1111/j.1600-0447.1999.tb05985.x>

- Friston, K., Brown, H. R., Siemerkus, J., & Stephan, K. E. (2016). The dysconnection hypothesis (2016). *Schizophrenia Research*, *176*(2–3), 83–94. <https://doi.org/10.1016/j.schres.2016.07.014>
- Fryer, S. L., Woods, S. W., Kiehl, K. A., Calhoun, V. D., Pearlson, G. D., Roach, B. J., ... Mathalon, D. H. (2013). Deficient suppression of default mode regions during working memory in individuals with early psychosis and at clinical high-risk for psychosis. *Frontiers in Psychiatry*, *4*(SEP), 1–17. <https://doi.org/10.3389/fpsy.2013.00092>
- Glahn, D. C., Ragland, J. D., Abramoff, A., Barrett, J., Laird, A. R., Bearden, C. E., & Velligan, D. I. (2005). Beyond hypofrontality: A quantitative meta-analysis of functional neuroimaging studies of working memory in schizophrenia. *Human Brain Mapping*, *25*(1), 60–69. <https://doi.org/10.1002/hbm.20138>
- Grot, S., Légaré, V. P., Lipp, O., Soulières, I., Dolcos, F., & Luck, D. (2017). Abnormal prefrontal and parietal activity linked to deficient active binding in working memory in schizophrenia. *Schizophrenia Research*, *188*, 68–74. <https://doi.org/10.1016/j.schres.2017.01.021>
- Gu, S., Satterthwaite, T. D., Medaglia, J. D., Yang, M., Gur, R. E., Gur, R. C., & Bassett, D. S. (2015). Emergence of system roles in normative neurodevelopment. *Proceedings of the National Academy of Sciences of the United States of America*, *112*(44), 13681–13686. <https://doi.org/10.1073/pnas.1502829112>
- Hwang, K., Velanova, K., & Luna, B. (2010). Strengthening of top-down frontal cognitive control networks underlying the development of inhibitory control: A functional magnetic resonance imaging effective connectivity study. *Journal of Neuroscience*, *30*(46), 15535–15545. <https://doi.org/10.1523/JNEUROSCI.2825-10.2010>
- Ioakeimidis, V., Haenschel, C., Yarrow, K., Kyriakopoulos, M., & Dima, D. (2020). A Meta-analysis of Structural and Functional Brain Abnormalities in Early-Onset Schizophrenia. *Schizophrenia Bulletin Open*, *1*(1), 1–12. <https://doi.org/10.1093/schizbullopen/sgaa016>
- Karlsgodt, K. H., Sanz, J., van Erp, T. G. M., Bearden, C. E., Nuechterlein, K. H., & Cannon, T. D. (2009). Re-evaluating dorsolateral prefrontal cortex activation during working memory in schizophrenia. *Schizophrenia Research*, *108*(1–3), 143–150. <https://doi.org/10.1016/j.schres.2008.12.025>
- Kaufmann, T., Alnæs, D., Doan, N. T., Brandt, C. L., Andreassen, O. A., & Westlye, L. T. (2017). Delayed stabilization and individualization in connectome development are related to psychiatric disorders. *Nature Neuroscience*, *20*(4), 513–515. <https://doi.org/10.1038/nn.4511>
- Kay, S. R., Fiszbein, A., & Opler, L. A. (1987). The Positive and Negative Syndrome Scale (PANSS) for Schizophrenia. *Schizophrenia Bulletin*, *13*(2), 261–276. <https://doi.org/10.1093/schbul/13.2.261>
- Keshavan, M. S., & Paus, T. (2015). Neurodevelopmental trajectories, disconnection, and schizophrenia risk. *JAMA Psychiatry*, Vol. 72, pp. 943–945. <https://doi.org/10.1001/jamapsychiatry.2015.1119>

- Kyriakopoulos, M., Dima, D., Roiser, J. P., Corrigall, R., Barker, G. J., & Frangou, S. (2012). Abnormal Functional Activation and Connectivity in the Working Memory Network in Early-Onset Schizophrenia. *Journal of the American Academy of Child & Adolescent Psychiatry, 51*(9), 911-920.e2. <https://doi.org/10.1016/j.jaac.2012.06.020>
- Lee, H., Dvorak, D., Kao, H. Y., Duffy, áine M., Scharfman, H. E., & Fenton, A. A. (2012). Early Cognitive Experience Prevents Adult Deficits in a Neurodevelopmental Schizophrenia Model. *Neuron, 75*(4), 714–724. <https://doi.org/10.1016/j.neuron.2012.06.016>
- Loeb, F. F., Zhou, X., Craddock, K. E. S., Shora, L., Broadnax, D. D., Gochman, P., ... Liu, S. (2018). Reduced Functional Brain Activation and Connectivity During a Working Memory Task in Childhood-Onset Schizophrenia. *Journal of the American Academy of Child and Adolescent Psychiatry, 57*(3), 166–174. <https://doi.org/10.1016/j.jaac.2017.12.009>
- Luo, Q., Pan, B., Gu, H., Simmonite, M., Francis, S., Liddle, P. F., & Palaniyappan, L. (2020). Effective connectivity of the right anterior insula in schizophrenia: The salience network and task-negative to task-positive transition. *NeuroImage: Clinical, 28*(August), 102377. <https://doi.org/10.1016/j.nicl.2020.102377>
- Mennigen, E., Jolles, D. D., Hegarty, C. E., Gupta, M., Jalbrzikowski, M., Olde Loohuis, L. M., ... Bearden, C. E. (2019). State-Dependent Functional Dysconnectivity in Youth With Psychosis Spectrum Symptoms. *Schizophrenia Bulletin, 1*–14. <https://doi.org/10.1093/schbul/sbz052>
- Menon, V. (2011). Large-scale brain networks and psychopathology: A unifying triple network model. *Trends in Cognitive Sciences, Vol. 15*, pp. 483–506. <https://doi.org/10.1016/j.tics.2011.08.003>
- Meule, A. (2017). Reporting and Interpreting Working Memory Performance in n-back Tasks. *Frontiers in Psychology, 8*(8), 578–587. <https://doi.org/10.3389/fpsyg.2017.00352>
- Minzenberg, M. J., Laird, A. R., Thelen, S., Carter, C. S., & Glahn, D. C. (2009). Meta-analysis of 41 Functional Neuroimaging Studies of Executive Function in Schizophrenia. *Archives of General Psychiatry, 66*(8), 811–822.
- Nelson, H. R., Willison, J. R. (1991). *National Adult Reading Test (NART)*. Windsor: NFER-Nelson.
- Nielsen, J. D., Madsen, K. H., Wang, Z., Liu, Z., Friston, K. J., & Zhou, Y. (2017). Working Memory Modulation of Frontoparietal Network Connectivity in First-Episode Schizophrenia. *Cerebral Cortex, 27*(7), 3832–3841. <https://doi.org/10.1093/cercor/bhx050>
- Niendam, T. A., Laird, A. R., Ray, K. L., Dean, Y. M., Glahn, D. C., & Carter, C. S. (2012). Meta-analytic evidence for a superordinate cognitive control network subserving diverse executive functions. *Cognitive, Affective and Behavioral Neuroscience, 12*(2), 241–268. <https://doi.org/10.3758/s13415-011-0083-5>
- Niendam, T. A., Ray, K. L., Iosif, A. M., Lesh, T. A., Ashby, S. R., Patel, P. K., ... Carter, C. S. (2018). Association of Age at Onset and Longitudinal Course of Prefrontal Function in Youth with

- Schizophrenia. *JAMA Psychiatry*, 75(12), 1217–1224.
<https://doi.org/10.1001/jamapsychiatry.2018.2538>
- Rapoport, J. L., Giedd, J. N., & Gogtay, N. (2012). Neurodevelopmental model of schizophrenia: update 2012. *Molecular Psychiatry*, 17(12), 1228–1238. <https://doi.org/10.1038/mp.2012.23>
- Rolls, E. T., Huang, C. C., Lin, C. P., Feng, J., & Joliot, M. (2020). Automated anatomical labelling atlas 3. *NeuroImage*, 206(August 2019), 116189. <https://doi.org/10.1016/j.neuroimage.2019.116189>
- Rottschy, C., Langner, R., Dogan, I., Reetz, K., Laird, A. R., Schulz, J. B., ... Eickhoff, S. B. (2012). Modelling neural correlates of working memory: A coordinate-based meta-analysis. *NeuroImage*, 60(1), 830–846. <https://doi.org/10.1016/j.neuroimage.2011.11.050>
- Schaefer, J., Giangrande, E., Weinberger, D. R., & Dickinson, D. (2013). The global cognitive impairment in schizophrenia: Consistent over decades and around the world. *Schizophrenia Research*, Vol. 150, pp. 42–50. <https://doi.org/10.1016/j.schres.2013.07.009>
- Soltaninejad, Z., Nejati, V., & Ekhtiari, H. (2019). Effect of Anodal and Cathodal Transcranial Direct Current Stimulation on DLPFC on Modulation of Inhibitory Control in ADHD. *Journal of Attention Disorders*, 23(4), 325–332. <https://doi.org/10.1177/1087054715618792>
- Tang, J., Liao, Y., Song, M., Gao, J.-H., Zhou, B., Tan, C., ... Chen, X. (2013). Aberrant Default Mode Functional Connectivity in Early Onset Schizophrenia. *PLoS ONE*, 8(7), e71061. <https://doi.org/10.1371/journal.pone.0071061>
- Wu, S., Wang, H., Chen, C., Zou, J., Huang, H., Li, P., ... Wang, G. (2017). Task performance modulates functional connectivity involving the dorsolateral prefrontal cortex in patients with schizophrenia. *Frontiers in Psychology*, 8(FEB), 1–14. <https://doi.org/10.3389/fpsyg.2017.00056>
- Zhang, S., Yang, G., Ou, Y., Guo, W., Peng, Y., Hao, K., ... Lv, L. (2019). Abnormal default-mode network homogeneity and its correlations with neurocognitive deficits in drug-naïve first-episode adolescent-onset schizophrenia. *Schizophrenia Research*, (xxxx). <https://doi.org/10.1016/j.schres.2019.10.056>
- Zhao, C., Zhu, J., Liu, X., Pu, C., Lai, Y., Chen, L., ... Hong, N. (2018). Structural and functional brain abnormalities in schizophrenia: A cross-sectional study at different stages of the disease. *Progress in Neuro-Psychopharmacology and Biological Psychiatry*, 83(11), 27–32. <https://doi.org/10.1016/j.pnpbp.2017.12.017>

Tables

Table 4.1. Demographic, clinical, and behavioural characteristics for the EOS and HC groups				
	EOS	HC		
	n = 15	n = 17	statistic	p value
Demographic data				
Age (years)	20.82 (1.71)	21.00 (2.11)	$t = 0.275$.786
Range (years)	18.08 – 23.92	17.33 - 25.83		
Gender (M/F)	10/5	11/6	$\chi^2 = 0.014$.907
Handedness (L/R)	14/1	15/2	$\chi^2 = 0.621$.621
IQ (NART)	100.33 (7.87)	111.41 (4.35)	$t = 5.009$	< 0.001
Clinical data				
AIO (years)	14.39 (2.25)	-		
Range (years)	7.58 – 17.14	-		
Illness-duration (years)	6.10 (1.84)	-		
Range (years)	3.48 – 10.50	-		
<u>Symptoms</u>				
PANSS positive	10.53 (3.38)	-		
PANSS negative	12.07 (4.53)	-		
PANSS total	47.27 (9.95)	-		
<u>Medication (mg)</u>				
Cumulative CPZE	26,174 (31,1109)	-		
n-back				
<u>Accuracy, % correct; Median (IQR)</u>				
one-back	100% (25%)	100% (13%)	$U = 101.00$.254
two-back	87.5% (75%)	100% (13%)	$U = 86.50$.085
three-back	75% (63%)	87.5% (25%)	$U = 99.00$.265
<u>Reaction time, s; Mean (SD)</u>				
one-back	0.57 (0.12)	0.51 (0.08)	$t = -1.654$.109
two-back	0.55 (0.27)	0.57 (0.10)	$t = 0.247$.808
three-back	0.67 (0.31)	0.62 (0.15)	$t = -0.498$.624

Abbreviations: **AIO**: Age of illness onset; **CPZE**: Chlorpromazine equivalents; **EOS**: Early-onset schizophrenia; **F**: Female; **HC**: Healthy controls; **IQR**: interquartile range; **L**: Left; **M**: Male; **NART**: National adult reading test; **PANSS**: Positive and negative symptoms scale; **R**: Right; **SD**: Standard deviation

Table 4.2. BOLD activations at two-back in healthy controls and patients with EOS								
					Peak coordinates			
#	k	Regions	BA	L/R	x	y	z	Z-value
Healthy controls								
1	536	Inferior parietal lobule	40	L	-36	-46	32	7.26
		Inferior parietal lobule	40	L	-42	-43	38	7.15
		Superior parietal lobule	7	L	-21	-67	59	5.46
2	607	Angular gyrus	40	R	36	-43	32	6.65
		Angular gyrus	40	R	33	-55	38	6.13
		Supramarginal gyrus	40	R	48	-40	44	5.70
3	169	Superior frontal gyrus	6	R	27	5	53	6.27
		Superior frontal gyrus	6	R	15	14	53	4.71
4	241	Precentral gyrus	6	L	-42	-1	35	5.81
		Middle frontal gyrus	6	L	-30	-1	53	5.58
5	85	Superior frontal gyrus	6	L	-12	8	53	5.07
		Supplementary motor area	32	L/R	-3	17	47	4.99
6	39	Inferior frontal gyrus, triangular	46	R	39	32	26	4.89
7	32	Inferior frontal gyrus, triangular	46	L	-45	32	23	4.77
		Inferior frontal gyrus, triangular	46	L	-39	26	20	4.76
8	8	Insula	47	L	-33	26	-1	4.58
9	2	Middle frontal gyrus	10	L	-36	47	17	4.46
10	2	Middle frontal gyrus	10	R	36	50	11	4.41
Patients with EOS								
1	394	Angular gyrus	40	R	33	-52	41	6.28
2	103	Insula	13	R	33	23	5	5.83
3	144	Inferior frontal gyrus, operculum	9	L	-45	8	26	5.76
		Precentral gyrus	6	L	-33	2	41	5.08
		Superior frontal gyrus	6	L	-24	-1	50	4.72
4	236	Inferior parietal lobule	40	L	-39	-46	41	5.67
		Inferior parietal lobule	7	L	-30	-58	47	5.51
5	32	Middle frontal gyrus	10	R	36	50	-4	5.66
6	322	Inferior frontal gyrus, operculum	9	R	42	8	29	5.59
		Superior frontal gyrus	6	R	27	8	50	5.20
		Middle cingulate gyrus	24	R	21	5	38	5.11
7	42	Inferior frontal gyrus, triangular	46	R	39	29	26	5.10
8	4	Inferior frontal gyrus, triangular	46	L	-39	26	26	4.80
9	1	Insula	13	L	-30	17	8	4.66

Coordinates reported in MNI space and corrected for multiple comparisons at FWE 0.05

Table 4.3. BOLD deactivations at two-back in healthy controls and patients with EOS								
					Peak coordinates			
#	k	Regions	BA	L/R	x	y	z	Z-value
Healthy controls								
1	78	Posterior cingulate gyrus	31	L	-6	-52	26	5.03
2	21	Precuneus	31	L	-9	-43	44	4.89
3	30	Medial superior frontal gyrus	10	L/R	0	59	20	4.78
4	5	Middle cingulate gyrus	31	L	-6	-25	41	4.48
Patients with EOS								
1	66	Precuneus	30	R	12	-55	11	5.71
2	49	Medial superior frontal gyrus	10	L	-12	62	26	5.39
3	96	Cuneus	31	L	-12	-58	20	5.21
		Precuneus	31	L	-6	-55	26	5.01
4	4	Parahippocampal gyrus	37	L	-27	-43	-10	4.65
5	10	Precuneus	7	L	-6	-46	47	4.59
6	2	Parahippocampal gyrus	36	L	-24	-31	-13	4.42
7	1	Medial superior frontal gyrus	10	R	6	65	20	4.39
8	1	Middle occipital gyrus	39	R	45	-76	11	4.38

Coordinates reported in MNI space and corrected for multiple comparisons at FWE 0.05

Table 4.4. Peak coordinates of within- and between-group PPI for left and right DLPFC seed								
					Peak coordinates			
#	k	Regions	BA	L/R	x	y	z	Z-value
Healthy controls								
<i>Negative PPI – R-DLPFC</i>								
1	462	Angular gyrus	7	R	36	-64	44	4.99
2	213	Middle cingulate gyrus	23	L/R	0	-31	32	4.85
3	390	Supplementary motor area	8	R	3	23	56	4.77
4	161	Superior parietal lobule	7	L	-24	-64	41	4.21
5	95	Precuneus	7	L/R	6	-76	38	3.82
<i>Negative PPI – L-DLPFC</i>								
1	204	Angular gyrus	40	R	39	-61	41	4.09
Controls > EOS								
<i>Negative PPI R-DLPFC</i>								
1	52	Posterior cingulate gyrus	31	L/R	0	-34	32	4.26
2	11	Angular gyrus	40	R	45	-61	41	3.55
3	13	Medial superior frontal gyrus	9	L/R	0	35	35	3.40

Coordinates reported in MNI space and reported at FWE 0.05, $p < 0.001$ for within-group PPI and at an uncorrected $p < 0.001$ for between-group PPI

Chapter 5: Functional neurodevelopment of working memory in early-onset schizophrenia: a longitudinal fMRI study from adolescence to early adulthood

Abstract: Schizophrenia, a debilitating disorder with typical manifestation of clinical symptoms in early adulthood, is characterised by widespread cognitive impairments in executive processes such as in working memory (WM). However, there is a rare case of individuals with early-onset schizophrenia (EOS) starting before their 18th birthday, while WM and its neural substrates are still undergoing maturational processes. Using the WM-inducing n-back task concurrently with functional magnetic resonance imaging, we assessed the functional neurodevelopment of WM in adolescents with EOS and age- and gender-matched typically developing controls. Participants underwent neuroimaging in the same scanner twice, once at age 17 and at 21 (mean interscan interval = 4.3 years). General linear model analysis was performed to explore WM neurodevelopmental changes within and between groups. Psychopathological scores were entered in multiple regressions to detect brain regions whose longitudinal functional change was predicted by baseline symptoms in EOS. WM neurodevelopment was characterised by widespread functional reductions in frontotemporal and cingulate brain areas in patients and controls, but we found no between-group differences in the trajectory of WM change. Finally, baseline symptom scores predicted functional neurodevelopmental changes in frontal, cingulate, parietal, occipital, and cerebellar areas. The adolescent brain undergoes developmental processes such as synaptic pruning, which may underly the refinement WM of network. Prefrontal and parietooccipital activity reduction may be specific to WM neurodevelopment in EOS and affected by clinical presentation of symptoms. Using longitudinal neuroimaging methods in a rare diagnostic sample of patients with EOS may help the advancement of neurodevelopmental biomarkers intended as pharmacological targets to tackle WM impairment.

1. Introduction

Early-onset schizophrenia (EOS) patients are diagnosed with the disorder earlier than their 18th birthday and constitute around 5% of all schizophrenia cases (Cannon et al., 1999). EOS is rarer and often more debilitating than its adult onset counterpart, as manifested by more severe premorbid educational, social, and cognitive deficits (Jacobsen & Rapoport, 1998). The neurodevelopmental model suggests that schizophrenia is associated with disrupted brain maturation stemming from genetic, perinatal, and environmental factors (Mané et al., 2009). Individuals who develop schizophrenia experience premorbid neurocognitive deficits by early childhood. These are expressed as a neurodevelopmental delay in the acquisition of cognitive skills (neurodevelopmental model), rather than cognitive decline of skills that have already been acquired (neurodegenerative model) (Bora, 2015). Evidence that further reinforce the neurodevelopmental basis of schizophrenia include structural and functional brain changes in patients with first-episode psychosis (Farrow et al., 2005; Li et al., 2018), in individuals at clinical high risk for developing schizophrenia (Chung et al., 2017; Fryer et al., 2013), healthy siblings of schizophrenia patients (Gogtay et al., 2007; Loeb et al., 2018) as well as in adolescent cases with the disorder (Haenschel et al., 2007; Voets et al., 2008).

The study of typical development is useful in informing neurodevelopmental accounts of schizophrenia, as it allows the detection of deviant cognitive function or brain structure by case-control comparisons (Dima et al., 2021; Frangou et al., 2021). Adolescence is an especially critical period for the developmental maturation of executive function and its relevant processes that include for instance cognitive control, working memory (WM) and error monitoring. These processes together with their

neural substrates continue to develop up to the third decade of life (Crone & Steinbeis, 2017; Tamnes et al., 2013). Cortical and subcortical grey matter volume decreases from childhood to adulthood, while white matter increases, following normative maturation processes that include synaptic pruning and myelination, respectively (Marsh et al., 2008). Grey matter volume reduction from childhood to adolescence starts from sensorimotor areas and progresses to higher association areas, such as the dorsolateral prefrontal cortex, posterior parietal, superior and inferior temporal cortices (Gogtay et al., 2004). During adolescence the brain is marked by accelerated cortical thinning relative to childhood and adulthood (Zhou et al., 2015). For instance, cortical thickness in the cingulate cortex at the frontal lobe and the temporal poles are last to reach peak thickness around age 13 and then follow complex quadratic and cubic thinning trajectories (Shaw et al., 2008). Cortical development agrees with cognitive performance; visual WM capacity (Isbell et al., 2015) and WM accuracy at the n-back have been shown to increase throughout childhood to adulthood (Satterthwaite et al., 2013), while thinning in the frontal lobe is further associated with better verbal WM performance during development (Sowell et al., 2001). As grey matter volume reduces in areas of the cognitive control network, performance in executive function, and emotion discrimination further matures (Breukelaar et al., 2017).

Longitudinal functional brain changes that occur in typical development and associate with WM encoding, maintenance, and retrieval activity were found to fluctuate in typically developing (TD) participants from 8 to 30 years in sensorimotor and executive brain regions (Simmonds et al., 2017). From adolescence to early adulthood (ages 16-23 years), functional WM development involves progressively reduced recruitment in the anterior cingulate, the insula and inferior parietal lobule,

while the dorsolateral prefrontal cortex (DLPFC) is not engaged by adulthood at the same rate as it is during childhood (Simmonds et al., 2017).

Cognitive brain function in EOS is manifested, at large, as hypoactivation relative to age-matched TD adolescents in key executive areas that include the anterior cingulate cortex and posterior parietal cortices (Ioakeimidis et al., 2020). WM function is further associated with aberrant brain activity and connectivity in occipital, temporal, anterior cingulate regions (White, Hongwanishkul, et al., 2011), and in bilateral middle frontal gyri (DLPFC) (Bittner et al., 2015; Kyriakopoulos et al., 2012; Pauly et al., 2008), and between bilateral temporal and anterior cingulate areas (White, Schmidt, et al., 2011), similar to adult-onset cases (Glahn et al., 2005). In addition to functional studies, structural cingulate deficits are also shown in EOS. Cortical volume (Marquardt et al., 2005) and neuronal density in the anterior cingulate decrease with age (Brüne et al., 2010), while aberrant cingulate white matter integrity is associated with psychotic symptoms (Paillère-Martinot et al., 2001; Tang et al., 2010) in EOS.

Longitudinally, cortical development in EOS is characterised by altered maturational trajectories of cortical thickness in the inferior frontal, superior temporal and cingulate gyri (Alexander-Bloch et al., 2014). Grey matter volume loss is prominent in frontotemporal and anterior cingulate regions in a 2-year between-scan interval in a group of adolescents and young adults with first episode schizophrenia (Farrow et al., 2005). A 5-year follow-up study found grey matter loss starting in the parietal cortices progressing anteriorly to the frontal and temporal lobes, with the DLFC and superior temporal gyri being affected last, in a sample of adolescents with EOS (Thompson et al., 2001). Another study of the same sample found volume loss in the medial frontal and parietal wall to be affected early in the disease and later progressing to the cingulate gyrus (Vidal et al., 2006). While there is a considerable body of literature concerned

with long-term longitudinal structural neurodevelopment of EOS, there are no studies, to date, to investigate the longitudinal functional neurodevelopmental course of patients with onset-age strictly below 18 years. In fact, majority of longitudinal functional imaging studies in schizophrenia include samples mixed with post-adolescent patients and are primarily focused on the effects of short pharmacological interventions in longitudinal brain function rather than the neurodevelopmental course of the illness. Short-term longitudinal studies exploring task-dependent BOLD changes relative to pharmacological interventions and symptomatic recovery predominantly report increases in activation in patients after interventions that last 2-14 weeks (and up to 2 years in one study); these are found in frontal (dorsolateral, ventrolateral, medial, precentral, postcentral), cingulate (ACC), temporal (inferior, middle, superior), insular, parietal (inferior, precuneus), occipital (fusiform, cuneus, lingual), as well as subcortical areas (striatum, cerebellum) (Aasen et al., 2005; Ballmaier et al., 2004; Brewer et al., 2007; Cadena et al., 2018; Gurler et al., 2020; Honey et al., 1999; Keshavan et al., 2017; Kumari et al., 2015; Meisenzahl et al., 2006; Reske et al., 2007; Schlagenhauf et al., 2008, 2010; Smee et al., 2011; Snitz et al., 2005; Wolf et al., 2007). These intervention-related increases have been reported in fMRI studies focusing on WM (Honey et al., 1999; Meisenzahl et al., 2006; Schlagenhauf et al., 2008, 2010; Wolf et al., 2007), verbal fluency (Smee et al., 2011), procedural learning (Kumari et al., 2015), cognitive control (Brewer et al., 2007; Cadena et al., 2018; Keshavan et al., 2017; Snitz et al., 2005), sustained attention (Aasen et al., 2005) and memory encoding (Gurler et al., 2020), as well as social cognition (Lee et al., 2006; Reske et al., 2007). Even though such studies are extremely helpful to elucidate functional brain changes associated with changes in medication intake and recovery from acute episodes, they do not provide any insight on the functional neurodevelopment of patients with schizophrenia.

Here we studied longitudinal functional brain changes during WM performance in adolescents with EOS and age- and gender-matched TD controls into early adulthood. Research in adolescents with EOS is important because it allows to examine disorder-specific brain changes during a developmentally sensitive period wherein cognitive functions and their neural substrates still mature. It also removed variance introduced by confounding characteristics of the illness such as age-of-illness onset and cumulative exposure to antipsychotic medication. We examined differences in WM functional maturation by employing a longitudinal fMRI design that allowed us to scan EOS and controls twice with a 4.3-year inter-scan interval (mean age at first scan 17 years old and at second 21) using the same scanner and the same n-back paradigm. This aimed to identify longitudinal BOLD activity change from adolescence to early adulthood associated with WM. To our knowledge, this is the first longitudinal task-dependent fMRI investigation of whole-brain changes in functional brain recruitment in a developing sample of patients with schizophrenia onset before their 18th year of age.

2. Methods

2.1. Participants

The baseline sample included 45 EOS and control participants aged 16.2 (± 1.8) years (Kyriakopoulos et al., 2012) at the time of recruitment. Thirty-four participants returned for the follow-up session, with twenty-nine (age 21.08 \pm 1.78) being fully eligible for image analysis ([Table 5.1](#)). Patients were recruited from the South London and Maudsley NHS Foundation Trust Child and Adolescent mental health services based on the following criteria: (a) fulfilling Diagnostic and Statistical Manual of Mental Disorders - Fourth Edition (DSM-IV) criteria for schizophrenia; (b) aged 12-19 years; (c) age-of-illness onset (AIO) before the 18th birthday; (d) no co-morbid Axis I diagnosis; and (e) IQ>70. Psychopathology was assessed in patients with the Positive and Negative Syndrome Scale (PANSS) (Kay et al., 1987). Total cumulative antipsychotic exposure was calculated in chlorpromazine equivalents (CPZE). The demographic, clinical and medication status of patients that were present in both baseline and follow-up scanning sessions are summarized in [Table 5.1](#). Seventeen healthy individuals who were recruited from the same geographic area and had no personal history of psychiatric disorder and no family history of psychosis in their first-degree relatives, returned for the follow-up study. Exclusion criteria for all participants were: (a) history of head injury; (b) lifetime history of substance dependence as defined by the DSM-IV; (c) substance abuse as defined by the DSM-IV within the 6 months preceding study entry; (d) any concomitant medical condition; and (e) history of hereditary neurological disorders. All participants were assessed by qualified child psychiatrists using the Structured Clinical Interview for DSM-IV Axis I Disorders (First et al 2002a, b). In all participants, the National Adult Reading Test (NART) (Nelson &

Willison, 1991) was used to obtain an estimate of general intellectual ability and the Annett handedness scale to assess hand dominance (Annett, 1970). Patients filled in the PANSS positive syndrome sub-scale for two consecutive weeks prior to scanning to ensure that they were clinically stable defined as scoring ≤ 3 on each item.

2.2. N-back task

The n-back task was administered as a block design, incorporating alternating active and control conditions. At the beginning of each condition, participants were explicitly instructed to respond by button press to the target letter. In the control condition (X-back) the designated target letter was “X”. In the active conditions (one-, two-, and three-back), the target letter was defined as any letter that was identical to the one presented one, two or three trials back, respectively. In each condition, a series of 14 letters were presented visually, with each letter displayed for 2 seconds. Responses were monitored via an MRI-compatible button box held in the subject’s dominant hand.

There were 18 epochs in all, each lasting 30 seconds, with total experiment duration of 9 minutes. Performance of the n-back was recorded as the number of correct responses (accuracy) and reaction time. Participants were excluded for scoring $< 50\%$ accurate trials at the low-load conditions (X- and one-back) at baseline or follow-up, leading to the exclusion of three EOS patients from analysis. This resulted in a longitudinal sample of 14 EOS patients.

All participants received training before scanning to ensure they understood the task instructions. Within group longitudinal differences for n-back accuracy were assessed with the Wilcoxon test due to non-normal distribution of performance accuracy.

2.3. Image acquisition

The same scanner and image acquisition parameters were used at baseline and at follow-up. fMRI and anatomical data were acquired during the same session on a 1.5-T imaging system (Signa; GE Medical Systems, Milwaukee, Wisconsin) using a gradient-echo echo-planar imaging sequence and a 3D T1-weighted Inversion Recovery prepared Spoiled GRASS sequence respectively. A total of 270 T2*-weighted gradient echo-planar imaging (EPI) brain volumes depicting blood-oxygenation level-dependent (BOLD) contrasts were acquired at each of 16 axial planes (echo time = 40ms, repetition time = 2s, voxel dimensions = 3.75 x 3.75 x 7mm³, interslice gap = 0.7mm, matrix size = 64 x 64, flip angle = 70°). Structural images were acquired using a 3D axial T1-weighted Inversion Recovery prepared Spoiled GRASS sequence from 128 slices (echo time = 5.1ms, repetition time = 2s, inversion time = 450ms, voxel dimensions = 0.9375 × 0.9375 x 1.5 mm³, matrix size = 256 x 192, field of view = 240 x 180 mm², flip angle = 20°, number of excitations = 1).

2.4. Image analysis

2.4.1. Pre-processing

Image processing and analysis were implemented using the Statistical Parametric Mapping (SPM12) software (www.fil.ion.ucl.ac.uk/spm/). Pre-processing involved realignment (slice timing and motion correction) of the functional images, co-registration of the mean functional image to each participant's structural one, normalisation into standard stereotactic space to the Montreal Neurological Institute (MNI) template and smoothing with an isotropic Gaussian kernel of 8 mm full-width-at-half-maximum. No subjects were excluded due to excessive inter-scan motion (defined as >4 mm translation, >4° rotation).

2.4.2. *First-level image analysis*

fMRI responses were high-pass filtered (128s) and modelled using a canonical haemodynamic response function (hrf) convolved with the vectors of interest, namely the one-, two-, and three-back blocks. First-level models were constructed for each subject whereby scans from both time points were modelled as different sessions with their respective motion parameters as nuisance regressors in the fMRI model specification module on SPM12. Therefore, longitudinal first-level images were constructed to examine baseline (t1) to follow-up (t2) BOLD activity changes (Δ_{BOLD}) for each different load of n-back blocks (one-, two-, three-back), and these images were used as the dependent variable in all subsequent second-level analysis.

At the time of the longitudinal analysis the baseline scans from two control subjects were irretrievable, which led a final sample of fifteen TD adolescents available for analysis.

2.4.3. *Second-level statistical analysis*

2.4.3.1. GLM

Longitudinal first-level images (Δ_{BOLD}) for the three n-back loads were entered in a 3×2 flexible factorial model with task (one-, two-, three-back) and group (TD adolescents, adolescents with EOS) as within- and between-subject factors, respectively. We were interested in within-, and between-group differences in longitudinal Δ_{BOLD} , expressed as reduction or increase across the two time points for the three n-back loads separately (one-, two-, three-back) and together (one-, two-, three-back combined; process-general contrast). We examined Δ_{BOLD} with the following main effects and interactions: main effects of task, main effects of group, and the interactions of task \times group. Therefore, we assessed the main effects of task on Δ_{BOLD} in all n-back levels (process-general) as

well as in each level individually, across diagnosis status. Additionally, we were interested in the main effects of group on Δ_{BOLD} in process-general and in individual loads of the n-back, for within- and between-groups contrasts. Gender and age at follow-up were used as covariates of no interest. Results are reported at FWE $p < 0.05$.

2.4.3.2. Multiple regressions

First-level images of Δ_{BOLD} at two- and three-back for our entire sample (controls and patients) were entered into multiple regression models in SPM12, with Δ_{accuracy} at two- and three-back as covariates of interest, respectively, while diagnosis and gender were entered as covariates of no interest. Additionally, multiple regressions for Δ_{accuracy} and Δ_{BOLD} were ran in separate models for each group. One-back blocks were skipped from this analysis because median accuracy was 100% in both groups in both scanning sessions.

Regression models with baseline PANSS symptoms scores were further analysed to explore whether symptoms could predict Δ_{BOLD} in patients. Additionally, we performed multiple regression analyses to explore whether Δ_{BOLD} would be predicted by age-of-onset or cumulative medication intake. Gender was used as a covariate of no interest in all analyses. Reported results are thresholded at FWE of $p < 0.05$.

Peak coordinates were labelled with the AAL SPM extension (Rolls et al., 2020) and most proximal Brodmann areas (BA) were identified through the Talairach client (Lancaster et al., 2000). For visualisation, SPMs were thresholded at an uncorrected $p < 0.001$ with k_e greater than the minimum number of voxels with FWE < 0.05 and were overlaid on the Colin27_T1_seg_MNI template in Mango (<http://rii.uthscsa.edu/mango/>).

3. Results

For the baseline study, cross-sectional analyses for demographic, clinical, behavioural, and functional brain differences are reported in detail in Kyriakopoulos et al. (2012) and for the follow-up session in the supplementary material. The results presented in the following sections only concern the longitudinal cohort that participated in both scanning sessions.

3.1. Participants

The longitudinal sample consisted of twenty-nine individuals (fifteen TD adolescents and fourteen adolescents with EOS ([Table 5.1](#)). Figure 5.1 shows the distribution of ages in both time points. The interscan interval between baseline and follow-up was 4.3 (± 0.82) years for all participants.

Mean age of schizophrenia onset was 14.87 years (± 1.28) (age range 11.70 – 17.14) ([Table 5.1](#); Figure 5.1), while illness duration at baseline was 2.20 years (± 1.44) and 6.14 (± 1.62) years at follow-up. PANSS scores (positive, negative and total) remained stable through the 4-year course of the longitudinal study ($p > .271$). Cumulative antipsychotic exposure (in chlorpromazine equivalents) increased significantly across the 4-year follow-up ($\Delta_{CPZE-t1>t2} = 16,716$ mg, $p < .001$) ([Table 5.1](#)).

NART scores increased, yet not significantly, in patients with EOS ($\Delta_{NART-t1>t2} = -2.76$, $p = 0.149$; [Table 5.1](#)) but were significantly improved in TD adolescents from baseline to follow-up ($\Delta_{NART-t1>t2} = -10.70$, $p < .001$; [Table 5.1](#)). Accuracy in one- and two-back blocks did not change significantly from baseline to follow-up, in neither of the groups. Three-back accuracy was significantly improved in individuals with EOS ($Z = -2.157$, $p = 0.031$), whereas TD adolescents showed a trend of accuracy improvement

($Z = -1.949$, $p = 0.051$) (Table 5.1). RT was not statistically different from baseline to follow-up in all n-back levels ($p > .413$)

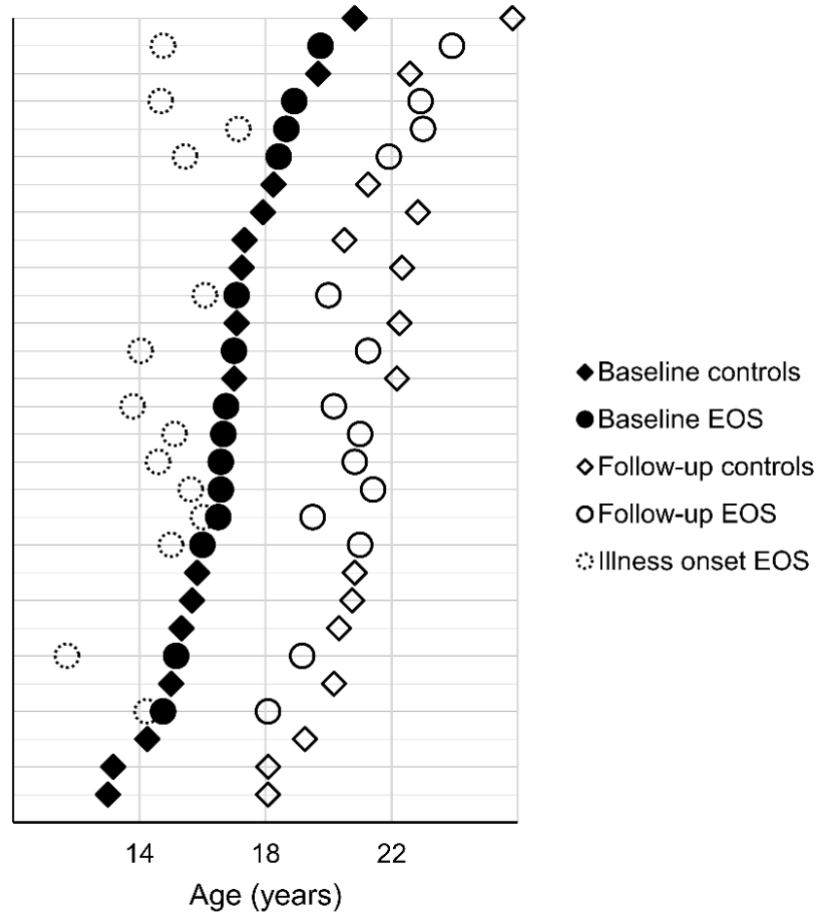


Figure 5.1. The graph shows the age distribution (in years) of the participants (Y axis) from baseline and follow-up scans. Age of illness-onset for EOS patients is also shown. It also shows the interscan interval for each participant (follow-up age minus baseline age) as well as the duration of illness for EOS patients at each scan (age minus illness-onset)

3.2. Longitudinal BOLD activity change in the entire sample

Main effects of task (one-, two-, three-back) in the entire sample showed that there were only longitudinal reductions ($\Delta_{\text{BOLD}(t1>t2)}$); these were located in the right superior frontal gyrus (SFG), bilaterally in the middle frontal gyri (MFG), the right fusiform gyrus, bilateral in the superior temporal poles, and from middle to posterior cingulate

gyrus, for the process-general contrast (Table 5.2; Figure 5.2A). There were significant $\Delta_{\text{BOLD}(t1>t2)}$ changes at the highest n-back load (three-back) which was observed in a cluster expanding from the right superior frontal gyrus to the anterior cingulate gyrus and supplementary motor area (SMA). One- and two-back blocks did not show significant longitudinal main effects of task.

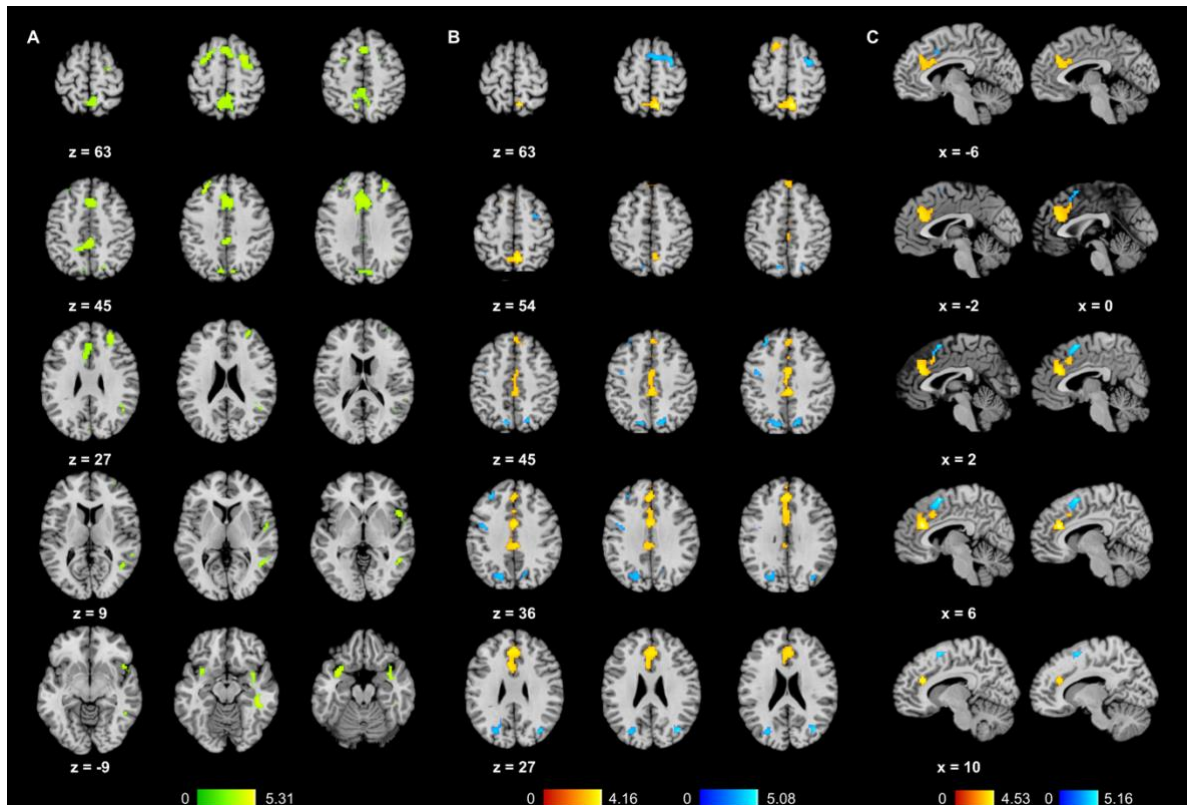


Figure 5.2. A) Brain areas with main effects of task on process-general $\Delta_{\text{BOLD}(t1>t2)}$ from baseline to follow-up in the entire sample of developing adolescents; B) Brain areas with process-general $\Delta_{\text{BOLD}(t1>t2)}$ in typically developing adolescents (red) and in adolescents with EOS (blue) and C) Sagittal layout of $\Delta_{\text{BOLD}(t1>t2)}$ in typically adolescents (red) and adolescents with EOS (blue), showing the non-overlapping reductions in ACC (red) and SMA (blue) areas at three-back trials. The EOS threshold SPM was extracted from the model with the additional covariates, i.e., onset-age, cumulative antipsychotic medication, and interscan interval, but it is not showing the left middle/superior temporal cluster because we wanted to show the absence of overlap in the two midline areas. Colour bars represent the T-values of the overlain clusters. Multiple comparisons correction at FWE $p < 0.05$

3.3. Longitudinal BOLD activity change within and between groups

Task main effects for healthy adolescents showed significant longitudinal process-general reduction of brain activity ($\Delta_{\text{BOLD}(t1>t2)}$) in medial areas bilaterally in the

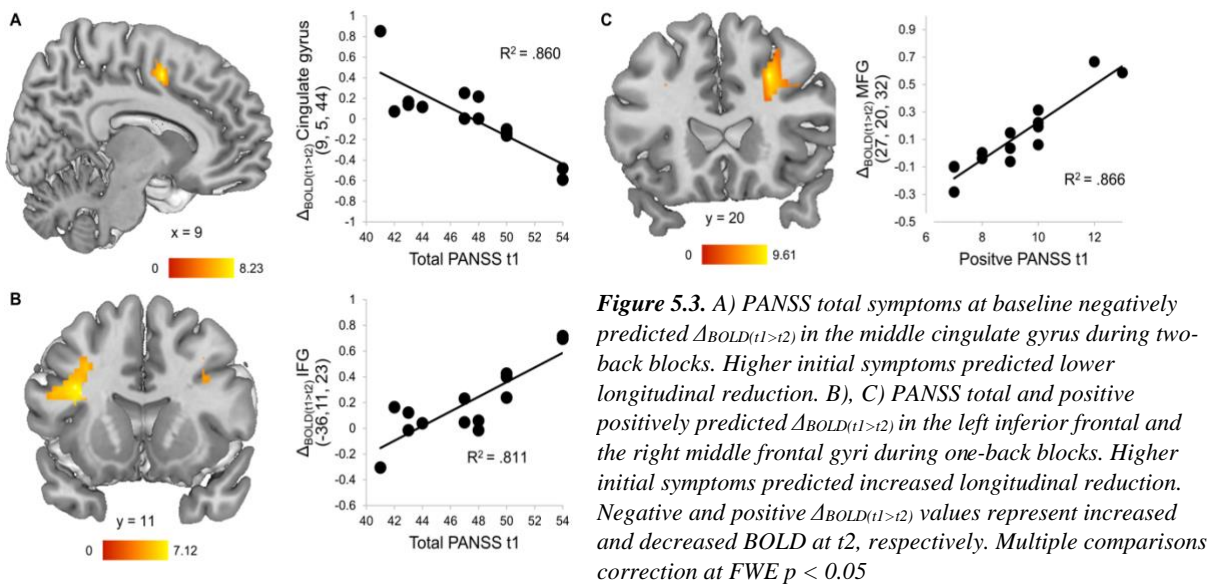
precuneus and the anterior cingulate gyrus expanding posteriorly to the posterior cingulate portion ([Table 5.3](#); Figure 5.2B). Significant changes $\Delta_{\text{BOLD}(t_1>t_2)}$ were also apparent for the three-back in the anterior cingulate gyrus.

Adolescents with EOS had significant process-general changes $\Delta_{\text{BOLD}(t_1>t_2)}$ in more lateral regions in the cortex; these were observed in the right middle occipital and the superior frontal gyri, and the left middle frontal gyrus (DLPFC) and the precuneus expanding to the superior parieto-occipital gyri ([Table 5.3](#); Figure 5.2B). Additionally, patients with EOS showed significant changes $\Delta_{\text{BOLD}(t_1>t_2)}$ at the right putamen/insula (BA 13) during the one-back ([Table 5.3](#)).

In addition to the previous analyses, we performed an exploratory GLM in the EOS group only, where we added the clinical covariates of age of illness-onset, cumulative CPZE and the interscan interval. This was done to identify changes in longitudinal brain activity after ruling out variance caused by confounding factors that are secondary to the illness (Karlsgodt et al., 2008). Duration of illness was not included as a covariate to this model because it is strongly correlated with age at follow-up ($r = 0.682$, $p = 0.007$) which would violate the collinearity assumption of ANCOVA. Clusters of significant changes $\Delta_{\text{BOLD}(t_1>t_2)}$ for process-general are shown in Figure 5.2C and reported in [Table 5.4](#). Significant clusters were located at the right middle occipital gyrus and left parieto-occipital regions, similar to the original analysis without the clinical covariates, but the effect in left middle frontal gyrus ($x = -30$, $y = 38$, $z = 38$, $k_e = 34$, $Z = 4.35$) was now at trend level (*peak-FWE* $p = 0.063$). Furthermore, significant process-general $\Delta_{\text{BOLD}(t_1>t_2)}$ was seen in the supplementary motor area, the right insula and parietooccipital region ([Table 5.4](#); Figure 5.2C). Unlike the model without the clinical covariates, there were no voxels surviving correction for multiple comparisons for the EOS \times one-back interaction. In contrast, $\Delta_{\text{BOLD}(t_1>t_2)}$ changes in the

supplementary motor area and the left superior temporal gyrus were found during three-back (Table 5.4).

No between-group effects that survived FWE correction were found for Δ_{BOLD} . Therefore, longitudinal changes were not significantly different between the two groups.



3.4. Prediction of longitudinal BOLD activity change by clinical characteristics of EOS

PANSS total, PANSS positive, and PANSS negative scores at t1 were entered in multiple regression models to examine if baseline psychotic symptoms could predict $\Delta_{\text{BOLD}(t1>t2)}$ changes in EOS at one-, two-, three-back, and process-general contrasts. At one-back, total PANSS symptoms scores at baseline predicted increased reduction in $\Delta_{\text{BOLD}(t1>t2)}$ changes in the left inferior frontal gyrus and right middle frontal gyrus, whereas baseline positive PANSS symptoms predicted increased reduction in $\Delta_{\text{BOLD}(t1>t2)}$ changes in the right portions of middle frontal, lingual, and angular gyri, as well as in the left inferior frontal gyrus (Table 5.5; Figure 5.3A). For the two-back n-

back, higher baseline scores in PANSS positive and total scales predicted lower reduction in $\Delta_{\text{BOLD}(t1>t2)}$ changes around the ACC and supplementary motor area, while more severe negative symptoms predicted lower reduction in $\Delta_{\text{BOLD}(t1>t2)}$ changes in the cerebellum ([Table 5.5](#); Figure 5.3B).

Age of illness-onset and cumulative CPZE did not account for significant prediction of $\Delta_{\text{BOLD}(t1>t2)}$ changes.

4. Discussion

To our knowledge, this is the first longitudinal fMRI study to investigate the functional development of WM in patients with EOS and age-matched controls from adolescence to early adulthood. We found that (1) functional brain changes associated with WM did not differ between patients with EOS and typically developing participants in a 4-year period, while (2) WM development is associated with widespread functional reductions in frontotemporal and cingulate regions in the entire sample. Finally, (3) severity of schizophrenia symptoms at baseline was associated with functional longitudinal changes mostly in frontal and cingulate areas.

EOS patients displayed stable WM performance and did not show any deterioration in their positive and negative symptoms at the time of testing, which is in line with the neurodevelopmental model (Zipursky et al., 2013). Accuracy was already developed at adult levels for the one-back and two-back in both groups, since there were no differences from baseline-to-follow-up. However, the ability to perform accurately the three-back continued to increase into early adulthood in both groups of developing adolescents. In the 4-year period spanning from adolescence to early adulthood, WM-related brain activation did not differ between EOS patients and typically developing participants. Similar neuroimaging findings were reported in a longitudinal study exploring cognitive control in young patients (12-28 years) with recent-onset schizophrenia which identified stable activation in DLPFC over a 1.5-year period in both schizophrenia and healthy controls (Niendam et al., 2018).

Even though longitudinal functional change between the groups was statistically comparable, when visually inspecting Figure 5.2 it becomes apparent that the functional reductions in TD controls and those in EOS patients do not overlap. Instead, adolescents

with EOS had reduced recruitment of brain areas located more laterally, i.e., prefrontal and parieto-occipital areas. These reductions were seen despite the patients' longitudinal cognitive performance and symptom status that remained stable across the 4-year follow-up period. Hence, WM functional neurodevelopment in EOS is manifested by reduced recruitment in executive brain regions that do not overlap with the developmental reductions in controls. Longitudinally, activity reductions in brain areas of the posterior parietal and occipital cortex together with prefrontal areas may be specific to schizophrenia dysfunction as the disease progresses (Hahn et al., 2018; Huang et al., 2019). Such dysfunction may result from altered brain maturation mechanisms in EOS, such as synaptic pruning. It is possible that EOS is characterised by additional factors, like social adversity and stress, during this later maturational period that affect the refinement of the executive circuitry and the elimination of extraneous synapses that normally occur in typical development (Karlsgodt et al., 2008; Thormodsen et al., 2013) to the degree of observable reduction in function over time. This could then translate into progressively different functional reorganisation of WM in EOS adolescents and TD ones during transition into adulthood.

Irrespective of group membership, WM maturation was associated with reduced recruitment in bilateral prefrontal cortex (right superior and left middle frontal), bilateral superior temporal poles, right fusiform gyrus, and posterior cingulate gyrus, irrespective of n-back load. Reductions were also seen in ACC, superior frontal gyrus, and supplementary motor area were found at three-back; as adolescents matured to adulthood, they relied less in the aforementioned regions to complete the n-back task. Similarly, Simmonds and colleagues (2017) found reductions in executive regions during typical development of WM function from childhood to adulthood. Hence, decreasing WM function in development consists of a normal process that is seen in

both EOS and TD adolescents in executive brain areas and it parallels normative structural developmental trajectories (Gogtay et al., 2004).

Our results indicate that typical WM maturation in the transition to adulthood is associated with decreased activation in regions in the medial wall that spanned from the anterior to the posterior cingulate and to the precuneus. Activation of the ACC/midcingulate cortex is relevant to conflict and error monitoring, redirection of attention and action whereas the posterior cingulate and precuneus are more related to self-referential activity (Rolls, 2019). Decreased activation in these areas could be related to performing the n-back by doing less errors, while also relying less on internalised thinking processes in early adulthood. It could also highlight the refinement of error monitoring to guide action towards more successful trials, which is suggested by the trend improvement in the three-back performance which is paralleled by the significant reduction on the activation in ACC and supplementary motor area during these high-load and error-prone blocks. Functional activity reduction in the ACC was not only significant in the whole n-back process-general and the three-back contrasts, but it was also predicted by improving accuracy at the two-back. Taken together these results indicate a central role of the ACC in WM development during late adolescence.

Positive, negative, and total schizophrenia psychopathology at baseline was associated with functional longitudinal changes in a widespread brain network including midline cingulate, frontal, parietal, and occipital areas, as well as the cerebellum. More severe initial total and positive PANSS scores predicted greater degree of hypoactivation in middle and inferior frontal areas located in the DLPFC in adulthood in EOS patients. Reduced DLPFC activation in EOS patients when tested in adolescence has been consistently reported (Kyriakopoulos et al., 2012; Pauly et al., 2008). Although, Simmonds et al. (2017) found that in TD participants from 16 to 23

years old, while functional WM development does not engage the DLPFC at the same rate as it does during childhood, it is still playing an integral role in WM. In our study, EOS patients with more severe adolescent psychopathology at age 17 activated their DLPFC less in early adulthood at age 21. This hypoactivity is consistent with findings from previous adult schizophrenia studies in WM (for meta-analysis see Wu & Jiang, 2019). On the other hand, more severe initial positive and total symptoms predicted linearly reduced functional change in the ACC. This means that EOS patients that scored higher at PANSS total scales had lesser functional reductions in the ACC. These results are consistent with previous meta-analyses on schizophrenia and WM memory (Wu & Jiang, 2019). The hypo-activation of the DLPFC and the hyper-activation of the dorsal ACC appear to be intrinsically linked; the DLPFC provides top-down cognitive control (Miller & Cohen, 2001) and the ACC is responsible for conflict monitoring (Kerns et al., 2004). Within this framework, the hyper-activation of the ACC could occur if the hypo-activation of the DLPFC leads to impaired cognitive control and demands increased conflict monitoring and adjustments in control from the ACC (Carter et al., 2001). Our results strengthen the case for DLPFC and ACC pathology in the pathogenesis of schizophrenia and at the same time highlight the importance of time of scanning in brain development.

Several methodological issues require further consideration. First, possible medication effects on the study results cannot be conclusively refuted. However, we found no significant relationship between medication and measures of regional activation. Second, our study's sample size may be small, although it is similar to the sample size of recent longitudinal studies that include neuroimaging and EOS patients (Epstein & Kumra, 2015; Palaniyappan et al., 2013; Sun et al., 2016). EOS is a rare disorder, which makes enrolment and retention of participants more difficult. However,

we improved our power by acquiring a homogeneous diagnostic sample that is matched to the HC group. Finally, potential signal drifts of MRI scanners are a common problem in longitudinal studies. Nevertheless, the same MRI scanner was used for baseline and follow-up investigations and was frequently tested for signal stability.

References

- Aasen, I., Kumari, V., & Sharma, T. (2005). Effects of rivastigmine on sustained attention in schizophrenia: An fMRI study. *Journal of Clinical Psychopharmacology*, *25*(4), 311–317. <https://doi.org/10.1097/01.jcp.0000169267.36797.76>
- Alexander-Bloch, A. F., Reiss, P. T., Rapoport, J., McAdams, H., Giedd, J. N., Bullmore, E. T., & Gogtay, N. (2014). Abnormal cortical growth in schizophrenia targets normative modules of synchronized development. *Biological Psychiatry*, *76*(6), 438–446. <https://doi.org/10.1016/j.biopsych.2014.02.010>
- Annett, M. (1970). A classification of hand preference by association analysis. *British Journal of Psychology*, *61*(3), 303–321. <https://doi.org/10.1111/j.2044-8295.1970.tb01248.x>
- Ballmaier, M., Toga, A. W., Siddarth, P., Blanton, R. E., Levitt, J. G., Lee, M., & Caplan, R. (2004). Thought disorder and nucleus accumbens in childhood: A structural MRI study. *Psychiatry Research - Neuroimaging*, *130*(1), 43–55. <https://doi.org/10.1016/j.psychresns.2003.10.001>
- Bittner, R. A., Linden, D. E. J., Roebroek, A., Härtling, F., Rotarska-Jagiela, A., Maurer, K., Goebel, R., Singer, W., & Haenschel, C. (2015). The When and Where of Working Memory Dysfunction in Early-Onset Schizophrenia—A Functional Magnetic Resonance Imaging Study. *Cerebral Cortex*, *25*(9), 2494–2506. <https://doi.org/10.1093/cercor/bhu050>
- Bora, E. (2015). Neurodevelopmental origin of cognitive impairment in schizophrenia. *Psychological Medicine*, *45*(1), 1–9. <https://doi.org/10.1017/S0033291714001263>
- Breukelaar, I. A., Antees, C., Grieve, S. M., Foster, S. L., Gomes, L., Williams, L. M., & Korgaonkar, M. S. (2017). Cognitive control network anatomy correlates with neurocognitive behavior: A longitudinal study. *Human Brain Mapping*, *38*(2), 631–643. <https://doi.org/10.1002/hbm.23401>
- Brewer, W. J., Yücel, M., Harrison, B. J., McGorry, P. D., Olver, J., Egan, G. F., Velakoulis, D., & Pantelis, C. (2007). Increased Prefrontal Cerebral Blood flow in First-Episode Schizophrenia Following Treatment: Longitudinal Positron Emission Tomography Study. *Australian & New Zealand Journal of Psychiatry*, *41*(2), 129–135. <https://doi.org/10.1080/00048670601109899>
- Brüne, M., Schöbel, A., Karau, R., Benali, A., Faustmann, P. M., Juckel, G., & Petrasch-Parwez, E. (2010). Von Economo neuron density in the anterior cingulate cortex is reduced in early onset schizophrenia. *Acta Neuropathologica*, *119*(6), 771–778. <https://doi.org/10.1007/s00401-010-0673-2>
- Cannon, M., Jones, P., Huttunen, M. O., Tanskanen, A., Huttunen, T., Rabe-Hesketh, S., & Murray, R. M. (1999). School performance in Finnish children and later development of schizophrenia: A population-based longitudinal study. *Archives of General Psychiatry*, *56*(5), 457–463. <https://doi.org/10.1001/archpsyc.56.5.457>

- Cadena, E. J., White, D. M., Kraguljac, N. V., Reid, M. A., & Lahti, A. C. (2018). Evaluation of fronto-striatal networks during cognitive control in unmedicated patients with schizophrenia and the effect of antipsychotic medication. *Npj Schizophrenia*, 4(1). <https://doi.org/10.1038/s41537-018-0051-y>
- Carter, C. S., MacDonald, A. W., Ross, L. L., & Stenger, V. A. (2001). Anterior cingulate cortex activity and impaired self-monitoring of performance in patients with schizophrenia: An event-related fMRI study. *American Journal of Psychiatry*, 158(9), 1423–1428. <https://doi.org/10.1176/appi.ajp.158.9.1423>
- Chung, Y., Haut, K. M., He, G., van Erp, T. G. M., McEwen, S., Addington, J., Bearden, C. E., Cadenhead, K., Cornblatt, B., Mathalon, D. H., McGlashan, T., Perkins, D., Seidman, L. J., Tsuang, M., Walker, E., Woods, S. W., & Cannon, T. D. (2017). Ventricular enlargement and progressive reduction of cortical gray matter are linked in prodromal youth who develop psychosis. *Schizophrenia Research*, 189, 169–174. <https://doi.org/10.1016/j.schres.2017.02.014>
- Crone, E. A., & Steinbeis, N. (2017). Neural Perspectives on Cognitive Control Development during Childhood and Adolescence. In *Trends in Cognitive Sciences* (Vol. 21, Issue 3, pp. 205–215). Elsevier Ltd. <https://doi.org/10.1016/j.tics.2017.01.003>
- Dima, D., Modabbernia, A., Papachristou, E., Doucet, G. E., Agartz, I., Aghajani, M., Akudjedu, T. N., Albajes-Eizagirre, A., Alnæs, D., Alpert, K. I., Andersson, M., Andreasen, N. C., Andreassen, O. A., Asherson, P., Banaschewski, T., Bargallo, N., Baumeister, S., Baur-Streubel, R., Bertolino, A., ... Frangou, S. (2021). Subcortical volumes across the lifespan: Data from 18,605 healthy individuals aged 3–90 years. *Human Brain Mapping*, December 2020, hbm.25320. <https://doi.org/10.1002/hbm.25320>
- Epstein, K. A., & Kumra, S. (2015). White matter fractional anisotropy over two time points in early onset schizophrenia and adolescent cannabis use disorder: A naturalistic diffusion tensor imaging study. *Psychiatry Research - Neuroimaging*, 232(1), 34–41. <https://doi.org/10.1016/j.psychresns.2014.10.010>
- Farrow, T. F. D., Whitford, T. J., Williams, L. M., Gomes, L., & Harris, A. W. F. (2005). Diagnosis-related regional gray matter loss over two years in first episode schizophrenia and bipolar disorder. *Biological Psychiatry*, 58(9), 713–723. <https://doi.org/10.1016/j.biopsych.2005.04.033>
- First M. B., Spitzer R. L., Gibbon M., Williams J. B. W. (2002a). *Structured Clinical Interview for DSM-IV-TR Axis I Disorders, Research Version, Non-patient Edition*. (SCID-I/NP). New York: Biometrics Research, New York State Psychiatric Institute
- First M. B., Spitzer R. L., Gibbon M., Williams J. B. W. (2002b). *Structured Clinical Interview for DSM-IV-TR Axis I Disorders, Research Version, Patient Edition*. (SCID-I/P). New York: Biometrics Research, New York State Psychiatric Institute
- Frangou, S., Modabbernia, A., Williams, S. C. R., Papachristou, E., Doucet, G. E., Agartz, I., Aghajani, M., Akudjedu, T. N., Albajes-Eizagirre, A., Alnæs, D., Alpert, K. I., Andersson, M., Andreasen, N.

- C., Andreassen, O. A., Asherson, P., Banaschewski, T., Bargallo, N., Baumeister, S., Baur-Streubel, R., ... Dima, D. (2021). Cortical thickness across the lifespan: Data from 17,075 healthy individuals aged 3–90 years. *Human Brain Mapping*, 1–21. <https://doi.org/10.1002/hbm.25364>
- Fryer, S. L., Woods, S. W., Kiehl, K. A., Calhoun, V. D., Pearlson, G. D., Roach, B. J., Ford, J. M., Srihari, V. H., McGlashan, T. H., & Mathalon, D. H. (2013). Deficient suppression of default mode regions during working memory in individuals with early psychosis and at clinical high-risk for psychosis. *Frontiers in Psychiatry*, 4(SEP), 1–17. <https://doi.org/10.3389/fpsy.2013.00092>
- Glahn, D. C., Ragland, J. D., Abramoff, A., Barrett, J., Laird, A. R., Bearden, C. E., & Velligan, D. I. (2005). Beyond hypofrontality: A quantitative meta-analysis of functional neuroimaging studies of working memory in schizophrenia. *Human Brain Mapping*, 25(1), 60–69. <https://doi.org/10.1002/hbm.20138>
- Gogtay, N., Giedd, J. N., Lusk, L., Hayashi, K. M., Greenstein, D., Vaituzis, a C., Nugent, T. F., Herman, D. H., Clasen, L. S., Toga, A. W., Rapoport, J. L., & Thompson, P. M. (2004). Dynamic mapping of human cortical development during childhood through early adulthood. *Proceedings of the National Academy of Sciences of the United States of America*, 101(21), 8174–8179. <https://doi.org/10.1073/pnas.0402680101>
- Gogtay, N., Greenstein, D., Lenane, M., Clasen, L., Sharp, W., Gochman, P., Butler, P., Evans, A., & Rapoport, J. (2007). Cortical Brain Development in Nonpsychotic Siblings of Patients With Childhood-Onset Schizophrenia. *Archives of General Psychiatry*, 64(7), 772–780. <https://doi.org/10.1001/archpsyc.64.7.772>
- Gurler, D., White, D. M., Kraguljac, N. V., Ver Hoef, L., Martin, C., Tennant, B., & Lahti, A. C. (2020). Neural Signatures of Memory Encoding in Schizophrenia Are Modulated by Antipsychotic Treatment. *Neuropsychobiology*, 1–13. <https://doi.org/10.1159/000506402>
- Haenschel, C., Bittner, R. A., Haertling, F., Rotarska-Jagiela, A., Maurer, K., Singer, W., & Linden, D. E. J. (2007). Contribution of Impaired Early-Stage Visual Processing to Working Memory Dysfunction in Adolescents With Schizophrenia. *Archives of General Psychiatry*, 64(11), 1229. <https://doi.org/10.1001/archpsyc.64.11.1229>
- Hahn, B., Robinson, B. M., Leonard, C. J., Luck, S. J., & Gold, J. M. (2018). Posterior parietal cortex dysfunction is central to working memory storage and broad cognitive deficits in schizophrenia. *Journal of Neuroscience*, 38(39), 8378–8387. <https://doi.org/10.1523/JNEUROSCI.0913-18.2018>
- Honey, G. D., Bullmore, E. T., Soni, W., Varatheesan, M., Williams, S. C. R., & Sharma, T. (1999). Differences in frontal cortical activation by a working memory task after substitution of risperidone for typical antipsychotic drugs in patients with schizophrenia. *Proceedings of the National Academy of Sciences of the United States of America*, 96(23), 13432–13437. <https://doi.org/10.1073/pnas.96.23.13432>
- Huang, A. S., Rogers, B. P., Anticevic, A., Blackford, J. U., Heckers, S., & Woodward, N. D. (2019).

- Brain function during stages of working memory in schizophrenia and psychotic bipolar disorder. *Neuropsychopharmacology*, 44(12), 2136–2142. <https://doi.org/10.1038/s41386-019-0434-4>
- Ioakeimidis, V., Haenschel, C., Yarrow, K., Kyriakopoulos, M., & Dima, D. (2020). A Meta-analysis of Structural and Functional Brain Abnormalities in Early-Onset Schizophrenia. *Schizophrenia Bulletin Open*, 1(1), 1–12. <https://doi.org/10.1093/schizbullopen/sgaa016>
- Isbell, E., Fukuda, K., Neville, H. J., & Vogel, E. K. (2015). Visual working memory continues to develop through adolescence. *Frontiers in Psychology*, 6(May), 1–10. <https://doi.org/10.3389/fpsyg.2015.00696>
- Jacobsen, L. K., & Rapoport, J. L. (1998). Research Update: Childhood-onset Schizophrenia: Implications of Clinical and Neurobiological Research. *Journal of Child Psychology and Psychiatry*, 39(1), 101–113. <https://doi.org/10.1111/1469-7610.00305>
- Karlsgodt, K. H., Sun, D., Jimenez, A. M., Lutkenhoff, E. S., Willhite, R., Van erp, T. G. M., & Cannon, T. D. (2008). Developmental disruptions in neural connectivity in the pathophysiology of schizophrenia. *Development and Psychopathology*, 20(4), 1297–1327. <https://doi.org/10.1017/S095457940800062X>
- Kay, S. R., Fiszbein, A., & Opler, L. A. (1987). The Positive and Negative Syndrome Scale (PANSS) for Schizophrenia. *Schizophrenia Bulletin*, 13(2), 261–276. <https://doi.org/10.1093/schbul/13.2.261>
- Kerns, J. G., Cohen, J. D., Iii, A. W. M., Cho, R. Y., Stenger, A., & Carter, C. S. (2004). Anterior Cingulate Conflict Monitoring and Adjustments in Control. *Science*, 303(5660), 1023–1026.
- Keshavan, M. S., Eack, S. M., Prasad, K. M., Haller, C. S., & Cho, R. Y. (2017). Longitudinal functional brain imaging study in early course schizophrenia before and after cognitive enhancement therapy. *NeuroImage*, 151(November 2016), 55–64. <https://doi.org/10.1016/j.neuroimage.2016.11.060>
- Kumari, V., Ettinger, U., Lee, S. E., Deuschl, C., Anilkumar, A. P., Schmechtig, A., Corr, P. J., Ffytche, D. H., & Williams, S. C. R. (2015). Common and distinct neural effects of risperidone and olanzapine during procedural learning in schizophrenia: A randomised longitudinal fMRI study. *Psychopharmacology*, 232(17), 3135–3147. <https://doi.org/10.1007/s00213-015-3959-1>
- Kyriakopoulos, M., Dima, D., Roiser, J. P., Corrigall, R., Barker, G. J., & Frangou, S. (2012). Abnormal Functional Activation and Connectivity in the Working Memory Network in Early-Onset Schizophrenia. *Journal of the American Academy of Child & Adolescent Psychiatry*, 51(9), 911–920.e2. <https://doi.org/10.1016/j.jaac.2012.06.020>
- Lancaster, J. L., Woldorff, M. G., Parsons, L. M., Liotti, M., Freitas, C. S., Rainey, L., Kochunov, P. V., Nickerson, D., Mikiten, S. A., & Fox, P. T. (2000). Automated Talairach Atlas labels for functional brain mapping. *Human Brain Mapping*, 10(3), 120–131. [https://doi.org/10.1002/1097-0193\(200007\)10:3<120::AID-HBM30>3.0.CO;2-8](https://doi.org/10.1002/1097-0193(200007)10:3<120::AID-HBM30>3.0.CO;2-8)
- Lee, K., Brown, W. H., Egleston, P. N., Green, R. D. J., Farrow, T. F. D., Hunter, M. D., Parks, R. W.,

- Wilkinson, I. D., Spence, S. A., & Woodruff, P. W. R. (2006). A Functional Magnetic Resonance Imaging Study of Social Cognition in Schizophrenia During an Acute Episode and After Recovery. *American Journal of Psychiatry*, *163*(11), 1926–1933.
<https://doi.org/10.1176/ajp.2006.163.11.1926>
- Li, M., Deng, W., Das, T., Li, Y., Zhao, L., Ma, X., Wang, Y., Yu, H., Li, X., Meng, Y. jing, Wang, Q., Palaniyappan, L., & Li, T. (2018). Neural substrate of unrelenting negative symptoms in schizophrenia: a longitudinal resting-state fMRI study. *European Archives of Psychiatry and Clinical Neuroscience*, *268*(7), 641–651. <https://doi.org/10.1007/s00406-017-0851-5>
- Loeb, F. F., Zhou, X., Craddock, K. E. S., Shora, L., Broadnax, D. D., Gochman, P., Clasen, L. S., Lalonde, F. M., Berman, R. A., Berman, K. F., Rapoport, J. L., & Liu, S. (2018). Reduced Functional Brain Activation and Connectivity During a Working Memory Task in Childhood-Onset Schizophrenia. *Journal of the American Academy of Child and Adolescent Psychiatry*, *57*(3), 166–174. <https://doi.org/10.1016/j.jaac.2017.12.009>
- Mané, A., Falcon, C., Mateos, J. J., Fernandez-Egea, E., Horga, G., Lomeña, F., Bargalló, N., Prats-Galino, A., Bernardo, M., & Parellada, E. (2009). Progressive gray matter changes in first episode schizophrenia: A 4-year longitudinal magnetic resonance study using VBM. *Schizophrenia Research*, *114*(1–3), 136–143. <https://doi.org/10.1016/j.schres.2009.07.014>
- Marquardt, R. K., Levitt, J. G., Blanton, R. E., Caplan, R., Asarnow, R., Siddarth, P., Fadale, D., McCracken, J. T., & Toga, A. W. (2005). Abnormal development of the anterior cingulate in childhood-onset schizophrenia: A preliminary quantitative MRI study. *Psychiatry Research - Neuroimaging*, *138*(3), 221–233. <https://doi.org/10.1016/j.psychresns.2005.01.001>
- Marsh, R., Gerber, A. J., & Peterson, B. S. (2008). Neuroimaging Studies of Normal Brain Development and Their Relevance for Understanding Childhood Neuropsychiatric Disorders. *Journal of the American Academy of Child & Adolescent Psychiatry*, *47*(11), 1233–1251.
<https://doi.org/10.1097/CHI.0b013e318185e703>
- Meisenzahl, E. M., Scheuerecker, J., Zipse, M., Ufer, S., Wiesmann, M., Frodl, T., Koutsouleris, N., Zetzsche, T., Schmitt, G., Riedel, M., Spellmann, I., Dehning, S., Linn, J., Brückmann, H., & Möller, H. J. (2006). Effects of treatment with the atypical neuroleptic quetiapine on working memory function: A functional MRI follow-up investigation. *European Archives of Psychiatry and Clinical Neuroscience*, *256*(8), 522–531. <https://doi.org/10.1007/s00406-006-0687-x>
- Miller, E., & Cohen, J. (2001). An integrative theory of prefrontal cortex function. *Annual Review of Neuroscience*, 167–202. <http://www.annualreviews.org/doi/abs/10.1146/annurev.neuro.24.1.167>
- Nelson, H. R., Willison, J. R. (1991). *National Adult Reading Test (NART)*. Windsor: NFER-Nelson.
- Niendam, T. A., Ray, K. L., Iosif, A. M., Lesh, T. A., Ashby, S. R., Patel, P. K., Smucny, J., Ferrer, E., Solomon, M., Ragland, J. D., & Carter, C. S. (2018). Association of Age at Onset and Longitudinal Course of Prefrontal Function in Youth with Schizophrenia. *JAMA Psychiatry*, *75*(12), 1217–1224.

<https://doi.org/10.1001/jamapsychiatry.2018.2538>

- Paillère-Martinot, M.-L., Caclin, A., Artiges, E., Poline, J.-B., Joliot, M., Mallet, L., Recasens, C., Attar-Lévy, D., & Martinot, J.-L. (2001). Cerebral gray and white matter reductions and clinical correlates in patients with early onset schizophrenia. *Schizophrenia Research*, *50*(1), 19–26. [https://doi.org/10.1016/S0920-9964\(00\)00137-7](https://doi.org/10.1016/S0920-9964(00)00137-7)
- Palaniyappan, L., Crow, T. J., Hough, M., Voets, N. L., Liddle, P. F., James, S., Winmill, L., & James, A. C. (2013). Gyrfication of Broca's region is anomalously lateralized at onset of schizophrenia in adolescence and regresses at 2year follow-up. *Schizophrenia Research*, *147*(1), 39–45. <https://doi.org/10.1016/j.schres.2013.03.028>
- Pauly, K., Seiferth, N. Y., Kellermann, T., Backes, V., Vloet, T. D., Shah, N. J., Schneider, F., Habel, U., & Kircher, T. T. (2008). Cerebral Dysfunctions of Emotion—Cognition Interactions in Adolescent-Onset Schizophrenia. *Journal of the American Academy of Child & Adolescent Psychiatry*, *47*(11), 1299–1310. <https://doi.org/10.1097/CHI.0b013e318184ff16>
- Reske, M., Kellermann, T., Habel, U., Jon Shah, N., Backes, V., von Wilmsdorff, M., Stöcker, T., Gaebel, W., & Schneider, F. (2007). Stability of emotional dysfunctions? A long-term fMRI study in first-episode schizophrenia. *Journal of Psychiatric Research*, *41*(11), 918–927. <https://doi.org/10.1016/j.jpsychires.2007.02.009>
- Rolls, E. T. (2019). The cingulate cortex and limbic systems for emotion, action, and memory. *Brain Structure and Function*, *224*(9), 3001–3018. <https://doi.org/10.1007/s00429-019-01945-2>
- Rolls, E. T., Huang, C. C., Lin, C. P., Feng, J., & Joliot, M. (2020). Automated anatomical labelling atlas 3. *NeuroImage*, *206*(August 2019), 116189. <https://doi.org/10.1016/j.neuroimage.2019.116189>
- Satterthwaite, T. D., Wolf, D. H., Erus, G., Ruparel, K., Elliott, M. A., Gennatas, E. D., Hopson, R., Jackson, C., Prabhakaran, K., Bilker, W. B., Calkins, M. E., Loughead, J., Smith, A., Roalf, D. R., Hakonarson, H., Verma, R., Davatzikos, C., Gur, R. C., & Gur, R. E. (2013). Functional maturation of the executive system during adolescence. *Journal of Neuroscience*, *33*(41), 16249–16261. <https://doi.org/10.1523/JNEUROSCI.2345-13.2013>
- Schlagenhauf, F., Dinges, M., Beck, A., Wüstenberg, T., Friedel, E., Dembler, T., Sarkar, R., Wrase, J., Gallinat, J., Juckel, G., & Heinz, A. (2010). Switching schizophrenia patients from typical neuroleptics to aripiprazole: Effects on working memory dependent functional activation. *Schizophrenia Research*, *118*(1–3), 189–200. <https://doi.org/10.1016/j.schres.2010.01.022>
- Schlagenhauf, F., Wüstenberg, T., Schmack, K., Dinges, M., Wrase, J., Koslowski, M., Kienast, T., Bauer, M., Gallinat, J., Juckel, G., & Heinz, A. (2008). Switching schizophrenia patients from typical neuroleptics to olanzapine: Effects on BOLD response during attention and working memory. *European Neuropsychopharmacology*, *18*(8), 589–599. <https://doi.org/10.1016/j.euroneuro.2008.04.013>
- Shaw, P., Kabani, N. J., Lerch, J. P., Eckstrand, K., Lenroot, R., Gogtay, N., Greenstein, D., Clasen, L.,

- Evans, A., Rapoport, J. L., Giedd, J. N., & Wise, S. P. (2008). Neurodevelopmental trajectories of the human cerebral cortex. *Journal of Neuroscience*, 28(14), 3586–3594. <https://doi.org/10.1523/JNEUROSCI.5309-07.2008>
- Simmonds, D. J., Hallquist, M. N., & Luna, B. (2017). Protracted development of executive and mnemonic brain systems underlying working memory in adolescence: A longitudinal fMRI study. *NeuroImage*, 157(January), 695–704. <https://doi.org/10.1016/j.neuroimage.2017.01.016>
- Smee, C., Krabbendam, L., O'Daly, O., Prins, A. M., Nalesnik, N., Morley, L., Samson, G., & Shergill, S. (2011). An fMRI study of prefrontal dysfunction and symptomatic recovery in schizophrenia. *Acta Psychiatrica Scandinavica*, 123(6), 440–450. <https://doi.org/10.1111/j.1600-0447.2010.01632.x>
- Snitz, B. E., MacDonald, A., Cohen, J. D., Cho, R. Y., Becker, T., & Carter, C. S. (2005). Lateral and medial hypofrontality in first-episode schizophrenia: Functional activity in a medication-naive state and effects of short-term atypical antipsychotic treatment. *American Journal of Psychiatry*, 162(12), 2322–2329. <https://doi.org/10.1176/appi.ajp.162.12.2322>
- Sowell, E. R., Delis, D., Stiles, J., & Jernigan, T. L. (2001). Improved memory functioning and frontal lobe maturation between childhood and adolescence: A structural MRI study. *Journal of the International Neuropsychological Society*, 7(3), 312–322. <https://doi.org/10.1017/S135561770173305X>
- Sun, Y., Chen, Y., Lee, R., Bezerianos, A., Collinson, S. L., & Sim, K. (2016). Disruption of brain anatomical networks in schizophrenia: A longitudinal, diffusion tensor imaging based study. *Schizophrenia Research*, 171(1–3), 149–157. <https://doi.org/10.1016/j.schres.2016.01.025>
- Tamnes, C. K., Walhovd, K. B., Grydeland, H., Holland, D., Østby, Y., Dale, A. M., & Fjell, A. M. (2013). Longitudinal Working Memory Development Is Related to Structural Maturation of Frontal and Parietal Cortices. *Journal of Cognitive Neuroscience*, 25(10), 1611–1623. https://doi.org/10.1162/jocn_a_00434
- Tang, J., Liao, Y., Zhou, B., Tan, C., Liu, T., Hao, W., Hu, D., & Chen, X. (2010). Abnormal anterior cingulum integrity in first episode, early-onset schizophrenia: A diffusion tensor imaging study. *Brain Research*, 1343, 199–205. <https://doi.org/10.1016/j.brainres.2010.04.083>
- Thompson, P. M., Vidal, C., Giedd, J. N., Gochman, P., Blumenthal, J., Nicolson, R., Toga, A. W., & Rapoport, J. L. (2001). Mapping adolescent brain change reveals dynamic wave of accelerated gray matter loss in very early-onset schizophrenia. *Proceedings of the National Academy of Sciences*, 98(20), 11650–11655. <https://doi.org/10.1073/pnas.201243998>
- Thormodsen, R., Rimol, L. M., Tamnes, C. K., Juuhl-Langseth, M., Holmén, A., Emblem, K. E., Rund, B. R., & Agartz, I. (2013). Age-related cortical thickness differences in adolescents with early-onset schizophrenia compared with healthy adolescents. *Psychiatry Research - Neuroimaging*, 214(3), 190–196. <https://doi.org/10.1016/j.psychres.2013.07.003>

- Vidal, C. N., Rapoport, J. L., Hayashi, K. M., Geaga, J. A., Sui, Y., McLemore, L. E., Alaghband, Y., Giedd, J. N., Gochman, P., Blumenthal, J., Gogtay, N., Nicolson, R., Toga, A. W., & Thompson, P. M. (2006). Dynamically Spreading Frontal and Cingulate Deficits Mapped in Adolescents With Schizophrenia. *Archives of General Psychiatry*, *63*(January), 25–34.
- Voets, N. L., Hough, M. G., Douaud, G., Matthews, P. M., James, A., Winmill, L., Webster, P., & Smith, S. (2008). Evidence for abnormalities of cortical development in adolescent-onset schizophrenia. *NeuroImage*, *43*(4), 665–675. <https://doi.org/10.1016/j.neuroimage.2008.08.013>
- White, T., Hongwanishkul, D., & Schmidt, M. (2011). Increased anterior cingulate and temporal lobe activity during visuospatial working memory in children and adolescents with schizophrenia. *Schizophrenia Research*, *125*(2–3), 118–128. <https://doi.org/10.1016/j.schres.2010.11.014>
- White, T., Schmidt, M., Kim, D. II, & Calhoun, V. D. (2011). Disrupted functional brain connectivity during verbal working memory in children and adolescents with schizophrenia. *Cerebral Cortex*, *21*(3), 510–518. <https://doi.org/10.1093/cercor/bhq114>
- Wolf, R. C., Vasic, N., Höse, A., Spitzer, M., & Walter, H. (2007). Changes over time in frontotemporal activation during a working memory task in patients with schizophrenia. *Schizophrenia Research*, *91*(1–3), 141–150. <https://doi.org/10.1016/j.schres.2006.12.001>
- Wu, D., & Jiang, T. (2019). Schizophrenia-related abnormalities in the triple network: a meta-analysis of working memory studies. *Brain Imaging and Behavior*, *14*(4), 971–980. <https://doi.org/10.1007/s11682-019-00071-1>
- Zhou, D., Lebel, C., Treit, S., Evans, A., & Beaulieu, C. (2015). Accelerated longitudinal cortical thinning in adolescence. *NeuroImage*, *104*, 138–145. <https://doi.org/10.1016/j.neuroimage.2014.10.005>
- Zipursky, R. B., Reilly, T. J., & Murray, R. M. (2013). The myth of schizophrenia as a progressive brain disease. *Schizophrenia Bulletin*, *39*(6), 1363–1372. <https://doi.org/10.1093/schbul/sbs135>

Tables

Table 5.1. Demographic, clinical, and behavioural characteristics for adolescents with EOS and TD adolescent groups at baseline and follow-up with respective p-values for longitudinal within-group change						
	Baseline (t1)		Follow-up (t2)		Within-group Δ longitudinal (p-value)	
	EOS	TD	EOS	TD		
	n = 14	n = 15	n = 14	n = 15	<i>EOS</i>	<i>TD</i>
Demographic data						
Age (years)	17.03 (1.42)	16.51 (2.22)	21.01 (1.60)	21.15 (1.99)		
Range (years)	14.75 – 19.75	13.00 – 20.83	18.08 – 23.92	18.08 - 25.83		
Gender (M/F)	9/5	10/5				
Handedness (L/R)	13/1	13/2				
NART	97.57 (10.65)	100.71 (8.02)	100.33 (7.87)	111.41 (4.35)	.149	<.001
Clinical data						
<u>Symptoms</u>						
PANSS positive	9.21 (1.81)	-	10.36 (3.43)	-	.271	-
PANSS negative	14.00 (1.80)	-	12.21 (4.66)	-	.229	-
PANSS total	47.21 (4.19)	-	47.64 (10.21)	-	.879	-
<u>Medication (mg)</u>						
Cumulative CPZE	10,967.86 (16,292.93)	-	27,683.57 (31,708.83)	-	.001	-
Behavioural data						
<u>Accuracy</u> (% correct); Median (IQR)						
one-back	100% (19%)	100% (0%)	100% (25%)	100% (13%)	.739	.705
two-back	81.25% (44%)	100% (13%)	93.75% (56%)	100% (13%)	.506	.234
three-back	56.25% (44%)	62.5 (50%)	81.25% (53%)	87.5% (25%)	.031	.051
<u>Reaction time</u> (s); Mean (SD)						
one-back	0.58 (0.12)	0.51 (0.08)	0.58 (0.12)	0.53 (0.08)	.924	.716
two-back	0.62 (0.12)	0.57 (0.11)	0.58 (0.25)	0.56 (0.11)	.587	.994
three-back	0.66 (0.14)	0.65 (0.14)	0.71 (0.29)	0.62 (0.13)	.413	.450

Abbreviations: **CPZE**: chlorpromazine equivalents; **EOS**: early-onset schizophrenia; **F**: female; **IQR**: interquartile range; **L**: left; **M**: male; **mg**: milligrams; **NART**: national adult reading test; **PANSS**: positive and negative syndrome scale; **R**: right; **TD**: typically developing controls

Table 5.2. Main effects of task on Δ_{BOLD} while controlling for gender and age at follow-up								
					Peak coordinates			
#	k	Regions	BA	L/R	x	y	z	Z-value
Main effects of task (t1>t2)								
<i>Process-general (one-, two, three-back)</i>								
1	568	Superior frontal gyrus	6	R	24	5	59	4.91
		Superior frontal gyrus	6	R	27	-7	62	4.36
2	66	Superior temporal pole	38	L	-36	5	-22	4.50
3	202	Fusiform gyrus	37	R	45	-37	-19	4.47
4	66	Middle frontal gyrus	9	L	-33	35	38	4.38
5	88	Superior temporal pole	22	R	54	11	-7	4.32
6	135	Middle frontal gyrus	10	R	30	47	29	4.14
7	380	Posterior cingulate gyrus	31	L/R	-3	-37	41	4.03
<i>Three-back</i>								
1	778	Superior frontal gyrus	6	R	24	5	59	4.67
		Supplementary motor area	6	R	9	5	59	4.60
		Anterior cingulate gyrus	32	R	9	14	38	4.28

Coordinates reported in MNI space and corrected for multiple comparisons at FWE 0.05

Table 5.3. Main effects of group (\times task) on Δ_{BOLD} while controlling for gender and age at follow-up								
					Peak coordinates			
#	k	Regions	BA	L/R	x	y	z	Z-value
Typically developing adolescents (t1>t2)								
<i>Process-general (one-, two, three-back)</i>								
1	146	Precuneus	7	L/R	6	-61	56	4.26
2	755	Anterior/Middle cingulate gyrus	32	L/R	3	35	26	4.02
<i>Three-back</i>								
1	345	Anterior cingulate gyrus	24	L/R	9	29	20	4.26
Adolescents with early onset schizophrenia (t1>t2)								
<i>Process-general (one-, two, three-back)</i>								
1	75	Middle occipital gyrus	19	R	39	-76	23	4.73
2	77	Superior frontal gyrus	6	R	30	-1	59	4.35
3	34	Middle frontal gyrus	9	L	-33	35	38	4.30
4	205	Precuneus/Superior occipital gyrus	7	L	-12	-76	44	4.09
<i>One-back</i>								
1	68	Putamen/Insula	13	R	30	8	20	4.32

Coordinates reported in MNI space and corrected for multiple comparisons at FWE 0.05

Table 5.4. Main effects of task on $\Delta_{\text{BOLD}(t_1 > t_2)}$ for EOS patients while controlling for gender, age at follow-up, age-of-illness onset, cumulative antipsychotic medication, and interscan interval

#	k	Regions	BA	L/R	Peak coordinates			Z-value
					x	y	z	
<i>Process-general (one-, two, three-back)</i>								
1	267	Middle occipital gyrus	19	R	39	-76	20	5.06
2	81	Insula	22	R	51	11	-4	4.48
3	183	Supplementary motor area	6	L/R	0	5	59	4.32
3	279	Superior occipital gyrus	7	L	-18	-73	38	4.07
4	130	Cuneus	7	R	15	-70	35	4.01
<i>Three-back</i>								
1	179	Supplementary motor area	6	L/R	6	8	59	4.40
2	147	Superior temporal gyrus	21	L	-57	-1	-13	4.00

Coordinates reported in MNI space and corrected for multiple comparisons at FWE 0.05

Table 5.5. Brain areas with $\Delta_{\text{BOLD}} (t_{1>12})$ predicted by baseline PANSS (total, positive, negative) scores in developing adolescents with EOS								
					Peak coordinates			
#	k	Regions	BA	L/R	x	y	z	Z-value
<i>One-back</i>								
Total symptoms: positive regression								
1	174	Inferior frontal gyrus, opercular	13	L	-36	11	23	4.26
2	88	Middle frontal gyrus	9	R	30	23	35	4.14
Positive symptoms: positive regression								
1	219	Middle frontal gyrus	9	R	27	20	32	4.87
2	131	Lingual gyrus	19	R	27	-61	-1	4.70
3	78	Angular gyrus	39	R	33	-61	35	4.38
4	92	Inferior frontal gyrus, opercular	9	L	-45	11	23	4.12
<i>Two-back</i>								
Total symptoms: negative regression								
1	177	Anterior Cingulate gyrus	32	L/R	9	5	44	4.56
Positive symptoms: negative regression								
1	136	Supplementary motor area	23	L/R	-6	-1	50	4.45
Negative symptoms: negative regression								
1	79	Cerebellum, Vermis, 3		L	0	-34	-13	5.22

Coordinates reported in MNI space and corrected for multiple comparisons at FWE 0.05

General discussion

Summary of main goals and findings

In this thesis we aimed to address the following: **(1)** to evaluate the expression of neurophysiological schizophrenia biomarkers within factors that increase the risk and vulnerability for developing schizophrenia; **(2)** to appraise the regional convergence of structural and functional brain differences within the imaging literature of patients with early onset schizophrenia (EOS), and **(3)** to assess changes in brain function, connectivity and longitudinal neurodevelopment connected with working memory (WM) performance in developing patients with EOS and typically developing individuals.

First, using EEG during the auditory roving oddball paradigm, we extracted the P50 sensory gating and MMN change detection ERPs and investigated their relation to state and trait anxiety. We then used the hollow mask illusion (HMI) experiment, to explore the influence of state and trait anxiety, and neuroticism with the P300/P600 ERPs that hint allocation of attentional resources. We assessed the *second* goal with the use of coordinate-based meta-analysis. We performed a database literature search of peer-reviewed studies using morphometric and task-based functional imaging techniques in the EOS population that reported their results in standard stereotactic coordinate space. The meta-analytically derived clusters of brain changes in EOS were entered in a further database search that this time was carried out to detect the normative core coactivation network of the aberrant brain regions in EOS, as well as their functional associations profile. Finally, the *third* goal was assessed by investigating the longitudinal 4.3-year follow-up of an EOS and typically developing cohort. The developing adolescents performed the n-back task twice while acquiring their fMRI

scans, first at 17 years old (Kyriakopoulos et al., 2012) and at 21. The follow-up scans were analysed to decipher cross-sectional brain activation in the WM network within and between the two groups, as well as functional connectivity of the dorsolateral prefrontal cortex (DLPFC) modulated by WM performance, as is shown by psychophysiological interactions analysis. Then, the baseline and follow-up scans were compared to examine the developmental changes from baseline to follow-up while performing the WM task, and finally functional neurodevelopmental brain changes were predicted by initial EOS symptom severity.

In **Chapter 1** we showed that during the oddball paradigm, high state anxiety participants did not inhibit their P50 response to the second repeating tone in a new stimulus train, displaying reduced capability to gate out redundant information. Meanwhile, trait anxiety influenced the detection of a new deviant tone which was expressed by enhanced MMN amplitude. This was pertinent with hypervigilant change detection, where the new tone in the stimulus train was perceived as more salient for those who were more trait anxious. Following with **Chapter 2**, in the visual modality, those with high state anxiety showed sensitisation to concave faces, stimuli that are mismatches to the convex face representation, by allocating more attentional resources to them. These results confirm the hindering role of anxiety in the cognitive control of attention (Eysenck et al., 2007). In **Chapter 3**, we discovered that the study-wide, task-based cognitive hypoactivation in patients with EOS converges in regions of the anterior cingulate cortex (ACC) and right temporoparietal junction (TPJ), while the WM dysfunction lies in posterior parietal cortices (precuneus, inferior parietal lobule) and the TPJ. These areas co-activate with a core network that is formed by the anterior midcingulate cortex and bilateral insulae, known as the salience network whose role is to attribute salience to internal and external events, while serving as the switch between

the default mode (DMN) and central executive networks (Sridharan et al., 2008). Next, WM accuracy and brain function in EOS individuals did not differ significantly from healthy controls in **Chapter 4**. There was, however, a reduction in negative modulatory connectivity from the DLPFC to nodes of the DMN, which suggests that WM dysfunction is more pronounced in connectivity measures rather than in brain activation in patients with EOS. This may be relevant with disease chronicity, as the EOS patients had been chronically ill for approximately 9 year at the time of the second scan. It also confirms the dysconnectivity hypothesis that describes schizophrenia as a disconnection syndrome between and within distinct functional systems (Friston, 1999). The final set of analyses of the thesis in **Chapter 5** revealed that longitudinally, WM brain function is reduced in frontotemporal and cingulate regions in EOS and typical development. However, whilst the longitudinal reduction between the groups it was not statistically different, qualitatively typically developing adolescents had reductions in the midline of the brain expanding from the ACC to the PCC and precuneus, whereas the EOS adolescents showed decreases in prefrontal, insular and parietooccipital regions. Notably, lack of maturation (lower BOLD signal reduction) in the cingulate cortex and exaggerated frontal and parietooccipital functional reduction were predicted by more severe psychotic and PANSS total symptoms at the first scan, thus highlighting again the central role of the prefrontal and cingulate cortices in cognitive function and development in EOS.

The following sections will attempt to critically review the implications of our findings in psychology and cognitive neuroscience research by putting together a short integrative discussion linking the central concepts that are dealt with in this thesis. Finally, we will examine the strengths, limitations, and future directions that result from this piece of work.

Is anxiety a risk factor for schizophrenia?

We established that anxiety levels, measured by the state-trait anxiety inventory (STAI) (Spielberger, 1983), influenced the ERPs in the oddball and HMI experiments which tap into bottom-up and top-down processes of attentional control. Increased anxiety levels are characterised by failure to inhibit an early EEG response to a repeating auditory stimulus, as shown by reduced P50 sensory gating, and by hypervigilant allocation of attentional resources to mismatches of memory representations (as seen jointly by the deviant oddball and the concave face stimuli). The sensory gating deficit in state anxiety that we observed in **Chapter 1** is in line with schizophrenia patients who normally do not inhibit the response to the second tone (Shan et al., 2010), as well as in those with familial or at clinical risk for psychosis. However, while anxiety drives hypervigilant change detection (Fucci et al., 2019) that is also supported by our findings, the opposite pattern is obvious in schizophrenia; MMN in schizophrenia and high-risk states is almost uniformly reduced (Näätänen et al., 2015) and so are the P300 and P600 ERPs for concave faces (Dima et al., 2011). Higher anxiety levels produced enhanced detection of mismatch stimuli (including the deviant tones and concave faces in **Chapters 1 & 2**, respectively) that were (subconsciously) perceived as more salient – which may serve as a safety mechanism against potential threats. In schizophrenia on the other hand, reduced change detection may represent a difficulty to distinguish potential bottom-up, stimulus-driven salience or a challenge to apply top-down control from prior knowledge to model expectations about the surrounding environment (Javitt, 2009).

Individual differences in anxiety in healthy participants impair goal directed attention (Eysenck & Derakshan, 2011), which is confirmed by other ERP studies (Ansari & Derakshan, 2011; Osinsky et al., 2012) as well as by **Chapters 1 & 2**. At the

same time, increased anxiety is associated with poor self-reported attentional control (including attention shifting, focusing and divided attention), enhanced cognitive biases and psychotic like experiences, in otherwise healthy individuals (Prochwicz & Kłosowska, 2018). Increased arousal to mismatch or redundant stimuli may negatively impact the interpretation of threat through cognitive, attributional and attentional biases that inform delusional and paranoid beliefs (Underwood et al., 2016). In addition, anxiety disrupts the equilibrium of feedforward and feedback control by favouring stimulus-driven connections, which can then be reversed by administering benzodiazepine anxiolytic drugs that enhance inhibitory GABAergic receptor activity (Cornwell et al., 2017). Dysregulation in prefrontal interneuron GABAergic activity is also a characteristic of schizophrenia (Adams et al., 2013). Assumably, the deleterious effects of anxiety on attentional control (Eysenck & Derakshan, 2011) and regulation of neurotransmitter activity may explain the role of anxiety in the formation of psychotic symptoms (Freeman et al., 2002; Freeman & Fowler, 2009), since anxiety is viewed as a major component in schizophrenia (Pallanti et al., 2013).

Another interesting set of findings concerns the interdependent effects of nicotine smoking, anxiety, ERPs, and schizophrenia. Smoking nicotine is reported to mitigate self-reported anxiety and to reduce arousal in late positive ERPs (Choi et al., 2015). Additionally, it reverses attentional impairments that are related to schizotypy (Wan et al., 2006). There may be a link in the increased prevalence of tobacco use in schizophrenia (Kelly & McCreadie, 2000), possibly as self-medication (either consciously or subconsciously) to alleviate stress or improve attentional performance. Opposing views however regarding nicotine and which are similar to cannabis, point to it being potentially causally related to psychosis (Quigley & MacCabe, 2019). Thus, the

plausible interconnectedness between nicotine use in schizophrenia for anxious symptoms relief and attentional improvement need further investigation.

Self-reported anxiety levels in patients with schizophrenia correlate with delusions, hallucinations (Guillem, Pampoulova, Stip, Lalonde, et al., 2005), and paranoid symptoms (Cowles & Hogg, 2019). Anxiety may mediate psychotic symptom severity through its effects on cognitive and attentional control processing, as described by our results of impaired P50 sensory gating at increasing anxiety and emphasised further by findings that underline a relationship of severe auditory verbal hallucinations with sensory gating impairment in schizophrenia patients (Thoma et al., 2017).

Worsened attentional performance and enhanced distractibility by irrelevant stimuli is also expressed with increased anxiety in individuals with high schizotypal traits (Braunstein-Bercovitz, 2000). Moreover, high trait anxiety in schizophrenia patients leads to increased P600 amplitude (as in **Chapter 2**), which is assumed to represent mnemonic binding processes, suggesting improper binding or attributional biases while viewing old versus new faces (Guillem, Pampoulova, Stip, Todorov, et al., 2005).

Anxiety also mediates task-dependent brain function measured by fMRI in the psychosis spectrum. Higher state anxiety in schizophrenia patients correlates with hyperactivation in the orbitofrontal cortex during scenes of social rejection (Lee et al., 2014) whereas reduced activation in patients' left supramarginal, left postcentral and right middle occipital gyri is moderated by their anxiety levels during object perception (Stephan-Otto et al., 2016). Anterior insula activation relative to fear conditioning is reduced with increasing trait anxiety in individuals at clinical-high risk and with overt schizophrenia (Quarmley et al., 2019), while individuals with familial risk for psychosis (first-degree relatives of patients) have inversely correlated trait anxiety levels with decreased connectivity in a network comprising limbic and visual cortical areas during

emotional face perception (Cao et al., 2016). Additionally, anxiety modulates the expression of brain network dynamics in populations with genetic and chromosomal mutations that are considered high risk for schizophrenia. For example, being a carrier of the Disrupted-In-Schizophrenia (DISC1) gene alters activation profiles in the anterior cingulate cortex in anxiety patients, causing hyperactivation during a visuospatial planning paradigm (Opmeer et al., 2015). Similarly, anxiety levels in individuals with 22q11.2 deletion syndrome underly modulatory changes of the amygdala/hippocampus complex from language and DLPFC networks (Zöllner et al., 2019).

Neuroticism on the other hand, did not show any significant effects in the neurophysiological indices of attentional and cognitive control. In a general population cohort, high neuroticism in childhood predicted later anxiety and depression (Rodgers, 1990) as well as schizophrenia. This led to the suggestion that there is “an area of shared liability” between neuroticism, non-affective schizophrenia and affective disorders (Van Os & Jones, 2001). Neuroticism may constitute an overlapping vulnerability that is shared between different psychopathologies which will later manifest as distinct diagnoses, i.e., schizophrenia or anxiety, potentially due to separate underlying mechanisms (Van Os & Jones, 2001). Neuroticism perhaps is a more complex concept than anxiety that can conceal functional brain activity changes since it can contribute to conditions (anxiety or schizophrenia) that have mixed cognitive brain activation profiles in the paradigms and ERPs tested in this thesis.

Addressing the overarching question “is anxiety a risk factor for schizophrenia?” is not a straight-forward answer. While epidemiological evidence suggests that anxiety is highly prevalent prior to the emergence of schizophrenia and is comorbid with the disorder, our results offer a mixed landscape. We expected that the effects of anxiety and schizophrenia on the ERPs would demonstrate continuity considering the status of

anxiety as a risk factor. This view however might be oversimplistic. Seeing psychopathology as a continuum in a broad spectrum of deficits may help us better understand how different factors affect neurophysiological indices of impaired cognition. Evidence showing genetic risk for schizophrenia to be associated with anxiety symptoms in unaffected adolescents (Jones et al., 2016) might suggest that anxiety predates the manifestation of psychotic symptoms. It also points to anxiety being a trait marker for schizophrenia, potentially increasing vulnerability to express an overt psychotic state. Perhaps anxiety with its detrimental role on attentional control, taps on systems that underly cognitive impairments in those with a genetic vulnerability for schizophrenia. Such impairments could include misdirecting attentional resources to threat, or misattributing saliency and threatening status to a stimulus, which could act as an “on” switch that signals hyperarousal to novel and otherwise harmless or irrelevant events. This switch could give rise to delusional beliefs and hallucinatory percepts to individuals who are placed at the furthest end of the psychopathological spectrum when also triggered by a ‘secondary hit’ (Maynard et al., 2001), such as anxiety.

Is salience network dysfunction the connective link across paradigms and diagnoses?

Schizophrenia is broadly considered a disorder of aberrant salience processing (Kapur, 2003). Salience is a multifaceted system allowing prioritisation of stimuli that are goal-relevant (Winton-Brown et al., 2014). Dysfunction in this system can mean impaired salience attribution to goal-relevant exogenous or endogenous stimuli and thoughts, or deficits in novelty detection. The idea of aberrant salience in psychosis and psychosis proneness is tied to dysregulated dopaminergic signalling through assignment of maladaptive reward-driven salience on otherwise harmless stimuli (Howes & Kapur, 2009) which is related to prediction errors for punishments and rewards (Heinz &

Schlagenhauf, 2010) or simply novelty (Winton-Brown et al., 2014). Aberrations in systems that underly salience processing interfere with attentional and action selection, which in individuals with prodromal symptoms could induce delusions through directing importance to irrelevant internal or external events (Winton-Brown et al., 2014). Such disturbances are present even in ultra-high risk subjects who attribute salience to irrelevant features and are longitudinally associated with a reduction of activation in middle and anterior cingulate, insular, and inferior frontal areas (Schmidt et al., 2017). Increased severity of delusional symptoms in schizophrenia patients associate with higher degree of impairment in salience processing (Roiser et al., 2009) and abnormal beliefs are associated with brain activation changes in areas subserving salience (Schmidt et al., 2017). In **Chapter 3** we reported a coactivation network located in the anterior midcingulate and bilateral insulae, which are nodes of the salience network (Seeley et al., 2007), to form the core of the clusters with convergent hypoactivation across the EOS neuroimaging studies. Anatomically these regions correspond closely to the cingulo-opercular network, which is considered as a second executive network (in addition to the frontoparietal) (Petersen & Posner, 2012), and it additionally forms a core system that displays sustained activity across various cognitive tasks (Dosenbach et al., 2006), and it monitors performance (Becerril & Barch, 2013). Interestingly, the right TPJ, which in **Chapter 3** converged as a common area of hypoactivation across cognitive and WM paradigms in EOS, and is anchored in the ventral-attention network (Petersen & Posner, 2012), is also considered to be part of the salience network (Kucyi et al., 2012). Therefore, there is a regional overlap across systems that were originally believed to be different, namely the salience, cingulo-opercular, and ventral-attention networks. This confirms the multifaced nature in functional relevance of the cingulate-insular-temporoparietal regions which have a

central role in the psychopathology of schizophrenia. Furthermore, disruptions in these overlapping systems are common across many psychiatric disorders during cognitive and emotion discrimination tasks (McTeague et al., 2017, 2020), therefore being a candidate as a transdiagnostic marker for psychopathology that requires more attention.

In addition to salience network disruption, in **Chapter 4**, EOS patients showed dysconnectivity between the DLPFC and regions of the DMN that were additionally deactivated when performing the WM task. These results combined with those in **Chapter 3** can be unified by three influential theories of schizophrenia neuropathology; the dopaminergic state-driven salience dysregulation that characterises psychosis (Kapur, 2003), the disconnection hypothesis (Friston, 1999; Friston et al., 2016), and the triple network model (Menon, 2011). The triple network model places three intrinsically organised networks, the central executive (commonly referred as frontoparietal network), the DMN (midline brain task-negative areas), and the salience network in the centre of psychopathology (Menon, 2011), tapping into the first two theories, i.e., dopamine and disconnection. According to this model, the salience network mediates switching between the central executive and DMN, when behaviourally relevant salience is detected in the internal or external environments. In the case of schizophrenia, deficits in the salience network can manifest as resting-state or task-dependent functional deficits. For example, there have been reports to show disconnection between the salience network and the DLPFC to characterise schizophrenic patients at resting state (Palaniyappan et al., 2013), as well as dysconnectivity within the salience network to be associated with difficulty in disengaging the DMN during cognitive task performance (Luo et al., 2020). Furthermore, abnormal functional activation in central executive, salience, and DMN nodes is reported in a meta-analysis of WM studies in schizophrenia (Wu & Jiang,

2019), whilst hypoactivation in DMN/self-referential processing areas is associated to impaired salience processing in patients (Pankow et al., 2016). Crucially, in addition to the functional deficits, the ACC and bilateral insulae demonstrate decreased grey matter volume across psychiatric disorders (including anxiety, bipolar, schizophrenia, and depression disorders) (Goodkind et al., 2015), pointing to salience network abnormality also being structurally prevalent. Finally, increased psychotic experiences in non-schizophrenic children are associated with reduced resting-state functional connectivity in the salience network and DMN (Karcher et al., 2019), suggesting that disturbances in functional systems of the triple network may be endophenotypic.

Working memory neurodevelopment as an endophenotypic marker for EOS

An endophenotype is a quantifiable, heritable trait that lies between genotype and phenotype and is considered to be reliably informative as index for illness liability (Park & Gooding, 2014). WM deficit is a fundamental cognitive impairment and consistently indicated as endophenotypic in schizophrenia; such impairment is obvious from prodromal to chronic patients as well as their first-degree relatives (Park & Gooding, 2014), and thus fitting the heritability requirement. Importantly, EOS is considered more genetically loaded than the adult-onset form, therefore core impairments that are observed in EOS may be more easily categorizable as endophenotypic. WM was indicated to have the highest genetic influence amongst other neurocognitive measures including IQ, verbal comprehension, perceptual disorganisation, and processing speed based on a twin study in schizophrenia probands and their unaffected monozygotic or dizygotic twins (Toulopoulou et al., 2007). In addition relatives of schizophrenia patients demonstrate abnormalities in WM-related activation and functional connectivity (Bakshi et al., 2011; Meda et al., 2008; Repovš & Barch, 2012; Thermenos

et al., 2004; Zhang et al., 2016). Therefore, apart from behavioural WM deficits, activation and functional profiles related to WM activity are candidate endophenotypes for the cognitive impairment in schizophrenia and trait markers that are not solely attributable to psychotic symptoms.

Functional hypoactivation of the posterior parietal cortices during WM performance in EOS may be as good an endophenotypic marker as the DLPFC. However WM studies in schizophrenia relatives often employ biased *a priori* DLPFC region-of-interest analyses (Delawalla et al., 2008). Bilateral DLPFC and posterior parietal cortex function shows an intermediate activation profile during WM in relatives of schizophrenia (Karlsgodt et al., 2007; Loeb et al., 2018), that is significantly different from healthy controls (Meda et al., 2008) and this has been also shown meta-analytically (Zhang et al., 2016). Similarly, developing offspring of schizophrenia patients show hypoactivation in the left superior parietal cortex during WM activity in the n-back (Bakshi et al., 2011). These studies suggest that functional WM abnormalities in the DLPFC and parietal cortices may be a trait impairment for schizophrenia, and thus heritable as they are expressed in first-degree relatives of probands. The results in **Chapter 3** suggest that the EOS posterior parietal hypoactivation may constitute an endophenotypic feature of WM impairment. Our results further propose that developmental trajectories related to the maturation of WM function may also be distinct endophenotypes for EOS. In **Chapter 5** we extended observations of structural EOS and their relatives' abnormal developmental trajectories in fronto-temporal and parietal regions (Gogtay et al., 2007; Greenstein et al., 2006) and showed that EOS demonstrate developmental trajectories of functional WM reductions in posterior parietooccipital, superior and middle frontal, as well as striatal (putamen), insular, and superior temporal areas. These may as well serve as endophenotypic

markers for disrupted WM maturation as they were independent of medication or illness duration. Longitudinal functional alterations in parietooccipital areas during a spatial WM task was also identified in a study with adult subjects with clinical high risk for schizophrenia (Fusar-Poli et al., 2010). On the other hand, in **Chapter 5** the WM functional developmental changes in some areas, i.e., in middle and inferior frontal, angular, lingual, cingulate, and supplementary motor, as well as subcortical cerebellar, were correlated with initial positive and negative symptoms scores. It may be that genetic susceptibility for schizophrenia increases the vulnerability of fronto-parietal, cingulate, temporal, as well as subcortical dysmaturation, in agreement with the ‘two-hit’ hypothesis (Maynard et al., 2001), which then deteriorates in isolated areas (e.g., prefrontal, cingulate) as the symptoms of the disease progress. Similarly, in individuals with genetic risk who later developed schizophrenia the trajectory of grey matter volume change in prefrontal areas was related to the severity of psychotic symptoms (McIntosh et al., 2011), suggesting that parallel functional and structural trajectories may correspond as endophenotypic illness markers.

In addition to BOLD hypo-/hyper-activation, it is proposed that functional connectivity may be an even better endophenotypic marker to understand schizophrenia liability (Karcher et al., 2019). WM-related functional connectivity of the ACC with DLPFC and parietal cortex increase in offspring of schizophrenia patients (Bakshi et al., 2011). The ACC, that has been related to cognitive control and behavioural adaptation following errors (Ham et al., 2013) and is hypoactive in EOS patients across cognitive paradigms (see **Chapter 3**) may pose another central role in the endophenotypic manifestation of WM deficit. Similarly, WM functional connectivity across several seeds of the WM network was found to be intermediate for siblings of that of EOS and control (Loeb et al., 2018). Whether DLPFC negative modulation of areas of the DMN

is endophenotypic to the WM impairment in EOS it remains to be explored with studies in subjects with familial high risk. We did however report that longitudinal reduction in DMN, posterior midline cingulate and parietal areas are observed in typically developing adolescents (see **Chapter 5**). This pattern of longitudinal maturation of WM function was not observed in the EOS adolescents. It is compelling to assume that the DMN system that guides internal thought at the resting state and deactivates with attention grabbing conditions during task, does not mature as effectively in EOS patients. This impairment may be relevant to the WM dysconnectivity of the right DLPFC that was observed in **Chapter 4**, and proposed failure in EOS to negatively modulate activation in posterior cingulate, medial prefrontal and right angular areas during the two-back.

Strengths

A strength in this thesis is the use of different neuroimaging techniques to address the overarching questions about functional boundaries in cognition in schizophrenia and relation to anxiety. EEG and fMRI techniques are crucial for the assessment of temporal and spatial characteristics of functional activation in the brain concurrently with different cognitive tasks. Such non-invasive in vivo imaging methods in human subjects are indispensable tools for psychology and have become the staple in cognitive neuroscience research. There is added clinical significance in identifying biological disease markers that are useful for locating pharmacological targets, which is useful for psychiatry. Neuroimaging provides access to the neural substrates of cognition in living performing subjects and allows to compare diagnostic groups on the presence or absence of overlapping, transdiagnostic boundaries of neurobiological dysfunction which is an invaluable tool for the characterisation of the psychopathological spectrum. Furthermore, the use of meta-analysis for determining spatial convergence in the

structural and functional neuroimaging literature of EOS is another significant asset of the thesis. By applying the statistical methods employed by the ALE algorithms, we dissect the degree of overlap in EOS abnormalities more systematically, objectively, and quantifiably, which would have not been possible to assess with a simple systematic review.

The study of cognitive function and neurodevelopment in EOS is another central advantage in this thesis. The hypothesis that schizophrenia is a neurodevelopmental disorder is being given more and more magnitude. By studying the longitudinal correlates of WM functional maturation in a cohort of developing adolescents with EOS and age-matched controls, we have the opportunity to examine this hypothesis in more depth. We get to explore how one of the major neurocognitive impairments in schizophrenia (WM) changes with time during the sensitive developmental period that marks the transition from adolescence to adulthood, which is also a time when WM and its neural substrates still mature. Again, the clinical implications for this are crucial in promoting the advancement of pharmacological targets that could one day alleviate the cognitive impairment in schizophrenia which currently has no known effective medication.

Limitations & future directions

We investigated the effects of neuroticism, state and trait anxiety as risk factors for schizophrenia through exploring known biomarker ERPs in healthy controls based on their individual differences in these psychometric measures. While this is a valid method to explore transdiagnostic markers for various disorders based on overlap and similarity of effects, a more direct way to answer our question would be by employing two extra groups; one consisted by patients with schizophrenia and one by subjects at high risk. This would permit us to identify how psychometric levels of anxiety and

neuroticism interact with the ERPs in these two patient groups as well as with psychotic symptoms dimensions. Future research should focus on exploring the interaction of the neurophysiological biomarkers of schizophrenia and anxiety, as anxiety is considered a core component of schizophrenia (Pallanti et al., 2013). In addition, this would allow to disentangle the mechanisms with which anxiety mediates delusions and psychotic symptoms in general. Since trait anxiety levels and anxiety disorders can alter the functional connections concerning the salience network (Geng et al., 2016; MacNamara et al., 2016; Massullo et al., 2020), anxiety might explain the pathogenesis of biases that reinforce delusional ideations through its links with positive psychotic symptoms (Guillem, Pampoulova, Stip, Lalonde, et al., 2005) and with salience dysregulation.

One other limitation is that we did not control for nicotine intake, which can affect the ERPs (Choi et al., 2015; Wan et al., 2006) as well as anxiety levels. The effects of anxiety on attentional control and the interplay with cognition and symptoms dimensions in schizophrenia together with the moderating effects of self-medicating practices such as nicotine use should be accounted for in future studies and be further explored.

Some limitations also arise with regards to statistical power and sample/experiment sizes in our studies. The sample sizes in the EEG studies were not determined by performing power analysis *a priori* but instead they were based on sample sizes of similar investigations. In **Chapter 1** the sample size that we used was well within the range of similar studies interested with the MMN or sensory gating ERPs in the oddball task concurrently with EEG. For example, Ermutlu et al. (2005) investigate the effects of cold stress in the sensory gating and MMN responses in a sample of fifteen participants, whereas Fucci and colleagues (2019) report the effects of safe and threat conditions in the MMN response and the effects of trait anxiety in thirty-

six participants. Another study by Haenschel and colleagues (2005) that tested repetition positivity effects in the P50 with the auditory roving oddball paradigm used an sample size of forty participants. In **Chapter 1** we included thirty-four participants, which in conjunction with the strong effect sizes, we were confident about our choice of sample size.

In **Chapter 2**, the sample size of twenty participants was determined by consulting the only similar investigation of the hollow mask experiment using EEG by Dima et al. (2011). In this study, the authors used a sample consisting of twenty patients with schizophrenia and twenty controls. Since we only used control subjects to explore influences of anxiety and neuroticism, in **Chapter 2** we decided to use a sample size corresponding to the control participants of Dima et al. (2011). After applying a similar statistical procedure as in the study by Dima et al. (2011), our observed effect sizes were strong and therefore once again increased our confidence in our decision.

In **Chapter 3**, the power of our meta-analysis was constrained by the available studies that were eligible for inclusion based on our research question. In Eickhoff et al. (2016) it is recommended that a minimum of 17 experiments is used in activation-likelihood estimation meta-analyses. According to the authors, this decreases the chance of a single experiment being the sole contributor to the observed significant clusters, especially when there is heterogeneity between each experiment's sample sizes (Eickhoff et al., 2016). Our VBM meta-analysis did not return significant clusters, potentially due to the low experiment number or the heterogeneity in sample sizes. Our fMRI meta-analyses (Cognitive and WM ALEs) have at least half of the total experiments contributing to the significant clusters (Table 3.4), despite being consisted by fewer experiments than the recommendation in Eickhoff and colleagues (2016). Importantly there is relative absence of heterogeneity in sample sizes amongst

experiments, except in Loeb et al. (2018) that had a slightly bigger sample size than the rest, which can be seen in [Table 3.1](#).

In **Chapter 4** and **Chapter 5** the sample size was determined by the number of participants from the baseline study of Kyriakopoulos and colleagues (2012) who returned to take part in the follow-up scanning session. From a total sample size of 45 (20 control and 25 EOS participants) only 34 returned for the follow-up study (17 EOS and 17 controls) in **Chapter 4**, while two more EOS were excluded due to low performance in the easier levels of the n-back task. Continuing with **Chapter 5**, one more EOS participant was excluded due to unmatched performance in the baseline scanning session and two controls had unretrievable baseline scans, making the total sample size twenty-nine. High attrition rates are a common issue with developmental and clinical longitudinal studies, especially ones with adolescents who may move cities after finishing high school or with patients with schizophrenia that may experience relapse of symptoms (Clemmensen et al., 2012; Díaz-Caneja et al., 2015). For this reason, we were principally motivated to use family-wise error correction for multiple comparisons, to have more robust confidence in our results.

Another point of discussion arises from the different methodological approaches in the preprocessing pipelines in the EEG studies. Taking a closer look to **Chapter 1**, the two ERP components that were extracted from the same oddball task were pre-processed with different filters. Similarly, in **Chapter 2** the pipeline is also different than this of Chapter 1. Filter settings as well as order of preprocessing steps are still a matter of debate within the EEG community as they can introduce time-domain distortions while enhancing type I and type II errors (de Cheveigné & Nelken, 2019; Liljander et al., 2016). We determined our pipeline after examining the scientific literature of the components that were under investigation (Dima et al., 2011; Hsieh et

al., 2019; Light et al., 2010) after careful consideration, while trying to replicate pipelines of other studies for better interpretability of our results. Different preprocessing pipelines may be better suited when isolating ERPs with different methods, such as peak detection or average amplitude in a time window, when examining early-, mid-, or late-latency components, or between different modalities, i.e., auditory, visual, and tactile as the signal is processed at different speed therefore may be optimised to customise the pipeline.

Finally, we approached statistical analysis in **Chapter 1** and **Chapter 2** by splitting the samples according to their median scores in the state and trait anxiety measures. Median-split analysis followed correlation or interaction findings between psychometric and ERP measures. While this method is not uncommon in neuroimaging research involving the STAI (Basten et al., 2011; Bishop, 2009; Chen et al., 2017; Modi et al., 2018) it should be used with caution. Even though arguments exist that it may be appropriate when dealing with skewed data, median-split tends to give more reliable results with normally distributed continuous variables (DeCoster et al., 2011). Trait anxiety in **Chapter 1** and state anxiety in **Chapter 2** appear to be normally distributed, however, state anxiety in **Chapter 1** appears to be right skewed as higher number of participants were at the lower range of the measure. Hence a different approach might have been more appropriate in this case.

An alternative approach to frequentist statistics would be the use of Bayesian analysis. Whilst frequentist statistics can tell us the probability of observing our results given the null hypothesis, it does not indicate evidence in support of observing the alternative hypothesis (Morey et al., 2016). Bayesian inference, however, could address prior beliefs on whether there is evidence in favour of the null or the alternative hypothesis, which is seen as more robust and flexible approach compared to null

hypothesis significance testing (Kruschke, 2010). Bayes Factor can serve as a good odds ratio metric that evaluates support to either one of the two hypotheses (Wagenmakers et al., 2018). Therefore, future studies would benefit by exploring this alternative to the classical frequentist hypothesis testing, although scientists have not yet reached full consensus on how to conduct and report its results (Aczel et al., 2020).

While WM impairment is a reliable endophenotype for schizophrenia and is established both behaviourally and functionally in studies with EOS patients and their siblings, a lot less is known about the functional neurodevelopment of WM. Our longitudinal design assessing fMRI changes in patients with EOS, while rarely found in the literature, it does not fully delineate the endophenotypic markers of WM neurodevelopment associated with schizophrenia. We elaborated the interpretation of our findings on the assumptions that EOS is more genetically loaded than adult-onset disorder and that longitudinal changes in WM function when we covaried for clinical characteristics constitute neurodevelopmental effects that are specific to EOS trait but not diseased state. To better address WM neurodevelopmental effects that are related with the genetic load to schizophrenia, future research would benefit by longitudinally studying first-degree relatives of schizophrenia patients. This will further the advancement of developmental endophenotypes that underly one of the most prominent cognitive deficits in schizophrenia, WM. Longitudinal fMRI studies that include first degree relatives will allow a more detailed examination of the endophenotypic implications that subserve the neurodevelopmental hypothesis that has been influential for over three decades in explaining the pathogenesis of schizophrenia (Weinberger, 1988).

References

- Aczel, B., Hoekstra, R., Gelman, A., Wagenmakers, E. J., Klugkist, I. G., Rouder, J. N., Vandekerckhove, J., Lee, M. D., Morey, R. D., Vanpaemel, W., Dienes, Z., & van Ravenzwaaij, D. (2020). Discussion points for Bayesian inference. *Nature Human Behaviour*, *4*(6), 561–563. <https://doi.org/10.1038/s41562-019-0807-z>
- Adams, R. A., Stephan, K. E., Brown, H. R., Frith, C. D., & Friston, K. J. (2013). The Computational Anatomy of Psychosis. *Frontiers in Psychiatry*, *4*(May), 47. <https://doi.org/10.3389/fpsy.2013.00047>
- Ansari, T. L., & Derakshan, N. (2011). The neural correlates of impaired inhibitory control in anxiety. *Neuropsychologia*, *49*(5), 1146–1153. <https://doi.org/10.1016/j.neuropsychologia.2011.01.019>
- Bakshi, N., Pruitt, P., Radwan, J., Keshavan, M. S., Rajan, U., Zajac-Benitez, C., & Diwadkar, V. A. (2011). Inefficiently increased anterior cingulate modulation of cortical systems during working memory in young offspring of schizophrenia patients. *Journal of Psychiatric Research*, *45*(8), 1067–1076. <https://doi.org/10.1016/j.jpsychires.2011.01.002>
- Basten, U., Stelzel, C., & Fiebach, C. J. (2011). Trait anxiety modulates the neural efficiency of inhibitory control. *Journal of Cognitive Neuroscience*, *23*(10), 3132–3145. https://doi.org/10.1162/jocn_a_00003
- Becerril, K. E., & Barch, D. M. (2013). Conflict and error processing in an extended cingulo-opercular and cerebellar network in schizophrenia. *NeuroImage: Clinical*, *3*, 470–480. <https://doi.org/10.1016/j.nicl.2013.09.012>
- Bishop, S. J. (2009). Trait anxiety and impoverished prefrontal control of attention. *Nature Neuroscience*, *12*(1), 92–98. <https://doi.org/10.1038/nn.2242>
- Braunstein-Bercovitz, H. (2000). Is the attentional dysfunction in schizotypy related to anxiety? *Schizophrenia Research*, *46*(2–3), 255–267. [https://doi.org/10.1016/S0920-9964\(00\)00021-9](https://doi.org/10.1016/S0920-9964(00)00021-9)
- Cao, H., Bertolino, A., Walter, H., Schneider, M., Schafer, A., Taurisano, P., Blasi, G., Haddad, L., Grimm, O., Otto, K., Dixon, L., Erk, S., Mohnke, S., Heinz, A., Romanczuk-Seiferth, N., Muhleisen, T. W., Mattheisen, M., Witt, S. H., Cichon, S., ... Meyer-Lindenberg, A. (2016). Altered functional subnetwork during emotional face processing a potential intermediate phenotype for schizophrenia. *JAMA Psychiatry*, *73*(6), 598–605. <https://doi.org/10.1001/jamapsychiatry.2016.0161>
- Chen, C., Hu, C. H., & Cheng, Y. (2017). Mismatch negativity (MMN) stands at the crossroads between explicit and implicit emotional processing. *Human Brain Mapping*, *38*(1), 140–150. <https://doi.org/10.1002/hbm.23349>

- Choi, D., Ota, S., & Watanuki, S. (2015). Does cigarette smoking relieve stress? Evidence from the event-related potential (ERP). *International Journal of Psychophysiology*, 98(3), 470–476. <https://doi.org/10.1016/j.ijpsycho.2015.10.005>
- Clemmensen, L., Vernal, D. L., & Steinhausen, H. C. (2012). A systematic review of the long-term outcome of early onset schizophrenia. *BMC Psychiatry*, 12(1), 1. <https://doi.org/10.1186/1471-244X-12-150>
- Cornwell, B. R., Garrido, M. I., Overstreet, C., Pine, D. S., & Grillon, C. (2017). The Unpredictive Brain Under Threat: A Neurocomputational Account of Anxious Hypervigilance. *Biological Psychiatry*, 82(6), 447–454. <https://doi.org/10.1016/j.biopsych.2017.06.031>
- Cowles, M., & Hogg, L. (2019). An Experimental Investigation into the Effect of State-Anxiety on State-Paranoia in People Experiencing Psychosis. *Behavioural and Cognitive Psychotherapy*, 47(1), 52–66. <https://doi.org/10.1017/S1352465818000401>
- de Cheveigné, A., & Nelken, I. (2019). Filters: When, Why, and How (Not) to Use Them. *Neuron*, 102(2), 280–293. <https://doi.org/10.1016/j.neuron.2019.02.039>
- DeCoster, J., Gallucci, M., & Iselin, A.-M. R. (2011). Best Practices for Using Median Splits, Artificial Categorization, and their Continuous Alternatives. *Journal of Experimental Psychopathology*, 2(2), 197–209. <https://doi.org/10.5127/jep.008310>
- Delawalla, Z., Csernansky, J. G., & Barch, D. M. (2008). Prefrontal Cortex Function in Nonpsychotic Siblings of Individuals with Schizophrenia. *Biological Psychiatry*, 63(5), 490–497. <https://doi.org/10.1016/j.biopsych.2007.05.007>
- Díaz-Caneja, C. M., Pina-Camacho, L., Rodríguez-Quiroga, A., Fraguas, D., Parellada, M., & Arango, C. (2015). Predictors of outcome in early-onset psychosis: a systematic review. *Npj Schizophrenia*, 1(1), 14005. <https://doi.org/10.1038/npjrschz.2014.5>
- Dima, D., Dillo, W., Bonnemann, C., Emrich, H. M., & Dietrich, D. E. (2011). Reduced P300 and P600 amplitude in the hollow-mask illusion in patients with schizophrenia. *Psychiatry Research - Neuroimaging*, 191(2), 145–151. <https://doi.org/10.1016/j.psychresns.2010.09.015>
- Dosenbach, N. U. F., Visscher, K. M., Palmer, E. D., Miezin, F. M., Wenger, K. K., Kang, H. C., Burgund, E. D., Grimes, A. L., Schlaggar, B. L., & Petersen, S. E. (2006). A Core System for the Implementation of Task Sets. *Neuron*, 50(5), 799–812. <https://doi.org/10.1016/j.neuron.2006.04.031>
- Eickhoff, S. B., Nichols, T. E., Laird, A. R., Hoffstaedter, F., Amunts, K., Fox, P. T., Bzdok, D., & Eickhoff, C. R. (2016). Behavior, sensitivity, and power of activation likelihood estimation characterized by massive empirical simulation. *NeuroImage*, 137, 70–85. <https://doi.org/10.1016/j.neuroimage.2016.04.072>
- Ermütlu, M. N., Karamürsel, S., Ugur, E. H., Senturk, L., & Gokhan, N. (2005). Effects of cold stress on

- early and late stimulus gating. *Psychiatry Research*, *136*(2–3), 201–209.
<https://doi.org/10.1016/j.psychres.2003.03.002>
- Eysenck, M. W., & Derakshan, N. (2011). New perspectives in attentional control theory. *Personality and Individual Differences*, *50*(7), 955–960. <https://doi.org/10.1016/j.paid.2010.08.019>
- Eysenck, M. W., Derakshan, N., Santos, R., & Calvo, M. G. (2007). Anxiety and cognitive performance: Attentional control theory. *Emotion*, *7*(2), 336–353. <https://doi.org/10.1037/1528-3542.7.2.336>
- Freeman, D., & Fowler, D. (2009). Routes to psychotic symptoms: Trauma, anxiety and psychosis-like experiences. *Psychiatry Research*, *169*(2), 107–112. <https://doi.org/10.1016/j.psychres.2008.07.009>
- Freeman, D., Garety, P. A., Kuipers, E., Fowler, D., & Bebbington, P. E. (2002). A cognitive model of persecutory delusions. *British Journal of Clinical Psychology*, *41*(4), 331–347.
<https://doi.org/10.1348/014466502760387461>
- Friston, K. (1999). Schizophrenia and the disconnection hypothesis. *Acta Psychiatrica Scandinavica*, *99*(s395), 68–79. <https://doi.org/10.1111/j.1600-0447.1999.tb05985.x>
- Friston, K., Brown, H. R., Siemerkus, J., & Stephan, K. E. (2016). The dysconnection hypothesis (2016). *Schizophrenia Research*, *176*(2–3), 83–94. <https://doi.org/10.1016/j.schres.2016.07.014>
- Fucci, E., Abdoun, O., & Lutz, A. (2019). Auditory perceptual learning is not affected by anticipatory anxiety in the healthy population except for highly anxious individuals: EEG evidence. *Clinical Neurophysiology*, *130*(7), 1135–1143. <https://doi.org/10.1016/j.clinph.2019.04.010>
- Fusar-Poli, P., Broome, M. R., Matthiasson, P., Woolley, J. B., Johns, L. C., Tabraham, P., Bramon, E., Valmaggia, L., Williams, S. C., & McGuire, P. (2010). Spatial working memory in individuals at high risk for psychosis: Longitudinal fMRI study. *Schizophrenia Research*, *123*(1), 45–52.
<https://doi.org/10.1016/j.schres.2010.06.008>
- Geng, H., Li, X., Chen, J., Li, X., & Gu, R. (2016). Decreased Intra- and Inter-Saliency Network Functional Connectivity is Related to Trait Anxiety in Adolescents. *Frontiers in Behavioral Neuroscience*, *9*(January), 1–10. <https://doi.org/10.3389/fnbeh.2015.00350>
- Gogtay, N., Greenstein, D., Lenane, M., Clasen, L., Sharp, W., Gochman, P., Butler, P., Evans, A., & Rapoport, J. (2007). Cortical Brain Development in Nonpsychotic Siblings of Patients With Childhood-Onset Schizophrenia. *Archives of General Psychiatry*, *64*(7), 772–780.
<https://doi.org/10.1001/archpsyc.64.7.772>
- Goodkind, M., Eickhoff, S. B., Oathes, D. J., Jiang, Y., Chang, A., Jones-Hagata, L. B., Ortega, B. N., Zaiko, Y. V., Roach, E. L., Korgaonkar, M. S., Grieve, S. M., Galatzer-Levy, I., Fox, P. T., & Etkin, A. (2015). Identification of a common neurobiological substrate for mental illness. *JAMA Psychiatry*, *72*(4), 305–315. <https://doi.org/10.1001/jamapsychiatry.2014.2206>
- Greenstein, D., Lerch, J., Shaw, P., Clasen, L., Giedd, J., Gochman, P., Rapoport, J., & Gogtay, N. (2006). Childhood onset schizophrenia: Cortical brain abnormalities as young adults. *Journal of*

- Child Psychology and Psychiatry*, 47(10), 1003–1012. <https://doi.org/10.1111/j.1469-7610.2006.01658.x>
- Guillem, F., Pampoulova, T., Stip, E., Lalonde, P., & Todorov, C. (2005). The relationships between symptom dimensions and dysphoria in schizophrenia. *Schizophrenia Research*, 75(1), 83–96. <https://doi.org/10.1016/j.schres.2004.06.018>
- Guillem, F., Pampoulova, T., Stip, E., Todorov, C., & Lalonde, P. (2005). Are there common mechanisms in sensation seeking and reality distortion in schizophrenia? A study using memory event-related potentials. *Psychiatry Research*, 135(1), 11–33. <https://doi.org/10.1016/j.psychres.2004.11.008>
- Haenschel, C., Vernon, D. J., Dwivedi, P., Gruzelier, J. H., & Baldeweg, T. (2005). Event-Related Brain Potential Correlates of Human Auditory Sensory Memory-Trace Formation. *Journal of Neuroscience*, 25(45), 10494–10501. <https://doi.org/10.1523/JNEUROSCI.1227-05.2005>
- Ham, T., Leff, A., de Boissezon, X., Joffe, A., & Sharp, D. J. (2013). Cognitive Control and the Salience Network: An Investigation of Error Processing and Effective Connectivity. *Journal of Neuroscience*, 33(16), 7091–7098. <https://doi.org/10.1523/JNEUROSCI.4692-12.2013>
- Heinz, A., & Schlagenhauf, F. (2010). Dopaminergic dysfunction in schizophrenia: Salience attribution revisited. *Schizophrenia Bulletin*, 36(3), 472–485. <https://doi.org/10.1093/schbul/sbq031>
- Howes, O. D., & Kapur, S. (2009). The dopamine hypothesis of schizophrenia: Version III - The final common pathway. *Schizophrenia Bulletin*, 35(3), 549–562. <https://doi.org/10.1093/schbul/sbp006>
- Hsieh, M. H., Lin, Y.-T., Chien, Y.-L., Hwang, T.-J., Hwu, H.-G., Liu, C.-M., & Liu, C.-C. (2019). Auditory Event-Related Potentials in Antipsychotic-Free Subjects With Ultra-High-Risk State and First-Episode Psychosis. *Frontiers in Psychiatry*, 10(April), 1–11. <https://doi.org/10.3389/fpsy.2019.00223>
- Javitt, D. C. (2009). When doors of perception close: Bottom-up models of disrupted cognition in schizophrenia. *Annual Review of Clinical Psychology*, 5, 249–275. <https://doi.org/10.1146/annurev.clinpsy.032408.153502>
- Jones, H. J., Stergiakouli, E., Tansey, K. E., Hubbard, L., Heron, J., Cannon, M., Holmans, P., Lewis, G., Linden, D. E. J., Jones, P. B., Smith, G. D., O'Donovan, M. C., Owen, M. J., Walters, J. T., & Zammit, S. (2016). Phenotypic manifestation of genetic risk for schizophrenia during adolescence in the general population. *JAMA Psychiatry*, 73(3), 221–228. <https://doi.org/10.1001/jamapsychiatry.2015.3058>
- Kapur, S. (2003). Psychosis as a state of aberrant salience: A framework linking biology, phenomenology, and pharmacology in schizophrenia. In *American Journal of Psychiatry* (Vol. 160, Issue 1, pp. 13–23). <https://doi.org/10.1176/appi.ajp.160.1.13>
- Karcher, N. R., O'Brien, K. J., Kandala, S., & Barch, D. M. (2019). Resting-State Functional

- Connectivity and Psychotic-like Experiences in Childhood: Results From the Adolescent Brain Cognitive Development Study. *Biological Psychiatry*, 86(1), 7–15.
<https://doi.org/10.1016/j.biopsych.2019.01.013>
- Karlsgodt, K. H., Glahn, D. C., van Erp, T. G. M., Therman, S., Huttunen, M., Manninen, M., Kaprio, J., Cohen, M. S., Lönnqvist, J., & Cannon, T. D. (2007). The relationship between performance and fMRI signal during working memory in patients with schizophrenia, unaffected co-twins, and control subjects. *Schizophrenia Research*, 89(1–3), 191–197.
<https://doi.org/10.1016/j.schres.2006.08.016>
- Kelly, C., & McCreadie, R. (2000). Cigarette smoking and schizophrenia. *Advances in Psychiatric Treatment*, 6(5), 327–331. <https://doi.org/10.1192/apt.6.5.327>
- Kruschke, J. K. (2010). What to believe: Bayesian methods for data analysis. *Trends in Cognitive Sciences*, 14(7), 293–300. <https://doi.org/10.1016/j.tics.2010.05.001>
- Kucyi, A., Hodaie, M., & Davis, K. D. (2012). Lateralization in intrinsic functional connectivity of the temporoparietal junction with salience- and attention-related brain networks. *Journal of Neurophysiology*, 108(12), 3382–3392. <https://doi.org/10.1152/jn.00674.2012>
- Kyriakopoulos, M., Dima, D., Roiser, J. P., Corrigall, R., Barker, G. J., & Frangou, S. (2012). Abnormal Functional Activation and Connectivity in the Working Memory Network in Early-Onset Schizophrenia. *Journal of the American Academy of Child & Adolescent Psychiatry*, 51(9), 911–920.e2. <https://doi.org/10.1016/j.jaac.2012.06.020>
- Lee, H., Ku, J., Kim, J., Jang, D. P., Yoon, K. J., Kim, S. I., & Kim, J. J. (2014). Aberrant neural responses to social rejection in patients with schizophrenia. *Social Neuroscience*, 9(4), 412–423. <https://doi.org/10.1080/17470919.2014.907202>
- Light, G. A., Williams, L. E., Minow, F., Sprock, J., Rissling, A., Sharp, R., Swerdlow, N. R., & Braff, D. L. (2010). Electroencephalography (EEG) and Event-Related Potentials (ERPs) with Human Participants. *Current Protocols in Neuroscience*, 52(1), 6.25.1–6.25.24.
<https://doi.org/10.1002/0471142301.ns0625s52>
- Liljander, S., Holm, A., Keski-Säntti, P., & Partanen, J. V. (2016). Optimal digital filters for analyzing the mid-latency auditory P50 event-related potential in patients with Alzheimer’s disease. *Journal of Neuroscience Methods*, 266, 50–67. <https://doi.org/10.1016/j.jneumeth.2016.03.013>
- Loeb, F. F., Zhou, X., Craddock, K. E. S., Shora, L., Broadnax, D. D., Gochman, P., Clasen, L. S., Lalonde, F. M., Berman, R. A., Berman, K. F., Rapoport, J. L., & Liu, S. (2018). Reduced Functional Brain Activation and Connectivity During a Working Memory Task in Childhood-Onset Schizophrenia. *Journal of the American Academy of Child and Adolescent Psychiatry*, 57(3), 166–174. <https://doi.org/10.1016/j.jaac.2017.12.009>
- Luo, Q., Pan, B., Gu, H., Simmonite, M., Francis, S., Liddle, P. F., & Palaniyappan, L. (2020). Effective connectivity of the right anterior insula in schizophrenia: The salience network and task-negative to

- task-positive transition. *NeuroImage: Clinical*, 28(August), 102377.
<https://doi.org/10.1016/j.nicl.2020.102377>
- MacNamara, A., DiGangi, J., & Phan, K. L. (2016). Aberrant Spontaneous and Task-Dependent Functional Connections in the Anxious Brain. *Biological Psychiatry: Cognitive Neuroscience and Neuroimaging*, 1(3), 278–287. <https://doi.org/10.1016/j.bpsc.2015.12.004>
- Massullo, C., Carbone, G. A., Farina, B., Panno, A., Capriotti, C., Giacchini, M., Machado, S., Budde, H., Murillo-Rodríguez, E., & Imperatori, C. (2020). Dysregulated brain salience within a triple network model in high trait anxiety individuals: A pilot EEG functional connectivity study. *International Journal of Psychophysiology*, 157(June), 61–69. <https://doi.org/10.1016/j.ijpsycho.2020.09.002>
- Maynard, T. M., Sikich, L., Lieberman, J. A., & LaMantia, A. S. (2001). Neural development, cell-cell signaling, and the “two-hit” hypothesis of schizophrenia. *Schizophrenia Bulletin*, 27(3), 457–476. <https://doi.org/10.1093/oxfordjournals.schbul.a006887>
- McIntosh, A. M., Owens, D. C., Moorhead, W. J., Whalley, H. C., Stanfield, A. C., Hall, J., Johnstone, E. C., & Lawrie, S. M. (2011). Longitudinal volume reductions in people at high genetic risk of schizophrenia as they develop psychosis. *Biological Psychiatry*, 69(10), 953–958. <https://doi.org/10.1016/j.biopsych.2010.11.003>
- McTeague, L. M., Huemer, J., Carreon, D. M., Jiang, Y., Eickhoff, S. B., & Etkin, A. (2017). Identification of common neural circuit disruptions in cognitive control across psychiatric disorders. *American Journal of Psychiatry*, 174(7), 676–685. <https://doi.org/10.1176/appi.ajp.2017.16040400>
- McTeague, L. M., Rosenberg, B. M., Lopez, J. W., Carreon, D. M., Huemer, J., Jiang, Y., Chick, C. F., Eickhoff, S. B., & Etkin, A. (2020). Identification of common neural circuit disruptions in emotional processing across psychiatric disorders. *American Journal of Psychiatry*, 177(5), 411–421. <https://doi.org/10.1176/appi.ajp.2019.18111271>
- Meda, S. A., Bhattarai, M., Morris, N. A., Astur, R. S., Calhoun, V. D., Mathalon, D. H., Kiehl, K. A., & Pearlson, G. D. (2008). An fMRI study of working memory in first-degree unaffected relatives of schizophrenia patients. *Schizophrenia Research*, 104(1–3), 85–95. <https://doi.org/10.1016/j.schres.2008.06.013>
- Menon, V. (2011). Large-scale brain networks and psychopathology: A unifying triple network model. In *Trends in Cognitive Sciences* (Vol. 15, Issue 10, pp. 483–506). Elsevier Ltd. <https://doi.org/10.1016/j.tics.2011.08.003>
- Modi, S., Kumar, M., Nara, S., Kumar, P., & Khushu, S. (2018). Trait anxiety and neural efficiency of abstract reasoning: An fMRI investigation. *Journal of Biosciences*, 43(5), 877–886. <https://doi.org/10.1007/s12038-018-9800-3>
- Morey, R. D., Romeijn, J. W., & Rouder, J. N. (2016). The philosophy of Bayes factors and the quantification of statistical evidence. *Journal of Mathematical Psychology*, 72, 6–18.

<https://doi.org/10.1016/j.jmp.2015.11.001>

- Näätänen, R., Shiga, T., Asano, S., & Yabe, H. (2015). Mismatch negativity (MMN) deficiency: A breakthrough biomarker in predicting psychosis onset. *International Journal of Psychophysiology*, *95*(3), 338–344. <https://doi.org/10.1016/j.ijpsycho.2014.12.012>
- Opmeer, E. M., van Tol, M. J., Kortekaas, R., van der Wee, N. J. A., Woudstra, S., van Buchem, M. A., Penninx, B. W., Veltman, D. J., & Aleman, A. (2015). DISC1 gene and affective psychopathology: A combined structural and functional MRI study. *Journal of Psychiatric Research*, *61*, 150–157. <https://doi.org/10.1016/j.jpsychires.2014.11.014>
- Osinsky, R., Gebhardt, H., Alexander, N., & Hennig, J. (2012). Trait anxiety and the dynamics of attentional control. *Biological Psychology*, *89*(1), 252–259. <https://doi.org/10.1016/j.biopsycho.2011.10.016>
- Palaniyappan, L., Simmonite, M., White, T. P., Liddle, E. B., & Liddle, P. F. (2013). Neural primacy of the salience processing system in schizophrenia. *Neuron*, *79*(4), 814–828. <https://doi.org/10.1016/j.neuron.2013.06.027>
- Pallanti, S., Cantisani, A., & Grassi, G. (2013). Anxiety as a core aspect of schizophrenia. *Current Psychiatry Reports*, *15*(5), 1–5. <https://doi.org/10.1007/s11920-013-0354-7>
- Pankow, A., Katthagen, T., Diner, S., Deserno, L., Boehme, R., Kathmann, N., Gleich, T., Gaebler, M., Walter, H., Heinz, A., & Schlagenhauf, F. (2016). Aberrant Salience Is Related to Dysfunctional Self-Referential Processing in Psychosis. *Schizophrenia Bulletin*, *42*(1), 67–76. <https://doi.org/10.1093/schbul/sbv098>
- Park, S., & Gooding, D. C. (2014). Working memory impairment as an endophenotypic marker of a schizophrenia diathesis. *Schizophrenia Research: Cognition*, *1*(3), 127–136. <https://doi.org/10.1016/j.scog.2014.09.005>
- Petersen, S. E., & Posner, M. I. (2012). The Attention System of the Human Brain: 20 Years After. *Annual Review of Neuroscience*, *35*(1), 73–89. <https://doi.org/10.1146/annurev-neuro-062111-150525>
- Prochwicz, K., & Kłosowska, J. (2018). The interplay between trait anxiety, cognitive biases and attentional control in healthy individuals with psychotic-like experiences. *Psychiatry Research*, *259*(September 2017), 44–50. <https://doi.org/10.1016/j.psychres.2017.09.085>
- Quarmley, M., Gur, R. C., Turetsky, B. I., Watters, A. J., Bilker, W. B., Elliott, M. A., Calkins, M. E., Kohler, C. G., Ruparel, K., Rupert, P., Gur, R. E., & Wolf, D. H. (2019). Reduced safety processing during aversive social conditioning in psychosis and clinical risk. *Neuropsychopharmacology*, *44*(13), 2247–2253. <https://doi.org/10.1038/s41386-019-0421-9>
- Quigley, H., & MacCabe, J. H. (2019). The relationship between nicotine and psychosis. *Therapeutic Advances in Psychopharmacology*, *9*(6), 204512531985996.

<https://doi.org/10.1177/2045125319859969>

- Repovš, G., & Barch, D. M. (2012). Working Memory Related Brain Network Connectivity in Individuals with Schizophrenia and Their Siblings. *Frontiers in Human Neuroscience*, 6(May), 1–15. <https://doi.org/10.3389/fnhum.2012.00137>
- Rodgers, B. (1990). Behaviour and Personality in Childhood as Predictors of Adult Psychiatric Disorder. *Journal of Child Psychology and Psychiatry*, 31(3), 393–414. <https://doi.org/10.1111/j.1469-7610.1990.tb01577.x>
- Roiser, J. P., Stephan, K. E., Den Ouden, H. E. M., Barnes, T. R. E., Friston, K. J., & Joyce, E. M. (2009). Do patients with schizophrenia exhibit aberrant salience? *Psychological Medicine*, 39(2), 199–209. <https://doi.org/10.1017/S0033291708003863>
- Schmidt, A., Antoniadis, M., Allen, P., Egerton, A., Chaddock, C. A., Borgwardt, S., Fusar-Poli, P., Roiser, J. P., Howes, O., & McGuire, P. (2017). Longitudinal alterations in motivational salience processing in ultra-high-risk subjects for psychosis. *Psychological Medicine*, 47(2), 243–254. <https://doi.org/10.1017/S0033291716002439>
- Seeley, W. W., Menon, V., Schatzberg, A. F., Keller, J., Glover, G. H., Kenna, H., Reiss, A. L., & Greicius, M. D. (2007). Dissociable Intrinsic Connectivity Networks for Salience Processing and Executive Control. *Journal of Neuroscience*, 27(9), 2349–2356. <https://doi.org/10.1523/jneurosci.5587-06.2007>
- Shan, J.-C., Hsieh, M. H., Liu, C.-M., Chiu, M.-J., Jaw, F.-S., & Hwu, H.-G. (2010). More evidence to support the role of S2 in P50 studies. *Schizophrenia Research*, 122(1–3), 270–272. <https://doi.org/10.1016/j.schres.2010.05.026>
- Sridharan, D., Levitin, D. J., & Menon, V. (2008). A critical role for the right fronto-insular cortex in switching between central-executive and default-mode networks. *Proceedings of the National Academy of Sciences*, 105(34), 12569–12574. <https://doi.org/10.1073/pnas.0800005105>
- Stephan-Otto, C., Siddi, S., Cuevas Esteban, J., Senior, C., García-Álvarez, R., Cambra-Martí, M. R., Usall, J., & Brébion, G. (2016). Neural activity during object perception in schizophrenia patients is associated with illness duration and affective symptoms. *Schizophrenia Research*, 175(1–3), 27–34. <https://doi.org/10.1016/j.schres.2016.04.020>
- Thermenos, H. W., Seidman, L. J., Breiter, H., Goldstein, J. M., Goodman, J. M., Poldrack, R., Faraone, S. V., & Tsuang, M. T. (2004). Functional magnetic resonance imaging during auditory verbal working memory in nonpsychotic relatives of persons with schizophrenia: A pilot study. *Biological Psychiatry*, 55(5), 490–500. <https://doi.org/10.1016/j.biopsych.2003.11.014>
- Thoma, R. J., Meier, A., Houck, J., Clark, V. P., Lewine, J. D., Turner, J., Calhoun, V., & Stephen, J. (2017). Diminished auditory sensory gating during active auditory verbal hallucinations. *Schizophrenia Research*, 188, 125–131. <https://doi.org/10.1016/j.schres.2017.01.023>

- Toulopoulou, T., Picchioni, M., Rijdsdijk, F., Hua-Hall, M., Ettinger, U., Sham, P., & Murray, R. (2007). Substantial genetic overlap between neurocognition and schizophrenia: Genetic modeling in twin samples. *Archives of General Psychiatry*, *64*(12), 1348–1355.
<https://doi.org/10.1001/archpsyc.64.12.1348>
- Underwood, R., Kumari, V., & Peters, E. (2016). Cognitive and neural models of threat appraisal in psychosis: A theoretical integration. *Psychiatry Research*, *239*, 131–138.
<https://doi.org/10.1016/j.psychres.2016.03.016>
- Van Os, J., & Jones, P. B. (2001). Neuroticism as a risk factor for schizophrenia. *Psychological Medicine*, *31*(6), 1129–1134. <https://doi.org/10.1017/S0033291701004044>
- Wagenmakers, E. J., Marsman, M., Jamil, T., Ly, A., Verhagen, J., Love, J., Selker, R., Gronau, Q. F., Šmíra, M., Epskamp, S., Matzke, D., Rouder, J. N., & Morey, R. D. (2018). Bayesian inference for psychology. Part I: Theoretical advantages and practical ramifications. *Psychonomic Bulletin and Review*, *25*(1), 35–57. <https://doi.org/10.3758/s13423-017-1343-3>
- Wan, L., Crawford, H. J., & Boutros, N. (2006). P50 sensory gating: Impact of high vs. low schizotypal personality and smoking status. *International Journal of Psychophysiology*, *60*(1), 1–9.
<https://doi.org/10.1016/j.ijpsycho.2005.03.024>
- Weinberger, D. R. (1988). Implications of Normal Brain Development for the Pathogenesis of Schizophrenia. *Archives of General Psychiatry*, *45*(11), 1055.
<https://doi.org/10.1001/archpsyc.1988.01800350089019>
- Winton-Brown, T. T., Fusar-Poli, P., Ungless, M. A., & Howes, O. D. (2014). Dopaminergic basis of salience dysregulation in psychosis. In *Trends in Neurosciences* (Vol. 37, Issue 2, pp. 85–94). Elsevier Ltd. <https://doi.org/10.1016/j.tins.2013.11.003>
- Wu, D., & Jiang, T. (2019). Schizophrenia-related abnormalities in the triple network: a meta-analysis of working memory studies. *Brain Imaging and Behavior*, *14*(4), 971–980.
<https://doi.org/10.1007/s11682-019-00071-1>
- Zhang, R., Picchioni, M., Allen, P., & Toulopoulou, T. (2016). Working Memory in Unaffected Relatives of Patients With Schizophrenia: A Meta-Analysis of Functional Magnetic Resonance Imaging Studies. *Schizophrenia Bulletin*, *42*(4), 1068–1077. <https://doi.org/10.1093/schbul/sbv221>
- Zöllner, D., Sandini, C., Karahanoğlu, F. I., Padula, M. C., Schaer, M., Eliez, S., & Van De Ville, D. (2019). Large-Scale Brain Network Dynamics Provide a Measure of Psychosis and Anxiety in 22q11.2 Deletion Syndrome. *Biological Psychiatry: Cognitive Neuroscience and Neuroimaging*, *4*(10), 881–892. <https://doi.org/10.1016/j.bpsc.2019.04.004>

Appendix

Appendices A and B are attached in the next pages

Empirical Paper

Cite this article: Ioakeimidis V, Khachatoorian N, Haenschel C, Papathomas TA, Farkas A, Kyriakopoulos M, and Dima D. (2021) State anxiety influences P300 and P600 event-related potentials over parietal regions in the hollow-mask illusion experiment. *Personality Neuroscience*. Vol 4: e2, 1–10. doi: [10.1017/pen.2020.16](https://doi.org/10.1017/pen.2020.16)

Received: 27 April 2020
Revised: 20 October 2020
Accepted: 6 November 2020

Keywords:

Hollow-mask illusion; EEG; P300; P600; Neuroticism; Anxiety

Author for correspondence:

Danai Dima, Email: danai.dima@city.ac.uk

State anxiety influences P300 and P600 event-related potentials over parietal regions in the hollow-mask illusion experiment

Vasileios Ioakeimidis¹, Nareg Khachatoorian¹, Corinna Haenschel¹, Thomas A. Papathomas^{2,3}, Attila Farkas², Marinos Kyriakopoulos^{4,5} and Danai Dima^{1,6} 

¹Department of Psychology, School of Arts and Social Sciences, City, University of London, London, UK; ²Center for Cognitive Science, Rutgers University, Piscataway, NJ, USA; ³Department of Biomedical Engineering, Rutgers University, Piscataway, NJ, USA; ⁴National and Specialist Acorn Lodge Inpatient Children Unit, South London and Maudsley NHS Foundation Trust, London, UK; ⁵Department of Child and Adolescent Psychiatry, Institute of Psychiatry, Psychology and Neuroscience, King's College London, London, UK and ⁶Department of Neuroimaging, Institute of Psychiatry, Psychology and Neuroscience, King's College London, London, UK

Abstract

The hollow-mask illusion is an optical illusion where a concave face is perceived as convex. It has been demonstrated that individuals with schizophrenia and anxiety are less susceptible to the illusion than controls. Previous research has shown that the P300 and P600 event-related potentials (ERPs) are affected in individuals with schizophrenia. Here, we examined whether individual differences in neuroticism and anxiety scores, traits that have been suggested to be risk factors for schizophrenia and anxiety disorders, affect ERPs of healthy participants while they view concave faces. Our results confirm that the participants were susceptible to the illusion, misperceiving concave faces as convex. We additionally demonstrate significant interactions of the concave condition with state anxiety in central and parietal electrodes for P300 and parietal areas for P600, but not with neuroticism and trait anxiety. The state anxiety interactions were driven by low-state anxiety participants showing lower amplitudes for concave faces compared to convex. The P300 and P600 amplitudes were smaller when a concave face activated a convex face memory representation, since the stimulus did not match the active representation. The opposite pattern was evident in high-state anxiety participants in regard to state anxiety interaction and the hollow-mask illusion, demonstrating larger P300 and P600 amplitudes to concave faces suggesting impaired late information processing in this group. This could be explained by impaired allocation of attentional resources in high-state anxiety leading to hyperarousal to concave faces that are unexpected mismatches to standard memory representations, as opposed to expected convex faces.

Visual illusions are primarily, for research, a great tool to understand human perception (Carbon, 2014) and they occur when the subjective percept does not match the real physical properties of the observed object. This mismatch can be a result of stimulus-driven assumptions made by the visual system and other times they constitute an active recalibration of higher-level cognitive areas (Eagleman, 2001). They can be distinguished in two categories based on the brain networks which contribute to the illusory percept; illusions resulting from bottom-up signals are called physiological or low-level, whereas those occurring from top-down regulatory activity are cognitive illusions (Dima, Dillo, Bonnemann, Emrich & Dietrich, 2011; King, Hodgekins, Chouinard, Chouinard & Sperandio, 2017).

An interesting class of cognitive illusions is the binocular depth-inversion illusions that result in objects perceived in reverse depth, with distant points perceived to be closer than near points; thus, concavities are perceived as convexities and vice versa. The best-known binocular depth-inversion illusion is the hollow-mask illusion. One way to experience it is to swap the images of the left and right eyes of a stereoscopic pair; despite the strong stereoscopic cues that signal a concave mask, viewers report perceiving a normal convex face (Farkas, Papathomas, Silverstein, Kourtev & Papayanopoulos, 2016; Georgeson, 1979; Van den Eenden & Spekrijse, 1989). A similar experience can be perceived by using a physical hollow mask, prompting a misperception of the concave 3D surface as convex, despite visual depth cues suggesting the opposite (concave when a face is perceived as 3D going inwards and convex when it was going outwards, like a normal face) (Gregory, 1973; Hill & Bruce, 1993; Hill & Johnston, 2007; Papathomas & Bono, 2004). Healthy controls from 6 month of age (Corrow, Granrud, Mathison & Yonas, 2011) throughout adulthood incorrectly perceive concave faces as convex. Individuals with schizophrenia perceive the illusion to a much lesser degree than controls; instead, they have a veridical perception of the truthful concavity of the mask (Schneider et al., 2002). Schneider et al. (2002) argued that this incongruence is the result of disturbed

© The Author(s), 2021. Published by Cambridge University Press. This is an Open Access article, distributed under the terms of the Creative Commons Attribution licence (<http://creativecommons.org/licenses/by/4.0/>), which permits unrestricted re-use, distribution, and reproduction in any medium, provided the original work is properly cited.

top-down processes in individuals with schizophrenia, which can be reversed after the course of antipsychotic medication. This discrepancy in schizophrenia has been shown to be due to strengthened bottom-up and weakened top-down processing that allows schizophrenia patients to interpret the sensory cues of a hollow face that deviate from stored knowledge of faces being convex as concave (Dima, Dietrich, Dillo & Emrich, 2010; Dima et al., 2011, 2009). Apart from schizophrenic patients, individuals with other psychosis-prone states are also less likely to perceive the hollow-mask illusion, such as cannabis users (Leweke, Schneider, Radwan, Schmidt & Emrich, 2000; Semple, Ramsden & McIntosh, 2003), alcohol withdrawal (Schneider et al., 1996), sleep deprivation (Sternemann et al., 1997), youth at ultra-high risk for psychosis (Gupta et al., 2016), and anxiety patients (Passie et al., 2013). Therefore, disposition of veridical perception of concaveness in faces in the psychotic and pro-psychotic states mentioned above, could be of use in research aiming to identify susceptibility to mental illness.

In this study, we explore the electrophysiological signature of perception of the hollow-mask illusion. We use the P300 and P600 event-related potentials (ERPs), occurring between 300 to 600 ms and 600 to 800 ms after stimulus onset, respectively, to explore the timeline of the hollow-mask illusion. These ERPs have been previously shown to be significantly reduced in amplitude in schizophrenia patients who respond to the hollow-mask illusion experiment compared to controls (Dima et al., 2011). The P300 occurrence involves attentional engagement responsible for memory functioning and stimulus evaluation, with familiar stimuli activating context- and familiarity-related temporo-parietal top-down control. The P600 has been traditionally thought to reflect any linguistic processes; however, studies have also implicated it to similar processes as the P300, in that it is triggered when a subject encounters an “improbable” stimulus (Coulson, King & Kutas, 1998). Since ungrammatical sentences are relatively rare in natural speech, a P600 may not be simply a linguistic response but rather an effect of the subject’s “surprise” upon encountering an unexpected stimulus (Coulson et al., 1998). Higher amplitudes in P300 and P600 are believed to be associated with stimulus novelty and significance, which are modulated by late perceptual processes, such as remembering and attention (Stelmack, Houlihan & McGarry-Roberts, 1993), and lower amplitude in P300 and P600 during perceiving concave faces was assumed to be a result in late perceptual processing dysregulation in patients with schizophrenia (Dima et al., 2011). Electroencephalography (EEG) studies have associated these late positive event-related components with frontal, temporal and parietal scalp distribution (Polich, 2007).

In this study, we investigate the P300 and P600 ERPs during the presentation of hollow-mask stimuli in healthy participants in relation to their individual differences in neuroticism and anxiety self-report measures. Neuroticism, from the five-factor model (McCrae & Costa, 1992), is of particular interest in psychiatry, as it reflects dysregulation of the emotional equilibrium, anxiety proneness, and susceptibility to stress (Hettema, Neale, Myers, Prescott & Kendler, 2006). As such, high scores in neuroticism are also associated with comorbidity of schizophrenia and anxiety disorders (Caspi, Houts, Belsky & Goldman-mellor, 2015; Khan, Jacobson, Gardner, Prescott & Kendler, 2005). A meta-analysis on the five-factor model has found that higher levels of neuroticism in individuals with schizophrenia come in conjunction with lower levels of extroversion, with large effect sizes, and lower openness, agreeableness and conscientiousness, but with more moderate effect sizes (Ohi et al., 2016). Additionally, there is evidence that schizophrenia appears to be co-occurring along with anxiety disorders (Muller, Koen, Seedat, Emsley & Stein, 2004; Temmingh & Stein, 2015). There is a complex relationship between

anxiety and positive symptom expression in psychotic states. Trait and state anxiety (STAI; Spielberger et al., 1983) can be seen as predictors of paranoia in psychosis spectrum disorders (Freeman & Fowler, 2009; Cowles & Hogg, 2019), whereas state anxiety mediates intrusive thoughts in hallucinating schizophrenia patients (Bortolon, Capdevielle & Raffard, 2015). Previous reports have shown that trait anxiety is significantly associated with positive psychotic symptoms and auditory hallucinations in schizophrenia patients, making it a potential causal factor for the disorder (Guillem et al., 2005). However, when the authors controlled for state anxiety, the correlation with hallucinations became non-significant whilst a significant relationship with bizarre delusions was revealed (Guillem et al., 2005). Hence, state anxiety concealed the delusion-trait anxiety relationship and revealed that delusions mediate the relationship between hallucinations and trait anxiety (Guillem et al., 2005). Accordingly, there is a complex relationship of self-reported neuroticism and anxiety self-reports with psychopathology, and particularly with psychosis which is known to be implicated with abnormal ERPs during the presentation of hollow-mask stimuli.

Given the predisposition of elevated neuroticism and anxiety levels with general psychopathology and psychosis, we hypothesised that self-reported neuroticism and anxiety levels will have an effect on the late positive ERPs that reflect high-order cognitive processes and are generated by hollow-mask stimuli. Furthermore, based on the presented evidence, it is expected that our sample consisting of healthy participants will be susceptible to the illusion behaviourally and show no difference in P300 and P600 amplitude for the concave and convex face stimuli. However, we expect to find an effect of neuroticism and anxiety scores on the amplitude of the ERPs generated by the concave and convex faces.

1 Methods

1.1 Participants

Neuroticism data using the Neuroticism Extroversion Openness Personality Inventory-Revised (NEO PI-R) (McCrae & Costa, 1992) were collected from 94 participants from 18 to 59 years of age ($M = 26.21$, $SD = 11.67$), of which 72 were female and 22 were male (Table 1). Exclusion criteria consisted of: (i) lifetime history of mental disorder or substance use, (ii) reported head injury or medical disorder, and (iii) intake of prescribed psychiatric medication. Participants provided written informed consent prior to their inclusion and the study was approved by the Psychology Department Ethics Committee of City, University of London. Participants were self-referred from study advertisements throughout the university and word-of-mouth recommendation. All participants completed the mini-international neuropsychiatric interview (MINI) (Sheehan et al., 1998).

Upon analysis of the neuroticism trait, 20 out of the 94 subjects were invited to participate in the hollow-mask illusion EEG paradigm. The selection was designed to include a normal distribution of neuroticism scores (Table 2). Those who took part in the EEG session first completed the State-Trait Anxiety Inventory (STAI) to assess state and trait measures of anxiety (Spielberger, Gorsuch, Lushene, Vagg & Jacobs, 1983). Following this, they participated in the hollow-mask illusion experiment while their brain activity was being recorded with EEG.

1.2 The NEO PI-R and STAI self-report questionnaires

The NEO PI-R is a 240-item self-report questionnaire, grouped in five meta-factors, each having six distinct facets. It is used to measure five broad dimensions of personality traits in adults, namely

Table 1. Demographic and questionnaire data in the entire sample ($N = 94$)

Demographic data	
Gender (male: female)	22:72
Age in years, M (SD)	26.21 (11.67)
Age range	18–59
NEO PI-R scores	
Neuroticism, M (SD)	97.74 (22.76)
Neuroticism range	46–162

NEO PI-R: Neuroticism Extroversion Openness Personality Inventory-Revised; STAI: State-Trait Anxiety Inventory.

Table 2. Demographic, questionnaire, and behavioural data in the EEG sample ($N = 20$)

Demographic data	
Gender (male: female)	3:17
Age in years, M (SD)	25.70 (8.96)
Age range	18–59
NEO PI-R scores	
Neuroticism, M (SD)	103.60 (25.77)
Neuroticism range	46–142
STAI scores	
State anxiety, M (SD)	33.75 (9.42)
Trait anxiety, M (SD)	43.75 (9.95)
Correct responses to face stimuli (% correct), M (SD)	
Concave	16% (23%)
Convex	86% (18%)
Flat	69% (26%)
Response time for face stimuli in ms, M (SD)	
Concave	4117.68 (.36)
Convex	3181.45 (1202.75)
Flat	3400.43 (1072.18)

EEG: Electroencephalography; NEO PI-R: Neuroticism Extroversion Openness Personality Inventory-Revised; STAI: State-Trait Anxiety Inventory.

neuroticism, extroversion, openness, agreeableness, and conscientiousness resulting from the scores of their corresponding facets (McCrae & Costa, 1992). Responses for each item have a five-point scale ranging from strongly disagree to strongly agree. In our analysis, we only focus on neuroticism.

The STAI is a 40-item self-report questionnaire and was devised by Spielberger et al. (1983). It is used to measure state and trait measures of anxiety, which result from its two forms, Y-1 and Y-2 respectively, each consisting of 20 items. Responses for each item have a four-point scale: “not at all”, “somewhat”, “moderately so”, and “very much so”.

1.3 Stimuli and design

Participants were included in the study only if their vision was normal or corrected to normal, had normal colour vision, and had functional stereoscopic vision. Stereoscopic vision was tested using the TNO test, designed by the by the Institute for Perception, Netherlands

Organisation for Applied Scientific Research (Lameris Ootech BV, Utrecht, Netherlands; (<http://www.ootech.nl/>)). Furthermore, prior to the hollow-mask illusion experiment, participants took a further test to evaluate if they have functional stereopsis. They viewed images of 15 geometric shapes of three possible surface curvatures (concave, convex and flat) and were asked to respond according to their perception. They were included in the study only if they got all 15 correct.

Subsequently, the hollow-mask illusion experiment was conducted to test the perception of binocular depth inversion (Dima et al., 2011). During this experiment, participants observed images of upright or upside-down faces (real faces) on a computer monitor with the aid of a Wheatstone mirror stereoscope (Wheatstone, 1838, 1852). They were told that the curvature (depth perception) of the faces will vary and were instructed to press one of three keys according to their perception of the depth of the image: “Concave” when a face was perceived as 3D going inwards to the screen, “Convex” when it was going outwards (like normal faces), and “Flat” when they perceived the face as 2D.

In order to create the impression of 3D, each eye was presented with a photo of the same face taken from two angles that corresponded to the views of the left and right eyes. The participant was able to perceive a 3D face that was fused in the middle of the screen while looking through the stereoscope. The effect of binocular depth inversion was generated by swapping the images for the right and left eyes; this swapping has the effect of creating a stereo pair with opposite binocular disparities to those of the convex face and produce, a concave face. Flat (2D) faces were produced by presenting images from the same angle (i.e. the same photo) to both eyes.

Participants performed 12 blocks, each containing 24 stimuli (12 upright and 12 upside-down), one-third concave, one-third convex, and the other third flat, presented in a random order. This led to six different conditions (upright convex, upright concave, upright flat; upside-down convex, upside-down concave, upside-down flat), resulting in 288 images per participant during the course of a complete experimental session. Each stimulus was presented until participants responded. A tone was heard 1.2 s after stimulus onset that signalled to participants that they were free to make a response according to their depth perception of the stimulus. The inter-stimulus interval, following response, was 0.5 s and the whole session lasted for an average of 45 min, including breaks. In all subsequent analyses, only upright faces are included.

1.4 EEG acquisition and ERP analysis

The EEG signal was recorded using a 64-channel, BrainVision BrainAmp series amplifier (Brain Products, Herrsching, Germany) with a 1000 Hz sampling rate. The data were recorded with respect to FCz electrode reference. Ocular activity was recorded with an electrode placed underneath the left eye. Pre-processing was conducted in BrainVision Analyser (Brain Products, Herrsching, Germany) and the statistical analysis of the ERP was conducted in the Statistical Package for the Social Sciences software (SPSS 23, Armonk, NY: IBM Corp).

Pre-processing steps are described in their order of application. First, all EEG channels were individually inspected for high-frequency noise artefacts and slow drift. Those which were noisy throughout the whole EEG session were topographically interpolated by spherical splines. Subsequently, EEG data were down-sampled to 250 Hz and a high-pass filtered with a cut-off frequency of 0.5 Hz was applied. An automatic ocular correction was performed with the independent component analysis in BrainVision Analyser. Following re-referencing to TP9 and TP10 electrodes, data were segmented from 200 ms

prior to 1000 ms after stimulus presentation for each condition. A low-pass filter of 30 Hz was applied followed by automatic artefact rejection which excluded segments with a slope of 100 $\mu\text{V}/\text{ms}$, min–max difference of 200 μV in a 200 ms interval and low activity of 0.5 μV in a 100 ms interval. Baseline correction was applied using the 200 ms interval preceding the stimulus and averaging was performed across each condition (convex, flat, concave). Averaging included all trials per condition (≈ 48), as opposed to only focussing on accurate-only responses, since concave faces were almost impossible to identify correctly (Table 2). For illustration purposes, a high cut-off filter of 20 Hz was applied to the grand average ERPs in Figure 1 and 2.

1.5 Statistical analysis

After pre-processing, the grand average data were extracted from BrainVision Analyser and were taken into SPSS for statistical analysis. The mean amplitudes of the ERPs were separately analysed for the 300–600 ms (P300) and the 600–800 ms (P600) time windows after stimulus onset. The waveforms of the flat faces were used as a baseline to calculate the difference waves for the concave and convex faces. As discussed by Luck (2014), this process can be used to eliminate identical components between separate conditions and isolate those that differ. Difference waves of “concave minus flat” and “convex minus flat” were used to moderate for face processing-related activity and allow comparison of the different 3D features between depth-inverted and depth non-inverted conditions. This led to the creation of two new variables that were used in the analysis as the “condition” factor with two levels: (i) the mean amplitude of the concave minus flat (Concave) and (ii) the mean amplitude of the convex minus flat (Convex).

Electrodes from five separate regions-of-interest (ROIs) were included in the analyses: frontal (Fp1–Fp2–F7–F8–F3–F4–Fz), central (C3–C4–Cz), temporal (T7–T8–P7–P8), parietal (P3–P4–Pz), and occipital (O1–O2–Oz). The electrode ROIs were chosen to correspond with those used in Dima et al. (2011). Repeated measures analyses of variance (RM ANOVA) with factors electrode ROI \times condition as well as RM ANCOVA, with a .01 alpha-level (α) after Bonferroni correction (.05/5: for the five electrode ROIs) were run in SPSS to examine the main effects the condition factor (Concave vs Convex) and its interactions with neuroticism, state and trait anxiety scores as covariates. Additionally, Pearson’s correlations were used to test the associations of the anxiety and neuroticism measures.

2 Results

2.1 Personality and anxiety scores

Mean scores of neuroticism, state and trait anxiety, and their standard deviations are shown in Table 2 for the 20 participants in the EEG session. Neuroticism, state and trait anxiety scores were distributed normally based on Shapiro–Wilk tests ($p > .05$). Correlation analysis showed that neuroticism had a positive correlation with trait anxiety ($r = .673, p = .001$) and state anxiety ($r = .480, p = .032$). Also, state and trait anxiety were positively correlated with each other ($r = .447, p = .048$). Age or sex did not have effect on neuroticism or on state and trait anxiety ($p \geq .265$).

2.2 Behavioural data

Table 2 shows the percentages of correct classification of the stimuli in the three conditions (concave, convex and flat), as well as their

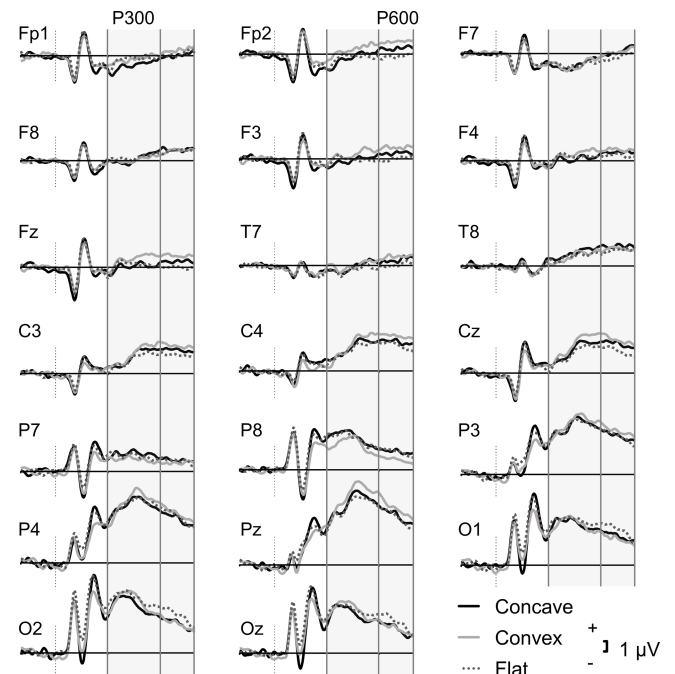


Figure 1. Grand average ERP waveforms for 3D normal faces, 3D inverted faces and flat faces in the whole sample ($N = 20$) in the 20 ROI electrodes.

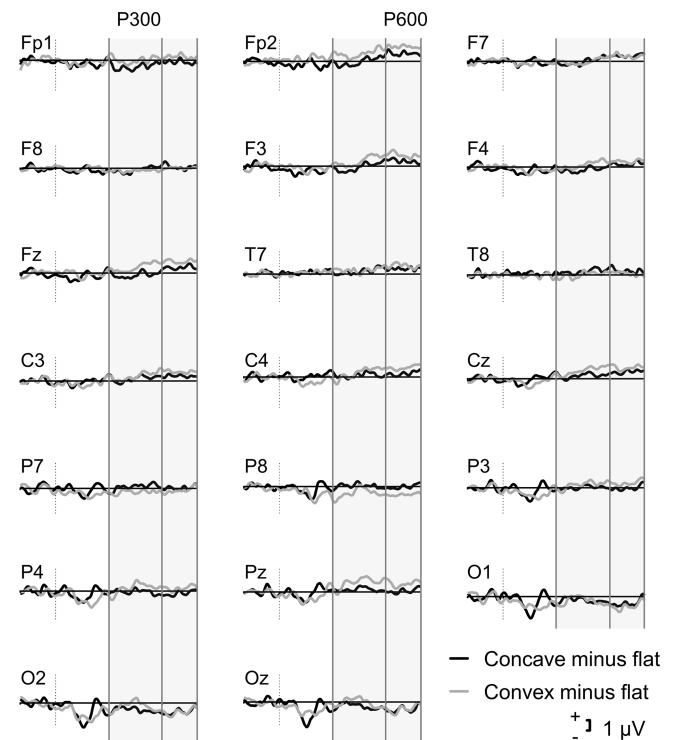


Figure 2. Grand average ERP difference waves for 3D normal faces minus flat faces and 3D inverted faces minus flat faces in the whole sample ($N = 20$) in the 20 ROI electrodes.

corresponding response times (RT). Correct responses for the concave faces, as expected, accounted only for 16% ($SD = \pm 23\%$) of the trials, far below the convex ($M = 87\%$; $SD = \pm 17\%$) and flat ($M = 66\%$; $SD = \pm 28\%$) faces. Correct responses for convex faces were significantly higher than for concave faces ($t_{19} = 11.330, p < .001$) but

not for flat ones ($t_{19} = 2.390, p = .270$). Whereas, correct responses for flat faces were significantly higher than the concave responses ($t_{19} = 9.120, p < .001$). Concave faces were misclassified equally as flat ($M = 47\%$, $SD = 21\%$) or convex ($M = 39\%$, $SD = 21\%$), $t_{19} = 1.000, p = .329$. RT for concave faces were significantly longer than convex RT ($t_{19} = 3.094, p = .006$), but not for the flat ones ($t_{19} = 1.939, p = .067$). Also, flat RT was not significantly different from convex RT ($t_{19} = 1.911, p = .071$).

RT and correct responses for the three types of stimuli (concave, convex, and flat faces) did not significantly correlate with neuroticism or either measure of anxiety.

2.3 ERP results

2.3.1 Main effects

Figure 1 illustrates the grand average ERP waveforms for the concave, convex, and flat stimuli trials in all electrode ROIs. The difference waves for the two conditions (concave minus flat; convex minus flat) are illustrated in Figure 2.

RM ANOVA revealed a significant main effect of condition (convex vs concave) in the mean amplitudes of the P300 difference wave in the temporal area ($F_{1,19} = 6.267, p = .022$), that did not survive Bonferroni correction. For the remaining four electrode groups, namely the frontal, central, parietal, and occipital, no significant main effects were detected in the P300 or P600 time windows ($p > .05$).

2.3.2 Neuroticism

Neuroticism did not interact significantly with condition (concave/convex) in either P300 or P600 time window in any of the five electrode ROIs that were tested ($p \geq .099$).

2.3.3 State anxiety

RM ANCOVA for the P300 ERP showed significant interactions for the condition \times covariate in the central ($F_{1,18} = 10.044, p = .005, \eta_p^2 = .358$) and parietal ($F_{1,18} = 9.243, p = .007, \eta_p^2 = .339$) ROIs. A significant interaction was found in the frontal ROI ($F_{1,18} = 4.820, p = .041, \eta_p^2 = .211$) that did not survive multiple correction.

In the P600, a condition \times state anxiety interaction that was significant for multiple comparisons was observed in the parietal ROI ($F_{1,18} = 13.270, p = .002, \eta_p^2 = .424$). For the temporal ($F_{1,18} = 4.772, p = .042, \eta_p^2 = .210$), central ($F_{1,18} = 4.712, p = .044, \eta_p^2 = .207$), and occipital ($F_{1,18} = 5.023, p = .037, \eta_p^2 = .218$) ROIs, significant interactions were found; however, they did not survive Bonferroni correction.

Subsequently, significant interactions of the continuous state anxiety covariate were explored by creating a categorical variable for state anxiety. Participants were separated according to their state anxiety scores by median split ($Mdn = 33$) into two groups of high-state and low-state anxiety (Bishop, Jenkins & Lawrence, 2007). Hence, 9 participants were included in the high-state anxiety group and 11 in the low-state anxiety group. There was no significant difference for behavioural scores between the two groups, except for correct responses to convex faces with low-state anxiety participants identifying them more correctly ($p = .031$). Subsequently, the mean difference amplitudes and standard errors were calculated for each electrode ROI that showed a significant interaction with the 3D condition, namely the central and parietal for the P300 time window and the parietal for the P600 (Figure 3). Post-hoc independent t -tests showed high- vs low-state anxious participants had significantly higher amplitudes for concave faces in the parietal ROI for the

P300 ($t_{18} = 2.498, p = .022, Cohen's d = 1.123$) and P600 ($t_{18} = 2.359, p = .030, Cohen's d = 1.060$), but not in the central P300 ($t_{18} = 1.507, p = .149, Cohen's d = .678$). Concurrently, paired-sample t -tests revealed significant differences between the 3D conditions only in the low-state anxiety group participants. The difference amplitude in the concave condition was significantly lower in the central and parietal P300 ($t_{10} = 3.810, p = .003, Cohen's d = 1.149; t_{10} = 3.527, p = .005, Cohen's d = 1.064$) and the parietal P600 ($t_{10} = 2.818, p = .018, Cohen's d = .850$) (Figure 3).

2.3.4 Trait anxiety

For the P300 time window, trait anxiety showed significant interactions with the condition factor at frontal ($F_{1,18} = 5.310, p = .033, \eta_p^2 = .228$) and central ($F_{1,18} = 5.879, p = .026, \eta_p^2 = .246$) ROIs, not surviving Bonferroni correction.

In the P600 time window, significant condition \times trait anxiety interactions in frontal ($F_{1,18} = 4.819, p = .042, \eta_p^2 = .211$) and central ($F_{1,18} = 6.732, p = .018, \eta_p^2 = .272$) ROIs did not survive Bonferroni correction.

3 Discussion

To our knowledge, this is the first study to assess neuroticism, state and trait anxiety in ERPs during the hollow-mask illusion. There are three key findings from our study. First, as expected, (i) controls rarely perceive concave 3D faces as they fail to correctly categorise them as such and (ii) there were no main significant effects of condition (convex/concave) in the P300 and P600 time windows (Dima et al., 2011). Second, there was no interaction of neuroticism or trait anxiety and concave/convex condition in the P300 and P600 time windows while viewing the hollow-mask illusion, not supporting our initial hypothesis. Third, there was a significant interaction of state anxiety and with the condition (concave/convex) in the P300 time window at central and parietal electrodes, and in the P600 time window at parietal ones.

The interaction effect between concave/convex faces and state anxiety revealed that the difference of amplitudes of the concave condition for the P300 ERP was significantly lower compared to the convex, only in the low-state anxiety group (Figure 3). This was the case despite the absence of conscious perception of concave stimuli in both groups. The P300 component is traditionally associated with the detection of an expected but unpredictable target in a series of stimuli, like the oddball task. The P300 is thought to be composed of two subcomponents, the “novelty” component (P300a), a large fronto-central positive wave elicited by novel stimuli that mainly reflects involuntary attention shifts to changes in the environment and the “target” component (P300b), more relevant to our study (Polich, 2007). The “target” component is generated in posterior-parietal brain areas and reflects memory access processes that are activated by stimuli that require an evaluation or input (Giraudet, St-Louis, Scannella & Causse, 2015).

In the low-state anxiety group, the concave condition elicited significantly smaller P300 amplitude than the convex condition. Although participants rarely reported concave faces as concave and misclassified them as convex or flat, they were highly accurate in correctly reporting both convex and flat faces. A recent study that tested different types of expectations (target stimuli could either confirm or disconfirm passive or active expectations) has shown that expected stimuli like the convex faces used in our study, could be related to larger P300 amplitudes (Król & El-Derey, 2015). The authors argued that conscious expectations can indirectly affect

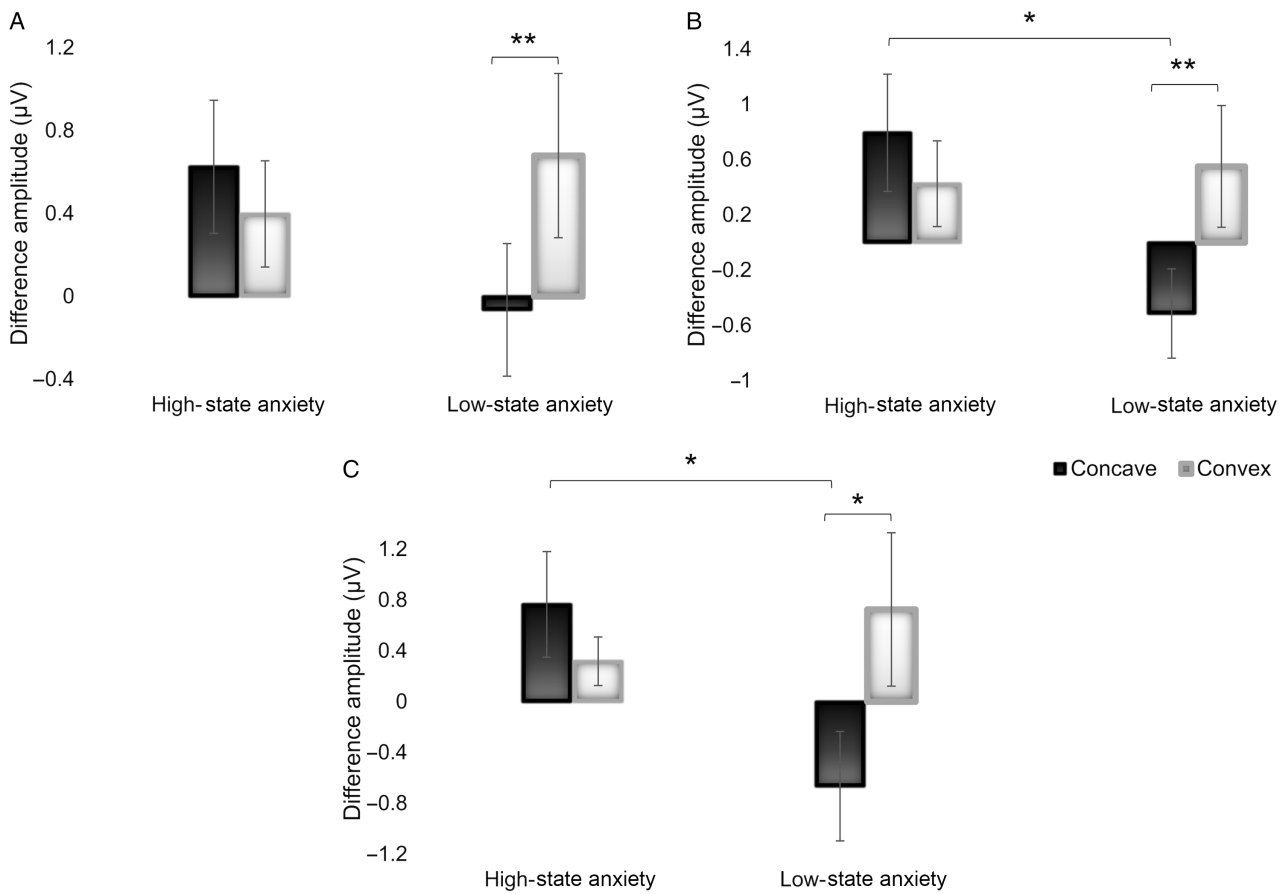


Figure 3. Mean difference amplitude (μV) of concave and convex ERPs minus flat for high-state anxiety and low-state anxiety groups by median split, in A) the P300 central, B) P300 parietal and C) P600 parietal time windows; * $p < .05$; ** $p < .01$ for between- and within-group comparisons.

expectancy and thus have an opposite direction effect of automatically formed expectations. Additionally, Kok (1988) showed that the P300 tends to be smaller when the stimulus does not match the active representation (template mismatch). In line with this, the P300 in our study was smaller when the concave face activated a convex face representation, compared to when a stimulus is less probable (probability mismatch) in the low-state anxiety group. There has also been evidence that the P300 is smaller for difficult tasks, especially when uncertainty is greater and a resolution much harder to reach (Polich, 1987); this uncertainty becomes evident by the longer RTs for concave faces. Our results also question the prevailing theory that the P300 amplitude increases with greater mental resource allocation (Polich & Kok, 1995) and increased informational content of the stimulus, reflecting extraction and utilisation of information (Gratton et al., 1990).

The high-state anxiety group compared to the low-state anxiety group showed a stronger P300 in response to the concave condition. Only a few studies have investigated the P300 in patients with anxiety disorders. In a study using the auditory oddball stimuli, the results showed not only clear differences between subjects who suffered from anxiety and controls but also showed opposite results between anxious patients and anxious controls; while anxious patients compared to controls showed a decreased P300, the group of anxious controls compared to anxious patients showed an increase of the P300 (Boudarene & Timsit-Berthier, 1997). Anxious participants have also been shown to display higher emotional sensitivity and enhanced P300 peak amplitude to negative emotional words compared to

non-anxious participants (De Pascalis, Strippoli, Riccardi & Vergari, 2004; Naumann, Bartussek, Diedrich & Laufer, 1992). An early P300 subcomponent (P315) was also larger in patients having an anxiety disorder alone when compared to depressed patients with or without an anxiety disorder and controls when performing an auditory oddball task; whereas a late P300 subcomponent (P400) was larger in patients having comorbidity of anxiety and depressive disorders than in the controls and depressed patients (Bruder et al., 2002). Another study looking at source characteristics of the P300b showed an anxiety-related pattern of hyperactive ventral attention networks for the anxiety group, indicating increased stimulus-driven attention to task-relevant stimuli (Li et al., 2015). In a recent meta-analysis of ERPs in post-traumatic stress disorder, results demonstrated that seven studies (out of eight) showed increased P300 responses to trauma related or aversive stimuli in the post-traumatic stress disorder group compared to the control group (Javanbakht, Liberzon, Amirsadri, Gjini & Boutros, 2011). In terms of P300, the present study disclosed a greater sensitivity to concave faces in anxious subjects, with a higher P300 amplitude indicating a greater effort investment for these subjects (Brocke, Tasche & Beauducel, 1997). There might be increased attentional resource allocation in anxious subjects to the concave faces showing sensitisation (sensitisation is a learning process in which repeated exposure of a stimulus results in the progressive amplification of a response) to stimuli that are not consciously correctly reported as concave. Our results therefore add support to the notion of impaired attentional resources in anxious participants leading to shifting more resources – hyperarousal – to

stimuli that are mismatches (concave faces) compared to stimuli that are expected (convex faces).

The same pattern of interaction between state anxiety and condition can be seen in the P600 time window at parietal electrodes. The P600 is a centro-parietal late positive ERP that has been associated with syntactic operations such as successful retrieval and recollection (Kaan & Swaab, 2003). The P600 amplitude is known to increase with words being consciously remembered (Smith, 1993), as well as remembering not only the words but also the context of encoding (Wilding, Doyle & Rugg, 1995; Wilding & Rugg, 1996). Furthermore, it is larger for deeply encoded items implying sensitivity to the levels of processing manipulation (Rugg et al., 1998). The language specificity of the P600 has been challenged with studies showing salience and probability of stimulus occurrence affecting P600 amplitude (Coulson et al., 1998; Gunter, Stowe & Mulder, 1997). In the Coulson et al. study (1998), both ungrammatical and improbable stimuli elicited larger P600 amplitude, while in the Gunter et al. (1997) study stimulus probability and sentence complexity had similar influence on the P600. Thus, it is not surprising that in the low-state anxiety group, convex faces elicit a strong P600 while the concave faces that are rarely correctly classified and are misrepresented as convex or flat faces elicit a much smaller P600. However, the opposite effect is seen in the high-state anxiety group implying the same mechanism we see in the P300 time window. Studies have demonstrated significantly higher amplitudes of the P600 in an obsessive-compulsive disorder patient group compared to controls in a working memory paradigm (Papageorgiou & Rabavilas, 2003) as well as in a selective attention task (Towey et al., 1994). Thus, the pattern of the results obtained in the current study suggests that the high-state anxiety group demonstrated impairments in the later stages of information processing as they are reflected by the stronger P600 elicited while viewing the concave face that involve or affect parietal brain areas.

Accordingly, it appears that the late perceptual ERPs of low-state anxiety participants are more like the group as a whole (i.e., the response to the convex stimuli is higher than the concave (when flat is subtracted)). Increased sensitisation to novel stimuli (concave faces) at the higher end of the state anxiety levels interferes with the allocation of attention to the expected ones (convex faces). Fucci, Abdoun & Lutz (2019) have demonstrated increased amplitude in an earlier auditory component (P2) corresponding to standard stimuli compared to deviant ones under safe but not under threatening conditions (Fucci et al., 2019). Likewise, under anxiety-inducing conditions the authors observed increased frontal P2 response to the deviant stimuli (Fucci et al., 2019). Similarly, increased P300 response was also observed in a sample of behaviourally inhibited adolescents with a history of an anxiety disorder compared to adolescents with no such history (Reeb-Sutherland et al., 2009). Our results suggest a dimensional effect of state anxiety on the attentional processes that underlie the hollow-mask illusion, the low-state anxiety individuals do not need to allocate as much attention to mismatch stimuli (concave faces) while individuals experiencing high anxiety orient excessive attention to it.

Even though the interaction between trait anxiety and neural correlates of the hollow-mask stimulus did not survive Bonferroni correction, it showed the same pattern as state anxiety. Anxiety in general has been related to hypervigilance and attentional biases (in terms of intrinsic negativity by selecting threatening stimuli instead of neutral or positive stimuli) (Eysenck, 1997); however, the effects of state vs trait on these processes are not well established. Trait anxiety influences state anxiety levels and is considered a stable personality characteristic, whereas state anxiety is more of a transitory response

to a situation (Meijer, 2001). There have been theories that posit that the two subtypes influence cognition differently; state anxiety decreases a person's threshold for threat stimuli and this occurs more frequently in participants with a high score on trait anxiety (Mathews & Mackintosh, 1998; Williams, Watts, MacLeod & Mathews, 1997). It seems that state anxiety is more sensitive to electrophysiological changes related to the hollow-mask illusion paradigm compared to trait anxiety, although both subtypes influence it in similar ways. It is, however, important to acknowledge that, in our sample, state anxiety levels are moderate. Future studies should recruit participants representing a wider range of state anxiety scores to include anxiety measures at the higher end of the spectrum. This could be better addressed by incorporating a bigger sample size, despite our large effect sizes, which would ensure the inclusion of a more substantial number of individuals to capture the whole gamut of state and trait anxiety measures. Finally, it would be important that future studies should control for effects of physiological arousal by measuring heart rate and cortisol levels, although one previous study did not find these to correlate with state anxiety (Jansen, Gispens-de Wied & Kahn, 2000).

With this study, we intended to explore the relationship between the electrophysiological response to hollow-mask stimuli and traits of personality and anxiety states in controls, to indirectly inform us as to whether certain individuals are more vulnerable to psychopathology. We expected to find a relationship between neuroticism and the ERPs generated by the concave and convex faces due to neuroticism's high occurrence in disorders that interact with the hollow-mask illusion, though this was not the case. Neuroticism has been indicated as an important risk factor for psychiatric traits including anxiety disorders (Hettema et al., 2006) and schizophrenia (Hayes, Osborn, Lewis, Dalman & Lundin, 2017; Van Os & Jones, 2001). A recent meta-analysis has found that a neurotic personality remained a significant risk factor for common mental disorders including anxiety, it was only identified as a vulnerability factor for psychotic disorders (Jeronimus, Kotov, Riese & Ormel, 2016). Research has yet to clarify whether the associations between neurotic traits and psychiatric disorders indicate whether neurotic personality characteristics are a causal factor or a consequence of psychiatric illnesses or both. In our study, we did however find significant correlations between neuroticism and state/trait anxiety. Neuroticism, also known as emotional instability (McCrae & Costa, 1997), and anxiety are closely related measures. This becomes apparent as anxiety itself makes up one of the six facets of neuroticism in the five-factor model of McCrae and Costa (1992). Trait anxiety positively correlated with neuroticism in a sample of patients with panic disorder (Foot & Koszycki, 2004). In a different study, high-state anxiety was associated with higher neuroticism scores in a healthy sample (Bonsaksen et al., 2019). In turn, state and trait anxiety was found to intercorrelate in a sample of patients with schizophrenia (Guillem, Pampoulova, Stip, Lalonde & Todorov, 2005) and schizophrenia patients tend to score higher in STAI measures than controls (Jansen et al., 2000). While state anxiety is thought more of as an effect of psychosis (Guillem et al., 2005) and has been demonstrated to be a predictor of state-paranoia (Cowles & Hogg, 2019), trait and state anxiety was shown to be related with positive symptoms of schizophrenia, such as bizarre delusions and auditory hallucinations (Guillem et al., 2005). Importantly, both anxiety measures affect cognitive control and attentional processes in controls (Pacheco-Unguetti, Acosta, Callejas & Lupiáñez, 2010). Hence, the interaction of state anxiety with the hollow-mask ERPs could explain an indirect relationship of self-report measures and proneness to mental illness.

Our paper serves as a stepping-stone to understanding psychiatric disorders and future research should parse out whether high- and low-state anxiety in different disorders, and especially in schizophrenia, alters the results found here.

In summary, our study points to a potential relationship between ERPs in the hollow-mask illusion and state anxiety. The most robust findings include a significant interaction of state anxiety with 3D condition in the P300 time window at central and parietal electrodes, and in the P600 time window at parietal ones. The high-state anxiety group shows disproportionately big P300 and P600 amplitudes to concave faces implying impaired late information processing in this group. Finally, anxious participants have impaired attentional resources by transferring more resources to the concave faces that are stimuli mismatches to our memory representations compared to convex faces that are expected.

Financial support. This work was supported by a Pump Priming Grant awarded to Danai Dima by City, University of London. Vasileios Ioakeimidis is funded by a City, University of London, PhD studentship.

Conflicts of interest. The authors have no conflicts of interest to report.

References

- Bishop, S. J., Jenkins, R., & Lawrence, A. D. (2007). Neural processing of fearful faces: Effects of anxiety are gated by perceptual capacity limitations. *Cerebral Cortex*, 17, 1595–1603. <https://doi.org/10.1093/cercor/bhl070>
- Bonsaksen, T., Heir, T., Ekeberg, Ø., Grimholt, T. K., Lerdal, A., Skogstad, L., & Schou-Bredal, I. (2019). Self-evaluated anxiety in the Norwegian population: Prevalence and associated factors. *Archives of Public Health*, 77, 1–8. <https://doi.org/10.1186/s13690-019-0338-0>
- Bortolon, C., Capdevielle, D., & Raffard, S. (2015). Face recognition in schizophrenia disorder: A comprehensive review of behavioral, neuroimaging and neurophysiological studies. *Neuroscience & Biobehavioral Reviews*, 53, 79–107. <https://doi.org/10.1016/j.neubiorev.2015.03.006>
- Boudarene, M., & Timsit-Berthier, M. (1997). Stress, anxiety and event related potentials. *Encephale*, 23, 237–250.
- Brocke, B., Tasche, K. G., & Beauducel, A. (1997). Biopsychological foundations of extraversion: Differential effort reactivity and state control. *Personality and Individual Differences*, 21, 727–738. [https://doi.org/10.1016/S0191-8869\(96\)00226-7](https://doi.org/10.1016/S0191-8869(96)00226-7)
- Bruder, G. E., Kayser, J., Tenke, C. E., Leite, P., Schneier, F. R., Stewart, J. W., & Quitkin, F. M. (2002). Cognitive ERPs in depressive and anxiety disorders during tonal and phonetic oddball tasks. *Clinical EEG and Neuroscience*, 22, 119–124. <https://doi.org/10.1177/155005940203300308>
- Carbon, C. C. (2014). Understanding human perception by human-made illusions. *Frontiers in Human Neuroscience*. <https://doi.org/10.3389/fnhum.2014.00566>
- Caspi, A., Houts, R. M., Belsky, D. W., & Goldman-mellor, S. J. (2015). The p factor: One general psychopathology factor in the structure of psychiatric disorders? *Clinical Psychology Science*, 2, 119–137. <https://doi.org/10.1177/2167702613497473>
- Corrow, S., Granrud, C. E., Mathison, J., & Yonas, A. (2011). Six-month-old infants perceive the hollow-face illusion. *Perception*, 40, 1376–1383. <https://doi.org/10.1068/p7110>
- Coulson, S., King, J. W., & Kutas, M. (1998). Expect the unexpected: Event-related brain response to morphosyntactic violations. *Language and Cognitive Processes*, 13, 21–58. <https://doi.org/10.1080/016909698386582>
- Cowles, M., & Hogg, L. (2019). An experimental investigation into the effect of state-anxiety on state-paranoia in people experiencing psychosis. *Behavioural and Cognitive Psychotherapy*, 47, 52–66. <https://doi.org/10.1017/S1352465818000401>
- De Pascalis, V., Strippoli, E., Riccardi, P., & Vergari, F. (2004). Personality, event-related potential (ERP) and heart rate (HR) in emotional word processing. *Personality and Individual Differences*, 36, 873–891. [https://doi.org/10.1016/S0191-8869\(03\)00159-4](https://doi.org/10.1016/S0191-8869(03)00159-4)
- Dima, D., Dietrich, D. E., Dillo, W., & Emrich, H. M. (2010). Impaired top-down processes in schizophrenia: A DCM study of ERPs. *NeuroImage*, 52, 824–832. <https://doi.org/10.1016/j.neuroimage.2009.12.086>
- Dima, D., Dillo, W., Bonnemann, C., Emrich, H. M., & Dietrich, D. E. (2011). Reduced P300 and P600 amplitude in the hollow-mask illusion in patients with schizophrenia. *Psychiatry Research – Neuroimaging*, 191, 145–151. <https://doi.org/10.1016/j.psychres.2010.09.015>
- Dima, D., Roiser, J. P., Dietrich, D. E., Bonnemann, C., Lanfermann, H., Emrich, H. M., & Dillo, W. (2009). Understanding why patients with schizophrenia do not perceive the hollow-mask illusion using dynamic causal modelling. *NeuroImage*, 46, 1180–1186. <https://doi.org/10.1016/j.neuroimage.2009.03.033>
- Eagleman, D. M. (2001). Visual illusions and neurobiology. *Nature Reviews Neuroscience*, 2, 920–926. <https://doi.org/10.1038/35104092>
- Eysenck, M. W. (1997). Anxiety and cognition: A unified theory. London: Psychology Press/Erlbaum (UK) Taylor & Francis.
- Farkas, A., Papathomas, T. V., Silverstein, S. M., Kourtev, H., & Papayanopoulos, J. F. (2016). Dynamic 3-D computer graphics for designing a diagnostic tool for patients with schizophrenia. *Visual Computer*, 32, 1499–1506. <https://doi.org/10.1007/s00371-015-1152-5>
- Foot, M., & Koszycki, D. (2004). Gender differences in anxiety-related traits in patients with panic disorder. *Depression and Anxiety*, 20, 123–130. <https://doi.org/10.1002/da.20031>
- Freeman, D., & Fowler, D. (2009). Routes to psychotic symptoms: Trauma, anxiety and psychosis-like experiences. *Psychiatry Research*, 169, 107–112. <https://doi.org/10.1016/j.psychres.2008.07.009>
- Fucci, E., Abdoun, O., & Lutz, A. (2019). Auditory perceptual learning is not affected by anticipatory anxiety in the healthy population except for highly anxious individuals: EEG evidence. *Clinical Neurophysiology*, 130, 1135–1143. <https://doi.org/10.1016/j.clinph.2019.04.010>
- Georgeson, M. A. (1979). Random-dot stereograms of real objects: Observations on stereo faces and moulds. *Perception*, 8, 585–588. <https://doi.org/10.1068/p080585>
- Giraudet, L., St-Louis, M. E., Scannella, S., & Causse, M. (2015). P300 event-related potential as an indicator of inattentive deafness? *PLoS ONE*, 10. <https://doi.org/10.1371/journal.pone.0118556>
- Gratton, G., Bosco, C. M., Kramer, A. F., Coles, M. G. H., Wickens, C. D., & Donchin, E. (1990). Event-related brain potentials as indices of information extraction and response priming. *Electroencephalography and Clinical Neurophysiology*, 75, 419–432. [https://doi.org/10.1016/0013-4694\(90\)90087-Z](https://doi.org/10.1016/0013-4694(90)90087-Z)
- Gregory, R. L. (1973). The confounded eye. In R. L. Gregory & E. H. Gombrich (Eds.), *Illusion in nature and art* (pp. 49–96). London: Duckworth.
- Guillem, F., Pampoulova, T., Stip, E., Lalonde, P., & Todorov, C. (2005). The relationships between symptom dimensions and dysphoria in schizophrenia. *Schizophrenia Research*, 75, 83–96. <https://doi.org/10.1016/j.schres.2004.06.018>
- Gunter, T. C., Stowe, L. A., & Mulder, G. (1997). When syntax meets semantics. *Psychophysiology*, 34, 660–676.
- Gupta, T., Silverstein, S. M., Bernard, J. A., Keane, B. P., Papathomas, T. V., Pelletier-Baldelli, A., ... Mittal, V. A. (2016). Disruptions in neural connectivity associated with reduced susceptibility to a depth inversion illusion in youth at ultra high risk for psychosis. *NeuroImage: Clinical*, 12, 681–690. <https://doi.org/10.1016/j.nicl.2016.09.022>
- Hayes, J. F., Osborn, D. P. J., Lewis, G., Dalman, C., & Lundin, A. (2017). Association of late adolescent personality with risk for subsequent serious mental illness among men in a Swedish nationwide cohort study. *JAMA Psychiatry*, 74, 703–711. <https://doi.org/10.1001/jamapsychiatry.2017.0583>
- Hetteema, J. M., Neale, M. C., Myers, J. M., Prescott, C. A., & Kendler, K. S. (2006). A Population-based twin study of the relationship between neuroticism and internalizing disorders. *American Journal of Psychiatry*, 163, 857–864. <https://doi.org/10.1176/ajp.2006.163.5.857>
- Hill, H., & Bruce, V. (1993). Independent effects of lighting, orientation, and stereopsis on the hollow-face illusion. *Perception*, 22, 887–897. <https://doi.org/10.1068/p220887>
- Hill, H., & Johnston, A. (2007). The hollow-face illusion: Object-specific knowledge, general assumptions or properties of the stimulus? *Perception*, 36, 199–223. <https://doi.org/10.1068/p5523>

- Jansen, L. M. C., Gispens-de Wied, C. C., & Kahn, R. S. (2000). Selective impairments in the stress response in schizophrenic patients. *Psychopharmacology*, 149, 319–325. <https://doi.org/10.1007/s002130000381>
- Javanbakht, A., Liberzon, I., Amirsadri, A., Gjini, K., & Boutros, N. N. (2011). Event-related potential studies of post-traumatic stress disorder: A critical review and synthesis. *Biology of Mood & Anxiety Disorders*, 1, 5. <https://doi.org/10.1186/2045-5380-1-5>
- Jeronimus, B. F., Kotov, R., Riese, H., & Ormel, J. (2016). Neuroticism's prospective association with mental disorders halves after adjustment for baseline symptoms and psychiatric history, but the adjusted association hardly decays with time: A meta-analysis on 59 longitudinal/prospective studies with 443 313 participants. *Psychological Medicine*, 46, 2883–2906. <https://doi.org/10.1017/S0033291716001653>
- Kaan, E., & Swaab, T. Y. (2003). Repair, revision, and complexity in syntactic analysis: An electrophysiological differentiation. *Journal of Cognitive Neuroscience*, 15, 98–110. <https://doi.org/10.1162/089892903321107855>
- Khan, A. A., Jacobson, K. C., Gardner, C. O., Prescott, C. A., & Kendler, K. S. (2005). Personality and comorbidity of common psychiatric disorders. *British Journal of Psychiatry*, 186, 190–196. <https://doi.org/10.1192/bjp.186.3.190>
- King, D. J., Hodgekings, J., Chouinard, P. A., Chouinard, V.-A., & Sperandio, I. (2017). A review of abnormalities in the perception of visual illusions in schizophrenia. *Psychonomic Bulletin & Review*, 24, 734–751. <https://doi.org/10.3758/s13423-016-1168-5>
- Kok, A. (1988). Probability mismatch and template mismatch: A paradox in P300 amplitude? *Behavioral and Brain Sciences*, 11, 388–389. <https://doi.org/10.1017/S0140525X00058143>
- Król, M., & El-Deredy, W. (2015). The clash of expectancies: Does the P300 amplitude reflect both passive and active expectations? *Quarterly Journal of Experimental Psychology*, 68, 1723–1724. <https://doi.org/10.1080/17470218.2014.996166>
- Leweke, F. M., Schneider, U., Radwan, M., Schmidt, E., & Emrich, H. M. (2000). Different effects of nabilone and cannabidiol on binocular depth inversion in man. *Pharmacology Biochemistry and Behavior*, 66, 175–181. [https://doi.org/10.1016/S0091-3057\(00\)00201-X](https://doi.org/10.1016/S0091-3057(00)00201-X)
- Li, Y., Wang, W., Liu, T., Ren, L., Zhou, Y., Yu, C., ... Hu, Y. (2015). Source analysis of P3a and P3b components to investigate interaction of depression and anxiety in attentional systems. *Scientific Reports*, 5, 17138. <https://doi.org/10.1038/srep17138>
- Luck, S. T. (2014). *An introduction to the event-related potential technique*. 2nd edition. Cambridge, MA: MIT Press.
- Mathews, A., & Mackintosh, B. (1998). A cognitive model of selective processing in anxiety. *Cognitive Therapy and Research*, 22, 539–560. <https://doi.org/10.1023/A:1018738019346>
- McCrae, R., & Costa, P. (1992). An introduction to the five-factor model and its applications. *Journal of Personality*, 60, 175–215. <https://doi.org/10.1111/j.1467-6494.1992.tb00970.x>
- McCrae, R. R., & Costa, P. T., Jr. (1997). Personality trait structure as a human universal. *American Psychologist*, 52, 509–516. <https://doi.org/10.1037/0003-066X.52.5.509>
- Meijer, J. (2001). Stress in the relation between trait and state anxiety. *Psychological Reports*, 88, 947–964. <https://doi.org/10.2466/pr0.2001.88.3c.947>
- Muller, J. E., Koen, L., Seedat, S., Emsley, R. A., & Stein, D. J. (2004). Anxiety disorders and schizophrenia. *Current Psychiatry Reports*, 6, 255–261. <https://doi.org/10.1007/s11920-004-0074-0>
- Naumann, E., Bartussek, D., Diedrich, O., & Laufer, M. E. (1992). Assessing cognitive and affective information processing functions of the brain by means of the late positive complex of the event-related potential. *Journal of Psychophysiology*, 6, 285–298.
- Ohi, K., Shimada, T., Nitta, Y., Kihara, H., Okubo, H., Uehara, T., & Kawasaki, Y. (2016). The Five-Factor Model personality traits in schizophrenia: A meta-analysis. *Psychiatry Research*, 240, 34–41. <https://doi.org/10.1016/j.psychres.2016.04.004>
- Pacheco-Unguetti, A. P., Acosta, A., Callejas, A., & Lupiáñez, J. (2010). Attention and anxiety: Different attentional functioning under state and trait anxiety. *Psychological Science*, 21, 298–304. <https://doi.org/10.1177/0956797609359624>
- Papageorgiou, C. C., & Rabavilas, A. D. (2003). Abnormal P600 in obsessive-compulsive disorder. A comparison with healthy controls. *Psychiatry Research*, 119, 133–143. [https://doi.org/10.1016/S0165-1781\(03\)00109-4](https://doi.org/10.1016/S0165-1781(03)00109-4)
- Papathomas, T. V., & Bono, L. M. (2004). Experiments with a hollow mask and a reverspective: Top-down influences in the inversion effect for 3-D stimuli. *Perception*, 33, 1129–1138. <https://doi.org/10.1068/p5086>
- Passie, T., Schneider, U., Borsutzky, M., Breyer, R., Emrich, H. M., Bandelow, B., & Schmid-Ott, G. (2013). Impaired perceptual processing and conceptual cognition in patients with anxiety disorders: A pilot study with the binocular depth inversion paradigm. *Psychology, Health & Medicine*, 18, 363–374. <https://doi.org/10.1080/13548506.2012.722649>
- Polich, J. (1987). Task difficulty, probability, and inter-stimulus interval as determinants of P300 from auditory stimuli. *Electroencephalography and Clinical Neurophysiology/Evoked Potentials*, 68, 311–320. [https://doi.org/10.1016/0168-5597\(87\)90052-9](https://doi.org/10.1016/0168-5597(87)90052-9)
- Polich, J. (2007). Updating P300: An integrative theory of P3a and P3b. *Clinical Neurophysiology*, 118, 2128–2148. <https://doi.org/10.1016/j.clinph.2007.04.019>
- Polich, J., & Kok, A. (1995). Cognitive and biological determinants of P300: An integrative review. *Biological Psychology*, 41, 103–146. [https://doi.org/10.1016/0301-0511\(95\)05130-9](https://doi.org/10.1016/0301-0511(95)05130-9)
- Reeb-Sutherland, B. C., Vanderwert, R. E., Degnan, K. A., Marshall, P. J., Pérez-Edgar, K., Chronis-Tuscano, A., ... Fox, N. A. (2009). Attention to novelty in behaviorally inhibited adolescents moderates risk for anxiety. *Journal of Child Psychology and Psychiatry*, 50, 1365–1372. <https://doi.org/10.1111/j.1469-7610.2009.02170.x>
- Rugg, M. D., Mark, R. E., Walla, P., Schloerscheidt, A. M., Birch, C. S., & Allan, K. (1998). Dissociation of the neural correlates of implicit and explicit memory. *Nature*, 392, 595–598. <https://doi.org/10.1038/33396>
- Schneider, U., Borsutzky, M., Seifert, J., Leweke, F. M., Huber, T. J., Rollnik, J. D., & Emrich, H. M. (2002). Reduced binocular depth inversion in schizophrenic patients. *Schizophrenia Research*, 53, 101–108. [https://doi.org/10.1016/S0920-9964\(00\)00172-9](https://doi.org/10.1016/S0920-9964(00)00172-9)
- Schneider, U., Leweke, F. M., Niemczyk, W., Sternemann, U., Bevilacqua, M., & Emrich, H. M. (1996). Impaired binocular depth inversion in patients with alcohol withdrawal. *Journal of Psychiatric Research*, 30, 469–474. [https://doi.org/10.1016/S0022-3956\(96\)00031-3](https://doi.org/10.1016/S0022-3956(96)00031-3)
- Semple, D. M., Ramsden, F., & McIntosh, A. M. (2003). Reduced binocular depth inversion in regular cannabis users. *Pharmacology Biochemistry and Behavior*, 75, 789–793. [https://doi.org/10.1016/S0091-3057\(03\)00140-0](https://doi.org/10.1016/S0091-3057(03)00140-0)
- Sheehan, D. V., Lecrubier, Y., Sheehan, K. H., Amorim, P., Janavs, J., Weiller, E., ... Dunbar, G. C. (1998). The Mini-International Neuropsychiatric Interview (M.I.N.I.): The development and validation of a structured diagnostic psychiatric interview for DSM-IV and ICD-10. *Journal of Clinical Psychiatry*, 59, 22–23.
- Smith, M. E. (1993). Neurophysiological manifestations of recollective experience during recognition memory judgments. *Journal of Cognitive Neuroscience*, 5, 1–13. <https://doi.org/10.1162/jocn.1993.5.1.1>
- Spielberger, C. D., Gorsuch, R. L., Lushene, R., Vagg, P. R., Jacobs, G. A. (1983). *Manual for the state-trait anxiety inventory*. Palo Alto, CA: Consulting Psychologists Press
- Stelmack, R. M., Houlihan, M., & McGarry-Roberts, P. A. (1993). Personality, reaction time, and event-related potentials. *Journal of Personality and Social Psychology*, 65, 399–409. <https://doi.org/10.1037//0022-3514.65.2.399>
- Sternemann, U., Schneider, U., Leweke, F. M., Bevilacqua, C. M., Dietrich, D. E., & Emrich, H. M. (1997). Pro-psychotic change of binocular depth inversion by sleep deprivation. *Der Nervenarzt*, 68, 593–596. <https://doi.org/10.1007/s001150050167>
- Temmingh, H., & Stein, D. J. (2015). Anxiety in patients with schizophrenia: Epidemiology and management. *CNS Drugs*, 29, 819–832. <https://doi.org/10.1007/s40263-015-0282-7>
- Towey, J. P., Tenke, C. E., Bruder, G. E., Leite, P., Friedman, D., Liebowitz, M., & Hollander, E. (1994). Brain event-related potential correlates of overfocused attention in obsessive-compulsive disorder. *Psychophysiology*, 31, 535–543. <https://doi.org/10.1111/j.1469-8986.1994.tb02346.x>
- Van den Enden, A., & Spekrijse, H. (1989). Binocular depth reversals despite familiarity cues. *Science*, 244, 959–961. <https://doi.org/10.1126/science.2382135>

- Van Os, J., & Jones, P. B.** (2001). Neuroticism as a risk factor for schizophrenia. *Psychological Medicine*, *31*, 1129–1134. <https://doi.org/10.1017/S0033291701004044>
- Wheatstone, C.** (1838). Contributions to the physiology of vision: I. On some remarkable, and hitherto unobserved, phenomena of binocular vision. *Philosophical Transactions of the Royal Society London*, *128*, 371–394.
- Wheatstone, C.** (1852). Contributions to the physiology of vision: II. On some remarkable, and hitherto unobserved, phenomena of binocular vision (continued). *Philosophical Transactions of the Royal Society London*, *142*, 1–17.
- Wilding, E. L., Doyle, M. C., & Rugg, M. D.** (1995). Recognition memory with and without retrieval of context: An event-related potential study. *Neuropsychologia*, *33*, 1–25. [https://doi.org/10.1016/0028-3932\(95\)00017-W](https://doi.org/10.1016/0028-3932(95)00017-W)
- Wilding, E. L., & Rugg, M. D.** (1996). An event-related potential study of recognition memory with and without retrieval of source. *Brain*, *119*, 889–905. <https://doi.org/10.1093/brain/119.3.889>
- Williams, J. M. G., Watts, F. N., MacLeod, C. M., & Mathews, A.** (1997). Cognitive psychology and emotional disorders. In *The Wiley series in clinical psychology*.

A Meta-analysis of Structural and Functional Brain Abnormalities in Early-Onset Schizophrenia

Vasileios Ioakeimidis^{1,*}, Corinna Haenschel¹, Kielan Yarrow¹, Marinos Kyriakopoulos^{2,3}, and Danai Dima^{*1,4}

¹Department of Psychology, School of Arts and Social Sciences, City, University of London, London, UK; ²National and Specialist Acorn Lodge Inpatient Children Unit, South London & Maudsley NHS Trust, London, UK; ³Department of Child and Adolescent Psychiatry, Institute of Psychiatry, Psychology and Neuroscience, King's College London, London, UK; ⁴Department of Neuroimaging, Institute of Psychiatry, Psychology and Neuroscience, King's College London, London, UK

*To whom correspondence should be addressed; Department of Psychology, School of Arts and Social Sciences, City, University of London, 10 Northampton Square, London EC1V 0HB, UK; tel: +44-(0)20-7040-0125, e-mail: danai.dima@city.ac.uk

Early-onset schizophrenia (EOS) patients demonstrate brain changes that are similar to severe cases of adult-onset schizophrenia. Neuroimaging research in EOS is limited due to the rarity of the disorder. The present meta-analysis aims to consolidate MRI and functional MRI findings in EOS. Seven voxel-based morphometry (VBM) and 8 functional MRI studies met the inclusion criteria, reporting whole-brain analyses of EOS vs healthy controls. Activation likelihood estimation (ALE) was conducted to identify aberrant anatomical or functional clusters across the included studies. Separate ALE analyses were performed, first for all task-dependent studies (Cognition ALE) and then only for working memory ones (WM ALE). The VBM ALE revealed no significant clusters for gray matter volume reductions in EOS. Significant hypoactivations peaking in the right anterior cingulate cortex (rACC) and the right temporoparietal junction (rTPJ) were detected in the Cognition ALE. In the WM ALE, consistent hypoactivations were found in the left precuneus (IPreC), the right inferior parietal lobule (rIPL) and the rTPJ. These hypoactivated areas show strong associations with language, memory, attention, spatial, and social cognition. The functional co-activated networks of each suprathreshold ALE cluster, identified using the BrainMap database, revealed a core co-activation network with similar topography to the salience network. Our results add support to posterior parietal, ACC and rTPJ dysfunction in EOS, areas implicated in the cognitive impairments characterizing EOS. The salience network lies at the core of these cognitive processes, co-activating with the hypoactivating regions, and thus highlighting the importance of salience dysfunction in EOS.

Key words: activation likelihood estimation/working memory/salience/psychosis/neurodevelopment/fMRI

Introduction

Early-onset schizophrenia (EOS) is a rare and severe form of schizophrenia which has its onset before early adulthood. Research usually distinguishes between childhood- and adolescent-onset cases; the former considering diagnoses up to 13 and the latter from 13 to 18 years old.¹ In this article, the term EOS encompasses both childhood- and adolescent-onset schizophrenia and is used as an umbrella term for all diagnosed cases of schizophrenia up to 18 years of age. Schizophrenia is diagnosed in 1% of the worldwide population,² but epidemiological findings for EOS suggest a rate of prevalence in less than 5% of all schizophrenia cases,³ making the literature for the disorder scarce. EOS patients have higher premorbid developmental and social deficits, more hospitalizations, and poorer psychosocial outcomes compared to adult schizophrenia patients.⁴ Like adult schizophrenia, EOS is characterized by diverse symptomatology, which includes the presence of positive and negative symptoms, along with cognitive impairments. Cognitive processes that are affected include working memory (WM),⁵ attention,⁶ and processing of salience.⁷

Regional gray matter volume loss and cortical thinning in EOS, although inconsistent, has been reported in numerous brain areas; these are seen bilaterally in the ventral prefrontal cortex, dorsolateral prefrontal cortex, superior parietal cortex (SPL), middle temporal gyrus, inferior temporal gyrus, thalamus, and the cerebellum; whereas left-sided reductions have been observed in the anterior cingulate cortex (ACC), paracingulate gyrus, cuneus, precuneus (PreC), and superior temporal gyrus (STG).^{1,8} EOS patients also demonstrate decreased insular volumes.⁹ Other findings in EOS include sensorimotor

areas, namely the right pre- and post-central gyri, the SMA and pre-SMA areas.¹⁰ Juuhl-Langseth et al,¹¹ found subcortical volume increases in the ventricles and bilaterally in the caudate, but no other differences were detected. However, a recent meta-analysis on longitudinal volumetric changes in early-onset psychosis has identified only frontal gray matter loss,¹² whereas only frontal lobe gray matter decreases were found in a different study.¹³ Reduced gray matter thickness was found bilaterally in the anterior midcingulate gyrus and sulcus, the insula, and the middle frontal sulci, as well as in the left hemisphere in superior temporal, the parietooccipital, the post-central and superior frontal sulci.¹⁴ Right hemisphere cortical thickness reductions were observed in the posterior midcingulate gyrus and sulcus, sub-parietal sulcus, the STG, and inferior frontal gyrus. Longitudinal studies have revealed that the cortical reductions observed in EOS are dynamically spreading during adolescence and follow a back-to-front and top-to-bottom pattern¹⁵; the medial frontal wall is affected early, whereas the ACC volume decreases later on.¹⁶ Thompson et al¹⁷ reported that the accelerated pattern of gray matter loss in an EOS sample is not a medication-related side effect and begins in parietal and motor areas, with reductions in superior and dorsolateral frontal cortices and temporal regions following later in adolescence.

Correspondingly, gray matter volume decreases in adult-onset schizophrenia that converge meta-analytically across studies include bilaterally the insula, the thalamus, the ACC (ventral, dorsal, and subgenual), and the left parahippocampal gyrus, post-central gyrus and middle frontal gyrus.¹⁸ A more recent meta-analysis of schizophrenia by the ENIGMA consortium also found bilateral decreases of cortical thickness in the fusiform gyrus, the inferior temporal gyrus, the cingulate cortex, the STG and the superior temporal sulcus, and lateralized reductions included the right inferior frontal gyrus and right posterior cingulate cortex, whereas left-hemisphere thickness decreases were found on the middle temporal gyrus and lateral orbitofrontal cortex.¹⁹ van Erp et al,¹⁹ also found cortical thickness increases in the SPL, PreC and paracentral lobule bilaterally, and right-side increases in the inferior parietal lobule (IPL), the rostral ACC and precentral gyrus.

Schizophrenia is characterized by cognitive deficits, especially in WM⁵ and attentional processing,⁶ linked with aberrant activation of their neural substrates. EOS patients demonstrate impairments in change detection²⁰ that are dependent on ACC and STG activity²¹ and are associated with positive symptoms.²⁰ Furthermore, WM-related dysfunction in schizophrenia is tied to reduced activity in the prefrontal cortex, which is more specific to an encoding malfunction.²² However, there are inconsistent reports revealing cases of prefrontal²³ and anterior cingulate^{24,25} hyperactivation in EOS and adult schizophrenia. Correspondingly, increasing WM load

predicts suppression deficiency in the medial frontal and bilateral posterior parietal cortices in EOS²⁶ and such suppression reduction is associated with WM capacity deficits.²⁷ Reduced activity during WM performance is also shown in the temporoparietal junction (TPJ)^{22,28} as well as the ACC.^{28,29} WM encoding deficits are further associated with functional connectivity disruptions between the ACC and the temporal lobes.³⁰ ACC- and TPJ-related dysfunction in EOS has also been observed during emotional,³¹ language processing,³² as well as change detection²¹ tasks.

In the present study, we used the activation likelihood estimation (ALE) meta-analysis method, a coordinate-based meta-analytic technique, using the available voxel-based morphometry (VBM) and task-dependent functional magnetic resonance imaging (fMRI) literature in EOS. To our knowledge, this is the first coordinate-based meta-analysis for the VBM and fMRI literature in EOS and we sought to identify brain areas with gray matter volume abnormalities and aberrant activation that converge across studies. In addition, we conducted post hoc analyses using meta-data from a large-scale neuroimaging database (BrainMap) to decode any cognitive correlates that associate with these brain areas and to identify functional networks that embed these areas in the healthy population. The overarching goal of the study was to draw inferences about the structural, functional cognitive and connectivity profiles of brain dysfunction that lies in EOS.

Methods

Literature Search and Study Selection

We conducted a systematic PubMed search to identify all neuroimaging studies on EOS up to January 2020, using the PRISMA guidelines.³³ The search was performed by 2 independent investigators using the following set of keywords:

“(schizophrenia [Title/Abstract]) AND (early onset schizophrenia OR childhood onset schizophrenia OR adolescent onset schizophrenia) AND (VBM [Title/Abstract] OR fMRI [Title/Abstract] OR magnetic resonance imaging [Title/Abstract] OR MRI [Title/Abstract] OR voxel based morphometry [Title/Abstract] OR cortical thickness [Title/Abstract])”

This process returned a total of 530 abstracts that were initially screened for inclusion. Studies were included if they: (1) were conducted in an EOS sample with age-of-illness onset (AIO) below 18 years old, (2) employed whole-brain analysis using VBM or fMRI, and (3) presented group comparisons of EOS and healthy controls (HC). Full-text review of the pre-selected studies was followed to determine eligibility. Studies were excluded if they: (1) did not report coordinate data on standard stereotactic space, (2) performed region-of-interest (ROI)

or small-volume correction analyses, (3) did not report second-level analysis of case-control contrasts, (4) analyzed samples reported by a previous study, (5) were longitudinal studies but did not report cross-sectional contrasts, (6) were case-studies, or (7) were resting-state fMRI studies. Whole-brain analyses were preferred over seed-based ones, that were excluded to eliminate risk-of-bias.^{34,35} Figure 1 displays the flow diagram of the search and selection process.

Database Construction

The complete selection process yielded a total of 15 whole-brain analysis studies that met criteria and reached consensus by 2 researchers (supplementary table S1). These were then divided into VBM and fMRI, with 7 and 8 studies, respectively (figure 1). For each of the studies, we extracted data on sample size, participants' mean age, and sex. For the patients, we also extracted AIO and duration of illness, mean and SD of symptom severity as well as chlorpromazine equivalents, where available (supplementary table S1).

We use the term “study” to refer to each published article and “experiment” to reflect a single contrast or analysis. For all experiments, we recorded all foci with significant case-control differences and their respective *P*-values and peak coordinates, as well as the direction of the signal change compared to the control group. For each fMRI study, we also recorded the experimental design and type of task. Coordinates reported in the Talairach & Tournoux³⁶ space were transformed into MNI³⁷ space.

Together the VBM studies included 7 experiments (or contrasts), from which only the HC > EOS contrast yielded significant differences, which located around 37 anatomical foci. The fMRI studies revealed 147 foci obtained from 36 cognitive experiments. These were then separated into HC > EOS contrasts (EOS hypoactivations; 22 experiments and 98 foci) and EOS > HC contrasts (EOS hyperactivations; 14 experiments and 49 foci). The fMRI studies were further organized into WM-only experiments, which yielded 15 experiments and 55 foci for EOS hypoactivation and 10 experiments and 35 foci for EOS hyperactivations (supplementary table S2). In the analysis, we only included coordinate

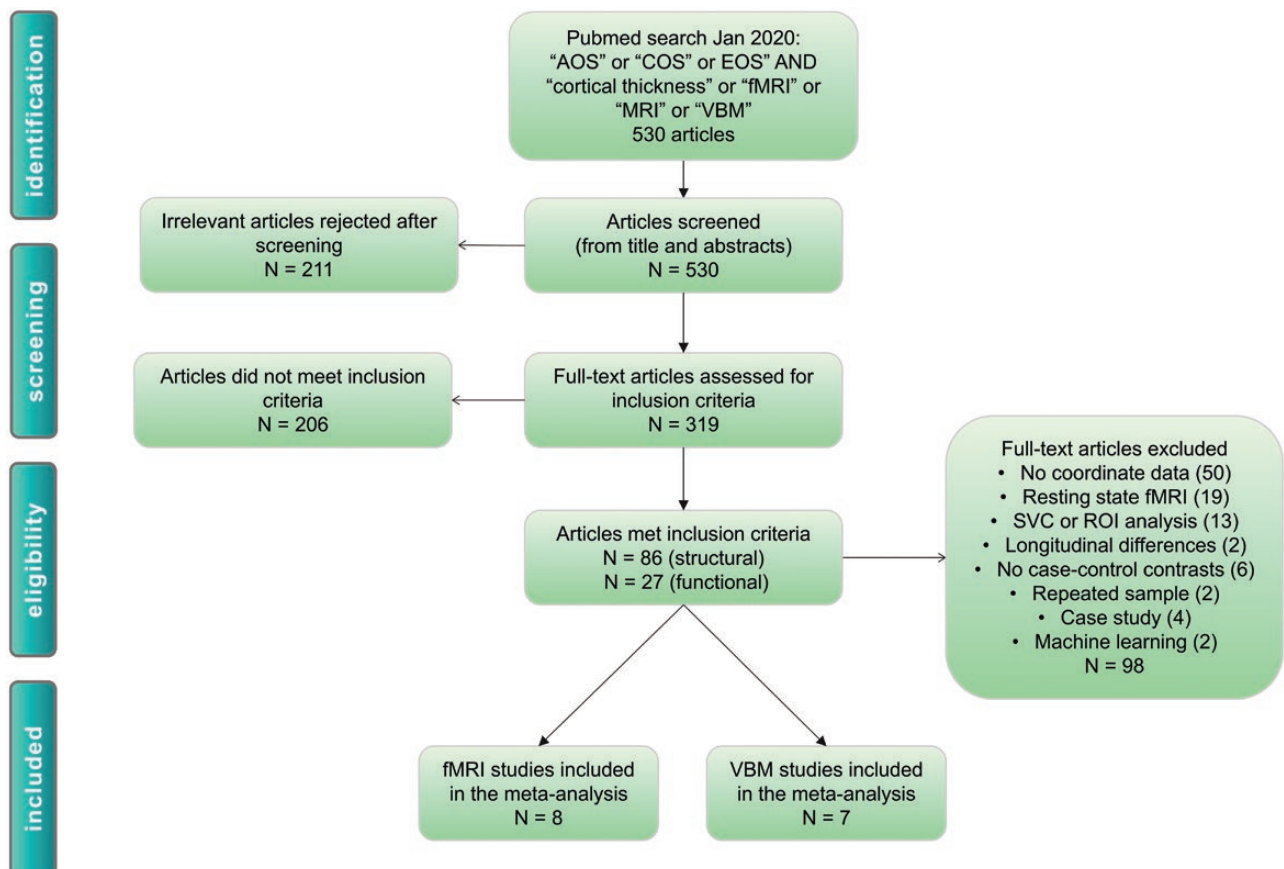


Fig. 1. Preferred Reporting Items for Systematic Reviews and Meta-Analyses (PRISMA) flowchart shows the detailed selection process of the studies used in the voxel-based morphometry (VBM) and functional magnetic resonance imaging (fMRI) meta-analyses. AOS (adolescent-onset schizophrenia); COS (childhood-onset schizophrenia); EOS (early-onset schizophrenia); SVC (small-volume correction); ROI (region-of-interest analysis).

data shown in case-control comparisons. To control for within-group effects, datasets were conservatively organized “per subject group” instead of “per experiment,” to avoid inflating the contribution of studies with more than one experiments and retain more balanced distribution of contributing foci from each study.³⁸

Activation Likelihood Estimation

All statistical analyses were carried out separately for the VBM and fMRI experiments following the same procedure. We used the revised version of the ALE algorithm^{39,40} implemented in GingerALE version 2.3.6³⁸ (www.brainmap.org/ale) to identify clusters of convergent activation across experiments. For more information on the method, please see [supplementary material](#). Within the fMRI studies, we performed separate ALE studies, one for all cognitive experiments (Cognition ALE) and the other, including only the working memory (WM ALE) ones. To correct for multiple comparisons, we applied a cluster-level FWE correction at $P < .05$ with a cluster-forming threshold of $P < .01$.^{41,42}

Follow-up Analyses for fMRI ALE

Meta-analytic Co-activation Modeling. Meta-analytic co-activation modeling (MACM) is a meta-analytic technique that investigates significant whole-brain task-dependent co-activation patterns of user-specified ROI.^{43,44} MACM allows one to make inferences about functional connectivity between the ROIs (seeds) and the rest of the brain.⁴⁵ The suprathreshold clusters of convergent activation from our ALE studies were used as seeds in the search criteria of the BrainMap database. In our study, this technique allowed the exploration of the networks which our ALE suprathreshold clusters (2 resulting from the Cognitive ALE and 3 from the WM ALE) co-activate, and subsequently could point to a network dysfunction.

First, ROI images of the clusters were created in Mango (<http://ric.uthscsa.edu/mango/>) and then used as seeds separately in Sleuth 2.4 (<http://brainmap.org/sleuth>),^{46,47} to identify fMRI experiments in the BrainMap database reporting at least one focus of activation within the respective seed in healthy controls. The resulting co-activation foci from each seed-search were exported into separate datasets and a single ALE analysis was performed for each dataset. A threshold of voxel-level FWE at 0.05 was applied, with a minimum cluster volume of 50 mm³ for all co-activation maps of each of our ROIs.⁴⁸

Secondly, the resultant voxel-level FWE thresholded functional connectivity (ie, MACM) maps for each seed were used in conjunction analyses to find where these maps overlap using the minimum statistic method.⁴⁹ We explored the conjunction across significantly co-activating brain regions resulting from the cognition ALE and WM ALE separately. This method was chosen to locate the

core network that was formed by the impaired ALE clusters in EOS.

Cognitive Associations. Finally, we explored the cognitive associations of our significantly impaired clusters in EOS that resulted from our Cognition and WM ALE studies. This procedure helped elucidate the roles of these clusters in cognition in the healthy population. We explored these cognitive associations by using the BrainMap meta-data that provides information on the *behavioral domains* of each neuroimaging experiment included in the database.⁴⁶ For more information, refer to the [supplementary material](#).

We used the contingency table approach to calculate the odds ratio of finding a behavioral domain given activation within a particular ROI relative to finding that same behavioral domain given activation elsewhere in the brain, similar to the reverse inference approach.⁵⁰ The benefit of the reverse inference method is that it allows us to assign multiple mental processes to a certain ROI⁵¹ instead of associating only a single function to a brain region as in the classical forward inference method.⁵² Significance was assessed with Fisher’s exact test and was corrected for multiple comparisons using the false discovery rate (FDR).⁵³

Results

The initial search returned 530 articles, of which 319 full-text articles were assessed for eligibility and 15 were retained for the quantitative meta-analysis, 7 of them for the VBM meta-analysis, and 8 for the task-dependent fMRI ([figure 1](#)).

VBM

Study Sample and Characteristics. The VBM meta-analysis returned a sample of 194 EOS individuals (58% male) with range of sub-sample mean ages from 15.4 to 16.9 and range of mean AIO 14.9–16.5 (3 studies had AIO < 18 but did not report the mean). The HC sample size was 254 (HC; 61% male) with range of mean ages 15.4–16.8 ([supplementary table S1](#)). The HC > EOS study included contrasts from all 7 experiments; however, no studies reported EOS > HC contrasts.^{54–60}

Anatomical Likelihood Estimation From VBM Studies. No significant clusters were found at $P < .05$ following cluster-level FWE correction for the contrasts HC > EOS in the VBM studies.

fMRI

Study Sample and Characteristics. The analysis across all functional studies (Cognition ALE) yielded a sample consisting of 148 EOS (69% male) with range of mean age from 13.3 to 21.3 and AIO range 10–16.5 (3 studies

did not mention the AIO but had ages of inclusion below 18 years). The HC sample included 152 individuals (70% male) with range of mean age from 12.8 to 20 years ([supplementary table S1](#)).

The studies with the WM experiments (WM ALE) returned a sample of 122 individuals with EOS (66% male), with range of mean age from 15 to 21.3 years old and AIO range from 10 to 16.5. The HC sample included 126 individuals (67% male) with range of mean age from 15 to 20 years old.

ALE From fMRI Studies

Cognition ALE. The analysis for all cognitive tasks yielded 2 significant clusters of reduced activation in EOS compared to HC ([table 1](#); [figure 2A](#)). One cluster was located at the right anterior cingulate cortex (rACC; $x = 6, y = 38, z = 14$) and the second cluster was located at the right superior temporal gyrus/ temporoparietal junction (rTPJ) ($x = 60, y = -46, z = 20$). No clusters of hyperactivation in EOS survived cluster-level FWE correction.

WM ALE. ALE revealed 3 significant clusters, where EOS individuals showed hypoactivation when engaging in WM tasks. These clusters were found at parietal and temporoparietal areas, with the first peaking at the left SPL/precuneus (lPreC; $x = -22, y = -66, z = 44$). The

second cluster was centered at the right inferior parietal lobule (rIPL; $x = 38, y = -50, z = 46$) and the third at the right supramarginal gyrus/rTPJ ($x = 60, y = -46, z = 22$) ([table 1](#); [figure 2B](#)). No FWE corrected clusters were significant for the EOS > HC contrasts, reflecting hyperactivations in the EOS group. Diagnostics for both the Cognitive and WM ALEs are shown in [supplementary table S3](#).

Follow-up: MACM

As a first follow-up step to our ALE studies, we were interested to investigate whole-brain task-dependent co-activations with the 5 seed-ROIs ([figure 2](#)) identified with the Cognition and WM ALE. The results for each seed are presented separately for the Cognition ALE and WM ALE studies in detail in SM and [supplementary tables S4 and S5](#).

Secondly, clusters forming a conjunction between the MACM maps for the 2 seed-ROIs (rACC and rTPJ) of the Cognition ALE and the 3 seeds (lPreC, rIPL, and rTPJ) from the WM ALE study are shown in [supplementary tables S4 and S5](#), respectively. The core co-activation networks for Cognition ALE and WM ALE resulting from the conjunction analyses were almost identical, with conjunctions bilaterally in the insula and the area of the anterior midcingulate gyrus (aMCC)/medial frontal gyrus ([figure 3](#)).

Table 1. Clusters Showing Significant Convergence of Hypoactivation in EOS

Cluster	Volume (mm ³)	Location	Local Extrema					ALE value (10 ⁻³)
			BA	L/R	x	y	z	
<i>Cognition ALE</i>								
Healthy controls > Early-onset schizophrenia								
1	1752	Anterior cingulate	32	R	6	38	14	9.781
		Cingulate gyrus	32	R	6	28	24	9.531
		Cingulate gyrus	32	R	12	36	22	9.23
		Anterior cingulate	24	L	0	36	14	9.161
		Medial frontal gyrus	6	R	8	34	32	9.063
		Cingulate gyrus	32	L	-2	36	26	8.94
2	1520	Superior temporal gyrus	13	R	60	-46	20	17.758
		Superior temporal gyrus	39	R	60	-56	26	8.899
<i>Working memory ALE</i>								
Healthy controls > Early-onset schizophrenia								
1	2488	Precuneus	7	L	-22	-66	44	16.062
		Middle temporal gyrus	39	L	-28	-56	34	9.312
		Precuneus	7	L	-10	-68	44	9.244
		Angular gyrus	39	L	-30	-60	44	9.187
2	1640	Inferior parietal lobule	40	R	38	-50	46	13.521
		Superior temporal gyrus	39	R	36	-52	36	10.426
3	1448	Supramarginal gyrus	40	R	60	-46	22	10.53
		Inferior parietal lobule	40	R	62	-40	26	9.141
		Superior temporal gyrus	39	R	60	-56	26	8.878

Note: MNI coordinates, $P < .05$ cluster-level FWE. ALE, activation likelihood estimation; BA, Brodmann area; HC, healthy controls; EOS, early-onset schizophrenia.

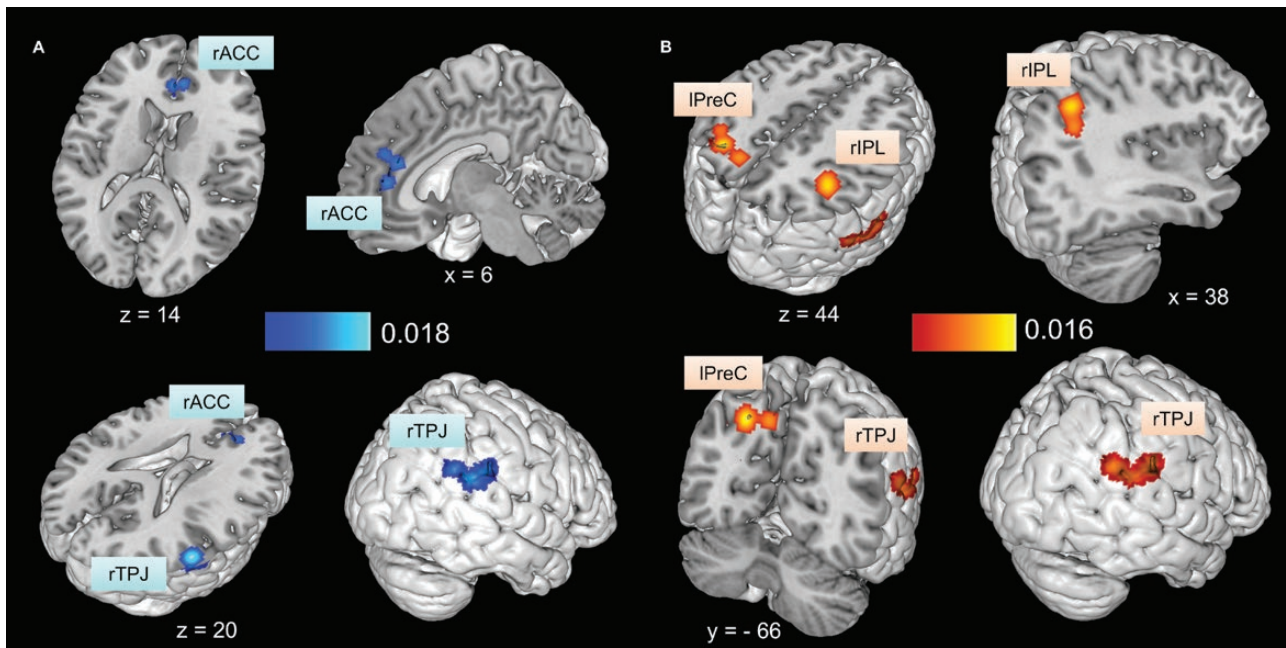


Fig. 2. Clusters of early-onset schizophrenia (EOS) hypoactivation in the Cognition ALE and WM ALE. (A) Significant convergence across all cognitive experiments was found in the ACC and rTPJ for the HC > EOS contrasts. (B) The WM ALE showed significant convergence at the IPreC, rIPL, and rTPJ. Results are cluster-FWE corrected at 0.05 with cluster-forming value at $P < .01$. The same clusters were later used as seed-ROIs for the MACM and functional associations analyses. rACC (right anterior cingulate cortex); rIPL (right inferior parietal lobule); IPreC (left precuneus); rTPJ (right temporoparietal junction); ALE (activation likelihood estimation); WM (working memory); ROI (region-of-interest).

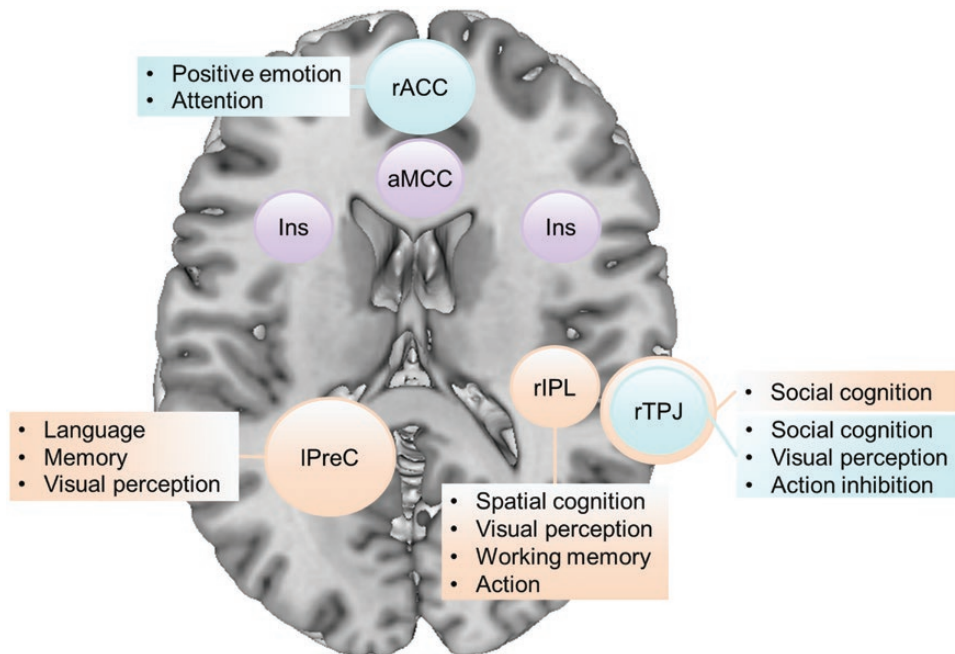


Fig. 3. Schematic representation of the relative positions of the suprathreshold Cognition ALE clusters in blue and WM ALE clusters in orange, with their respective associate behavioral domains. The core network resulting from the conjunction analysis of the respective MACM maps, in purple. Axial brain slice from Colin27_T1_MN1 at $z = 15$. ALE (activation likelihood estimation); WM (working memory)

Follow-up: Cognitive Associations

We were interested to explore the mental processes that show cognitive associations with the significant clusters from our ALE studies.

The rACC ROI that resulted from the Cognition ALE was found to be significantly associated with positive emotion/reward, attention, and broad cognition. The rTPJ ROI revealed a strong and significant association with social cognition and high associations with visual motion perception and action inhibition (figure 4A).

Our ROIs deriving from the WM ALE study showed prevalent cognitive associations with behavioral domains of cognition, perception, and action (figure 4B). More specifically, the IPreC ROI was found to be predominantly associated with language processing (orthography, speech, and phonology), memory, and visual perception. The rIPL ROI was more strongly associated with spatial cognition. Additional cognitive associations were found for motion perception and WM, as well as the broad domain of action. The rTPJ ROI had a single, very strong, and highly significant association with social cognition.

Discussion

In the present study, we investigated structural and functional changes in EOS vs HC using ALE, a coordinate-based meta-analysis method. By doing so, we sought to outline all structural and functional findings in EOS and to establish whether a structural or functional biomarker exists for the disorder. Additionally, we were interested to define brain regions with abnormal function across cognition and during WM performance in the developing brains of EOS patients compared to typically developing controls. We followed up with post hoc analyses that sought to explore task-wide co-activation brain patterns of our ALE-derived clusters within the healthy population and their cognitive associations with behavioral domains. These analyses allowed us to explore the behavioral profile of the affected brain regions and to pinpoint, where the EOS dysfunction lies in terms of functional network connectivity.

VBM

The VBM meta-analysis for gray matter volume reductions returned no significantly convergent clusters

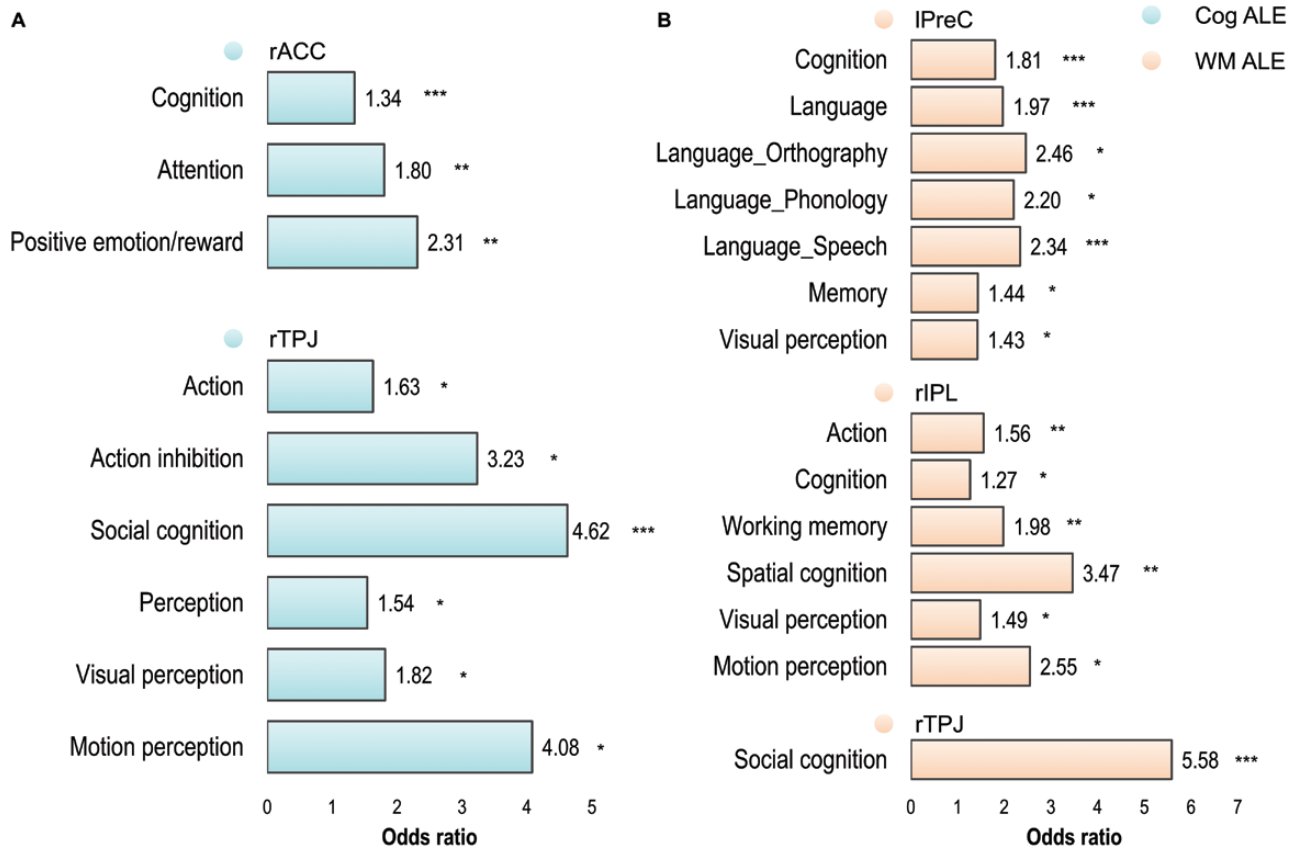


Fig. 4. Cognitive associations for the seed-ROIs resulting from (A) the Cognition ALE in blue and (B) WM ALE in orange. A 2x2 contingency table approach was used along with Fisher's test as a method of reverse inference to determine the odds of detecting a behavioral domain given activation of a certain ROI relative to the odds of detecting it given activation elsewhere in the brain. Only significant (FDR corrected) behavioral domains are presented in bar graphs, with odds of activating the ROI higher than 1. *P < .05; **P < .01; ***P < .001. ALE (activation likelihood estimation); WM (working memory); ROI (region-of-interest).

between controls and EOS patients. This result is consistent with previous studies that failed to demonstrate EOS – HC gray matter differences.^{61,62} However, our result could be due to limited statistical power owing to the very small number of studies ($n = 7$)⁴⁸ that met our inclusion criteria, even though some individual studies have found brain-volume reductions in EOS.⁵⁵ Different brain areas follow different developmental trajectories in controls⁶³ and gray matter volume loss in EOS is dynamic and follows a back-to-front pattern starting in parietal and progressing in temporal and prefrontal regions.¹⁷ Thus, differences in age, duration of illness, AIO, or medication in individual studies could be some of the factors creating variability and contributing to the absence of structural convergence. Alternatively, lack of convergence in the VBM analysis could suggest the EOS brain-volume reduction to be not specific to a particular brain region.

fMRI

ACC. In the Cognition ALE, the ACC and rTPJ were the 2 clusters showing reduced activation in the EOS patients when compared with typically developing controls. Following the post hoc cognitive association analysis, we found the ACC cluster activity to be related with attentional and reward-related processes.

The ACC shows sustained activity during WM delays,⁶⁴ plays a role in conflict monitoring and avoidance learning,⁶⁵ responds to errors,⁶⁶ and drives the reallocation of attentional resources according to task-demands and salience.⁶⁷ These processes have been shown to be affected in schizophrenia patients and coupled with reduced activation in areas of the ACC compared to HC.^{66,68,69} Thus hypoactivation of the ACC in EOS is shared with the adult / chronic populations of the disorder.⁶⁸ One study has shown that the conflict- and error-monitoring related ACC activity reduction in schizophrenia relates to the absence of behavioral adjustments to improve performance.⁶⁸ The ACC hypoactivation is believed to reflect impaired attribution of salience to errors, which then leads to impaired performance.⁶⁶ Hence, the ACC could serve as a neural substrate across a range of cognitive disturbances in EOS, which are shared with adult schizophrenia patients.

rTPJ. Our meta-analysis provides evidence that the rTPJ has significantly reduced activation in EOS patients across different cognitive tasks and this dysfunction persists also within WM-only tasks. Even though the rTPJ clusters from both functional ALE analyses overlap to a high degree, our cognitive association analyses revealed a slightly different pattern of behavioral domains coded by each cluster. The rTPJ cluster corresponding to the Cognition ALE was primarily involved in social cognition, visual perception, and action inhibition, whereas

the one corresponding to WM was primarily involved in social cognition-related behaviors.

Apart from attention reorienting to salient stimuli,⁷⁰ the rTPJ also facilitates an individual's sense of agency,⁷¹ which is impaired in schizophrenia.⁷² The rTPJ plays a domain-general role in social cognition (such as mental state attribution) through gating low-level attentional processes that generate internal predictions about external sensory events.⁷³ Attentional shifting mediated by the rTPJ is done by detecting unexpected events in the environment and the formation of spatial or social predictions that are held in WM.⁷⁴ Thus, the cognitive associations' findings of the Cognition ALE could be interpreted in light of the rTPJ sub-serving social cognitive processes through motor control (action inhibition) and the integration of sensory stimuli (visual perception). These processes could play a part in a wider cognitive framework that involves the detection of saliency, under any circumstances that require cognitive control (eg, detection of performance errors)⁷⁵ and executive functioning, such as WM. Therefore, the hypoactivation we observed here could indicate inefficient salience processing of stimuli that are relevant for cognitive and WM performance. The same dysfunctional processes could also explain impaired social cognition processes that are observed in the disorder.

Additionally, in schizophrenia, TPJ hypoactivation has previously been shown during auditory distraction from a visual attention task.⁷⁶ This suggests that deficient processing for exogenous/bottom-up cues is mediated by impaired TPJ activation, as observed in an adult and chronically ill sample.⁷⁶ In a recent meta-analysis, Kim⁷⁷ supported the existence of a frontoparietal network involving the rTPJ activated for subsequent forgetting after repetition enhancement. The author inferred that rTPJ activation results in the suppression of task-irrelevant mind wandering.⁷⁷ Hence, rTPJ hypoactivity, as observed in our meta-analysis, could signal the inefficiency of EOS subjects to “shut down” distracting thoughts and focus their attention on WM performance. Additionally, morphological examination of rTPJ in adult patients has shown that an abnormal sulcal pattern was associated with deficits in sense of agency and auditory hallucinations.⁷⁸ We suggest that the rTPJ is tied to the neurodevelopment of the disorder, an idea which is reinforced by the early insult in its sulcal development, as sulcal patterns are determined in utero,⁷⁸ and by reduced activity related to cognitive and WM processes in the EOS population, as our results suggest.

Posterior Parietal Cortices: Attentional and Executive Dysfunction. Focusing only on the WM experiments, our results not only showed hypoactivation in the rTPJ cluster but also bilaterally in the posterior parietal cortex (IPreC and rIPL). The paradigms in this meta-analysis included verbal and visuospatial WM. In our ALE results,

the cluster with the highest ALE value was located in the IPreC. Our cognitive association analysis of this cluster showed it was associated with cognitive functions of language and memory, as well as visual perception. On the right hemisphere, the hypoactivation peaked on the more inferior part of the parietal lobe (rIPL) with activity related to WM, spatial cognition, action, and motion perception.

Evidence from anatomical studies reveals parietal gray matter loss starting early in patients with childhood-onset schizophrenia, whereas bilateral SPL gray matter demonstrates the highest loss rate.¹⁷ Early parietal abnormalities are a consistent finding in schizophrenia research.^{79,80} There is supporting evidence that the IPreC volume is a successful classifier for EOS in a multivariate machine learning study,⁸¹ while rIPL and bilateral PreC resting-state BOLD abnormalities accurately predicted adolescents with schizophrenia against typically developing controls.⁸² Yildiz et al⁸³ proposed the “parietal type” of schizophrenia in which parietal, both anatomical and functional, impairments mark the second insult (the first insult being early in life before the overt manifestation of clinical symptoms in line with the neurodevelopmental model of the disorder including genetic, pregnancy and infancy factors) that triggers illness onset in some patients and is later progressing to frontal regions. This parietal impairment is first evidenced by WM impairment and sense of agency deficits⁸³ and hence could explain delusions of control seen in the disorder.⁸⁴

Functional imaging suggests that the posterior parietal areas that cover the PreC/IPS (BA: 7/40) are responsible for the manipulation of information in WM,⁸⁵ such as binding verbal and spatial stimuli⁸⁶ and for creating saliency maps for subsequent attentional selection.⁸⁷ Active binding in WM, which has been shown to be affected in schizophrenia patients, is partially explained by insufficient allocation of attentional resources and has a neural substrate located in the IPreC and bilateral IPL.⁸⁶ Our IPreC and rIPL clusters of hypoactivation in EOS could indicate patients’ reduced ability to manipulate verbal and spatial information in WM, as the included tasks comprised of both modalities with which our left and right parietal clusters were respectively functionally associated. Additionally, reduced connectivity of the frontoparietal network has been observed in schizophrenia: Dysconnectivity of the IPreC and rIPL to dorsal cingulate cortex has been linked to lack of cognitive control,⁸⁸ while frontoparietal dysconnectivity during WM performance has been suggested as a potential biomarker of the disorder.⁸⁹ Andre et al⁹⁰ found evidence for decreased rIPL activation and IPreC activation increase with aging in healthy subjects. Developmentally, this could mean that EOS patients reach a posterior parietal activation plateau similar to adult levels before actually entering adulthood. The results in this meta-analysis, together with previous studies in patients with

schizophrenia, highlight a parietal insult in multiple loci that extends from structure to activity.

MACM: Saliency Dysfunction. We followed up our ALE meta-analyses of cognition and WM in EOS by exploring the task-dependent co-activation patterns of our suprathreshold clusters with aberrant activation. EOS is marked with convergent hypoactivation in areas of the ACC and rTPJ across different cognitive processes. Using our clusters as seeds to explore their task-dependent functional connectivity, we discovered they are all co-activated with a more posterior part of the ACC or aMCC/medial frontal gyrus and bilateral insular cortices. Similarly, the posterior parietal and rTPJ seeds that demonstrate reduced activation during WM activate the same core network. This core network maps heavily on the salience network.⁹¹ As the salience network co-activates with the ACC, rTPJ, and posterior parietal cortices—areas responsible for attention (endogenous and exogenous), reward, WM, and visual perception—it becomes clear that this system integrates all these processes for successful cognitive and WM performance.

Decreased gray matter volume of the salience network (ACC/medial frontal gyrus and bilateral insula) has been a consistent finding across psychiatric conditions, and especially schizophrenia.⁹² In our meta-analysis, we did not detect consistent aberrant activity of the insular cortices in EOS; however, both our ALE results detected hypoactivation of the rTPJ. rTPJ is intimately linked to the ventral attentional network, responsible for reorienting attention to behaviorally relevant and salient stimuli.⁹³ Kucyi and colleagues⁹⁴ have previously argued that the ventral attention and salience networks are likely undifferentiated, owing to the high degree of functional and spatial overlap.⁹⁴ Therefore, the rTPJ could be considered a node of the salience network, and together with the ACC they show hypoactivation in EOS, which in turn could point to a central salience processing dysfunction relevant to general cognition.

Limitations, Strengths, and Conclusions

To our knowledge, we conducted the first ALE meta-analysis on VBM and fMRI EOS studies, following PRISMA guidelines. Given the severity of the disorder and the heterogeneity of the published findings, we thought it was imperative to use a coordinate-based meta-analytic method to track and trace statistical convergence in a standardized manner. Due to the nature of the ALE method, we were restricted to only using studies reporting results in standard stereotactic space. After screening 530 eligible papers, only few studies qualified to be included in our meta-analysis, mostly due to few reporting case-control comparison coordinates. Although a low number of eligible studies unavoidably create a low statistical power in our meta-analysis, it highlights

the need for more studies with EOS-only samples and for clear reporting of clinical characteristics such as AIO in addition to MNI or Talairach and Tournoux coordinates. Additionally, in the Cognitive ALE, the distribution of paradigms is unbalanced and mostly driven from the WM ones. However, as it is shown from the diagnostics in [supplementary table S3](#), each of the Cognitive ALE clusters contains at least one focus from a non-WM study. The ALE identified clusters in our meta-analysis could be used in future ROI and connectivity studies.

The VBM meta-analysis did not reveal any reduction of gray matter volume in EOS patients. Our fMRI results highlight brain areas of consistently reduced activation across studies that are common for EOS. These areas include the ACC during general cognition, the bilateral posterior parietal cortices during WM and the rTPJ during cognition and WM. Furthermore, our post hoc analysis showed that the salience network is functionally connected with these hypoactivating nodes identified here. Evidence from previous studies supports the idea that a salience processing impairment is central to schizophrenia and patients demonstrate disruptions of within- and between- salience network connectivity with other functional networks. Thus, saliency dysfunction could play a central role in EOS and lead to cognitive symptoms in the disorder, such as poor WM and goal-directed attention.

Supplementary Material

Supplementary data are available at *Schizophrenia Bulletin Open* online.

Funding

V.I. is funded by a studentship from City, University of London.

Acknowledgment

The authors have declared that there are no conflicts of interest in relation to the subject of this study.

References

- Kyriakopoulos M, Frangou S. Pathophysiology of early onset schizophrenia. *Int Rev Psychiatry*. 2007;19(4):315–324.
- Zwicker A, Denovan-Wright EM, Uher R. Gene–environment interplay in the etiology of psychosis. *Psychol Med*. 2018;48(12):1925–1936.
- Cannon M, Jones P, Huttunen MO, et al. School performance in Finnish children and later development of schizophrenia: a population-based longitudinal study. *Arch Gen Psychiatry*. 1999;56(5):457–463.
- Vyas NS, Patel NH, Puri BK. Neurobiology and phenotypic expression in early onset schizophrenia. *Early Interv Psychiatry*. 2011;5(1):3–14.
- Park S, Gooding DC. Working memory impairment as an endophenotypic marker of a schizophrenia diathesis. *Schizophr Res Cogn*. 2014;1(3):127–136.
- Luck SJ, Gold JM. The construct of attention in schizophrenia. *Biol Psychiatry*. 2008;64(1):34–39.
- Kapur S. Psychosis as a state of aberrant salience: a framework linking biology, phenomenology, and pharmacology in schizophrenia. *Am J Psychiatry*. 2003;160(1):13–23.
- Rapoport JL, Addington AM, Frangou S, Psych MR. The neurodevelopmental model of schizophrenia: update 2005. *Mol Psychiatry*. 2005;10(5):434–449.
- Moran ME, Weisinger B, Ludovici K, et al. At the boundary of the self: the insular cortex in patients with childhood-onset schizophrenia, their healthy siblings, and normal volunteers. *Int J Dev Neurosci*. 2014;32:58–63.
- Douaud G, Mackay C, Andersson J, et al. Schizophrenia delays and alters maturation of the brain in adolescence. *Brain*. 2009;132(Pt 9):2437–2448.
- Juuhl-Langseth M, Rimol LM, Rasmussen IA Jr, et al. Comprehensive segmentation of subcortical brain volumes in early onset schizophrenia reveals limited structural abnormalities. *Psychiatry Res*. 2012;203(1):14–23.
- Fraguas D, Díaz-Caneja CM, Pina-Camacho L, Janssen J, Arango C. Progressive brain changes in children and adolescents with early-onset psychosis: a meta-analysis of longitudinal MRI studies. *Schizophr Res*. 2016;173(3):132–139.
- Janssen J, Alemán-Gómez Y, Schnack H, et al. Cortical morphology of adolescents with bipolar disorder and with schizophrenia. *Schizophr Res*. 2014;158(1-3):91–99.
- Palaniyappan L, Das TK, Winmill L, Hough M, James A. Progressive post-onset reorganisation of MRI-derived cortical thickness in adolescents with schizophrenia. *Schizophr Res*. 2019;208:477–478.
- Gogtay N, Nugent TF III, Herman DH, et al. Dynamic mapping of normal human hippocampal development. *Hippocampus*. 2006;16(8):664–672.
- Vidal CN, Rapoport JL, Hayashi KM, et al. Dynamically spreading frontal and cingulate deficits mapped in adolescents with schizophrenia. *Arch Gen Psychiatry*. 2006;63(1):25–34.
- Thompson PM, Vidal C, Giedd JN, et al. Mapping adolescent brain change reveals dynamic wave of accelerated gray matter loss in very early-onset schizophrenia. *Proc Natl Acad Sci U S A*. 2001;98(20):11650–11655.
- Glahn DC, Laird AR, Ellison-Wright I, et al. Meta-analysis of gray matter anomalies in schizophrenia: application of anatomic likelihood estimation and network analysis. *Biol Psychiatry*. 2008;64(9):774–781.
- van Erp TG, Walton E, Hibar DP, et al. Cortical Brain Abnormalities in 4474 Individuals With Schizophrenia and 5098 Control Subjects via the Enhancing Neuro Imaging Genetics Through Meta Analysis (ENIGMA) Consortium. *Biol Psychiatry*. 2018;84(9):644–654.
- Rydkjær J, Møllegaard Jepsen JR, Pagsberg AK, Fagerlund B, Glenthøj BY, Oranje B. Mismatch negativity and P3a amplitude in young adolescents with first-episode psychosis: a comparison with ADHD. *Psychol Med*. 2017;47(2):377–388.
- Oknina LB, Wild-Wall N, Oades RD, et al. Frontal and temporal sources of mismatch negativity in healthy controls, patients at onset of schizophrenia in adolescence and others at 15 years after onset. *Schizophr Res*. 2005;76(1):25–41.
- Bittner RA, Linden DE, Roebroeck A, et al. The when and where of working memory dysfunction in early-onset

- schizophrenia—a Functional Magnetic Resonance Imaging Study. *Cereb Cortex*. 2015;25(9):2494–2506.
23. Thormodsen R, Jensen J, Holmèn A, *et al*. Prefrontal hyperactivation during a working memory task in early-onset schizophrenia spectrum disorders: an fMRI study. *Psychiatry Res*. 2011;194(3):257–262.
 24. Glahn DC, Ragland JD, Abramoff A, *et al*. Beyond hypofrontality: a quantitative meta-analysis of functional neuroimaging studies of working memory in schizophrenia. *Hum Brain Mapp*. 2005;25(1):60–69.
 25. White T, Hongwanishkul D, Schmidt M. Increased anterior cingulate and temporal lobe activity during visuospatial working memory in children and adolescents with schizophrenia. *Schizophr Res*. 2011;125(2-3):118–128.
 26. Fryer SL, Woods SW, Kiehl KA, *et al*. Deficient suppression of default mode regions during working memory in individuals with early psychosis and at clinical high-risk for psychosis. *Front Psychiatry*. 2013;4:92.
 27. Van Snellenberg JX, Girgis RR, Horga G, *et al*. Mechanisms of working memory impairment in schizophrenia. *Biol Psychiatry*. 2016;80(8):617–626.
 28. Pauly K, Seiferth NY, Kellermann T, *et al*. Cerebral dysfunctions of emotion-cognition interactions in adolescent-onset schizophrenia. *J Am Acad Child Adolesc Psychiatry*. 2008;47(11):1299–1310.
 29. Kyriakopoulos M, Dima D, Roiser JP, Corrigall R, Barker GJ, Frangou S. Abnormal functional activation and connectivity in the working memory network in early-onset schizophrenia. *J Am Acad Child Adolesc Psychiatry*. 2012;51(9):911–920.e2.
 30. White T, Schmidt M, Kim DI, Calhoun VD. Disrupted functional brain connectivity during verbal working memory in children and adolescents with schizophrenia. *Cereb Cortex*. 2011;21(3):510–518.
 31. Seiferth NY, Pauly K, Kellermann T, *et al*. Neuronal correlates of facial emotion discrimination in early onset schizophrenia. *Neuropsychopharmacology*. 2009;34(2):477–487.
 32. Borofsky LA, McNealy K, Siddarth P, Wu KN, Dapretto M, Caplan R. Semantic processing and thought disorder in childhood-onset schizophrenia: insights from fMRI. *J Neurolinguistics*. 2010;23(3):204–222.
 33. Moher D, Liberati A, Tetzlaff J, Altman DG; PRISMA Group. Preferred reporting items for systematic reviews and meta-analyses: the PRISMA statement. *PLoS Med*. 2009;6(7):e1000097.
 34. Tahmasian M, Eickhoff SB, Giehl K, *et al*. Resting-state functional reorganization in Parkinson's disease: an activation likelihood estimation meta-analysis. *Cortex*. 2017;92:119–138.
 35. Müller VI, Cieslik EC, Laird AR, *et al*. Ten simple rules for neuroimaging meta-analysis. *Neurosci Biobehav Rev*. 2018;84:151–161.
 36. Talairach J, Tournoux P. *Co-Planar Stereotaxic Atlas of the Human Brain*. New York, NY: Thieme Medical Publishers; 1988.
 37. Evans AC, Collins DL, Mills SR, Brown ED, Kelly RL, Peters TM. 3D statistical neuroanatomical models from 305 MRI volumes. In: 1993 IEEE Conference Record Nuclear Science Symposium and Medical Imaging Conference, San Francisco, CA, 31 October–6 November 1993. IEEE; 1994:1813–1817.
 38. Turkeltaub PE, Eickhoff SB, Laird AR, Fox M, Wiener M, Fox P. Minimizing within-experiment and within-group effects in Activation Likelihood Estimation meta-analyses. *Hum Brain Mapp*. 2012;33(1):1–13.
 39. Eickhoff SB, Laird AR, Grefkes C, Wang LE, Zilles K, Fox PT. Coordinate-based activation likelihood estimation meta-analysis of neuroimaging data: a random-effects approach based on empirical estimates of spatial uncertainty. *Hum Brain Mapp*. 2009;30(9):2907–2926.
 40. Eickhoff SB, Bzdok D, Laird AR, Kurth F, Fox PT. Activation likelihood estimation meta-analysis revisited. *Neuroimage*. 2012;59(3):2349–2361.
 41. Rasgon A, Lee WH, Leibu E, *et al*. Neural correlates of affective and non-affective cognition in obsessive compulsive disorder: a meta-analysis of functional imaging studies. *Eur Psychiatry*. 2017;46:25–32.
 42. Beissner F, Meissner K, Bär KJ, Napadow V. The autonomic brain: an activation likelihood estimation meta-analysis for central processing of autonomic function. *J Neurosci*. 2013;33(25):10503–10511.
 43. Robinson JL, Laird AR, Glahn DC, Lovallo WR, Fox PT. Metaanalytic connectivity modeling: delineating the functional connectivity of the human amygdala. *Hum Brain Mapp*. 2010;31(2):173–184.
 44. Robinson JL, Laird AR, Glahn DC, *et al*. The functional connectivity of the human caudate: an application of meta-analytic connectivity modeling with behavioral filtering. *Neuroimage*. 2012;60(1):117–129.
 45. Laird AR, Eickhoff SB, Rottschy C, Bzdok D, Ray KL, Fox PT. Networks of task co-activations. *Neuroimage*. 2013;80:505–514.
 46. Fox PT, Laird AR, Fox SP, *et al*. BrainMap taxonomy of experimental design: description and evaluation. *Hum Brain Mapp*. 2005;25(1):185–198.
 47. Laird AR, Lancaster JL, Fox PT. BrainMap: the social evolution of a human brain mapping database. *Neuroinformatics*. 2005;3(1):65–78.
 48. Eickhoff SB, Nichols TE, Laird AR, *et al*. Behavior, sensitivity, and power of activation likelihood estimation characterized by massive empirical simulation. *Neuroimage*. 2016;137:70–85.
 49. Nichols T, Brett M, Andersson J, Wager T, Poline JB. Valid conjunction inference with the minimum statistic. *Neuroimage*. 2005;25(3):653–660.
 50. Poldrack RA. Can cognitive processes be inferred from neuroimaging data? *Trends Cogn Sci*. 2006;10(2):59–63.
 51. Yarkoni T, Poldrack RA, Nichols TE, Van Essen DC, Wager TD. Large-scale automated synthesis of human functional neuroimaging data. *Nat Methods*. 2011;8(8):665–670.
 52. Henson R. Forward inference using functional neuroimaging: dissociations versus associations. *Trends Cogn Sci*. 2006;10(2):64–69.
 53. Benjamini Y, Hochberg Y. Controlling the false discovery rate: a practical and powerful approach to multiple testing. *J R Stat Soc Ser B*. 1995;57(1):289–300.
 54. Castro-Fornieles J, Bargalló N, Calvo A, *et al*. Gray matter changes and cognitive predictors of 2-year follow-up abnormalities in early-onset first-episode psychosis. *Eur Child Adolesc Psychiatry*. 2018;27(1):113–126.
 55. Douaud G, Smith S, Jenkinson M, *et al*. Anatomically related grey and white matter abnormalities in adolescent-onset schizophrenia. *Brain*. 2007;130(Pt 9):2375–2386.
 56. Janssen J, Reig S, Parellada M, *et al*. Regional gray matter volume deficits in adolescents with first-episode psychosis. *J Am Acad Child Adolesc Psychiatry*. 2008;47(11):1311–1320.
 57. Yoshihara Y, Sugihara G, Matsumoto H, *et al*. Voxel-based structural magnetic resonance imaging (MRI) study of patients with early onset schizophrenia. *Ann Gen Psychiatry*. 2008;7:25.
 58. Tang J, Liao Y, Zhou B, *et al*. Decrease in Temporal Gyrus Gray Matter Volume in First-Episode, Early Onset Schizophrenia: An MRI Study. Bruce A, ed *PLoS One*. 2012;7(7):1–6.

59. Ai Z, Wang Q, Yang Y, Manevski K, Zhao X, Eer D. Estimation of land-surface evaporation at four forest sites across Japan with the new nonlinear complementary method. *Sci Rep*. 2017;7(1):17793.
60. Zhang Y, Zheng J, Fan X, et al. Dysfunctional resting-state connectivities of brain regions with structural deficits in drug-naïve first-episode schizophrenia adolescents. *Schizophr Res*. 2015;168(1-2):353–359.
61. Thormodsen R, Rimol LM, Tamnes CK, et al. Age-related cortical thickness differences in adolescents with early-onset schizophrenia compared with healthy adolescents. *Psychiatry Res*. 2013;214(3):190–196.
62. Pagsberg AK, Baaré WF, Raabjerg Christensen AM, et al. Structural brain abnormalities in early onset first-episode psychosis. *J Neural Transm (Vienna)*. 2007;114(4):489–498.
63. Casey B, Jones RM, Somerville LH. Braking and accelerating of the adolescent brain. *J Res Adolesc*. 2011;21(1):21–33.
64. Petit L, Courtney SM, Ungerleider LG, Haxby JV. Sustained activity in the medial wall during working memory delays. *J Neurosci*. 1998;18(22):9429–9437.
65. Botvinick MM. Conflict monitoring and decision making: reconciling two perspectives on anterior cingulate function. *Cogn Affect Behav Neurosci*. 2007;7(4):356–366.
66. Polli FE, Barton JJ, Thakkar KN, et al. Reduced error-related activation in two anterior cingulate circuits is related to impaired performance in schizophrenia. *Brain*. 2008;131(Pt 4):971–986.
67. Crottaz-Herbette S, Menon V. Where and when the anterior cingulate cortex modulates attentional response: combined fMRI and ERP evidence. *J Cogn Neurosci*. 2006;18(5):766–780.
68. Kerns JG, Cohen JD, MacDonald AW III, et al. Decreased conflict- and error-related activity in the anterior cingulate cortex in subjects with schizophrenia. *Am J Psychiatry*. 2005;162(10):1833–1839.
69. Laurens KR, Kiehl KA, Ngan ET, Liddle PF. Attention orienting dysfunction during salient novel stimulus processing in schizophrenia. *Schizophr Res*. 2005;75(2-3):159–171.
70. Touroutoglou A, Hollenbeck M, Dickerson BC, Feldman Barrett L. Dissociable large-scale networks anchored in the right anterior insula subserved affective experience and attention. *Neuroimage*. 2012;60(4):1947–1958.
71. Hughes G. The role of the temporoparietal junction in implicit and explicit sense of agency. *Neuropsychologia*. 2018;113:1–5.
72. Koreki A, Maeda T, Okimura T, et al. Dysconnectivity of the agency network in schizophrenia: a functional magnetic resonance imaging study. *Front Psychiatry*. 2019;10:171.
73. Decety J, Lamm C. The role of the right temporoparietal junction in social interaction: how low-level computational processes contribute to meta-cognition. *Neuroscientist*. 2007;13(6):580–593.
74. Krall SC, Rottschy C, Oberwelland E, et al. The role of the right temporoparietal junction in attention and social interaction as revealed by ALE meta-analysis. *Brain Struct Funct*. 2015;220(2):587–604.
75. Ham T, Leff A, de Boissezon X, Joffe A, Sharp DJ. Cognitive control and the salience network: an investigation of error processing and effective connectivity. *J Neurosci*. 2013;33(16):7091–7098.
76. Smucny J, Rojas DC, Eichman LC, Tregellas JR. Neural effects of auditory distraction on visual attention in schizophrenia. *PLoS One*. 2013;8(4):e60606.
77. Kim H. Parietal control network activation during memory tasks may be associated with the co-occurrence of externally and internally directed cognition: a cross-function meta-analysis. *Brain Res*. 2018;1683:55–66.
78. Plaze M, Mangin JF, Paillère-Martinot ML, et al. “Who is talking to me?” - Self-other attribution of auditory hallucinations and sulcation of the right temporoparietal junction. *Schizophr Res*. 2015;169(1-3):95–100.
79. Burke L, Androustos C, Jogia J, Byrne P, Frangou S. The Maudsley Early Onset Schizophrenia Study: the effect of age of onset and illness duration on fronto-parietal gray matter. *Eur Psychiatry*. 2008;23(4):233–236.
80. Zhao C, Zhu J, Liu X, et al. Structural and functional brain abnormalities in schizophrenia: a cross-sectional study at different stages of the disease. *Prog Neuropsychopharmacol Biol Psychiatry*. 2018;83:27–32.
81. Greenstein D, Malley JD, Weisinger B, Clasen L, Gogtay N. Using multivariate machine learning methods and structural MRI to classify childhood onset schizophrenia and healthy controls. *Front Psychiatry*. 2012;3:53.
82. Liu Y, Zhang Y, Lv L, Wu R, Zhao J, Guo W. Abnormal neural activity as a potential biomarker for drug-naïve first-episode adolescent-onset schizophrenia with coherence regional homogeneity and support vector machine analyses. *Schizophr Res*. 2018;192:408–415.
83. Yildiz M, Borgwardt SJ, Berger GE. Parietal lobes in schizophrenia: do they matter? *Schizophr Res Treatment*. 2011;2011:581686.
84. Blakemore SJ, Frith C. Self-awareness and action. *Curr Opin Neurobiol*. 2003;13(2):219–224.
85. Champod AS, Petrides M. Dissociation within the frontoparietal network in verbal working memory: a parametric functional magnetic resonance imaging study. *J Neurosci*. 2010;30(10):3849–3856.
86. Grot S, Légaré VP, Lipp O, Soulières I, Dolcos F, Luck D. Abnormal prefrontal and parietal activity linked to deficient active binding in working memory in schizophrenia. *Schizophr Res*. 2017;188:68–74.
87. Bisley JW, Goldberg ME. Attention, intention, and priority in the parietal lobe. *Annu Rev Neurosci*. 2010;33:1–21.
88. Fornito A, Yoon J, Zalesky A, Bullmore ET, Carter CS. General and specific functional connectivity disturbances in first-episode schizophrenia during cognitive control performance. *Biol Psychiatry*. 2011;70(1):64–72.
89. Loeb FF, Zhou X, Craddock KES, et al. Reduced functional brain activation and connectivity during a working memory task in childhood-onset schizophrenia. *J Am Acad Child Adolesc Psychiatry*. 2018;57(3):166–174.
90. Andre J, Picchioni M, Zhang R, Touloupoulou T. Working memory circuit as a function of increasing age in healthy adolescence: a systematic review and meta-analyses. *Neuroimage Clin*. 2016;12:940–948.
91. Seeley WW, Menon V, Schatzberg AF, et al. Dissociable intrinsic connectivity networks for salience processing and executive control. *J Neurosci*. 2007;27(9):2349–2356.
92. Goodkind M, Eickhoff SB, Oathes DJ, et al. Identification of a common neurobiological substrate for mental illness. *JAMA Psychiatry*. 2015;72(4):305–315.
93. Corbetta M, Patel G, Shulman GL. The reorienting system of the human brain: from environment to theory of mind. *Neuron*. 2008;58(3):306–324.
94. Kucyi A, Hodaie M, Davis KD. Lateralization in intrinsic functional connectivity of the temporoparietal junction with salience- and attention-related brain networks. *J Neurophysiol*. 2012;108(12):3382–3392.